Charles University

Faculty of Science

Study programme: Analytical chemistry

Mgr. Lukáš Taraba

CHROMATOGRAPHIC CHARACTERIZATION OF POLYANILINE-COATED STATIONARY PHASES

CHROMATOGRAFICKÁ CHARAKTERIZACE POLYANILINEM POTAŽENÝCH STACIONÁRNÍCH FÁZÍ

Doctoral thesis

Supervisor: RNDr. Tomáš Křížek, Ph.D.

Prague, 2018

Prohlášení

Prohlašuji, že jsem tuto dizertační práci vypracoval samostatně a že jsem uvedl všechny použité informační zdroje a literaturu. Tato práce ani její podstatná část nebyla předložena k získání jiného nebo stejného akademického titulu.

Jsem si vědom, že případné využití výsledků, získaných v této práci, mimo Univerzitu Karlovu je možné pouze po písemném souhlasu této univerzity.

V Praze dne 26. 6. 2018 Mgr. Lukáš Taraba

This thesis summarizes the results obtained in the years 2014–2018 during my Ph.D. studies at the Charles University, Faculty of Science, Department of Analytical Chemistry, Hlavova 2030, 128 43, Prague 2, Czech Republic.

The work was financially supported by the Grant Agency of the Charles University (project No. 307 015) and by the Ministry of Education, Youth and Sports of the Czech Republic (projects SVV).

Supervisor: RNDr. Tomáš Křížek, Ph.D.
Department of Analytical Chemistry
Faculty of Science, Charles University

Supervisor-consultant: Prof. RNDr. Pavel Coufal, Ph.D.
Department of Analytical Chemistry
Faculty of Science, Charles University

ABSTRACT (EN)

This dissertation thesis is focused on physicochemical and chromatographic characterization of polyaniline-coated stationary phases. In the first part, surfaces of bare silica and octadecyl silica sorbents were modified by *in-situ* chemical polymerization of aniline hydrochloride and their subsequent systematic characterization was performed by using the linear solvation energy relationship approach in the HILIC mode of capillary LC. In addition, several common physicochemical techniques were used to characterize properties of these altered materials. The modified sorbents were then packed into capillary columns. The retention interactions taking place between solute and the separation system were evaluated on the basis of retention data of a number of various solutes. The results showed that polyaniline coating had a significant effect on the retention promoting interactions of both polyaniline-coated stationary phases. The assumed mixed-mode retention mechanism was proven for both the stationary phases.

The second part dealt with investigation of the separation potential of polyaniline-coated silica stationary phase in different chromatographic modes. The retention factor curves of structurally similar solutes were constructed as a function of organic modifier portion in the mobile phase. The obtained results showed that the stationary phase is applicable in more than one chromatographic mode. Next, the separation performance of polyaniline-coated sorbent was assessed for two sets of either hydrophobic or hydrophilic structural analogues in the NP, RP and HILIC modes. Due to the mixed-mode retention mechanism of this stationary phase, the elution order of solutes is not governed only by their polarity. In addition, selectivity of this stationary phase was compared to the selectivity of unmodified bare silica and octadecyl silica commercial sorbents.

The last part was focused on protonation ability of polyaniline-coated silica sorbent and its effect on retention behavior of various solutes in the mobile phase of different pH investigated by the linear solvation energy relationship in RP mode. The results show that pH of the eluent has a remarkable effect on the extent of dominant retention interactions. By tuning the mobile phase pH, we can modulate the retention of neutral hydrophobic solutes due to the pH-dependent charge and structure of polymer chains of the polyaniline-coated sorbent which shows a mixed-mode separation mechanism also in RP mode.

ABSTRAKT (CZ)

Tato dizertační práce se zabývá fyzikálně-chemickou charakterizací stacionárních fází potažených polyanilinem. V první části byly chemickou polymerizací anilinium(1+) chloridu *in-situ* modifikovány povrchy sorbentů na bázi čistého silikagelu a silikagelu s navázanou oktadecylovou skupinou. Jejich následná systematická charakterizace byla provedena s použitím modelu lineárních vztahů solvatačních energií v HILIC módu kapilární kapalinové chromatografie. Dále bylo k popisu vlastností modifikovaných materiálů použito několik běžných fyzikálně-chemických technik. Modifikované sorbenty byly ve formě suspenzí naplněny do kapilárních kolon. Retenční interakce probíhající mezi analytem a separačním systémem byly zhodnoceny na základě retenčních dat pro množství různých analytů. Výsledky ukázaly, že polyanilinový povlak měl významný vliv na retenci podporující interakce pro obě stacionární fáze. Předpokládaný smíšený retenční mechanismus byl prokázán pro obě stacionární fáze.

Druhá část se zabývá zkoumáním separačního potenciálu stacionární fáze potažené polyanilinem v různých chromatografických módech. Pro strukturně podobné látky byly zkonstruovány křivky retenčních faktorů závislé na podílu organického modifikátoru v mobilní fázi. Získané výsledky ukázaly, že tato stacionární fáze je použitelná ve více než jednom chromatografickém módu. Poté byl posouzen separační výkon polyanilinem potaženého sorbentu na skupině hydrofobních nebo hydrofilních strukturních analogů v NP, RP a HILIC módech. Eluční pořadí analytů není kvůli smíšenému retenčnímu mechanismu této stacionární fáze řízeno pouze jejich polaritou. Selektivita této stacionární fáze byla dále porovnána se selektivitami komerčních sorbentů na bázi čistého silikagelu a silikagelu s navázanou oktadecylovou skupinou.

Poslední část byla zaměřena na protonizační schopnost polyanilinem potaženého silikagelového sorbentu a její vliv na retenční chování různých analytů v mobilní fázi o různém pH zkoumaný pomocí modelu lineárních vztahů solvatačních energií v RP módu. Výsledky ukazují, že pH eluentu má pozoruhodný vliv na velikost dominantních retenčních interakcí. Retence neutrálních hydrofobních látek může být modulována volbou pH mobilní fáze díky náboji a struktuře polymerních řetězců v polyanilinem potaženém sorbentu, které na pH závisí. Tato stacionární fáze vykazuje smíšený separační mechanismus rovněž v RP módu.

Keywords: capillary liquid chromatography, chromatographic characterization, linear solvation energy relationship, polyaniline, stationary phase

Klíčová slova: chromatografická charakterizace, kapilární kapalinová chromatografie, model lineárních vztahů solvatačních energií, polyanilin, stacionární fáze

TABLE OF CONTENTS

LIST OF ABBREVIATIONS AND SYMBOLS

2AAP	2´-aminoacetophenone
3AAP	3´-aminoacetophenone
4AAP	4´-aminoacetophenone
AC	acetone
ACN	acetonitrile
APS	ammonium persulfate
AU	arbitrary unit
BET	Brunauer-Emmett-Teller theory of nitrogen adsorption
C_8	octyl (silica)
C_{18}	octadecyl (silica)
CA	caffeine
CE	capillary electrophoresis
CI	confidence interval
cLC	capillary liquid chromatography
FTIR	Fourier-transformation infrared (spectroscopy)
GC	gas chromatography
HCA	hierarchical cluster analysis
HETP	height equivalent to the theoretical plate
HI	hydrophobicity index
HILIC	hydrophilic interaction liquid chromatography
HPLC	high-performance liquid chromatography
HS	hydrophobic subtraction (model)
i.d.	inner diameter
IEC	ion-exchange chromatography
LC	liquid chromatography
LFER	linear free energy relationship
LSER	linear solvation energy relationship
MeOH	methanol
MMC	mixed-mode chromatography
MLR	multiple linear regression
NP	normal phase (separation mode of liquid chromatography)
PAHs	polycyclic aromatic hydrocarbons

PANI	polyaniline
PANI-SiO_2	polyaniline-coated silica
PANI-C_{18}	polyaniline-coated octadecyl silica
PCA	principal component analysis
PEEK	polyether ether ketone
PGC	porous graphitic carbon
PTFE	polytetrafluoroethylene
RP	reversed phase (separation mode of liquid chromatography)
RSD	relative standard deviation
ΔRSD	intermediate precision
SE	standard error
SEM	scanning electron microscopy
SFC	supercritical fluid chromatography
SI	silanol index
SSA	specific surface area
TB	theobromine
TPH	theophylline
TEM	transmission electron microscopy
TO	toluene
TU	thiourea
UV	ultraviolet electromagnetic radiation
VIS	visible region of electromagnetic spectrum
XPS	X-ray photoelectron spectroscopy
XRD	X-ray diffraction

a	hydrogen bond basicity (LSER)
A	overall hydrogen bond acidity (LSER), eddy diffusion
A_p	peak area
A_s	peak asymmetry
b	hydrogen bond acidity (LSER)
b	broad (peak intensity in Raman/IR spectrum)
B	overall hydrogen bond basicity (LSER), longitudinal diffusion
B	benzenoid segment

c	system intercept (LSER)
C_m	mass transfer resistance in the mobile phase
C_s	mass transfer resistance in the stationary phase
d^+	cation-exchange ability (LSER)
D^+	protonation ability of solute (LSER)
d^-	anion-exchange ability (LSER)
D^-	dissociation ability of solute (LSER)
d_f	thickness of particle porous layer
D_m	diffusion coefficient in the mobile phase
d_p	particle diameter
D_s	diffusion coefficient in the stationary phase
e	lone electron pair interactions and π-π stacking (LSER)
E	excess molar refraction (LSER)
E^0	standard electrode potential
$f(q)$	sorbent-properties-dependent function in van Deemter equation
F	Fisher's statistics
g	gravitational constant
ΔG°	standard free (or Gibbs) energy
ΔH°	standard enthalpy
k	retention factor
K	distribution constant
$\log D$	decadic logarithm of distribution coefficient
m	medium (peak intensity in Raman/IR spectrum)
n	number of measurements
N	theoretical plate number/separation efficiency
pH	negative decadic logarithm of hydroxonium cation activity
${}^{s}_{s}\mathrm{pH}$	effective pH obtained after mixing aqueous and organic solvents
${}^{s}_{w}\mathrm{pH}$	hydro-organic pH of the aqueous-organic solvent mixture
${}^{w}_{w}\mathrm{pH}$	purely aqueous pH
Pho	phenoxazine-like segment
Phz	phenazine-like segment
$\mathrm{p}K_\mathrm{a}$	negative decadic logarithm of dissociation constant of the acid
Q	quinoid segment

R	universal gas constant, chromatographic peak resolution
R^2	determination coefficient
rg	aromatic ring (assignment in Raman/IR spectrum)
s	dipole-dipole interactions (LSER)
s	strong (peak intensity in Raman/IR spectrum)
S	spreading coefficient, dipolarity/polarizability (LSER)
ΔS°	standard entropy
sh	shoulder (peak intensity in Raman/IR spectrum)
SQ	semiquinone segment
T	absolute temperature
t_R	retention time
t_{sed}	sedimentation time
u	linear flow rate velocity
v	settling rate, dispersion interactions (hydrophobicity, LSER)
V	McGowan's molecular volume (LSER)
vs	very strong (peak intensity in Raman/IR spectrum)
v/v	volume-to-volume ratio
w	weak (peak intensity in Raman/IR spectrum)
w/v	weight-to-volume ratio
α	selectivity factor
β	phase ratio
γ	short-wave electromagnetic radiation,
γ	out-of-plane bending vibration
γ_p	packing impedance factor
γ_L	surface energy of liquid phase
γ_{LS}	surface energy of liquid-solid interface
γ_S	surface energy of solid phase
δ	deformation or in-plane bending vibration
ε_f	fraction of a total particle volume
ε_i	particle porosity
η	dynamic viscosity of liquid
η_{kin}	kinematic viscosity of solvent
κ	particle/solvent-dependent constant

λ	flow path inequality coefficient
$\boldsymbol{\nu}$	stretching vibration
ϱ_l	liquid density
ϱ_p	stationary phase density
σ	electrical conductivity
$\boldsymbol{\tau}$	torsion vibration
φ	volume fraction
ψ	particle shape, size and porosity coefficient
ψ'	sorbent type related coefficient
$\boldsymbol{\omega}$	wagging vibration

1 PREFACE

High performance liquid chromatography (HPLC) belongs indisputably among the most frequently employed separation techniques at the present time, although the original concept was introduced by M. S. Tsvet more than hundred years ago. Using a simple apparatus consisting of a glass column packed with powder of calcium carbonate that was flushed with mixtures of organic solvents, he separated different forms of plant pigments as colored bands in the column. From that time, an unceasing desire for quicker, more selective and more efficient separations of increasing number of various analytes started off a boom of the instrumental development and improvement, design and testing of newly prepared stationary and mobile phases, and thorough investigation of theoretical background of the separation processes and retention mechanism. For instance, current challenges for HPLC are separations of chiral drugs, determination of residual contaminants occurring in medicine, or elaborate analysis of complex samples in omics which would be impossible to perform without newly developed stationary phases including ionic liquids, biomolecules, and polymer composites [1-3].

In spite of belonging among the oldest packing materials, silica (also called silica gel, SiO_2) is the most used inorganic sorbent in modern HPLC ever. Bare (native) SiO_2 has been employed for separation of polar analytes in normal phase (NP) and hydrophilic interaction liquid chromatography (HILIC) modes. Furthermore, SiO_2 is applied as a suitable supporting material for surface modification and subsequent use for reversed phase (RP) separations of low polar compounds. Its main benefits are very good mechanical strength and high-temperature endurance, uniformity of the surface area, and chemical purity and resistance against organics. Common silica is the porous, amorphous form of hydrated SiO_2 of various shapes and sizes with superficial silanols which can be functionalized with various groups [4-6]. A major downside of SiO_2-based stationary phases is the limited applicable pH range of approximately 2–8. The acidic hydrolysis of ligand attachment occurs under the lower pH thereby chromatographic performance of the stationary phase deteriorates. Oppositely, SiO_2 supporting material dissolves spontaneously at high pH, especially in high-aqueous mobile phases at elevated temperature.

A solution of this issue is use of a different sorbent, such as hybrid silica [7], porous graphitic carbon (PGC) [8], inorganic oxides (TiO_2, Al_2O_3, ZrO_2) [9], or polymers [10]. These alternative sorbents may be chemically stable over a wider pH

range, however, their chromatographic parameters cannot compete with SiO_2 thus far [11]. Alternatively, there are several approaches to prevent degradation of the SiO_2-based sorbent such as use of multidentate ligands, silanol single (trimethyl silane) or multiple (propylene bridges) endcapping, steric shielding of free silanols by bulky non-polar group (*e.g.*, isopropyl, *tert*-butyl residue) [12], embedding of polar group into non-polar ligand (whereby this polar, amide or dimethyl urea based group attracts solutes before they reach silica surface [13]), horizontally polymerized protection layer of siloxanes [14], and carbon or polymer coating [15, 16].

The latter approach, although not frequently used, provides an interesting way to protect the surface of stationary phase. Polymer-coated sorbents combine the mechanical strength of an inorganic supporting material with chemical properties and stability of the chosen polymer, therefore, it can lead to obtaining unique selectivity of the prepared stationary phase with mixed-mode retention mechanism [17]. Additionally, polymer coating is relatively simple procedure in comparison with modification of the sorbent with (complex) organic ligand(s) that may require a multiple-step process with a low yield, especially for stationary phases with more than one functionality [18, 19]. Using polymer coating, a plethora of miscellaneous stationary phases can be produced [20].

For practical application it is vital for the newly prepared stationary phases to be characterized and ranked so that an analyst can select the most appropriate sorbent for an intended separation. A subtle difference in sorbent chemistry, not only the length of alkyl chain or different embedded functionalities and their number, but also their sequence or distance in ligand/polymer chain, can have the substantial effect on the column selectivity [21]. New stationary phases, both developed in primary research and commercial ones, are usually characterized by physicochemical and chromatographic methods. Among general characterization techniques belongs elemental analysis, specific surface area (SSA) analysis, scanning electron microscopy (SEM), and infrared or Raman spectroscopy.

For investigation of chromatographic properties of a sorbent is first necessary to pack a separation column. Regarding the column dimensions, it can be convenient to choose smaller inner diameter (i.d.) than that of common analytical column (*i.e.*, 4.0−4.6 mm) for preliminary experiments in order to save prepared sorbent. Therefore, liquid chromatography performed in capillary columns represents an ideal option because it allows to spare also mobile phases, and thereby expenses and the

environment [22]. In the past decades, simple chromatographic tests were used predominantly to characterize sorbent properties and to compare individual stationary phases [23]. However, for a more precise description of interactions taking place between stationary phase and solutes and consequent proposal of (complex) retention mechanism, there were developed different approaches. These, new approaches join thermodynamics of the retention process with mathematical processing and statistical evaluation of obtained data, linear solvation energy relationship (LSER) model is the most applied [24]. The great advantage of LSER is its applicability for characterization of a system in different chromatographic modes (*e.g.*, RP and HILIC), in contrast to simple chromatographic tests having strictly fixed measurement conditions.

2 AIMS OF THE THESIS

This work was focused on physicochemical and chromatographic characterization of polyaniline-coated stationary phases and was divided into three parts:

- Preparation of chemically polymerized polyaniline coatings on stationary phases based on bare silica gel and octadecyl silica, characterization of these modified sorbents by common physicochemical techniques and by the linear solvation energy relationship approach in hydrophilic interaction liquid chromatography.

- Investigation of polyaniline-coated silica as a mixed-mode stationary phase showing the change of the elution order of structurally related solutes based on the varied portion of organic modifier and pH of the eluent and study of the application potential of this stationary phase to separate structural analogues of either slightly hydrophilic or slightly hydrophobic solutes in different modes of capillary liquid chromatography.

- Systematic chromatographic characterization of polyaniline-coated silica employing linear solvation energy relationship in reversed phase mode under different pH of the mobile phase and study of partitioning or adsorption retention processes.

3 POLYMER-COATED STATIONARY PHASES – PREPARATION AND CHARACTERIZATION

3.1 Polymer coating approaches

Polymer coating of a supporting substrate can be performed in many ways depending on physicochemical properties of both materials, required features of the complex product and intended purpose. However, we distinguish three general ways of preparation: sorption/immobilization of pre-synthesized polymer layer(s) onto the support surface (including pore filling by "nail-like" attachment), *in-column* dynamic coating, and *in-situ* polymerization of monomers adsorbed onto the supporting material [25].

Commonly used procedures for immobilization of already polymerized coatings are thermal immobilization, static solvent evaporation, self-immobilization, and microwave/ultraviolet (UV)/γ-irradiation [26]. The principle of dynamic coating of the particles is identical with the approach used to modify the inner silica capillary wall in capillary electrophoresis (CE); the coating solution passes through the column that has been previously packed with the support material [27]. *In-situ* polymerization, triggered mostly by radical initiation or UV irradiation, is less used approach because of limited number of monomers that can adsorb onto the supporting surface.

The formed attachment between a polymer (possibly with cross-linked chains) and a supporting material is based either on chemisorption (covalent chemical bonds) or physisorption (immobilization mediated via Coulombic or van der Waals interactions). Up to present day, there have been immobilized a lot of polymers of various chemical structures, both neutral (*e.g.*, polyethers, polytetrafluoroethylene (PTFE), polyvinylalcohol, polymethyl methacrylate, or styrene-divinyl benzene copolymers [10, 28, 29]) and charged (*e.g.*, polysiloxanes, polysulphonates, polyamines, polypeptides, polysaccharides [20, 30, 31]). In particular, polycations, *i.e.*, polymers whose repeating unit bears a positively charged functionality, represent very interesting group because they can adsorb on partially negatively charged silica particles due to electrostatic interactions over a wide range of pH (ideally for pH ≥ 3).

3.2 Polyaniline properties and synthesis

Polyaniline (PANI) belongs among the most studied polymers ever due to its unique physicochemical properties. PANI is readily synthesized, flexible, electrochromic, conductive polymer of high chemical and environmental stability [32]. Additionally, PANI is the eldest known electrochemically active polymer [33]. Figure 1 shows commonly accepted chemical structure of PANI. Polyaniline was reported for the first time in the 1840s, when aniline was oxidized using chromic acid [34]. For the next one hundred years, PANI was studied mainly to elucidate the relation between its various colors and exact chemical structures [35].

Thorough PANI investigation reinvigorated during the development of conducting polymers, also known as "synthetic metals", in the second half of 20th century; especially thanks to works of MacDiarmid, Shirakawa and Heeger (the Nobel prize for Chemistry laureates). They observed that PANI transfers to metallic regime after acid doping (simple acidification). The change of PANI electrical conductivity σ from 10^{-10} to 10^{3} $S \cdot cm^{-1}$ was observed. The presumed conductivity mechanism is based on formation of polarons and bipolarons (nitrogen radical cations) in PANI chains [36].

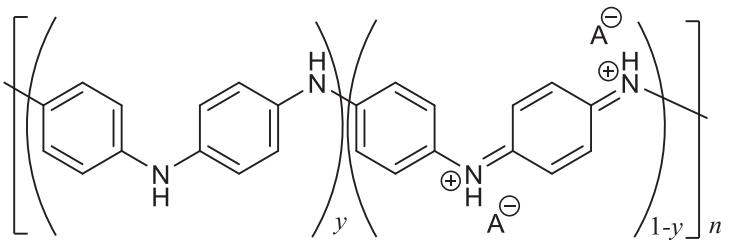

Figure 1 Chemical structure of polyaniline consisting of units built from reduced (y) and oxidized (1-y) blocks; here in form of acid-doped emeraldine salt

From the perspective of molecular structure, PANI generally occurs in three oxidation states: fully oxidized pernigraniline, half-oxidized emeraldine and fully reduced leucoemeraldine. Each PANI polymorph acts as an organic base in the undoped state. When acid-doped and, therefore, protonated, it transforms into salt (Figure 2); each form has individual color [37, 38]. Emeraldine salt is the only highly conductive form of PANI; other forms are either semiconductors or insulators. Stability of the individual form depends on several conditions, such as solution pH, salt counter-anion, temperature, applied potential or presence of another electroactive compound [39, 40].

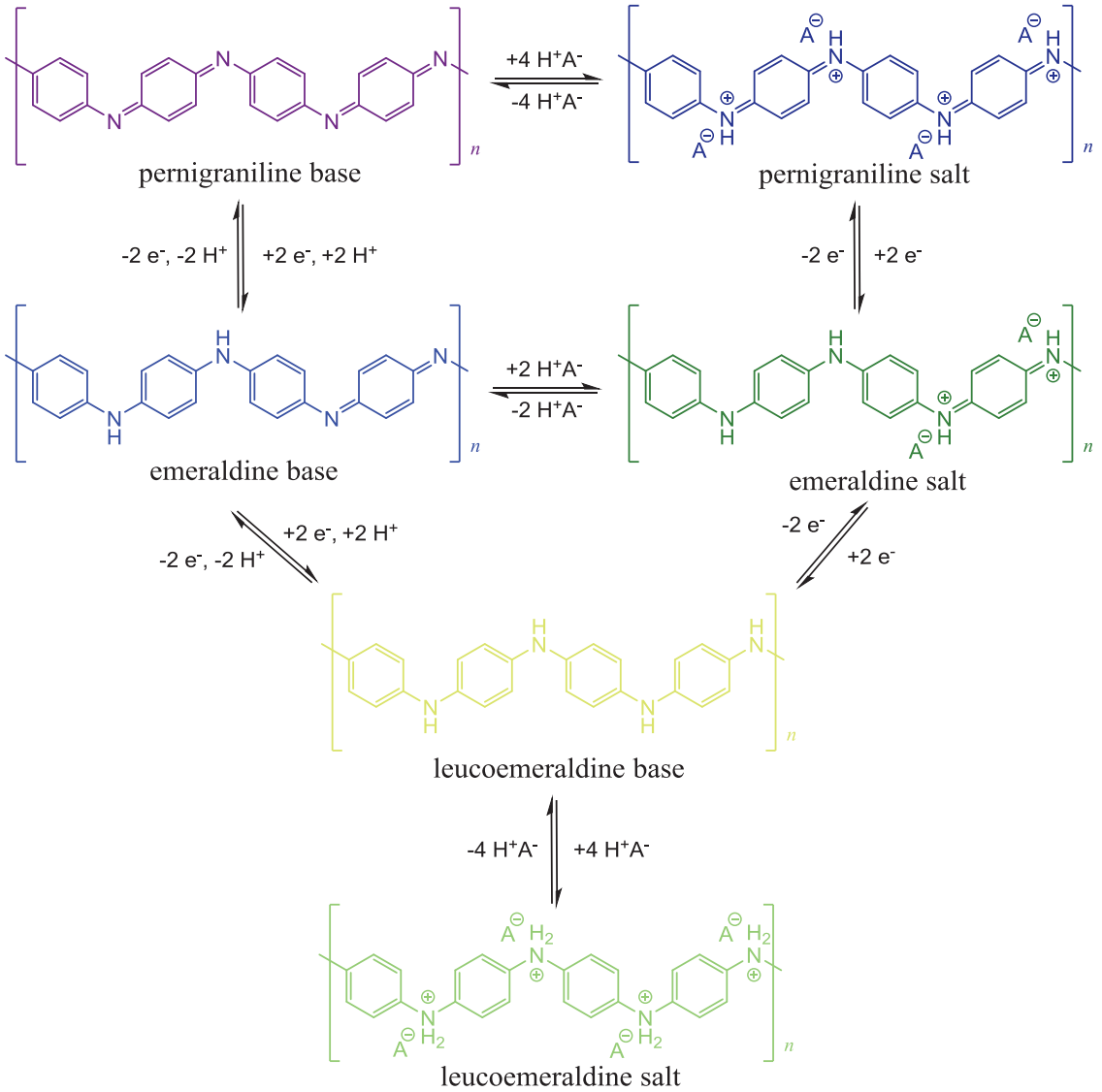

Figure 2 Oxidation states of PANI in forms of bases and salts; the color of individual PANI structures corresponds roughly to the real coloration of PANI in the specific state

PANI is typically prepared by oxidative electrochemical or chemical polymerization of aniline or anilinium(1+) salt [41]. The advantage of electrochemical way is the permanent control of the applied potential during the whole PANI polymerization process. PANI is deposited on a conducting substrate as a thin film of adjustable thickness [42]. Oppositely, chemical polymerization yields higher quantity of high molecular weight polymer [43]. In addition, the latter approach does not require use of a potentiostat, whereby makes polymerization instrumentally less demanding. Parameters of the PANI synthesis (both chemical and electrochemical) strongly affect its final morphology and properties. According to intended purpose of PANI, the following should be optimized in chemical polymerization: counter anion (dopant) [44],

oxidant (reaction initiator) [45], concentrations and ratios of reagents [46], reaction pH, temperature and time [47-49], and use of non-aqueous solvents (even aprotic) [50, 51] or irradiation (UV, γ) [52, 53]. Other two parameters have the effect on PANI features in electrochemical polymerization: electrode material (shape, dimensions, surface roughness) and chosen electrochemical technique (*e.g.*, cyclic voltammetry) [54]. Additionally, use of a chiral dopant leads to formation of optically active PANI [55].

The most used chemical preparation of PANI consists of addition of the aqueous solution of ammonium persulfate (APS, E^0 = 1.94 V) to the aqueous solution aniline hydrochloride at temperature below 5 °C [56]. Consistent temperature control is of great importance because increasing synthesis temperature yields PANI of lower molecular weight. Moreover, undesirable chain branching may occur because of *ortho*-coupling of monomers. The reaction is performed in acidic environment because low pH promotes the head-to-tail (*para*) coupling of aniline monomers. Conversely, high pH of polymerization leads to the formation of unwanted, short-chain, oligomeric material [32]. PANI prepared in usual way (low both temperature and pH of mixture) provides irregular or granular particles of approximately micron size. However, nano- and micro-scale diversity of PANI morphology is extensive. Small changes of reaction parameters and/or use of templates, both hard [57] and soft, such as immiscible solvents- and surfactant-based templates [58], affect substantially the final look of PANI. Reaction additives, such as substituted anilines, can remarkably alter the PANI structural growth [59]. Thus it is possible to obtain fibers (linear, cross-linked), wires, tubes, spheres, hollow spheres, plates, bloom-, brain-, leaf-, and sea urchin-like structures [34].

The molecular mechanism of the PANI polymerization process has not been described entirely and unambiguously yet [60]. Nonetheless, the generally accepted mechanism suggests adsorption (if available) of anilinium(1+) cation onto a substrate followed by the initial formation of aniline cation-radical; which is indicated by the change of polymerization mixture from colorless to transparent light pink [32]. In the next step, two cation-radicals couple into dication-diradical or recombine (as benzidine, phenazine, azobenzene or 4-aminophenylamine). During the rapid and exothermic propagation period free anilinium(1+) monomers are incorporated by (mostly) *para*-coupling into the oligomeric chain of pernigraniline [61]. *Ortho*- and *meta*-coupling is also possible, but less likely, leading to recombinant-like structures. As the polymerization proceeds, the reaction mixture becomes deep blue [62]. When the oxidant is completely consumed, the remaining monomers in the solution reduce fully

oxidized pernigraniline to emeraldine. The final product, emeraldine salt, has green color [63].

For hard template coating, formed oligomeric cation-radicals are more hydrophobic than the original monomeric cation-radicals. Therefore, they tend to cling together and separate themselves from the hydrophilic aqueous medium by adsorbing at surfaces in contact with the polymerization mixture [64]. The adsorbed oligomers have higher reactivity towards initiation of the PANI chains growth; the reaction is auto-accelerated (heterogeneous catalysis) [65]. As was experimentally proven, PANI polymerization at the surfaces precedes its polymerization in the bulk of the reaction mixture [66]. The PANI chain, earlier attached to the supporting surface, supposedly presents a nucleus of the forming film. PANI oligomers are thus formed and adsorbed close to the nucleus and stimulate the growth of other PANI chains. These chains proliferate along the surface and because of steric reasons they are preferentially oriented perpendicularly to the substrate [67, 68]. Microscopic lumpy deposits that merge together, thus forming compact layer, are observed in SEM images.

PANI formation as thin films or coatings was reported on various substrates, including colloidal dispersions, such as glass/silica [69-72], metals or metal oxides (Au [73], Pt and Pd [74], TiO_2 [75]), another polymer [76, 77], graphene [78], carbon nanotubes [79, 80], or even wood saw dust [81]. Oppositely, PANI matrix has been successfully used for deposition of noble metal nanoparticles (Cu [82], Ag [83], Au [84], Pd [85]). Thanks to the adsorption ability, PANI has been used as a surface modifier in multiple applications, such as flexible electrodes [86], photovoltaic devices [87], rechargeable batteries [88], sensors [89, 90], organic field transistors [91], supercapacitators [92], electrochromic glasses [93, 94], anticorrosive coatings [95], gas-separation membrane [96], antibacterial agent [97], and catalysts [98-100].

Despite immense number of PANI-related publications (over 40 000 references) in other scientific fields, there are only several references about PANI coatings applied in separation science. However, PANI has been employed as the inner-wall modifier in capillary electrophoresis (CE) [101-103] and continuous flow analysis [104], protonable modifier of polystyrene-divinylbenzene monolith [105], multiple-layer particle coating for capillary electrochromatography [106], conductive stationary phase for electrochemical separation technique [107, 108], and sorbent for thin layer chromatography (TLC) [109-112] and solid-phase microextraction (SPME)[113-116].

From the three PANI polymorphs, emeraldine is of particular interest from the chromatographic perspective. Indeed, alternation of diamine-benzenoid and imine-quinoid moieties is exceptional among polymers, let alone common organic ligand based stationary phases used in current HPLC separations. Moreover, charge tuning of PANI only by the change of mobile phase pH makes the polymer rare among other stationary phases. However, PANI, as polyelectrolyte polymer, lacks a single, clearly defined pK_a value of the functional groups. Instead, PANI shows a distribution of dissociation constants [117]. According to the available literature, the pK_a value of the transition from emeraldine base to emeraldine salt approximately ranges from 2 to 8 [118]. However, it should be noted that such a wide pK_a range is most likely related to the different techniques used for pK_a determination and to the heterogeneous experimental conditions used for preparation of PANI.

Christwanto and Wallace reported as first the preparation of polyaniline coatings on silica by oxidation of aniline. In their approach aniline was first diluted in hexane and mixed with the sorbent. Hexane was then evaporated and free-flowing aniline-coated particles were oxidized using potassium dichromate under ambient temperature in polymerization mixture containing 1.5 M hydrochloric acid [119]. Authors also performed a preliminary chromatographic study using as probes small organic molecules, inorganic anions, and polycyclic aromatic hydrocarbons (PAHs) to characterize the novel stationary phase. According to obtained results, they concluded that the sorbent behaved as typical RP stationary phase for neutral compounds, whereas it acted as anion-exchanger for anions. Moreover, their sorbent showed certain steric selectivity (on the basis of solute planarity) for PAHs tested.

Stejskal et al. proposed some improvements concerning the silica coating procedure [120]. In this approach, the polymerization mixture was cooled to 0–2 °C and spherical silica particles were continually dispersed by magnetic stirring in polymerization mixture containing aniline hydrochloride, which is more soluble in water than pure aniline. Moreover, they introduced colloidal silica as a stabilizer to prevent the formation of PANI macroscopic precipitate, which occurs besides PANI coating of silica. Authors presumed that PANI colloidal dispersion would have not settled down as PANI precipitate did, but kept floating in supernatant. Therefore, separation of PANI-coated particles and PANI precipitate based on different sedimentation time would be unnecessary. However, silica nanospheres were too abundantly present in PANI-silica microspheres, therefore, superficial free silanols of

nano-silica were accessible to interact with solutes, which is undesirable for chromatographic purpose. In addition, they coated also aminopropyl and octadecyl silica (C_{18}) sorbents to evaluate the quality of coating, expressed as percentage of nitrogen on the particle surface. Unfortunately, they did not perform any chromatographic study to show benefits of their improvements.

Sowa et al. adopted the approach from Stejskal et al. to prepare the PANI-silica stationary phase, characterized its physicochemical properties (elemental composition, porosity, density and particle size distribution), and studied the application potential in non-suppressed ion chromatography of small inorganic anions [121-123]. They also carried out pH and thermal stability study of the sorbent using high-resolution continuum source graphite furnace atomic absorption spectrometry and Raman spectroscopy. They concluded that PANI layer protected the supporting silica better than grafted C_{18}. Furthermore, the authors showed that the sorbent was stable in pH range of 1−12 under T range of 30−70 °C. Therefore, they assessed PANI-silica gel sorbent as appropriate stationary phase for liquid chromatography (LC) [124].

Despite such a detailed investigation of PANI-coated silica properties, its systematic chromatographic characterization, description of retention interactions, or comparative evaluation of applicability in different chromatographic modes have not been published yet.

3.3 Physicochemical characterization of stationary phases

Physicochemical characterization should accompany chromatographic characterization of newly prepared stationary phase because it provides information that clarifies and supports the obtained chromatographic data. In addition, description of physicochemical properties of a new commercial sorbent represents the integral part of its development today. Moreover, continual control of the sorbent properties is necessary for reproducible preparation of the well-defined stationary phase. A variety of techniques can be used depending on the type of sorbent or on required chemical and/or morphological information. The most common techniques are briefly introduced below.

Elemental analysis, also called combustion analysis, is used to compare the difference of sorbent elemental composition before and after attachment of a stationary phase modifier, and thus the efficiency of modification. Carbon, hydrogen and nitrogen

are usually determined elements, although modern elemental analyzers can also determine quantity of sulfur [120]. Carbon content is one of key descriptors for alkyl-ligand-based sorbents, such as C_{18} and octyl-bonded silica (C_8). Trace analysis, employing **inductively coupled plasma-mass spectrometry** (ICP-MS), is used to determine metal impurities because metals adversely increase the acidity of superficial silanols on silica-based sorbent [125].

Thermogravimetric analysis (TGA) allows evaluation of material characteristics related to either mass loss or gain due to loss of moisture, decomposition or oxidation of the material. The changes of chemical (*e.g.*, chemisorption) and physical (*e.g.*, vaporization, sublimation, adsorption/desorption) properties of materials are measured as the time function of either increasing or constant temperature [126, 127].

Nitrogen adsorption/desorption measurement determines material SSA and porosity, that comprises mean pore diameter or volume and pore size distribution. Shape of adsorption isotherm curve expressing adsorbed volume of nitrogen as a function of relative pressure is a primary characteristic. The values of related material properties are calculated subsequently. The nitrogen adsorption measurement is generally conducted at temperature of -196 °C. In literature, this technique is also referred as **BET** because it is based on theory suggested by Brunauer, Emmett and Teller [128].

Alternatively, porosity and specific surface area can be determined using **mercury intrusion porosimetry** [129]. Another sorbent characteristic, the sorbent bulk density, is calculated on the basis of **helium pycnometry** measurement. In principle, a sample volume of known weight is measured. Helium is recommended as a displacing fluid because its atomic dimensions enable entry into a pore of size down to 0.2 nm [123].

The exact distribution of particle sizes can be determined by **laser diffraction** method [130], by **Coulter-counter technique** [131], which is based on measurement of electric impedance of the aperture through which an electrolyte with suspended particles flows, or by measurement using microscopy, associated with the software suitable for statistic evaluation [132].

Several types of microscopy can be used to study surface morphology and dimensions of diverse objects. Classical **optical microscopy**, the eldest of the microscopic techniques, can be used for a rough assessment of macroscopic changes, such as damage or coloration, of contemporary micron-size stationary phases.

Scanning electron microscopy (SEM), the most used microscopic technique today, uses electrons of much shorter wavelength than is the wavelength range of visible light (VIS, 380–750 nm), which allows magnification of an object up to 500 000 times. The resolution higher than 0.5 nm thus can be achieved. SEM is particularly useful to reveal the shape and surface of stationary phase particles and possible presence of fine debris or other foreign materials before and after the sorbent modification [120, 133]. Alternative microscopic techniques providing information about the surface morphology of conductive materials are **atomic force microscopy** and **scanning electrochemical microscopy** [48, 134].

Transmission electron microscopy (TEM), the technique in which a beam of electrons is transmitted through an object to form an image, is used to investigate very small objects or an ultra-thin cross-section of materials. Because of the sample-thickness-limiting criterion, usually up to 100 nm, TEM technique is limited mostly to study of nanoparticles and peripheral parts of objects with changing thickness, such as thin-cut slices of porous layer in core-shell silica particle (dispersed in a transparent hardened resin) [135].

X-ray photoelectron spectroscopy (XPS), also known as **electron spectroscopy for chemical analysis** (ESCA), is a popular technique using X-ray radiation for surface analysis (up to the depth of 10 nm) requiring ultra-high vacuum conditions [136]. XPS provides information about elemental composition, oxidation state of elements and types of chemical bond from the electron binding energy. Hydrogen and helium are the only two elements that cannot be detected using XPS. The combination of SEM with XPS is used for surface elemental mapping of stationary phase particles. Elements can be highlighted or distinguished by coloration allowing thus the evaluation of sufficiently uniform distribution of surface-modifying ligand [137]. **Energy-dispersive X-ray spectroscopy** (EDS or EDX) is alternative technique to XPS providing the elemental analysis of a sample as a whole, not only its surface.

Another powerful X-ray-based technique called **X-ray diffraction** (XRD) gives information about the intrinsic space orientation and phase composition of measured objects including powder samples. According to XRD record, material is considered as amorphous or crystalline [127]. Additionally, crystalline domain abundance in a sample and their intrinsic structure are also possible to determine. Moreover, for crystalline sample, XRD specifies lattice parameters and crystal system, estimates nanoparticles

sizes, and measures the thickness of thin films. Advantageously, both mentioned X-ray techniques are non-destructive.

Raman spectroscopy and **infrared spectroscopy** are frequent techniques describing chemical bonds occurring in the studied material and their abundance. Infrared spectroscopy is usually accompanied with Fourier transformation (FTIR) [138]. Other spectroscopic analytical methods such as **UV-VIS-NIR** (NIR stands for near-infrared) **spectroscopy** and **fluorescence spectroscopy** are employed marginally [49].

Solid-state nuclear magnetic resonance (SS-NMR), more specifically called **cross-polarization magic-angle spinning nuclear magnetic resonance** (CP-MAS NMR), is other, relatively new, increasingly used technique for structural characterization of novel materials and composites [128].

Properties of electroactive materials are characterized by electrochemical methods either during the synthesis/modification or afterwards. **Cyclic voltammetry** (CV) is the most usual technique to describe redox behavior of a material [139, 140]. Besides, conductivity of a material can be measured in solution, suspension or in dry form, such as powder or oriented crystal [141].

Indeed, a number of techniques is applicable for thorough physicochemical characterization of a stationary phase, some of them provide complementary information whereas the others may be used to confirm results of another technique.

3.4 Column packing

In principle, column packing is a filtration of a sorbent suspension through the column outlet frit using elevated pressure (up to hundreds of MPa). The filtration is driven by high-pressure pump operating in either constant pressure or constant flow mode.

Several packing techniques are distinguished according to the way of column preparation. Dry packing uses a gas (usually nitrogen) as a sorbent transporting medium. Another similar procedure employs supercritical fluids (mostly carbon dioxide). The most frequently applied technique, slurry packing, uses a liquid solvent or a mixture of solvents. Further, electrokinetic packing procedure, where packing process is driven by electroosmotic flow together with gravity, can be used. Sol-gel packing procedure is common for monolithic columns [142]. Column packing by centripetal

forces using acceleration of particles with an in-house designed apparatus, capable of spinning several columns at once, is an instance of non-conventional approach [143]. Preparative columns employ besides slurry packing also radial compression or dynamic axial packing procedures [144].

Contemporary market offers columns of different geometries and various construction materials, such as untreated silica tubing (coated with polyimide to ensure flexibility of the column), polyether ether ketone (PEEK), PTFE, stainless steel, titanium, and glass or PEEK lined stainless steel tubes. Chemical inertness and perfect smoothness are basic requirements on the column inner wall. Otherwise, bumps in the column wall could brush or smash sorbent particles in contact with this wall during the subtle motion of the particles triggered by pressure change. As a consequence, rough surface if the inner wall would lead to the decline of column bed stability and separation efficiency. Nevertheless, in contrast to the latter statement, Agilent Technologies patented the technology of creating spiral patterns on the columns wall referred to as "structured walls" in 2016 to circumvent the issue with geometrical discontinuities occurring near the walls of all existing analytical and capillary columns [145]. In addition, there is an ongoing development of three-dimensional printed columns today [146].

Hardware for column slurry packing consists of the high-pressure pump connected to a packing (also called pushing) solvent reservoir, and slurry chamber filled with sorbent suspension, which is flushed by the packing solvent into an attached, empty column with a built-in outlet frit. Pores of such a frit have to be smaller than the diameter of stationary phase particles. Frit material, such as quartz wool, stainless steel, titanium, PEEK, PTFE, sintered silica particles, or organic monolith, has to be inert to the used solvents and solutes. Other parameters of the frit, such as thickness, position (inside/outside the column) and mounting, also affect the column efficiency [147-149].

Although the packing process itself is simple, there are operating parameters, such as packing pressure (including pressure ramp profile) [150], consolidation time [151], use of pre-column, flow distributor, or heating [152, 153], slurry stirring or column sonication during packing [154-156], packing orientation (downward [157, 158]/upward [159]/horizontal [160]), and connection of individual parts (diverse diameters, bends, seals shape), that have remarkable effect on the final performance of the column [161]. However, the systematical investigation of the parameters and their mutual effects has not been performed yet.

Concerning the most relevant variables, that are packing pressure and compaction time, most authors select the values at a guess or adopt those published by more experienced researchers in the field. For the case of the final packing pressure setup, there is general guideline that the value should be at least doubled to the expected operating pressure during separations [162]. Generally applies that for smaller diameter of the packed particles higher packing pressure is required [163]. Total packing time consisting of packing and compaction phases depends on the length of column. Even after complete filling of the column with the sorbent, the formed particle bed still compacts tighter, being rinsed with packing solvent (secondary consolidation process). Therefore, the column should be subjected to the maximal pressure at least for the period equal to the time during which twenty-fold inner volume of the column would flow through. Thus, packing time needed to achieve a stable bed depends on the column dimensions and flow rate [164]. Afterwards the column should be steadily depressurized to prevent abrupt expansion of the consolidated bed.

Optimal conditions for column packing are determined individually by the stationary phase. Besides chemistry of the sorbent, its physical properties, such as particle size (including size distribution), shape, and porosity, significantly affect the packed bed density and homogeneity [165]. The particles of the same type and nominal parameters provided by two different manufacturers may require different packing conditions because they could have been produced differently; in some cases even the batch-to-batch variability from a single producer makes a difference [166]. Today, the optimization of the packing process is mostly carried out by the "trial and error" approach. However, some attempts of the systematic optimization of slurry packing procedure have already appeared [150].

Some theoretical considerations in the column packing process to achieve excellent results are briefly mentioned below. The first problematic aspect is the particle uniformity. Presuming the perfect particle sphericity, the larger particle size distribution (despite a single nominal particulate size specified by manufacturer) can significantly affect the bed density and column performance in beneficial [167] or deleterious [168] ways. Addition of certain amount of larger particles (up to 10 %) than the nominal particle size to the packed slurry has been implemented by some manufacturers to make the packing process easier [156]. On the contrary, the presence of smaller particles than is the nominal particle size or "fines", *i.e.*, very small particles, in the particulate

material causes a serious problem as higher back pressure than expected from the nominal particle size is observed [169].

The behavior of particles in the slurry given by particle-particle and particle-solvent interactions is described below. Choice of appropriate and stable slurry solvent for the stationary phase is matter of high importance for successful packing procedure. The term "stable" denotes the fact that the suspension properties do not change significantly during the column packing process. Although all suspensions are thermodynamically unstable, most of suspensions used for column packing belong to the group of coarse suspensions with particle diameter (d_p) ≥ 1 μm which may be kinetically more resistant to settling compared with colloids (suspensions of d_p < 1 μm) [170]. Solvent features, such as density, dispersion rate, shear thickening/thinning, viscosity, and wettability, should be considered in practical choice of slurry and packing solvents.

Wettability, that is the ability of a solvent to wet a stationary phase surface, is logically one of basic requirements. An improper match leads to "creaming" when the stationary phase floats on the solvent surface (despite the higher density of the sorbent) as is shown in Figure 3.

Figure 3 C_{18} silica particles non-wettable in water (left flask) and wettable in methanol (right flask)

The wetting process originates from equilibrium of surface forces. According to thermodynamics, wettability depends on value of the spreading coefficient S defined as:

$$S = \gamma_S - (\gamma_L + \gamma_{LS}) \quad (1)$$

where γ_S and γ_L are surface energies of a solid and liquid phases, respectively, and γ_{LS} refers to the energy of liquid-solid interface [171, 172]. If the value of S is positive then wetting happens spontaneously. Surface energies of solids are usually higher than that

of liquids, therefore, solids are mainly wettable. However, organic materials such as polymeric phases have usually lower surface energies than inorganic sorbents what could explain why some of polymers are non-wettable in liquids of high surface energy. Generally applies that for sorbents of high surface energies (*e.g.*, unmodified silica) suit polar solvents of high surface energy (*e.g.*, MeOH or aqueous solutions), whereas for sorbents of low surface energies (e.g. C_{18}, C_8 or PGC) low surface energy solvents (hexane, acetone (AC), tetrahydrofuran, or mixtures such as acetonitrile (ACN)/chloroform) are preferred [162]. Wetting agents, such as cationic, neutral or anionic surfactants, generally diminish γ_L and γ_{LS} [173, 174]. Nevertheless, the difficulty related to getting rid of surfactants from the packed column should be considered.

According to Stokes' law on sedimentation velocity, both density and viscosity of the solvent(s) contribute to the slurry suspension stability [175]. The settling rate v is for the suspension of non-coagulated porous spherical particles of finite concentration (modified Stokes' equation) defined as:

$$v = \frac{(1-\varphi)^{-\kappa}\, d_p^2 \left[\varrho_p(1-\varepsilon_i) + \varrho_l(\varepsilon_f - 1)\right] g}{18\eta} \tag{2}$$

where $(1-\varphi)^{-\kappa}$ is the hindered settling function of particles in suspension of volume fraction φ, κ is the particle/solvent-dependent constant, d_p represents particle diameter, ϱ_p and ϱ_l correspond to the densities of packing material and the liquid, respectively, η is the dynamic viscosity of the liquid, g is the gravitational constant, ε_i stands for the particle porosity, and ε_f is the fraction of total particle volume [176]. From the equation is clear that higher solvent viscosity and lower particle density slow down the sedimentation process. Currently, solvent kinematic viscosity (η_{kin}), defined as the ratio of solvent dynamic viscosity to solvent density, is preferred as a metric for the choice of suitable solvent systems rather than dynamic viscosity. Binary solvent mixtures provide more flexibility in tuning the viscosity, density and surface energies of the slurry systems. Wahab et al. proposed a guide to choosing slurry solvents for capillary and conventional columns, however, this guide only overviews the most abundant sorbents and solvents used in slurry packing [150].

Thus far it is believed that a viscous dispersive suspension, where particle-solvent interaction prevails over particle-particle interaction, settles down in a "layer by

layer" fashion forming thus a random, uniform bed without channeling or voids. Such system presumably results in a tightly packed, high efficiency column. Oppositely, agglomerating particles can pack in clusters stacking to each other, leading thus to formation of voids and resulting in a loose bed (manifested by lower back pressure) causing higher peak asymmetry (A_s) and increase of the height equivalent of a theoretical plate (HETP) value [177, 178]. Paradoxically, capillaries packed with agglomerated suspension of C_{18} stationary phase (using sonication during packing) produced the best results [179, 180]. Concerning the optimal packing solvent, it should be incompressible at the packing pressure and of lower viscosity and density than slurry itself, furthermore, this solvent should agglomerate the used sorbent [150, 176].

Further, column dimensions, particularly inner diameter, have an effect on quality of the packed bed. We encounter two general wall effects that were described in literature [181]. The geometrical wall effect caused by the first (*circa* five) particle layers adjacent to the wall is characterized by higher than average external porosity. Packing bed of this circular region is ordered otherwise than in bulk packing region because the particles can only touch the wall, but not penetrate it [182]. The layer of particles in the closest wall proximity forms a highly ordered monolayer, followed by less ordered layers until transformed into a randomly, however, more ordered particle arrangement in the column center. As a result, the radial diffusion velocity fluctuates and leads to overall higher average flow velocity in the wall area [183].

The second wall effect is caused by radial tension which pushes particles against the column wall and friction between the packing bed and the column wall during the packing process. Usual bed tension balanced by compressibility and partial ductility of the bed in bulk packing region is hindered close to the wall. Hence, an intermediate bed region (approximately 5–50 d_p from the column wall towards the column center) is packed more densely than the center of the column [184].

Therefore, if the column diameter does not exceed approximately 100 d_p (typically for capillaries), the radial eddy dispersion is affected mostly by the geometrical wall effect. Intuitively, capillary columns provide higher permeability due to deteriorating wall effects, therefore, the column performance is lower. Under the same conditions of the packing procedure, HETP of capillaries is up to 2.5 times higher than that of their conventional counterparts (2.1–4.6 mm i.d.) even in the absence of extra-column contributions to the total dispersion.

Another variable to consider in column packing is the concentration of slurry. Besides its effect on the surface tension, slurry concentration affects the packing velocity through the slurry viscosity and bed homogeneity, and thus the column efficiency [185]. Low concentration of the slurry leads to increase of the local external porosity in the wall region from, whereas high concentration promotes formation of larger and more abundant voids [186]. At low slurry concentrations, particles arrive and settle down individually, thereby allowing particle rearrangement. Oppositely, at high slurry concentrations, particles arrive and pack as large clumps causing fluctuations in the shape of the column bed [187]. Too high concentration of slurry suspension, especially if it contains agglomerated particles, can cause even clogging of small diameter capillaries. This phenomenon is more likely for irregular shape particles of broad size distribution. For this reason, the recommended slurry concentration of capillary packing is lower (1–5 % weight to volume ratio – w/v) than that of conventional columns (7–10 % w/v).

Unfortunately, the current understanding of the slurry packing process is still incomplete because of complicated modeling of non-Newtonian suspension rheology and insufficiently explored behavior of the particle-solvent interface under extreme pressures. Therefore, there has been no universal guideline for all packing scenarios yet; just to quote the column packing pioneer and the expert in field J. W. Jorgenson: *"...column packing is an art rather than a science.*" [179]. Furthermore, column packing process and chromatography in capillary columns are perceived and handled separately for the narrow bore and conventional columns.

3.5 Capillary liquid chromatography

Miniaturization of instrumentation is one of contemporary trends in separation science, not only for reducing device cost and improving its portability. Like in other modern separation techniques, such as CE [188, 189], gas chromatography (GC) [190, 191], or supercritical fluid chromatography (SFC) [192, 193], capillaries have been applied as separation columns also in HPLC [194-197]. This miniaturized alternative has become popular especially in the field of primary research. Table 1 illustrates ranking of capillary columns among all HPLC column types according to currently accepted nomenclature of HPLC columns [198].

Table 1 Overview of HPLC column specification accompanied with column inner diameter and eluent flow rate

column type	column i.d. [mm]	eluent flow rate [mL/min]
process	> 50	> 150
preparative	20−50	10−150
semi-preparative	10−20	5−10
conventional/analytical	4.0−4.6	0.4−2.0
solvent saver	2.1−3.0	0.2−1.0
narrow-bore	1−2.1	0.1−0.5
micro-bore	0.5−1.0	0.05−0.1
capillary	0.1−0.5	0.001−0.02
nano	< 0.01	< 0.001

Diameter of most capillary liquid chromatography (cLC) columns varies from 100 to 500 μm with flow rate range of 1−20 μL/min; both of them are related to particle diameter (d_p) used. Origins of cLC date back to 1967 when Horvath et al. separated ribonucleotides in the stainless steel column of dimensions 1 mm × (up to) 2 m [199]. One decade later, cLC was used by Ishii et al., and by Scott and Kucera in separations of aromatic hydrocarbons and alkylbenzenes [200, 201], respectively.

Nowadays, cLC is frequently employed for testing and characterization of newly prepared or expensive stationary phases because this technique requires only small amount of sorbent to pack the column. Other advantages, compared with conventional HPLC, are low sample injection volume (usually hundreds of nL) and low consumption of mobile phase, allowing thus use of expensive mobile phases and additives (*e.g.*, deuterium water or cyclodextrins). Additionally, low heat capacity of cLC facilitates control of the column temperature. Next, low flow rates move cLC closer to the popular trend of "green chemistry" and allow its direct hyphenation with flame ionization detector and mass spectrometry using spray ionization [202]. Other beneficial feature is improved detection sensitivity because of less diluted injection band when operated at the same linear velocity as for wide bore columns.

The above mentioned advantages of cLC are the main drawbacks at the same time. Such low flow rates of the mobile phase and injection volumes are very demanding on the used instrumentation when taking into account extra-column

contributions of the system to the void volume and the necessity to ensure minimized pulsation while delivering mobile phase in gradient mode. Moreover, inhomogeneity of cLC column bed packings manifest itself more significantly compared with conventional HPLC columns, which is given by the ratio of capillary perimeter and diameter. Current market offers about seven hundred different commercial stationary phases but only some of them are available in capillary or nano columns. Therefore, preparation of own "low-cost" columns is still profitable, especially when a commercially unavailable "tailor-made" stationary phase is required. However, the preparation of the capillary column of excellent performance remains a very challenging task due to complexity of the procedure.

3.6 Chromatographic characterization of LC systems

The rapid development of HPLC in the last decades brought a wide choice of both commercial and tailor-made stationary phases of various properties. Selection of a suitable chromatographic column is a crucial step for successful solution of an intended separation of solutes. However, simple description of the column technical parameters cannot provide decisive information for such choice. Revelation of the relation between physicochemical features of the stationary phase and retention of the analyte represents a keystone of thorough understanding of the retention process. Employment of various testing procedures and their comparison provide the complex information about characteristics of the separation systems. Some of the tests were designed originally for RP liquid chromatography, however, they can be successfully applied also in other chromatographic modes after some modifications [23, 203, 204].

Empirical chromatographic tests are considered as powerful, easy-to-perform and time-sparing evaluation procedures, and thus are very popular with column producers. These tests were designed to describe the column under the fixed conditions. Individual tests evaluate various features of the sorbent, such as silanol activity (also expressed as donor/acceptor hydrogen-bond capacity or ion-exchange capacity), hydrophobicity (hydrophobic selectivity, methylene selectivity), steric resistance (shape selectivity), presence of metal impurities, and others [205]. The most frequent output of retention measurements for chosen group of solutes is expressed in form of certain chromatographic quantity, such as retention time (t_R), retention factor (k, also called

capacity factor), selectivity factor (α, also denoted as separation factor), peak asymmetry, or column efficiency (HETP) [206]. The obtained results serve to evaluate and compare the performance of various stationary phases, to verify the performance of the individual column at any moment of its lifetime, or to evaluate column-to-column or batch-to-batch reproducibility of the sorbent during the quality control process [207]. Among the most known tests belong Walters [208], Tanaka [209], Sander & Wise [210], Galushko [211], Engelhardt [212], or Neue [213], albeit plethora of tests was designed by other researchers [23]. Yet none of the tests has been accepted as universal for the evaluation of chromatographic columns, analysts have used them to facilitate choice of an appropriate column.

Statistical evaluation of the test can be also used to prove significance of the results. Three basic groups of statistical approaches are generally distinguished. First, simple plots enable to evaluate the differences between the columns as regards to one or two characteristics (two dimensional diagrams). Columns located in the plot close to each other show similar properties. For instance, Ibrahim et al. [214] proposed a simple graphical representation approach using the plot of ion-exchange (assessed by selectivity factor of benzyltrimethylammonium chloride/cytosine) versus hydrophilicity (assessed by selectivity factor of cytosine/uracil) for evaluation of HILIC phases. Radar chart (spider plot) is an example of advanced plane visualization of several dimensions without modification (except for normalization) used for a gross column classification [215].

Second, chemometric methods, such as principal component analysis (PCA) or hierarchical cluster analysis (HCA), can be used to compare the columns. In case of PCA, all the studied properties are collectively included in the comparison, processed by data projection to reduce the space in which the relevant information is located and assessed by orientation and angle of parameters and distance of points from the origin in the final PCA score plot [216]. HCA uses Euclidean distance calculation and comparison for a classifying drawing, mostly in the form of dendrogram [217]. Similarly to the simple plots, neighboring columns are expected to provide nearly identical chromatographic performances. Advantageously, PCA and HCA approaches can be combined.

The third way employs comparative equations to calculate a discrimination factor (discrimination criterion) from a reference column [218]. The lower this factor is,

the more similar are the column properties, as deduced from the Pythagorean theorem [219].

Like other chemical equilibrium processes, chromatographic separation is driven by rules of thermodynamics. Knowledge of separation thermodynamics thus contributes to the understanding of separation as a whole. In the basic equilibrium it applies:

$$\Delta G^{\circ} = -RT \ln K = \Delta H^{\circ} - T\Delta S^{\circ} \tag{3}$$

where ΔG° stands for the change of the standard free (or Gibbs) energy, R is the universal gas constant, T is the absolute temperature, K describes distribution constant, ΔH° stands for the change of standard enthalpy and ΔS° is the change of standard entropy. Simplified van't Hoff expression then relates the thermodynamic quantities with retention factor k of an analyte and phase ratio β as follows:

$$\ln k = -\frac{\Delta H^{\circ}}{RT} + \frac{\Delta S^{\circ}}{R} + \ln \beta. \tag{4}$$

The thermodynamic quantities are calculated employing van't Hoff plots that express $\ln k$ as a function of $1/T$ [220, 221]. Therefore, this thermodynamic approach provides information on the changes of ΔG°, $\Delta H^{\circ}$and ΔS° if the analyte transfers from mobile to stationary phase [24]. The output in the form of a non-linear curve indicates participation of more retention mechanisms. From the plot of $\ln k$ as a function of $1/T$ is also possible to observe a decrease of solute retention, peak coelution or shift of the elution order similarly as from the original chromatograms [222]. The drawback of this method is that it considers the system as a whole, and does not describe individual interactions participating in the retention process.

To circumvent the separation-related issues that require too much time, effort or cost, predictive models have been established on combination of the experimental data obtained during measurements for empirical tests and additional thermodynamics calculations. The model proposal is generally based on relation between solute k and separation conditions, such as column temperature, pH of the mobile phase, the volume fraction of the solvents of the mobile phase, slope of the gradient elution, and total gradient elution time. Such models can be applied to predict the retention behavior of the chosen solute for both isocratic and gradient elution [223, 224]. Additionally, *in-*

silico predictions and simulations, such as molecular dynamics or Monte Carlo method are gaining popularity [225, 226].

Furthermore, complex methods based on thermodynamics have been designed, providing outputs more perceptibly related to physicochemical characteristics of the separation processes. Hydrophobic subtraction (HS) model and linear solvation energy relationship (LSER) are the most frequent approaches. Both these models are categorized into so-called quantitative structure-retention relationship (QSRR) which generally relates retention of the solute to suitably chosen parameters characterizing this solute (*e.g.*, chemical structure, log *D* etc.) [227, 228]. The solute parameters, also called descriptors, express solute properties as numerical values, therefore, they can be treated by mathematics and statistics. Both LSER and HS have been steadily developed and optimized due to necessity of their generalization for more and more columns. The outputs of both models are based on the analysis of extensive sets of experimental data and provide the information about considered interactions participating in the chromatographic system.

HS model was introduced by Snyder et al. [229] as the RP-oriented alternative to the LSER. In the basic form of this model, selectivity factor of a given solute to ethylbenzene (nonpolar reference analyte) is the system-dependent variable. Analyte descriptors in HS model describe following characteristics of the solute: hydrophobicity, molecular "bulkiness"/resistance to insertion of the solute to the stationary phase, hydrogen-bond acidity and basicity, and approximate charge of the solute (the extended version of the model covers also π-π interactions and dipole-dipole interactions [230]). Some column parameters denote complementary properties to the solute descriptors, *e.g.*, column hydrogen-bond basicity versus solute hydrogen-bond acidity. The resulting multilinear equation comprises the sum of individual products (independent variables) of the solute descriptors and the column parameters. Because of internal standardization to ethylbenzene retention, the model parameters standing for properties of a stationary phase are independent on the composition of the mobile phase and the temperature. In contrast to LSER, the analyte descriptors of the HS model are acquired exclusively from chromatographic measurements on the same set of several columns; the procedure is rather complex (for details see ref. [231, 232]). In addition, a variant of the HS model applicable for HILIC was proposed in the recent years [233].

3.6.1 Linear solvation energy relationship

Understanding the retention-promoting interactions between analyte and stationary phase and the controlled manipulation of these interactions represent a keystone of chromatography as the separation method. Model of linear free energy relationship (LFER) is based on the measurement of a quantity related to the change of free energy of the chromatographic system during certain process, such as retention or dissolution [234]. The total ΔG° is the sum of the particular independent contributions related to dispersion, electrostatic, orientation and inductive interactions, and hydrogen bonding [235]. LSER is a specific subset of a broader class of thermodynamics relationships called LFERs. Use of the word "solvation" instead of "free" emphasizes that LSER stems from historical attempts to understand and predict the interaction abilities of different bulk solvents, more specifically the partition of the solute between two immiscible solvents [236]. The model evolved steadily over several decades. Vitha and Carr thoroughly overviewed the successive development of LSER, conversion of initial solvent parameters to solute parameters, their redefinitions and recalculations [237].

The advantage of LSER in comparison with simple chromatographic tests or the HS model is that LSER can characterize not only a stationary phase but a whole chromatographic system under changed temperature, pH or composition of the mobile phase [238-240]. Moreover, for the building of the LSER model, only one stationary phase is sufficient in contrast with the HS model requiring more similar phases [24]. Unlike the HS model, LSER is usually applied in different chromatographic modes (*e.g.*, RP and HILIC) [241], providing both qualitative and quantitative information about molecular interactions engaged in separation process.

Abraham et al. introduced the cavity-formation-based theory describing transfer of analyte from the mobile to the stationary phase (and *vice versa*) and derived the respective equation showing the relation of $\Delta G^{\circ}$of the characterized system, expressed explicitly as solute log k (albeit other ΔG°-related solute properties can be also employed) and solute parameters [242]:

$$\log k = eE + sS + aA + bB + vV + c \qquad (5)$$

where the uppercase letters E, S, A, B, V are the solute (also called Abraham) descriptors, the lowercase letters e, s, a, b, v are the system coefficients and term c is the model intercept.

The descriptor *E* describes the excessive molar refraction which defines the difference between the molar refraction of the analyte and the molar refraction of a hypothetic *n*-alkane of the same characteristic volume ($E = 0$) [243]. *E* reflects the ability of the solute to interact with the environment by the lone electron pairs interactions and π-π stacking. The descriptor *S* expresses the dipolarity/polarizability of the solute and describes dipole-dipole and dipole-induced dipole interactions. Similarly to *E*, term *S* has zero value for *n*-alkanes. The attempts to separate term dipolarity from term polarizability failed due to their interconnection. Term *A* expresses solute's overall hydrogen bond acidity (the proton donor), whereas term *B* expresses solute's overall hydrogen bond basicity (the proton acceptor). Descriptor *V* is McGowan's characteristic volume of the solute molecule and describes the cavity-forming effect (cohesive and dispersion forces) during transfer of solute from one phase to the other [244]. Usually, term *V* is identified as hydrophobicity in RP-LC systems.

The above mentioned descriptor meaning applies almost identically for GC. However, for transfer of analyte from the gaseous mobile phase to the liquid stationary phase the product *vV* is substituted with *lL*. Descriptor *L* describes the decadic logarithm of partition coefficient (log *P*) of the relevant gas to *n*-hexadecane at 25 °C [245]. The Abraham descriptors, obtained from experimental measurements (*E*), structure-based calculations (*V*) and subsequent recounts from Abraham equation, are mostly taken from the published literature, databases or from specialized predictive software (*e.g.*, ACD Labs/Percepta Predictor) [246, 247].

System coefficients *s*, *a*, and *b* characterizing the chromatographic system are complementary to the solute descriptors, *e.g.*, term *a* expresses the hydrogen bond basicity and term *b* the hydrogen bond acidity of the system (similarly to the HS model). Generally, the system coefficients express the dissimilar participation of the relevant molecular interaction in two environments – in the mobile phase and in the stationary phase. Term *c* stands for the LSER model intercept, it is characteristic for the given separation system and covers all the above unspecified interactions, such as mobile and stationary phase ratio, throughput capacity or steric selectivity of the stationary phase [248]. For determination of the values of the relevant coefficients, multiple linear regression (MLR) is employed [249]. A positive value of the coefficient indicates that a solute interacts stronger with the stationary phase, thereby the solute is more retained in the column. Conversely, the negative coefficient value expresses that the solute preferably interacts with components of the mobile phase, therefore, the

solute is weakly retained. The total retention of the solute is given by the sum of individual contributions.

The LSER model used five Abraham descriptors originally and was designed to describe only the interactions of neutral molecules in the RP systems [241, 250-252]. However, the urge to describe also HILIC systems by LSER increased in recent years [253-256]. Eq. (5) as such cannot completely and credibly describe all the interactions taking place in a HILIC system because the equation does not consider the contributions of ionic interactions, which are of substantial importance for HILIC-presumed retention mechanism [257-259]. Chirita et al. proposed a convenient inclusion of the interactions associated with the electric charges on both partially and totally ionized compounds [260]. They extended the original Abraham equation with two other descriptors:

$$\log k = eE + sS + aA + bB + vV + d^{-}D^{-} + d^{+}D^{+} + c \tag{6}$$

where D^{-} stands for the negative charge carried by anion or zwitterion and D^{+} corresponds to the positive charge carried by cation or zwitterion, according to Eqs. (7) and (8) which express the degree of dissociation and protonation of the solute, respectively:

$$D^{-} = \frac{10^{(pH^{*}-pK^{*})}}{1 + 10^{(pH^{*}-pK^{*})}} \tag{7}$$

$$D^{+} = \frac{10^{(pK^{*}-pH^{*})}}{1 + 10^{(pK^{*}-pH^{*})}} \tag{8}$$

where pK* is the dissociation constant of either the acid or the base in the hydro-organic mobile phase and pH* describes the effective ${}^{s}_{s}pH$ obtained after mixing aqueous buffer with the organic solvent and is, hence, different from aqueous ${}^{w}_{w}pH$ of the buffer before mixing with the organic solvent. Although the pH electrode should be in principle calibrated with organic buffers before correct measurement of the ${}^{s}_{s}pH$, in practice, ${}^{s}_{w}pH$ of the hydro-organic mobile phase is commonly estimated after calibrating the electrode in purely aqueous buffers, and the aqueous dissociation constant pK_a is often used in Eqs. (7) and (8) [260]. Coefficients d^{-} and d^{+} express anion-exchange and cation-exchange ability of the chromatographic system, respectively. Meaningfulness of the extended LSER model has been demonstrated by the increasing number of publications employing this approach [239, 261, 262].

Several criteria ensure the reliable LSER model. First, the testing set of solutes should be representative. Solutes of various chemistries, such as cations, anions, zwitterions, neutral hydrophobic or hydrophilic compounds, and even structurally similar solutes and isomers, should be involved. As the rule of thumb, sufficient statistical significance of the model requires at least four solutes per independent variable (minimum of 28 compounds for the proposed Eq. 6). The range of descriptor values should be as wide as possible. This requirement is usually confirmed by descriptive statistics, frequency plots and correlation matrix of the solutes. Mutual plotting of solute descriptors helps to reveal their possible over-correlation which should be precluded [260]. Simultaneously, the solute values should show random scattering because any clustering might have an adverse effect on the model building. Finally, as the mathematical solution of the chemical interactions model is based on strictly linear relationship between the dependent variable log k and independent variables (E, S, A, B, V, D^-, D^+), no mutual co-interactions are presumed. Otherwise, a multiple non-linear regression must be used. However, to propose multiple non-linear model would require a qualified guess of the equation (also called self-starting function), which is commonly unavailable due to enormous complexity of chemical interactions. Therefore, the output of the linear modelling, in the form of system coefficient values, is then subjected to statistical evaluation. Reliability of a proposed LSER model is then verified by the determination coefficient (R^2) and Fisher's statistics (F value) of the multilinear regression as well as by the standard error (SE) and confidence interval (CI, mostly for 0.95 confidence coefficient) of individual coefficients. The statistical p-value, expressing the probability of the error that the coefficient does not contribute to the model, can be employed too [263].

The LSER model has been adapted and applied also for chromatographic systems using ternary mobile phases [264, 265], chiral stationary phase [266, 267], and for gradient elution [268, 269]. Besides very wide application of the LSER concept in GC [270-272], it has been also employed in SFC and micellar electrokinetic chromatography [273-274].

3.7 Separation modes of liquid chromatography

Liquid chromatography offers several basic possibilities for separation of solutes of interest. Separation selectivity and efficiency depend on the choice of both the mobile phase composition and the stationary phase. Separation temperature, column dimensions and elution program are the next criteria to consider. This chapter briefly overviews the most common modes applied in column LC.

Normal phase (NP) chromatography is one of the eldest modes used in LC. In principle, the sorbent is polar, *e.g.*, bare silica, silica modified with diol, nitro, cyanopropyl and aminopropyl moieties, or polyethylene glycol chains, whereas the eluent is less polar, typically binary mixture of non-polar/low-polar organic solvents, such as hexane, xylene, chloroform, tetrachloromethane and AC [275]. Analytes of high polarity are retained stronger than low polarity ones; the retention characteristics are mostly related to the sorbent surface area. Selectivity and repeatability of NP separations are very sensitive to the amount of water adsorbed on the stationary phase because water acts as a highly polar active-site-blocking competitor to solutes.

The retention in **ion-exchange chromatography** (IEC) is based on electrostatic attraction between ionic solute and oppositely charged surface, more precisely superficial functional groups of the stationary phase, such as $-SO_3^-$, $-COO^-$, $-N(CH_3)_3^+$ and $-NH(C_2H_5)_2^+$. IEC is employed for separations of either cations or anions. The interaction strength is given by number of sorbent active sites and charged functionalities of the solute which are both controlled by pH of the eluent [276, 277].

Reversed phase (RP) chromatography, as the name suggests, has a reversed arrangement of the mobile and stationary phase compared with NP. The eluent is usually a mixture of water-miscible organic solvent(s), such as ACN, alcohols, tetrahydrofuran, with an aqueous component, such as water, diluted solution of acid/base or buffer. Stationary phase for RP separation is non-polar, it means that an original polar sorbent is modified with less polar, covalently attached organic ligand(s), polymer-based coating, or made of hybrid-polymer. Among the most known commercial RP stationary phases belong C_{18} and C_8, phenyl-alkyl, perfluoroalkyl, and pentafluoro-phenyl grafted silica, some stationary phases are identical for NP and RP, such as aminopropyl and cyanopropyl silica. Additionally, hundreds of tailor-made stationary phases of various chemistries have been prepared in primary research laboratories. In RP, solutes of decreasing polarity are increasingly retained on the

stationary phase, the elution order is theoretically exactly inverse to NP. However, the latter is not absolutely true due to the complexity of the retention processes on functionalized, non-rigid stationary phases [278, 279]. Access of solutes to active adsorption centers, such as silanols, capable of polar interactions is limited because of the surface modification of the RP stationary phase [280]. Originally, a partitioning mechanism similar to the water/*n*-octane partitioning was proposed for the RP retention process because the experimental data fitted to it far better than to older, adsorption-derived models. However, it was soon shown that separation process in RP mode combines both adsorption and partitioning phenomena. For some stationary phases prevails the former one and for different ones the latter [281]. Anyway, it is worth emphasizing that RP mode still dominates over other separation modes in modern LC.

Hydrophilic interaction liquid chromatography (HILIC) was developed in order to separate neutral solutes of high polarity which are hardly analyzed in previously mentioned modes. The term HILIC was coined by Alpert in 1990 to describe the separation system consisting of hydrophilic stationary phase and relatively hydrophobic mobile phase that contains certain amount of water [282]. Typical organic solvent used in HILIC is ACN, albeit MeOH is also common, in volume fraction range of 0.60 – 0.96. Aqueous component of the eluent has higher elution strength oppositely to RP and the elution order is similar to NP [257]. The favorable features of HILIC are higher peak symmetry for solutes of the basic nature, higher sensitivity of mass spectrometric detection, higher applicable flow rate due to lower back pressure related to high content of organic solvent in the eluent, and possible direct injection of a sample treated with solid phase extraction. Additionally, HILIC can conveniently replace less reproducible NP using non-polar mobile phases in which polar solutes are not soluble. Mechanism of HILIC retention has not been completely explained thus far, despite its thorough investigation. Generally accepted theory suggests the formation of a water-enriched layer on the surface of polar stationary phase. Analytes distribute themselves according to their hydrophilicity between the hydrophilic area near the sorbent surface and more hydrophobic bulk mobile phase in which organic solvent prevails. The retention depends directly on the solute polarity and inversely on the polarity of the eluent [283]. Furthermore, it has been shown that hydrogen bonding, electrostatic interactions, dipole-dipole interactions and dispersion interactions are also involved to certain extent in the separation mechanism [284]. Concerning adsorption or partitioning as the retention-governing mechanism, combination of both these mechanisms has been

proven to affect the overall retention, for some columns prevails the former and for others the latter [285]. Therefore, HILIC mode is considered as a multimodal retention process. Each stationary phase enabling formation of water-rich layer on its surface, such as neutral polar diol, amide, cyclodextrin, cyclofructan, polar charged bare silica, aminopropyl, and zwitterionic sulfobetaine, is suitable for HILIC [259].

Mixed-mode chromatography (MMC), also called multimodal chromatography, refers to chromatographic mode in which more than one interaction type between solute and stationary phase substantially affects the separation. MMC contrasts the conventional single modes where one type of interaction is dominant and others are considered as negligible. MMC can enable higher selectivity and/or loading capacity of some complex samples containing positively and negatively charged as well as neutral solutes [286, 287]. Single MMC column can replace two in series connected columns used for on-line two-dimensional analysis. MMC columns are classified as physical MMC and chemical MMC, the former are formed of two types of packing materials mixed/stepwise packed in the column, whereas the latter correspond to one packing material containing two or more functionalities. Therefore, mode combinations, such as HILIC/RP or IEC/RP are possible [288, 289]. The preferred retention interactions of MMC stationary phases and their extent depend on the choice of the mobile phase composition, thus one stationary phase can be shifted from RP mode to HILIC and back.

Other modes of LC designed and applied to separate samples containing more specific groups of analytes are briefly mentioned below.

A specific mode is used in chiral separations. In **polar ionic mode** (PIM) (alternatively called **polar organic mode** – POM) the eluent consists of a mixture of one or more common polar organic solvents (ACN or MeOH), organic acid (formic acid, acetic acid, trifluoroacetic acid) and/or base (diethylamine, triethylamine, ethylendiamine) and/or volatile organic salt (ammonium acetate, ammonium formate). This mode is asset for mass spectrometric detection because of facilitated ionization [290]. The typical stationary phases applied in chiral separations are based on attachment of polysaccharides, cyclodextrins, glycoproteins and crown-ethers as ligands to SiO_2 [291, 292].

Size-exclusion chromatography (SEC) refers to separation of biomolecules and polymers according to their size (sieving effect), related to the molar mass, in a column filled with a porous polymer gel, such as methacrylate, acrylamide, agarose, or dextran.

Theoretically, no chemical interaction of the analyzed sample and stationary phase participates in this mechanism [293].

Ion-pair chromatography (IPC) employs the formation of associates between ionic solutes and oppositely charged ions, whose molecules include relatively big non-polar part, for instance surfactants. Separation of ionic associates then takes place on the stationary phase designed for RP-LC. This mode advantageously affects selectivity of ionic analytes, whereas the retention of neutral compounds is almost unaffected [294].

Hydrophobic interaction chromatography (HIC) is applied for separation of proteins and uses (generally) aqueous buffered mobile phase with high content of organic or inorganic salts which reduce the solvation of sample solutes. The separation is based on the gradient elution with decreasing ionic strength of the eluent. Under low solvation, the hydrophobic regions of solute become exposed and adsorbed ("salting-out" effect) in the column. Decrease of salt content in the eluent then leads to solute elution according to increasing hydrophobicity [295].

Further important chromatographic modes include **micellar liquid chromatography** (MLC), **micellar electrokinetic chromatography** (MEKC) and **affinity chromatography** based on formation of pseudo-stationary phase in the mobile phase or very selective reaction(s) between solute and stationary phase, respectively.

In any case, the dominant position of NP, RP and HILIC among all separation modes used in modern LC is proven by the fact that these three modes cover 94 % of published works using LC separation between years 2001–2010 [291].

4. PUBLICATION I – Characterization of polyaniline-coated stationary phases by using the linear solvation energy relationship in the hydrophilic interaction liquid chromatography mode using capillary liquid chromatography

Taraba L., Křížek T., Hodek O., Kalíková K., Coufal P.

Journal of Separation Science 40 (2017) 677–687

Received: 12 July 2016 | Revised: 13 November 2016 | Accepted: 17 November 2016

DOI: 10.1002/jssc.201600785

RESEARCH ARTICLE

JOURNAL OF SEPARATION SCIENCE

Characterization of polyaniline-coated stationary phases by using the linear solvation energy relationship in the hydrophilic interaction liquid chromatography mode using capillary liquid chromatography

Lukáš Taraba[1] | Tomáš Křížek[1] | Ondřej Hodek[1] | Květa Kalíková[2] | Pavel Coufal[1]

[1]Department of Analytical Chemistry, Faculty of Science, Charles University, Prague, Czech Republic

[2]Department of Physical and Macromolecular Chemistry, Faculty of Science, Charles University, Prague, Czech Republic

Correspondence
RNDr. Tomáš Křížek, Department of Analytical Chemistry, Faculty of Science, Charles University, Hlavova 8, 128 43 Prague 2, Czech Republic.
Email: tomas.krizek@natur.cuni.cz

A polyaniline coating was used to modify the surface of bare silica gel and octadecyl silica stationary phases to characterize the properties of altered materials. It was assumed that the mixed-mode retention was established on the basis of the polyaniline chemical structure and its combination with the original sorbents. Polyaniline was deposited onto the original surfaces during the chemical polymerization of aniline hydrochloride. The prepared materials were slurry packed into capillary columns and systematic chromatographic characterization was performed using the linear solvation energy relationship, also employing descriptors that allow inclusion of ionic interactions in the proposed retention mechanism. The retention times of 80 solutes with various chemical structures were measured in the hydrophilic interaction liquid chromatography mode. The obtained results demonstrated the significant contribution of the polyaniline coating to the retention mechanism under the given conditions; the assumed mixed-mode retention was confirmed. The dominant retention interaction for both modified stationary phases was based on the protonation of nitrogen atoms in the polyaniline structure, leading to suitable retention and selectivity for the hydrophilic analytes, especially anionic and zwitterionic species. Thus, especially, the polyaniline-coated bare silica gel sorbent seems to be promising for potential applications related to the separation of polar compounds.

KEYWORDS

capillary liquid chromatography, hydrophilic interaction liquid chromatography, linear solvation energy relationship, polyaniline-coated silica gel, stationary phases

1 | INTRODUCTION

Modern analytical chemistry must provide methods for an increasingly extensive spectrum of miscellaneous analytes with various chemical structures. The design, preparation, and characterization of novel stationary phases, among other things for HPLC, are thus in the forefront of interest at the present time.

The development of suitable sorbents applicable as stationary phases has developed substantially over the past few decades. However, bare silica gel continues to be the best known and most extensively used untreated stationary phase. Regardless of the means of preparation, underivatized silica gel sorbents have, in general, good mechanical and high-temperature resistance and acceptable retention ability. On the other hand, their pH stability range is not broad enough to meet the current requirements of separation science (although type C silica gel is able to retain its properties at high pH values [1,2]). Grafting of the superficial hydroxyl groups of silica gel with a broad range of functional groups (i.e. from simple hydrophobic and functionalized short-chain residues to biomacromolecules, polymers and organometallic complexes) represents a turning point in the development of modern separation techniques.

The contemporary market offers an extensive variety of stationary phases; some of them have a simple and uniform scaffold, whereas others are suitable for the "mixed-mode" separation mechanism. Unfortunately, the latter are usually rather

Abbreviations: LSER, linear solvation energy relationship; MLR, multiple linear regression; N_2-BET, nitrogen adsorption measurement method using Brunauer–Emmett–Teller theory; PANI, polyaniline; PANI-SiO_2, polyaniline-coated Hypersil; PANI-C_{18}, polyaniline-coated Nucleosil C_{18}

Conflict of interest: The authors have declared no conflict of interest.

expensive because of their complicated production process. Therefore, the modification of a low-cost support material (e.g. silica gel or alumina beads; ideally with a solid spherical core) by coating with a polymer/copolymer with the required functional structure (e.g. polypyrrole, polyimidazole, polybenzimidazole, polythiophene, polyaniline (PANI)) seems to be a viable alternative to these phases. The new sorbent maintains the original mechanical stability from the inorganic substrate and acquires chemical resistance from the polymer [3]; the resulting selectivity and retention ability are given by a combination of these two individual materials.

PANI is a readily synthesized, highly stable, semiconducting polymer occurring in three different states depending on the degree of protonation and the oxidation state as fully protonated leucoemeraldine, partly protonated emeraldine (the generally accepted structure of which is shown in Fig. 1), or fully deprotonated pernigraniline. One of its interesting features is that, in addition to a bulk precipitate, it forms a thin film on the surface of the material (e.g. glass [4], another polymer [5,6], carbon nanotubes [7], silicon [8,9], noble metals [9–11], or even wood [12]) in direct contact with the polymerization mixture. Consequently, it has been thoroughly investigated as a surface modifier for multiple applications, such as flexible electrodes, conductive fibers, organic field transistors, electrochromic glasses, anticorrosive coatings, biosensors, gas separation membranes, or catalysts [6,13–17]. Some attempts have been made to employ PANI coatings as an inner-wall modifier in CE [18] and continuous flow analysis [19] and as a sorbent for SPME [20,21] and TLC [22,23]. Chriswanto and Wallace [24] carried out a preliminary investigation of the separation potential of PANI-coated silica beads with various sets of testing compounds comprising polyaromatic hydrocarbons, small organic molecules, and inorganic ions in the normal phase, RP, and ion-exchange modes, respectively. However, the material preparation method was tedious and inefficient. Stejskal et al. developed a simple coating method based on in situ polymerization of PANI on spherical silica gel dispersed in a reaction mixture containing aniline hydrochloride and ammonium persulfate [14]. Sowa et al. adopted the latter approach to synthesize the stationary phase and studied its potential application in nonsuppressed ion chromatography [25,26]. Although certain endeavors have been made to describe the major interactions participating in the retention mechanism, to the best of our knowledge thorough and systematic chromatographic characterization of this sorbent has not been performed.

The linear solvation energy relationship (LSER) is a chemometric approach based on multiple linear regression (MLR) [27]. It has been employed to provide an insight into the retention mechanism of the separation system (investigation is possible in GC, SFC and LC) [28,29]. This model (also called Abraham according to the denotation of the solute descriptors [30]) relates the retention of a given solute to its chemical structure and physicochemical properties; i.e., the retention is the sum of the contributions originating from several independent types of interactions. The most common LSER equation for LC consists of five types of retention interactions:

$$\log k = eE + sS + aA + bB + vV + c \tag{1}$$

where k is the solute retention factor, the capital letters E, S, A, B, V are the solute descriptors, the lower case letters e, s, a, b, v are the system coefficients and term c is the intercept. The solute descriptors describe certain structural characteristics of the solute (in the form of a numerical value); E denotes the excess molar refraction, S the dipolarity/polarizability, A the overall hydrogen bond acidity, B the overall hydrogen bond basicity, and V is McGowan's molecular volume. The system coefficients reflect the particular type of interaction; e corresponds to the lone electron pair interactions and π–π stacking, s the dipole–dipole interactions, a the hydrogen bond basicity, b the hydrogen bond acidity, v the dispersion interactions/hydrophobicity. Each of the terms in the equation is expressed as the product of the solute descriptor $(E - V)$ and the system coefficient $(e - v)$. The solute descriptors can be found in the literature or calculated and the system coefficients can thus be obtained after solving the MLR. Each coefficient describes the dissimilar ability of the stationary and mobile phase to interact with the solutes through the corresponding interaction mechanism. A positive value of the coefficient indicates that the relevant interaction is stronger with the stationary phase, thereby increasing the solute retention (conversely, a negative value expresses

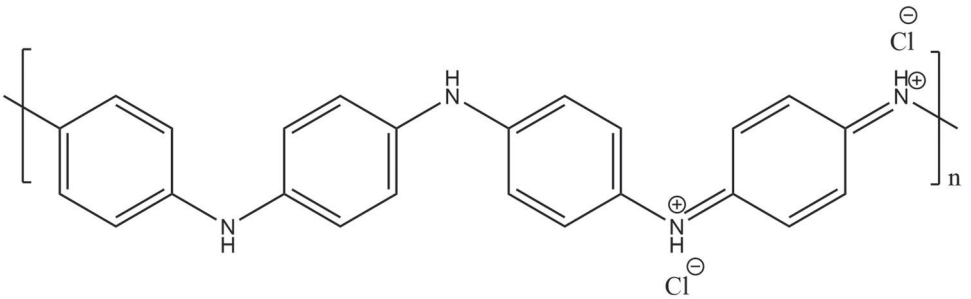

FIGURE 1 Chemical structure of partly protonated PANI—emeraldine salt

the decrease in retention due to preferred interaction between the solute and the mobile phase). Term c is characteristic for a given system. LSER using five Abraham descriptors was originally designed to describe only the interactions of neutral molecules. Although it is now generally used for characterization of RP systems, there is an increasing tendency to also employ the model to describe HILIC systems [31–36]. In fact, Eq. (1) as such cannot credibly describe all the interactions taking place in the HILIC mode, as it does not take into account the contributions of ionic interactions, although they form a substantial part of the HILIC retention process. To include the interactions associated with the electric charges present on partially and/or totally ionized compounds in the model, Chirita et al. [37] proposed extension of the original Abraham equation by including two other descriptors, leading to Eq. (2):

$$\log k = eE + sS + aA + bB + vV + d^{-}D^{-} + d^{+}D^{+} + c \quad (2)$$

where D^{-} corresponds to the negative charge carried by the anionic and zwitterionic species and D^{+} represents the positive charge carried by the cationic and zwitterionic species, according to Eqs. (3) and (4) expressing the degree of dissociation and protonation, respectively, of the solute.

$$D^{-} = \frac{10^{(\mathrm{pH}^{*}-\mathrm{pK}^{*})}}{1 + 10^{(\mathrm{pH}^{*}-\mathrm{pK}^{*})}} \quad (3)$$

$$D^{+} = \frac{10^{(\mathrm{pK}^{*}-\mathrm{pH}^{*})}}{1 + 10^{(\mathrm{pK}^{*}-\mathrm{pH}^{*})}} \quad (4)$$

where pK^{*} is the dissociation constant of either the acid or the base in the hydroorganic mobile phase and pH^{*} describes the effective ${}^{s}_{s}\mathrm{pH}$ obtained after mixing aqueous buffer with the organic solvent, and is hence different from the aqueous ${}^{w}_{w}\mathrm{pH}$ of the buffer before mixing with the organic solvent. Although organic buffers are required for calibration of the electrode before correct measurement of ${}^{s}_{s}\mathrm{pH}$, in practice it is common to estimate ${}^{s}_{w}\mathrm{pH}$ of the hydroorganic mobile phase after calibration of the electrode in aqueous buffers and to use the aqueous dissociation constant pK [37].

In this study, we concentrated on the primary characterization of the synthesized spherical PANI-coated bare silica gel and octadecyl-modified silica gel particles using optical microscopy, SEM, elemental analysis, and specific surface area determination using the Brunauer–Emmett–Teller (BET) theory. This was followed by packing of the capillary columns with the prepared sorbents and their characterization in HILIC using the LSER. With respect to the combination of the original support matrices and PANI coating, we assume formation of the stationary phases showing unique selectivity and unconventional mixed-mode retention mechanisms.

2 | MATERIALS AND METHODS

2.1 | Chemicals and reagents

Acetonitrile (HPLC gradient grade), benzyltrimethylammonium chloride, nicotinic acid, and analytes used for the LSER measurements (all of analytical grade purity) were purchased from Sigma–Aldrich (St. Louis, MO, USA). Supporting Information Table S1 lists the solutes with their corresponding molecular descriptors used in this publication. Formic acid, ammonium formate, ammonium acetate, and ammonium hydroxide were supplied by Lachner (Neratovice, Czech Rep.). The deionized water was purified with a Milli-Q water purification system from Millipore (Bedford, MA, USA).

2.2 | Eluent and sample preparation

Ammonium formate buffer (100 mmol/L) was prepared by dissolving the appropriate amount of ammonium formate in deionized water; the required ${}^{w}_{w}\mathrm{pH}$ value of 3.0 was adjusted by titration with formic acid. The mobile phase was obtained by mixing ACN and the buffer stock in the ratio ACN/buffer (90:10, v/v). The apparent ${}^{s}_{w}\mathrm{pH}$ of 5.4 was measured with a glass electrode calibrated with aqueous calibration buffers. Analyte solutions were prepared in a concentration range of 0.05–1.0 mg/mL either in pure ACN or in ACN/buffer (90:10, v/v), depending on their solubility.

2.3 | Instrumentation

Empty polyimide-coated fused-silica columns were supplied by Supelco (Bellefonte, PA, USA). Hypersil bare silica gel (spherical, average particle size 5 μm, average pore size 12 nm) and Nucleosil C_{18} (spherical, average particle size 5 μm, average pore size 10 nm, carbon load 15%) stationary phases were purchased from Shandon Southern (Cheshire, UK) and Macherey-Nagel (Düren, Germany), respectively. The Elmasonic S15H ultrasonic bath (P-Lab, Prague, Czech Republic) and LCP 4000 isocratic pump (Ecom, Prague, Czech Republic) were used for column packing. The slurry reservoir was made of an empty stainless-steel HPLC column with a volume of 1.7 mL.

Chromatographic measurements were performed using an Agilent 1200 HPLC System (Agilent Technologies, Waldbronn, Germany) ensuring a low flow rate (i.e. units of μL/min) and consisting of a degasser, binary pump, automated injector, column oven, and diode array detector. The ^{3D}HPLC ChemStation Software (Agilent Technologies) was used for acquisition and analysis of the experimental data. The injection volume was 0.1 μL for all the analytes and the flow rate was 5 μL/min. The capillary columns were thermostatted at 25°C. UV absorbance detection was performed at 230, 254, and 298 nm. The dead time (1.86 and 1.75 min

for PANI-coated Hypersil and PANI-coated Nucleosil C_{18}, respectively) was determined using a system peak.

Colored images of stationary phases confirming surface coating with PANI were obtained using an optical microscope (Jablocom, Jablonec nad Nisou, Czech Republic). The MIRA II scanning electron microscope (Tescan, Brno, Czech Republic), equipped with a tungsten filament as a cathode (applied voltage of 7 kV) and scintillating YAG detector, was employed to acquire the images displaying the sorbent surfaces and particle size uniformity. Before the analysis, the sample was deposited on a carbon tape and coated with platinum in a vacuum sputter.

Specific surface area determination based on Brunauer–Emmett–Teller nitrogen adsorption (N_2-BET) using the multipoint measurement approach was performed on a Nova 2000e instrument (Quantachrome Instruments, FL, USA). The sample was kept under vacuum for 2 h at 60°C for equilibration before analysis. The measurements were carried out at a bath temperature of −196°C; nitrogen was used as the adsorption gas. The elemental analysis was performed using a Thermo Finnigan Flash EA 1112 CHNS/O analyzer equipped with a thermal conductivity detector (Thermo Fisher Scientific, Waltham, MA, USA).

2.4 | Stationary phase preparation and characterization

2.4.1 | PANI coating procedure

Both original sorbents (i.e. Hypersil and Nucleosil C_{18}) were modified with PANI coating by in situ chemical polymerization of aniline hydrochloride. First, the stationary phases were suspended in pure methanol and dried in an oven at 60°C for 3 h. The dry Hypersil sorbent (1 g) was subsequently dispersed in 16 mL of 125 mM aniline hydrochloride and sonicated for 5 min. Because of its hydrophobicity, Nucleosil C_{18} (1 g) was dispersed in 8 mL of pure acetonitrile (to prevent phase collapse in aqueous solution) and mixed with 8 mL of 250 mM aniline hydrochloride. It was then treated in the same way as Hypersil.

Then the beaker with the mixture was immersed in a salt-ice cooling bath and gently stirred using a magnetic stirrer. Two milliliters of 0.5 M ammonium persulfate was added at once to initiate the oxidative polymerization of aniline. Since the reaction is exothermic [38], the temperature of the cooling bath was maintained at −5°C (±1°C) throughout the polymerization process to avoid undesirable formation of short-chain PANI oligomers at temperatures above 0°C [8]. The polymerization was left to proceed with continuous stirring at constant temperature for either 1 h for Hypersil or for 3 h when Nucleosil C_{18} was coated. After the relevant time, the reaction mixture was sealed with a sealing film and kept in a dark place overnight.

The next day the supernatant was poured off and the compact sediment of PANI-covered stationary phase was redispersed in 20 mL of 50% methanol v/v and further sonicated for 5 min. The supernatant liquid that could contain traces of bulk PANI precipitate was again separated after 15 min sedimentation of the coated particles.

The sorbent was collected on a 0.45 μm Nylon filter (Whatman, Maidstone, UK) and then repeatedly rinsed with small portions of 0.2 M hydrochloric acid, acetone, and methanol to ensure removal of all the short-chain oligomers [25]. The sorbent was then washed with the deionized water. Both prepared stationary phases were finally dried in an oven at 60°C and stored in glass vials.

2.4.2 | Slurry packing procedure

An empty column was prepared using capillary with inner diameter of 320 μm and outer diameter of 1.59 mm (1/16 inch). An outlet frit was prepared by inserting a piece of quartz wool filter into a polyether ether ketone union. Then the union was connected to the capillary. The packing procedure was based on the work of Franc et al. [39].

The prepared stationary phase was suspended in 50% methanol v/v acting as the slurry solvent to obtain a slurry concentration of 0.02 g/mL. Sonication of the slurry for 5 min was performed before its transfer into the reservoir. The column was packed at a pressure of 25 MPa using 65% acetonitrile v/v as a packing solvent. After the column was fully packed, the pressure was maintained for another 30 min and then the prepared column was slowly depressurized. Each prepared column was conditioned with the packing solvent before use for >12 h. Once the baseline was stable, the column was considered ready for use.

2.4.3 | Choice of HILIC mobile phase and solutes for the LSER

Investigation of the differences in the properties of PANI-modified stationary phases required operating conditions that would be suitable for both the studied stationary phases and was simultaneously able to emphasize their differences. Therefore, we employed the mobile phase composition proposed by Schuster and Lindner in a work dealing with the comparative characterization of various HILIC columns by LSER [40]. The retention time of each tested solute was measured three times in the HILIC mode under the following conditions: acetonitrile/100 mM ammonium formate aqueous solution of ${}^{w}_{w}$pH 3.0, (90:10, v/v) as the mobile phase at 25°C. The measured ${}^{s}_{w}$pH of the water-organic mobile phase had a value of 5.4 (for evaluation of the influence of aqueous ${}^{w}_{w}$pH versus apparent hydroorganic ${}^{s}_{w}$pH on D^- and D^+ values, see Supporting Information). We assumed that the elution strengths of the chosen mobile phases should yield sufficiently different retention factors but that the analysis times would remain reasonable for both our columns.

Our LSER testing set consisted of 80 solutes carefully chosen to cover a wide range of individual Abraham

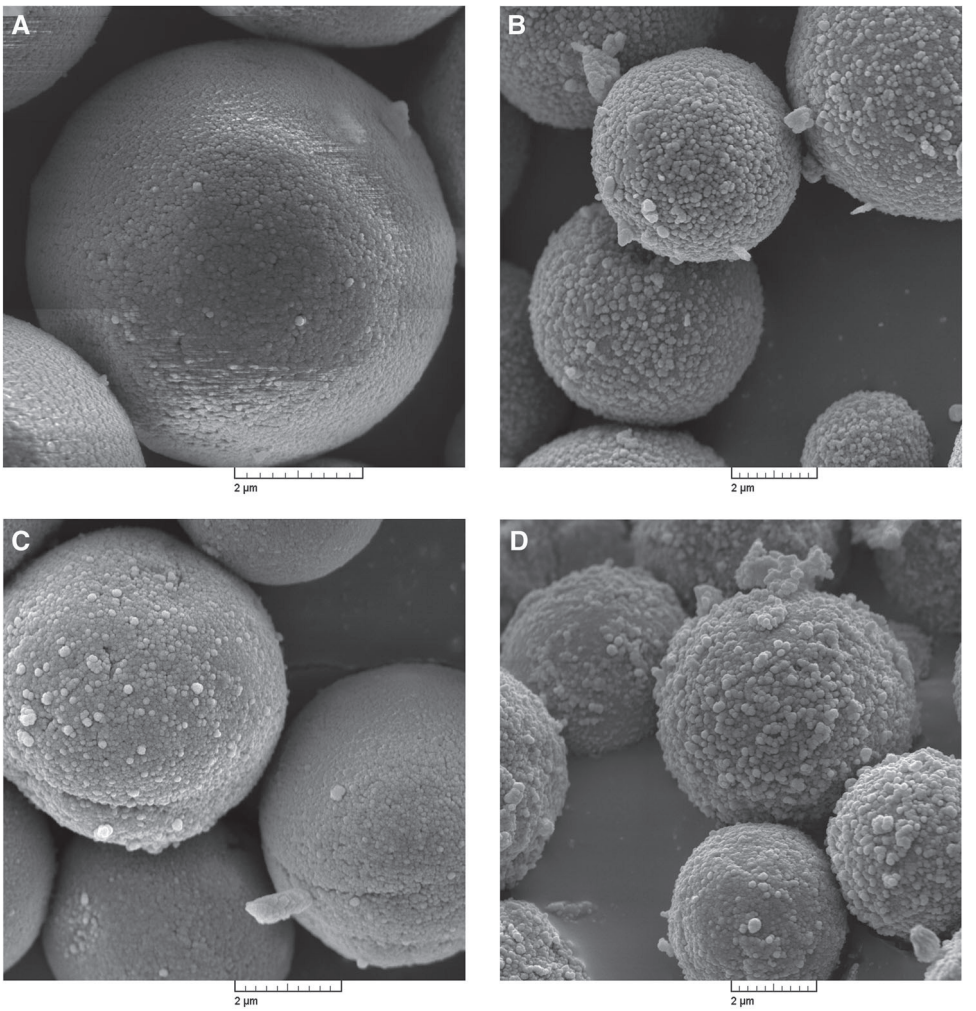

FIGURE 2 SEM images of Hypersil (A), PANI-Hypersil (B), Nucleosil C_{18} (C), and PANI-Nucleosil C_{18} (D), magnification 20 000 - 30 000×

descriptor values and not to prefer any individual interaction. This consisted of low-mass neutral, acidic, basic, and amphoteric molecules (shown in Supporting Information Table S1).

The affinity of the analytes for the stationary phase was expressed as the retention factor (k) for all the compounds. All Abraham descriptor values were taken from the published literature [36,37,40]; descriptors D^- and D^+ were calculated using the pK values of the relevant compounds that were either published or computed by Marvin software [41]. MLR analyses and evaluation of the models were performed using NCSS software [42].

3 | RESULTS AND DISCUSSION

3.1 | Polymerization of PANI on different stationary phases

The difference in polymerization time for the Hypersil and Nucleosil C_{18} sorbents was given by the different time (i.e. approximately six times longer for the latter) necessary to initiate the process indicated by blue coloration of the mixtures confirming the presence of aniline radical cations [43]. This is probably because, unlike Hypersil, the polymerization process was carried out in an acetonitrile/water mixture in the case of Nucleosil C_{18}. Nonetheless, at the end of the stated period both the polymerization mixtures were olive green. After thorough rinsing, the colorless supernatant affirmed the efficiency of the purification process and, furthermore, no bulk precipitate was observed.

The optical microscope images depict the stationary phases before and after the modification with PANI, demonstrating the success of the coating according to the observed color change (the relevant pictures are shown in Supporting Information Fig. S1). It seems that the coating was thinner for the octadecyl-bonded stationary phase although this cannot be decided conclusively from these images.

The elemental analysis showed that the PANI-coated Hypersil (PANI-SiO_2) and PANI-coated Nucleosil C_{18} (PANI-C_{18}) stationary phases have a carbon loading of 9.52 and 19.90%, hydrogen of 1.14 and 3.15%, and nitrogen of 1.53 and 1.19%, respectively (the original Nucleosil C_{18} has a carbon loading of 14.68% and hydrogen of 2.81%). Complete absence of sulfur in both the phases testifies for the high

quality purification process. From the elemental analysis results it is clear that both original support matrices are coated with a PANI layer. For PANI-C_{18} the lower amount of nitrogen could indicate lower thickness of the PANI coating, which is in an agreement with the optical microscopy observation.

Images obtained using SEM display the change in the surface morphology of the original sorbents after coating with PANI; in both cases, a surface roughening with minute PANI grains covering the original smooth spherical particles was observed (Fig. 2).

The specific surface analysis results probably correspond to a decrease in the specific surface area as the pores are filled with the polymer. In case of the PANI-SiO_2, the specific surface area decreased from 142 to 119 m^2/g (16.2%) whereas, for PANI-C_{18}, the area decreased slightly from 201 to 186 m^2/g (7.5%). The larger difference in the specific surface area supports the hypothesis of the better overall coating efficiency for the PANI-SiO_2.

The chemical stability of the newly prepared stationary phases was also examined. Recently, Wang et al. proposed a simple test based on measuring the changes in retention times of a positively charged (benzyltrimethylammonium chloride), a negatively charged (nicotinic acid) and a neutral analyte (adenine) under the same HILIC conditions (i.e. ACN/25 mM ammonium acetate, $^{w}_{w}$pH 6.8, (75:25, v/v); UV detection at 254 nm; flow rate 15 μL/min with respect to capillary LC; test analytes 0.05–0.5 mM in 80% ACN) for several hours to assess the hydrolytic stability of the ligand attachment [44]. Utilizing this approach, we observed a shift in retention times for the charged analytes at first, however, this trend subsequently diminished and the retention times stabilized for both PANI-SiO_2 and PANI-C_{18}. The duration of the testing period was 32 h. The overall change of the retention time for an individual analyte was expressed as percent change of the initial retention time. The retention time changed by –0.4 and +3.1% in the case of benzyltrimethylammonium chloride, by –1.1 and –0.6% for adenine, and by –12.1 and –6.1% for nicotinic acid on PANI-SiO_2 and PANI-C_{18} column. Thus, we consider the stability of these home-made columns to be comparable with the commercial ones [44]. It is important to note that no presaturating column was attached to prevent depreciation of the analytical column [45].

The separation efficiency of the prepared capillary columns packed with PANI-SiO_2 and PANI-C_{18} was evaluated using aniline, phenol, pyridine, toluene, and uracil, as commonly accepted probes, under LSER measurement conditions (detection wavelength 254 nm) and expressed as the height equivalent to the theoretical plate. The obtained values are shown in Table 1. The height equivalent to the theoretical plate values are higher than those obtained with commercially available capillary columns; however, the primary intention of this study was to assess chromatographic selectivity of the PANI-SiO_2 and PANI-C_{18} stationary phases and to investigate the potential mixed-mode retention mechanism. Further optimization and improvement of separation efficiency is the aim of our following research.

TABLE 1 Column efficiency of the PANI-SiO_2 and PANI-C_{18} packed capillary columns

Analyte	HETP (PANI-SiO_2) 10^{-4} m	HETP (PANI-C_{18}) 10^{-4} m
Aniline	4.7	9.6
Phenol	6.8	9.4
Pyridine	3.5	7.3
Toluene	4.8	6.7
Uracil	2.9	9.6

Chromatographic conditions: mobile phase consisted of acetonitrile/100 mM ammonium formate aqueous solution of $^{w}_{w}pH$ 3.0, (90:10, v/v), temperature 25°C, flow rate 5 μL/min, injection volume 0.1 μL.
HETP, height equivalent to the theoretical plate.

3.2 | Evaluation of the LSER model

The statistical significance of the proposed LSER model should be ensured by a sufficiently large set of testing solutes comprising 80 compounds to satisfy the rule of thumb that requires at least four solutes per independent variable (i.e., a minimum of 28 compounds in our case). However, the number of solutes is not the only requirement; a suitably established model should include diverse chemical structures (such as organic acids, bases, zwitterions, and neutral compounds with a broad range of polarities) so that no added solute would appreciably modify the result. Moreover, we introduced some positional isomers to investigate even a tiny influence on their retention. The diversity of solute descriptors used is demonstrated by descriptive statistics (Supporting Information Table S2) and frequency plots (Supporting Information Fig. S2). This could imply that there are some cross-correlations based on the values of the descriptor correlation matrix for the solute set (Supporting Information Table S3). However, no undesirable cross correlation was observed, as each descriptor was plotted two by two against another one, showing all the data points to be randomly scattered without any particular compound acting as a lever.

In recent years, the LSER model has frequently been used for the characterization of LC chromatographic systems, allowing comparison and ranking of a new characterized stationary phase. In the following text, we discuss our retention models for the PANI-modified stationary phases and point out the dominant retention interactions. The obtained system coefficients for both columns along with the statistics are displayed in Table 2. The experimental log k values for the set of 80 solutes for PANI-Hypersil and 75 solutes (five outliers excluded) for PANI-Nucleosil C_{18} show linear correlation with the calculated log k values with correlation coefficients of R 0.93 and 0.87, respectively. Since the least square regression estimation may be adversely influenced by

TABLE 2 System coefficients (statistically significant values in bold) and statistics for both modified stationary phases

Stationary phase	Model	*e*	*s*	*a*	*b*	*v*	d^-	d^+	*c*	*R*	*n*	*F*
PANI-Hypersil	CM	**0.56**	−0.19	**0.48**	**0.48**	**−0.84**	**0.82**	**0.39**	−0.52	0.93	80	66
	p-Value	0.00	0.13	0.00	0.00	0.00	0.00	0.00	0.00			
	SE	0.12	0.12	0.10	0.09	0.19	0.11	0.10	0.15			
	±CI	0.23	0.25	0.20	0.19	0.39	0.21	0.20	0.29			
PANI-Nucleosil C_{18}	CM	**0.21**	**−0.18**	0.01	0.00	0.00	**0.68**	−0.06	−0.45	0.87	75	29
	p-Value	0.00	0.03	0.92	0.94	0.97	0.00	0.34	0.00			
	SE	0.07	0.08	0.06	0.06	0.12	0.07	0.06	0.09			
	±CI	0.14	0.15	0.12	0.11	0.24	0.14	0.12	0.18			

CI represents the ± 95% confidence interval; SE is the standard error of the coefficients; the statistical *p*-value expresses the probability of the error that the individual coefficient does not contribute to the model; *F* corresponds to Fisher's statistics; *n* is the number of analytes considered in the regression. Chromatographic conditions: mobile phase consisted of acetonitrile/100 mM ammonium formate aqueous solution of ${}^{w}_{w}pH$ 3.0, (90:10, v/v), temperature 25°C, flow rate 5 μL/min.

outliers and hence yield misleading results, possible outliers should be found, for instance, by inspection of the plot of predicted against experimental log *k* values and removed from the input dataset—here in the case of the PANI-Nucleosil C_{18} column. The lower value of *R* for the latter stationary phase could be explained by inappropriate combination of the hydrophobic original sorbent (although modified with PANI) and the mobile phase suitable rather for HILIC separation. The octadecyl groups of the Nucleosil C_{18} support could disrupt the formation of stagnant water, which is dependent not only on the composition of the mobile phase but also on the stationary phase chemistry.

The intercept c relating to the phase ratio and interactions which are not covered by the system coefficients, is negative for both columns. Unfortunately, a simple discussion is impossible because of the variety of the phenomena contributing to the intercept. The remarkable ability of the stationary phase to interact with the *n* and π electrons of the solutes expressed by the high value of *e* is given by the chemical structure of the PANI coating. The somewhat lower value of this coefficient for PANI-C_{18} could be influenced by the presumably different amount of PANI coating on the surface of the original sorbent. The interaction between polar and/or polarizable solutes and the phase is indicated by the *s* coefficient that had almost the same negative value in both cases which was, moreover, evaluated as statistically insignificant for PANI-SiO_2. The polarizability of acetonitrile is higher compared to water and thus it makes the dipole–dipole interaction between analytes and the mobile phase slightly stronger than that with these stationary phases. The regression coefficients *a* (overall hydrogen bond basicity) and *b* (overall hydrogen bond acidity) differ significantly between the tested stationary phases. For the PANI-SiO_2 sorbent, they form substantial elements of the model, whereas for PANI-C_{18} they are not statistically significant. This difference for *b* is probably caused by the fact that the number of silanol groups able to interact with the solute is substantially higher on bare silica gel (Hypersil) compared to residual silanols after the silanization of Nucleosil C_{18}. Unfortunately, the cause for *a* is not so readily identifiable. The regression coefficient *v*, comprising the dispersion forces taking part in the separation system (mostly considered as hydrophobicity in the RP mode) and reflecting the different ease of cavity formation between the two solvents [46], was highly negative for PANI-SiO_2 sorbent, whereas for PANI-C_{18} this type of interaction does not contribute at all to the retention of the analytes. This result is meaningful since it qualifies PANI-SiO_2 as a true normal phase/HILIC sorbent. Conversely, the presence of nonpolar octadecyl chains (although coated with PANI) on PANI-C_{18} may impair the formation of a water-rich layer on the sorbent surface. The decrease in the absolute value of *v* for PANI-C_{18} clearly illustrates the higher overall similarity of the stationary and mobile phases for this parameter. Furthermore, it is obvious that, in the case of PANI-SiO_2, more energy is needed for a solute to form a cavity within a highly cohesive solvent (i.e. stagnant water-rich layer) than to transfer into a less organized liquid (here the bulk acetonitrile-containing mobile phase). Thus the analyte with a high *V* value more probably stays in the organic layer and hence is retained less. Regression coefficient d^-, denoting that the stationary phase behaves as a cation, represents the dominant interaction type for both investigated columns. This result stems again from the structure of PANI possessing protonated imino moieties under acidic conditions. The considerable value of d^+in the case of PANI-SiO_2 could be most likely related to the dissociation of the silanol groups of bare silica gel. On the other hand, the slightly negative value of d^+ was evaluated as statistically insignificant for the PANI-C_{18} sorbent.

Figure 3 depicts the plots of the experimental versus predicted log *k* values for PANI-SiO_2 and PANI-C_{18}. It can be observed that neutral compounds and bases have a wider range of retention time values on the PANI-SiO_2 column, whereas for PANI-C_{18} they formed a cluster of slightly higher than average retention values. This fact is in accordance with the values of the system coefficients *v*, *b*, d^+ discussed above. Acids and zwitterions also spread out more on

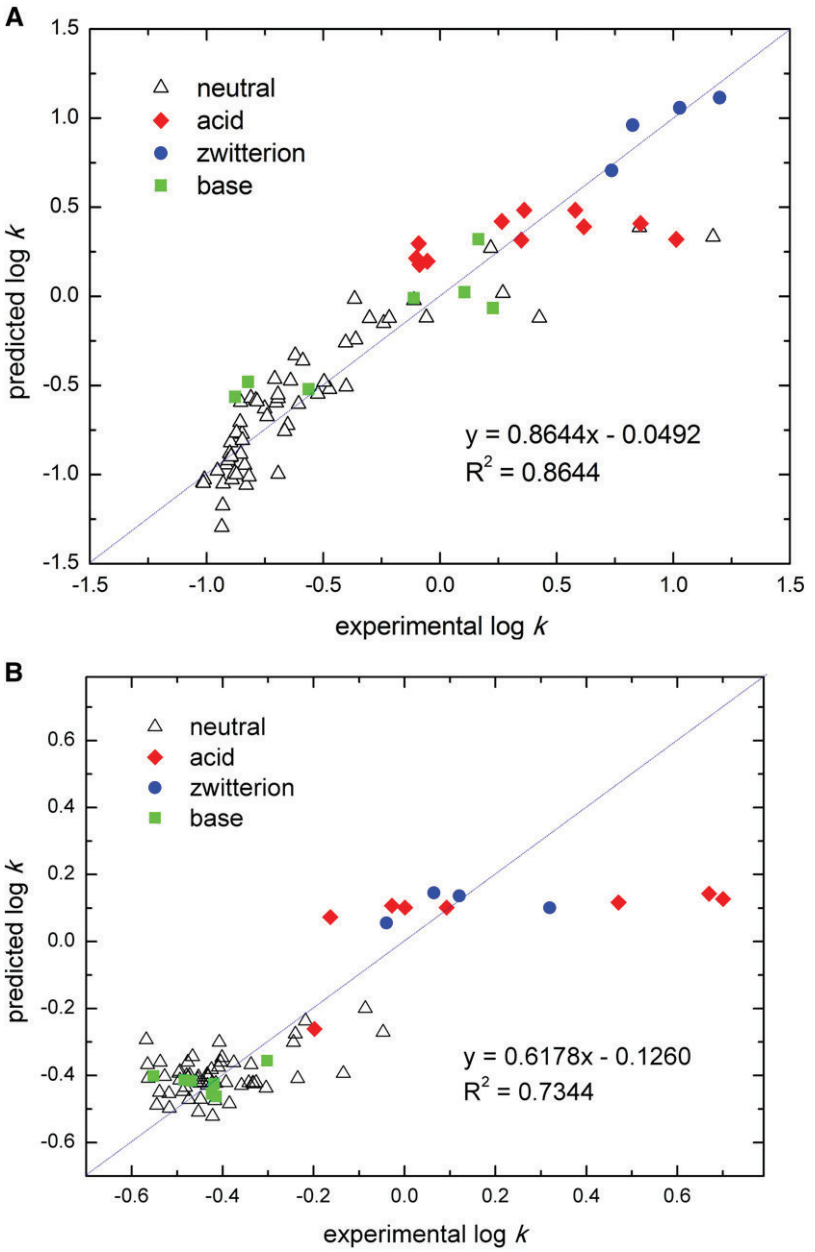

FIGURE 3 Plot of predicted versus experimental log k of PANI-Hypersil (A) and PANI-Nucleosil C_{18} (B) stationary phases; the dotted line denotes equal log k values

PANI-SiO_2, probably because of the greater influence of d^- and positive involvement of a in the retention mechanism. The dotted line denotes the ideal case in which the experimental and predicted log k values are equal. It seems that the experimentally obtained retention times of the more retained analytes are slightly higher than those predicted by the calculated model. The lower value of the determination coefficient R^2 obtained for the PANI-C_{18} phase may stem from the fact that most of the neutral species cluster in a rather small area of the graph. Overall, the column packed with PANI-SiO_2 shows better agreement between the experimental and predicted log k values according to the R^2 value (0.86 against 0.73 for PANI-C_{18}) and more importantly a greater selectivity.

For a further simple comparison, we plotted the experimentally obtained retention factors on PANI-SiO_2 and PANI-C_{18} columns (Fig. 4). It can be clearly seen that, with some exceptions among bases, ionizable compounds were retained more on PANI-SiO_2; the strength of retention is expressed by the position of the analyte relative to the dotted line, which defines equal log k values. A possible explanation for some bases being more retained on the PANI-C_{18} stationary phase is that they are relatively nonpolar under the given conditions (i.e. have a positive value of the distribution coefficient log D) in contrast to the rest of the bases (data not shown) and can thus be attracted by the latter sorbent rather than by PANI-SiO_2. On the contrary, neutral compounds, which are more retained on

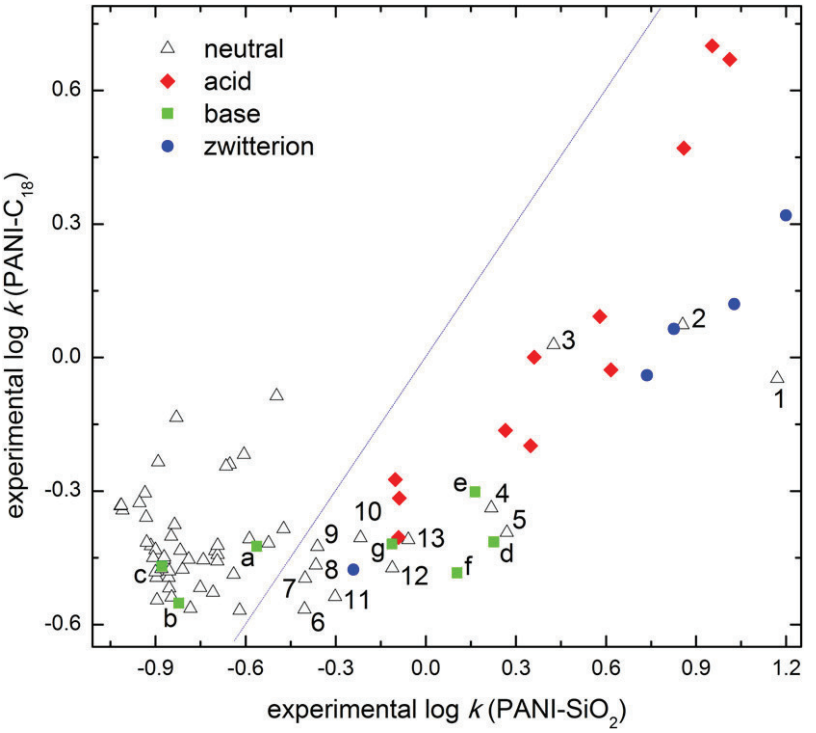

FIGURE 4 Comparison of solute retention on the different stationary phases; the dotted line denotes equal log *k* values; numbers refer to neutral analytes and letters to bases: 1, phloroglucinol; 2, guanine; 3, urea; 4, cytosine; 5, uridine; 6, thymine; 7, caffeine; 8, hydroquinone; 9, pyrocatechol; 10, theophylline; 11, theobromine; 12, 2-deoxyuridine; 13, resorcinol; a, pyridine; b, aniline; c, 1,4-toluidine; d, 4-aminopyridine; e, adenine; f, tyramine; g, 2-aminopyridine

PANI-SiO_2, have a slightly too highly hydrophilic nature. The application potential of PANI-SiO_2 is demonstrated by an isocratic separation of three structurally similar carboxylic acids (see Supporting Information).

Additionally the selectivity of PANI-SiO_2 and PANI-C_{18} stationary phases was compared at a rough estimate with other stationary phases commonly used in HILIC mode by means of a simple graphical representation [44,47]. This approach utilizes the plot of ion exchange, assessed by selectivity factor of benzyltrimethylammonium chloride/cytosine, versus hydrophilicity character, assessed by selectivity factor of cytosine/uracil, for evaluation of HILIC phases (experimental conditions: ACN/25 mM ammonium acetate, $^{w}_{w}$pH 6.8, (80:20, v/v); UV detection at 254 nm; flow rate 15 μL/min with respect to capillary LC; test analytes 0.05–0.5 mM in 80% ACN). With respect to the intellectual property of the above-mentioned articles, below we provide only the values of the selectivity factors denoting the position of PANI-SiO_2 and PANI-C_{18} stationary phases in the plot (Fig. 3 in [44] and Fig. 1 in [47]). According to the found selectivity factor values: $\alpha_{\text{benzyltrimethylammonium chloride/cytosine}} = 2.09$ (PANI-SiO_2) and 1.52 (PANI-C_{18}), and $\alpha_{\text{cytosine/uracil}} = 1.12$ (PANI-SiO_2) and 0.97 (PANI-C_{18}), both these phases display unique selectivity, mutually different (PANI-C_{18} is more hydrophobic). Both the phases are only very weak anion exchangers (PANI-SiO_2 is slightly stronger), halfway between hydrophobic octadecyl-based and amide-embedded stationary phases. The closest commercially available stationary phase to these homemade phases is distinctly more catex-like behaving ZORBAX SB-Aq.

4 | CONCLUDING REMARKS

Two stationary phases with different surface chemistry, bare silica gel (Hypersil) and octadecyl silica (Nucleosil C_{18}), were successfully coated with PANI deposited during the chemical polymerization of aniline hydrochloride. These materials were subsequently characterized by using optical microscopy and SEM, elemental analysis, as well as using specific surface area determination based on the multipoint N_2-BET method. In both cases, the specific surface area decreased slightly, as the pores were filled with PANI coating. The retention mechanism of the sorbents was systematically investigated chromatographically by the LSER approach after slurry packing of the sorbents into capillary columns. The original Abraham model enhanced with the variables corresponding to ionic interactions was employed for evaluation of the modified stationary phases. All the retention measurements were performed in the HILIC mode.

The general assignment of all the system coefficients corresponds to the structure of PANI-coated sorbents. The significant and opposite values of coefficients *b* and *v* for PANI-SiO_2 suggest that partition of the analytes occurs between the largely organic mobile phase and the water-rich

pseudostationary phase. Other system coefficients indicate a mixed-mode retention mechanism for this stationary phase in HILIC. Especially the large and positive value of d^- clearly indicates considerable retention of hydrophilic, especially anionic and zwitterionic solutes. Consequently, the phase could provide sufficient retention and appropriate selectivity in applications requiring separation of polar and ionic compounds.

Coefficient d^- was also the most significant for the PANI-C_{18} sorbent, where the other relevant coefficients are e and s. The rest of coefficients were not of particular significance, although the virtual elimination of v indicated substantial similarity in polarity between the mobile and stationary phases. In addition, this PANI-modified stationary phase exhibits relatively low retention ability and poorer selectivity in the HILIC mode. This sorbent appears to be of greater interest in the RP mode, which will be the subject matter of an upcoming research project.

To conclude, it is evident that the original sorbent substantially affects the chromatographic features of PANI-coated stationary phases. The chromatographic test comparing the selectivity of different stationary phases clearly testified unique selectivity for both PANI-SiO_2 and PANI-C_{18} stationary phases.

ACKNOWLEDGMENTS

We gratefully acknowledge financial support of the Grant Agency of Charles University, project no. 227233, and projects SVV and CZ0116. The authors would like to thank the Zentiva Group (Prague, Czech Republic) pharmaceutical company for cooperation in the measurement of the specific surface area of the sorbents and for recording SEM images, specifically Lukáš Krejčík and Radka Mikešová.

REFERENCES

1. Pesek, J. J., Matyska, M. T., Hydride-based silica stationary phases for HPLC: Fundamental properties and applications. *J. Sep. Sci.* 2005, *28*, 1845–1854.
2. Pesek, J. J., Bosch, E., Matyska, M. T., Larrabee, S., HPLC retention behavior on hydride-based stationary phases. *J. Sep. Sci.* 2007, *30*, 637–647.
3. Kirkland, J. J, Vanstraten, M. A., Claessens, H. A., High pH mobile-phase effects on silica-based reversed-phase high-performance liquid-chromatographic columns. *J. Chromatogr. A* 1995, *691*, 3–19.
4. Ayad, M. M., Shenashin, M. A., Film thickness studies for the chemically synthesized conducting polyaniline. *Eur. Polym. J.* 2003, *39*, 1319–1324.
5. Job, A. E., Alves, N., Zanin, M., Ueki, M. M., Increasing the dielectric breakdown strength of poly(ethylene terephthalate) films using a coated polyaniline layer. *J. Phys. D Appl. Phys.* 2003, *36*, 1414–1417.
6. Orlov, A. V., Kiseleva, S. G., Karpacheva, G. P., Teplyakov, V. V., Syrtsova, D. A., Starannikova, L. E., Lebedeva, T. L., Structure and gas separation properties of composite films based on polyaniline. *J. Appl. Polym. Sci.* 2003, *89*, 1379–1384.
7. Salvatierra, R. V., Zitzer, G., Savu, S. A., Alves, A. P., Zarbin, A. J. G., Chasse, T., Casu, M. B, Rocco, M. L. M., Carbon nanotube/polyaniline nanocomposites: Electronic structure, doping level and morphology investigations. *Synth. Met.* 2015, *203*, 16–21.
8. Riede, A., Helmstedt, M., Sapurina, I., Stejskal, J., In situ polymerized polyaniline films 4. Film formation in dispersion polymerization of aniline. *J. Colloid Interface Sci.* 2002, *248*, 413–418.
9. Rozlivkova, Z., Trchova, M., Sedenkova, I., Spirkova, M., Stejskal, J., Structure and stability of thin polyaniline films deposited in situ on silicon and gold during precipitation and dispersion polymerization of aniline hydrochloride. *Thin Solid Films* 2011, *519*, 5933–5941.
10. Ivanov, S., Mokreva, R., Tsakova, V., Terlemezyan, L., Electrochemical and surface structural characterization of chemically and electrochemically synthesized polyaniline coatings. *Thin Solid Films.* 2003, *441*, 44–49.
11. Chen, Y. J., Kang, E. T., Neoh, K. G, Electroless polymerization of aniline on platinum and palladium surfaces. *Appl. Surf. Sci.* 2002, *185*, 267–276.
12. Sapurina, I., Kazantseva, N. E, Ryvkina, N. G, Prokes, J., Saha, P., Stejskal, J., In-situ polymerized polyaniline films 3. Film formation. *J. Appl. Polym. Sci.* 2005, *95*, 807–814.
13. Travain, S. A., Bianchi, R. F., Colella, E. M. L., de Andrade, A. M., Giacometti, J. A., Flexible polyaniline devices for strain gauge and pH monitoring applications. *Polimeros* 2007, *17*, 334–338.
14. Stejskal, J., Quadrat, O., Sapurina, I., Zemek, J., Drelinkiewicz, A., Hasik, M., Krivka, I., Prokes, J., Polyaniline-coated silica gel. *Eur. Polym. J.* 2002, *38*, 631–637.
15. Sapurina, I., Riede, A., Stejskal, J., In-situ polymerized polyaniline films 3. Film formation. *Synth. Met.* 2001, *123*, 503–507.
16. Drelinkiewicz, A., Waksmundzka-Gora, A., Makowski, W., Stejskal, J., Pd/polyaniline(SiO_2) a novel catalyst for the hydrogenation of 2-ethylanthraquinone. *Catal. Commun.* 2005, *6*, 347–356.
17. Boeva, Z. A., Sergeyev, V. G., Polyaniline: Synthesis, properties, and application. *Polym. Sci. Ser. C* 2014, *56*, 144–153.
18. Bossi, A., Piletsky, S. A., Turner, A. P. F., Righetti, P. G., Repartition effect of aromatic polyaniline coatings on the separation of bioactive peptides in capillary electrophoresis. *Electrophoresis* 2002, *23*, 203–208.
19. Florea, L., Diamond, D., Benito-Lopez, F., Polyaniline coated microcapillaries for continuous flow analysis of aqueous solutions. *Anal. Chim. Acta* 2013, *759*, 1–7.
20. Ghassempour, A., Najafi, N., Mehdinia, M. A., Davarani, S. S. H, Fallahi, M., Nakhshab, M., Analysis of anatoxin-A using polyaniline as a sorbent in solid-phase microextraction coupled to gas chromatography-mass spectrometry. *J. Chromatogr. A* 2005, *1078*, 120–127.
21. Sowa, I., Wojciak-Kosior, M., Rokicka, K., Kocjan, R., Szymczak, G., Application of solid phase extraction with the use of silica modified with polyaniline film for pretreatment of samples from plant material before HPLC determination of triterpenic acids. *Talanta* 2014, *122*, 51–57.
22. Mohammad, A., Khatoon, S., Khan, A. M. T., Moheman, A., Synthetic and chromatographic studies on silica polyaniline: A new approach. *Arch. Appl. Sci. Res.* 2010, *2*, 233–240.
23. Siddiq, A., Ansari, M. O., Mohammad, A., Mohammad, F., El-Desoky, G. E., Synergistic effect of polyaniline modified silica gel for highly efficient separation of non resolvable amino acids. *Int. J. Polym. Mater. Polym. Biomater.* 2014, *63*, 277–281.
24. Chriswanto, H., Wallace, G. G., Characterization of polyaniline using chromatographic studies. *Chromatographia* 1996, *42*, 191–198.
25. Sowa, I., Wojciak-Kosior, M., Draczkowski, P., Strzemski, M., Kocjan, R., Synthesis and properties of a newly obtained sorbent based on silica gel coated with a polyaniline film as the stationary phase for nonsuppressed ion chromatography. *Anal. Chim. Acta* 2013, *787*, 260–266.
26. Sowa, I., Kocjan, R., Wojciak-Kosior, M., Swieboda, R., Zajdel, D., Hajnos, M., Physicochemical properties of silica gel coated with a thin layer of polyaniline (PANI) and its application in nonsuppressed ion chromatography. *Talanta* 2013, *115*, 451–456.
27. Gunst, R. F., Mason, R. L., Regression Analysis and Its Application: A Data-Oriented Approach, Marcel Dekker Inc., New York 1980.

28. Poole, C. F., Poole, S. K., Column selectivity from the perspective of the solvation parameter model. *J. Chromatogr. A* 2002, *965*, 263–299.

29. Sykora, D., Vozka, J., Tesarova, E., Chromatographic methods enabling the characterization of stationary phases and retention prediction in high-performance liquid chromatography and supercritical fluid chromatography. *J. Sep. Sci.* 2016, *39*, 115–131.

30. Abraham, M. H., Whiting, G. S., Doherty, R. M., Shuely, W. J., Hydrogen-bonding .16. A new solute solvation parameter, Π-2(H), from gas-chromatographic data. *J. Chromatogr*. 1991, *587*, 213–228.

31. Quiming, N. S., Denola, N. L., Saito, Y., Catabay, A. P., Jinno, K., Chromatographic behavior of uric acid and methyl uric acids on a diol column in HILIC. *Chromatographia* 2008, *67*, 507–515.

32. Quiming, N. S., Denola, N. L., Bin Samsuri, S. R., Saito, Y., Jinno, K., Development of retention prediction models for adrenoreceptor agonists and antagonists on a polyvinyl alcohol-bonded stationary phase in hydrophilic interaction chromatography. *J. Sep. Sci.* 2008, *31*, 1537–1549.

33. Jandera, P., Hajek, T., Skerikova, V., Soukup, J., Dual hydrophilic interaction-RP retention mechanism on polar columns: Structural correlations and implementation for 2-D separations on a single column. *J. Sep. Sci.* 2010, *33*, 841–852.

34. Michel, M., Baczek, T., Studzinska, S., Bodzioch, K., Jonsson, T., Kaliszan, R., Buszewski, B., Comparative evaluation of high-performance liquid chromatography stationary phases used for the separation of peptides in terms of quantitative structure-retention relationships. *J. Chromatogr. A* 2007, *1175*, 49–54.

35. Kalikova, K., Kozlik, P., Gilar, M., Tesarova, E., Properties of two amide-based hydrophilic interaction liquid chromatography columns. *J. Sep. Sci.* 2013, *36*, 2421–2429.

36. Kozlik, P., Simova, V., Kalikova, K., Bosakova, Z., Armstrong, D. W., Tesarova, E., Effect of silica gel modification with cyclofructans on properties of hydrophilic interaction liquid chromatography stationary phases. *J. Chromatogr. A* 2012, *1257*, 58–65.

37. Chirita, R. I., West, C., Zubrzycki, S., Finaru, A. L., Elfakir, C., Investigations on the chromatographic behaviour of zwitterionic stationary phases used in hydrophilic interaction chromatography. *J. Chromatogr. A* 2011, *1218*, 5939–5963.

38. Stejskal, J., Gilbert, R. G., Polyaniline. Preparation of a conducting polymer (IUPAC technical report). *Pure Appl. Chem.* 2002, *74*, 857–867.

39. Franc, M., Vojta, J., Sobotnikova, J., Coufal, P., Bosakova, Z., Performance and lifetime of slurry packed capillary columns for high performance liquid chromatography. *Chem. Pap.* 2014, *68*, 22–28.

40. Schuster, G., Lindner, W, Comparative characterization of hydrophilic interaction liquid chromatography columns by linear solvation energy relationships. *J. Chromatogr. A* 2013, *1273*, 73–94.

41. Marvin 16.4.11.0, ChemAxon, Budapest, Hungary 2015. Available from: http://www.chemaxon.com.

42. Hintze, J. L., *NCSS User's Guide II*. NCSS, *Kaysville*, UT, USA 2007.

43. Armes, S. P., Miller, J. F., Optimum reaction conditions for the polymerization of aniline in aqueous solution by ammonium persulphate. *Synth. Met.* 1988, *22*, 385–393.

44. Wang, Y., Wahab, M. F., Breitbach, Z. S., Armstrong, D. W., Carboxylated cyclofructan 6 as a hydrolytically stable high efficiency stationary phase for hydrophilic interaction liquid chromatography and mixed mode separations. *Anal. Methods* 2016, *8*, 6038–6045.

45. Kirkland, J. J., van Straten, M. A., Claessens, H. A., Reversed-phase high-performance liquid chromatography of basic compounds at pH11 with silica-based column packings. *J. Chromatogr. A* 1998, *797*, 111–120.

46. Vitha, M., Carr, P. W., The chemical interpretation and practice of linear solvation energy relationships in chromatography. *J. Chromatogr. A* 2006, *1126*, 143–194.

47. Ibrahim, M. E. A., Liu, Y., Lucy, C. A., A simple graphical representation of selectivity in hydrophilic interaction liquid chromatography. *J. Chromatogr. A* 2012, *1260*, 126-131.

SUPPORTING INFORMATION

Additional Supporting Information may be found online in the supporting information tab for this article.

How to cite this article: Taraba L, Křížek T, Hodek O, Kalíková K, Coufal P. (2017). Characterization of polyaniline-coated stationary phases by using the linear solvation energy relationship in the hydrophilic interaction liquid chromatography mode using capillary liquid chromatography. *J Sep Sci*, 40, 677–687. DOI: 10.1002/jssc.201600785.

Supporting Information

Characterization of polyaniline-coated stationary phases by LSER in the HILIC mode using capillary liquid chromatography

Lukáš Taraba[a], Tomáš Křížek[a,*], Ondřej Hodek[a], Květa Kalíková[b], Pavel Coufal[a]

[a] Charles University, Faculty of Science, Department of Analytical Chemistry, Hlavova 8, 128 43 Prague 2, Czech Republic

[b] Charles University, Faculty of Science, Department of Physical and Macromolecular Chemistry, Hlavova 8, 128 43 Prague 2, Czech Republic

[*] Corresponding author at: Charles University, Faculty of Science, Department of Analytical Chemistry, Hlavova 8, 128 43 Prague 2, Czech Republic.
Tel.: +420 221 951 229. E-mail address: tomas.krizek@natur.cuni.cz (T. Křížek)

Table S1 LSER test solutes with their molecular descriptors and retention factors.

No.	solute	E	S	A	B	V	$D^{-}_{5.4}$	$D^{+}_{5.4}$	$k_{PANI-SiO2}$	$k_{PANI-C18}$
1	adenine	1.68	1.80	0.70	1.13	0.923	0.00	0.39	1.46	0.50
2	cytosine	1.43	1.90	0.60	1.02	0.793	0.00	0.00	1.86	0.40
3	guanine	1.80	1.60	0.97	1.20	0.982	0.00	0.00	7.16	1.18
4	thymine	0.80	1.00	0.44	1.03	0.893	0.07	0.00	0.40	0.27
5	uracil	0.81	1.00	0.44	1.00	0.752	0.07	0.00	0.57	0.33
6	uridine	1.88	2.35	0.90	2.29	1.582	0.00	0.00	1.65	0.46
7	2-deoxyuridine	1.65	2.14	0.74	1.92	1.524	0.00	0.00	0.77	0.34
8	phenylalanine	0.95	1.39	0.78	1.02	1.313	1.00	1.00	5.45	0.91
9	tyrosine	1.18	1.60	1.28	1.29	1.372	1.00	1.00	15.82	2.09
10	tyramine	1.01	1.17	0.71	0.94	1.157	0.00	1.00	1.27	0.33
11	tryptophan	1.62	1.80	1.09	1.23	1.543	1.00	1.00	10.65	1.32
12	5-methyltryptophan	1.64	1.74	1.09	1.23	1.684	1.00	1.00	6.70	1.16
13	xanthine	1.50	1.60	0.97	1.07	0.941	0.15	0.00	2.23	0.63

14	theophylline	1.50	1.60	0.54	1.34	1.222	0.00	0.00	0.61	0.39
15	theobromine	1.50	1.60	0.50	1.38	1.222	0.00	0.00	0.50	0.29
16	caffeine	1.50	1.60	0.00	1.33	1.364	0.00	0.00	0.40	0.32
17	benzene	0.61	0.52	0.00	0.14	0.716	0.00	0.00	0.13	0.32
18	toluene	0.60	0.52	0.00	0.14	0.857	0.00	0.00	0.12	0.38
19	1,2-xylene	0.66	0.56	0.00	0.16	0.998	0.00	0.00	0.10	0.45
20	1,3-xylene	0.62	0.52	0.00	0.16	0.998	0.00	0.00	0.10	0.46
21	1,4-xylene	0.61	0.52	0.00	0.16	0.998	0.00	0.00	0.10	0.47
22	ethylbenzene	0.61	0.51	0.00	0.15	0.998	0.00	0.00	0.12	0.38
23	propylbenzene	0.60	0.50	0.00	0.15	1.139	0.00	0.00	0.12	0.44
24	butylbenzene	0.60	0.51	0.00	0.15	1.280	0.00	0.00	0.12	0.50
25	biphenyl	1.36	0.99	0.00	0.26	1.324	0.00	0.00	0.15	0.42
26	naphthalene	1.34	0.92	0.00	0.20	1.085	0.00	0.00	0.14	0.40
27	anthracene	2.29	1.34	0.00	0.26	1.454	0.00	0.00	0.25	0.61
28	phenanthrene	2.06	1.29	0.00	0.26	1.454	0.00	0.00	0.22	0.58
29	pyrene	2.81	1.71	0.00	0.29	1.585	0.00	0.00	0.32	0.82
30	phenol	0.81	0.89	0.60	0.30	0.775	0.00	0.00	0.20	0.30
31	pyrocatechol	0.97	1.07	0.88	0.47	0.834	0.00	0.00	0.44	0.38
32	resorcinol	0.98	1.11	1.09	0.52	0.834	0.00	0.00	0.87	0.39
33	phloroglucinol	1.36	1.12	1.40	0.82	0.893	0.00	0.00	14.80	0.90
34	1,2-cresol	0.84	0.86	0.52	0.31	0.916	0.00	0.00	0.14	0.33
35	1,3-cresol	0.82	0.88	0.57	0.34	0.916	0.00	0.00	0.15	0.33
36	1,4-cresol	0.82	0.87	0.57	0.31	0.916	0.00	0.00	0.16	0.35
37	2-nitrophenol	1.02	1.05	0.05	0.37	0.949	0.06	0.00	0.14	0.32
38	3-nitrophenol	1.05	1.57	0.79	0.23	0.949	0.00	0.00	0.30	0.38
39	4-nitrophenol	1.07	1.72	0.82	0.26	0.949	0.02	0.00	0.34	0.41
40	2-nitrotoluene	0.87	1.11	0.00	0.27	1.032	0.00	0.00	0.13	0.33
41	3-nitrotoluene	0.87	1.10	0.00	0.25	1.032	0.00	0.00	0.13	0.36
42	benzoic acid	0.73	0.90	0.59	0.40	0.932	0.95	0.00	0.82	0.48
43	4-hydroxybenzoic a.	0.93	0.90	0.81	0.56	0.990	0.91	0.00	4.14	0.94

44	4-aminobenzoic a.	1.08	1.65	0.94	0.60	1.032	0.81	0.00	0.82	0.39
45	salicylic a.	0.89	0.84	0.71	0.38	0.990	1.00	0.00	10.29	4.68
46	acetylsalicylic a.	0.78	0.80	0.49	1.00	1.288	0.99	0.00	9.88	5.02
47	cinnamic a.	1.14	1.00	0.58	0.57	1.171	0.89	0.00	0.79	0.53
48	mandelic a.	0.90	1.05	0.74	0.89	1.131	0.98	0.00	7.23	2.95
49	1.2-coumaric a.	1.13	1.39	1.07	0.79	1.229	0.96	0.00	2.30	1.00
50	1.4-coumaric a.	1.13	1.39	1.07	0.79	1.229	0.96	0.00	3.80	1.24
51	4-hydroxyphenylacetic a.	0.94	1.32	0.97	0.78	1.131	0.96	0.00	1.84	0.69
52	aniline	0.96	0.96	0.26	0.41	0.816	0.00	0.15	0.15	0.28
53	4-nitroaniline	1.22	1.83	0.45	0.38	0.990	0.00	0.00	0.18	0.30
54	1.2-toluidine	0.97	0.92	0.23	0.45	0.957	0.00	0.11	0.20	0.37
55	1.4-toluidine	0.92	0.95	0.23	0.45	0.957	0.00	0.28	0.13	0.34
56	bromobenzene	0.88	0.73	0.00	0.09	0.891	0.00	0.00	0.13	0.37
57	chlorobenzene	0.72	0.65	0.00	0.07	0.839	0.00	0.00	0.12	0.35
58	1.2-dichlorobenzene	0.87	0.78	0.00	0.04	0.961	0.00	0.00	0.11	0.47
59	1.2.3-trichlorobenzene	1.03	0.86	0.00	0.00	1.084	0.00	0.00	0.13	0.58
60	tetrachlorobenzene	1.18	0.92	0.00	0.00	1.206	0.00	0.00	0.15	0.73
61	2-chlorophenol	0.85	0.88	0.32	0.31	0.898	0.00	0.00	0.18	0.35
62	3-chlorophenol	0.91	1.06	0.69	0.15	0.898	0.00	0.00	0.20	0.36
63	4-chlorophenol	0.92	1.08	0.67	0.21	0.898	0.00	0.00	0.20	0.35
64	benzaldehyde	0.82	1.00	0.00	0.39	0.873	0.00	0.00	0.14	0.29
65	3-hydroxybenzaldehyde	0.99	1.38	0.74	0.40	0.932	0.00	0.00	0.23	0.33
66	benzamide	0.99	0.50	0.49	0.67	0.973	0.00	0.00	0.24	0.27
67	benzonitrile	0.74	1.11	0.00	0.33	0.871	0.00	0.00	0.13	0.28
68	benzophenone	1.45	1.50	0.00	0.50	1.481	0.00	0.00	0.15	0.37
69	benzylalcohol	0.80	0.87	0.33	0.56	0.916	0.00	0.00	0.16	0.27
70	2-naphthol	1.52	1.08	0.61	0.40	1.144	0.00	0.00	0.26	0.39
71	hydroquinone	1.00	1.00	1.16	0.60	0.834	0.00	0.00	0.43	0.34
72	dibenzothiophene	1.96	1.31	0.00	0.18	1.379	0.00	0.00	0.22	0.57
73	ethyl acetate	0.11	0.62	0.00	0.45	0.747	0.00	0.00	0.20	0.38

74	urea	0.50	1.49	0.83	0.84	0.465	0.00	0.00	2.67	1.07
75	pyridine	0.63	0.84	0.00	0.52	0.675	0.00	0.34	0.27	0.38
76	2-aminopyridine	0.98	1.10	0.32	0.63	0.775	0.00	0.96	0.77	0.38
77	4-aminopyridine	0.90	1.21	0.23	0.71	0.775	0.00	1.00	1.68	0.39
78	acetone	0.18	0.70	0.04	0.49	0.547	0.00	0.00	0.13	0.35
79	acetophenone	0.82	1.01	0.00	0.48	1.014	0.00	0.00	0.14	0.30
80	anisole	0.71	0.75	0.00	0.29	0.916	0.00	0.00	0.13	0.33

Table S2 Descriptive statistics for the solute set in Table S1

	E	S	A	B	V	D^-	D^+
minimum	0.110	0.500	0.000	0.000	0.465	0.000	0.000
maximum	2.810	2.350	1.400	2.290	1.684	0.910	1.000
average	1.061	1.125	0.433	0.564	1.037	0.762*	0.686*
standard deviation	0.448	0.416	0.410	0.443	0.245	0.381*	0.388*

*Only charged solutes were included.

Table S3 Correlation matrix for the solute descriptors of the set of solutes listed in Table S1

	E	S	A	B	V	D^-	D^+
E	1.000	0.694	0.192	0.369	0.695	0.093	0.091
S		1.000	0.516	0.696	0.466	0.219	0.218
A			1.000	0.561	0.086	0.403	0.190
B				1.000	0.360	0.320	0.292
V					1.000	0.400	0.063
D^-						1.000	0.455
D^+							1.000

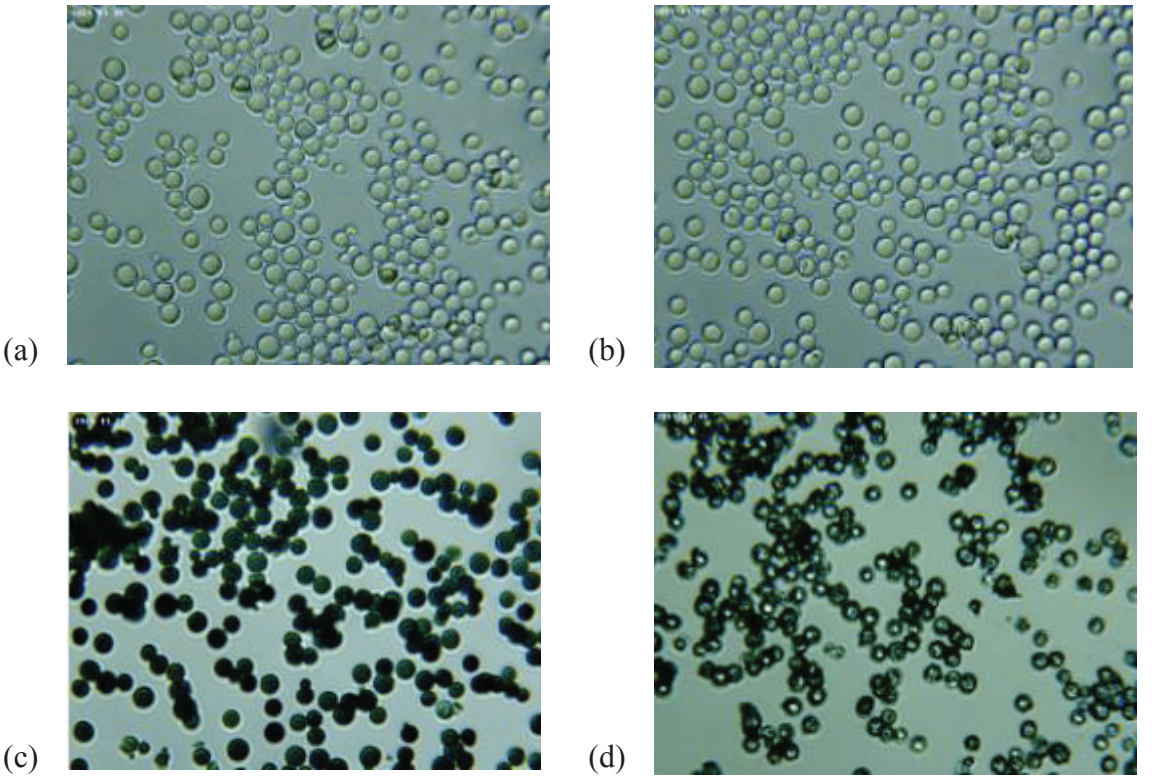

Figure S1 Optical microscope images of: untreated Hypersil (a) and Nucleosil C_{18} (b); and PANI-coated Hypersil (c) and Nucleosil C_{18} (d), magnification 1600×.

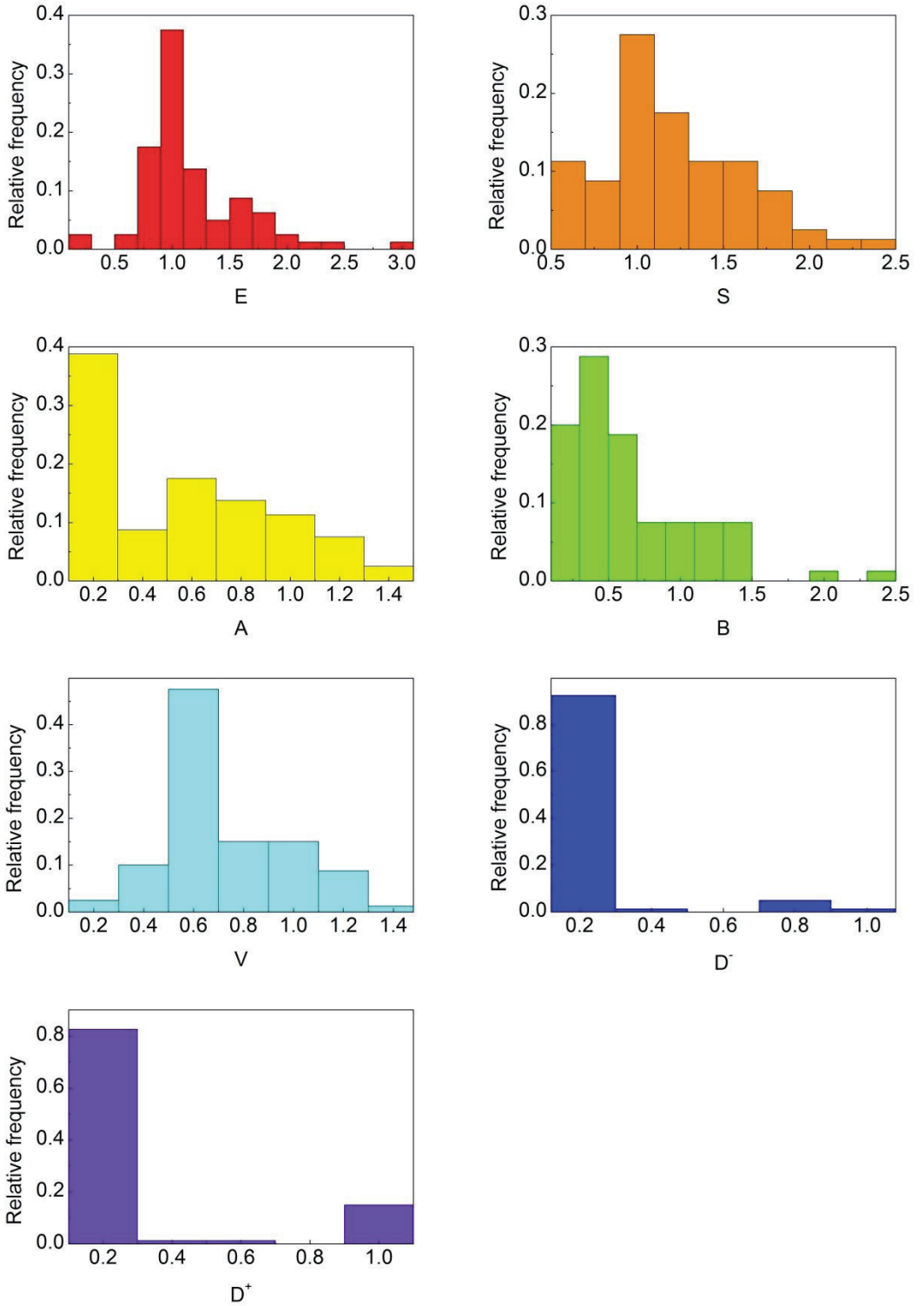

Figure S2 Frequency plots of the Abraham and D^-, D^+ descriptors of the solute set in Table S1.

Aqueous pH versus apparent hydro-organic pH

Discussions can be found in the literature as to whether it would be more appropriate to use the aqueous buffer pH for calculations of the D^-, D^+ descriptors instead of the apparent hydro-organic pH of the prepared mobile phase. Some of the works proposed that using ${}^{w}_{w}pH$ for the calculations could be more suitable since it agrees better with the HILIC theory assuming the formation of a stagnant water layer on the surface of the stationary phase, where the aqueous pH would be more likely to be present, as the water would be separated from the hydro-organic modifier [S1]. Nonetheless, most authors still tend to use ${}^{s}_{w}pH$ for the calculations [S2,S3]. For simplicity, we decided to use primarily ${}^{s}_{w}pH$ for D^-, D^+ calculations, although we also calculated the descriptors using ${}^{w}_{w}pH$ and evaluated the effect for our individual test setup.

As shown in Figure S3, the values of a, d^- and v coefficient increased slightly, whereas d^+ decreased and became statistically insignificant for ${}^{w}_{w}pH$ 3.0 for PANI-SiO_2; the correlation coefficient R decreased slightly to a value of 0.90. For the PANI-C_{18} sorbent at ${}^{w}_{w}pH$ 3.0, there was a minor increase for d^- and v and somewhat greater increase in a, thus making it statistically significant; the value of R again decreased to 0.83. It can be seen that the trend is the same for both stationary phases; however, we can conclude that no breakthrough change was observed in the individual coefficients and thus also in the devised model.

Separation of structurally similar organic acids using PANI-SiO_2

To demonstrate the application potential of the PANI-SiO_2 stationary phase, isocratic separations of three organic acids of similar structure, specifically cinnamic acid (i.e. (*E*)-3-phenylprop-2-enoic acid), 1,2-coumaric acid ((*E*)-3-(2-hydroxyphenyl)prop-2-enoic acid), 1,4-coumaric acid ((*E*)-3-(4-hydroxyphenyl)prop-2-enoic acid), were carried out under the LSER measurement conditions (see section 2.2 and 2.3) and optimized separation conditions (Figure S4). Cinnamic acid and 1,2-coumaric acid were baseline resolved ($R_{1,2}$ = 2.18) under the LSER conditions whereas a somewhat lower resolution ($R_{2,3}$ = 0.95) was obtained for positional isomers of coumaric acid. This observation is in agreement with the values of molecular descriptors of relevant solutes which are lower for cinnamic acid in almost all cases (only E and D^+ values are identical). On the other hand, coumaric acid isomers have the same values of all molecular descriptors. The calculated pK_a values of these compounds are of

a minute difference (i.e. 4.04 for 1,2-coumaric acid and 4.00 for 1,4-coumaric acid; the benzene-bound hydroxyl groups have no influence since their pK_a values are above 9). A possible explanation for the slightly higher retention of 1,4-isomer is given by the position of the hydroxyl group which is more readily accessible for stationary phase in *para* constitutional arrangement. In addition, the interaction of 1,2-isomer with the stationary phase may be weakened by formation of intramolecular hydrogen bond between carboxyl and hydroxyl moieties.

All solutes were baseline resolved ($R_{1,2}$ = 3.69; $R_{2,3}$ = 1.87) in optimized separation achieved by increasing of the portion of ACN in the mobile phase.

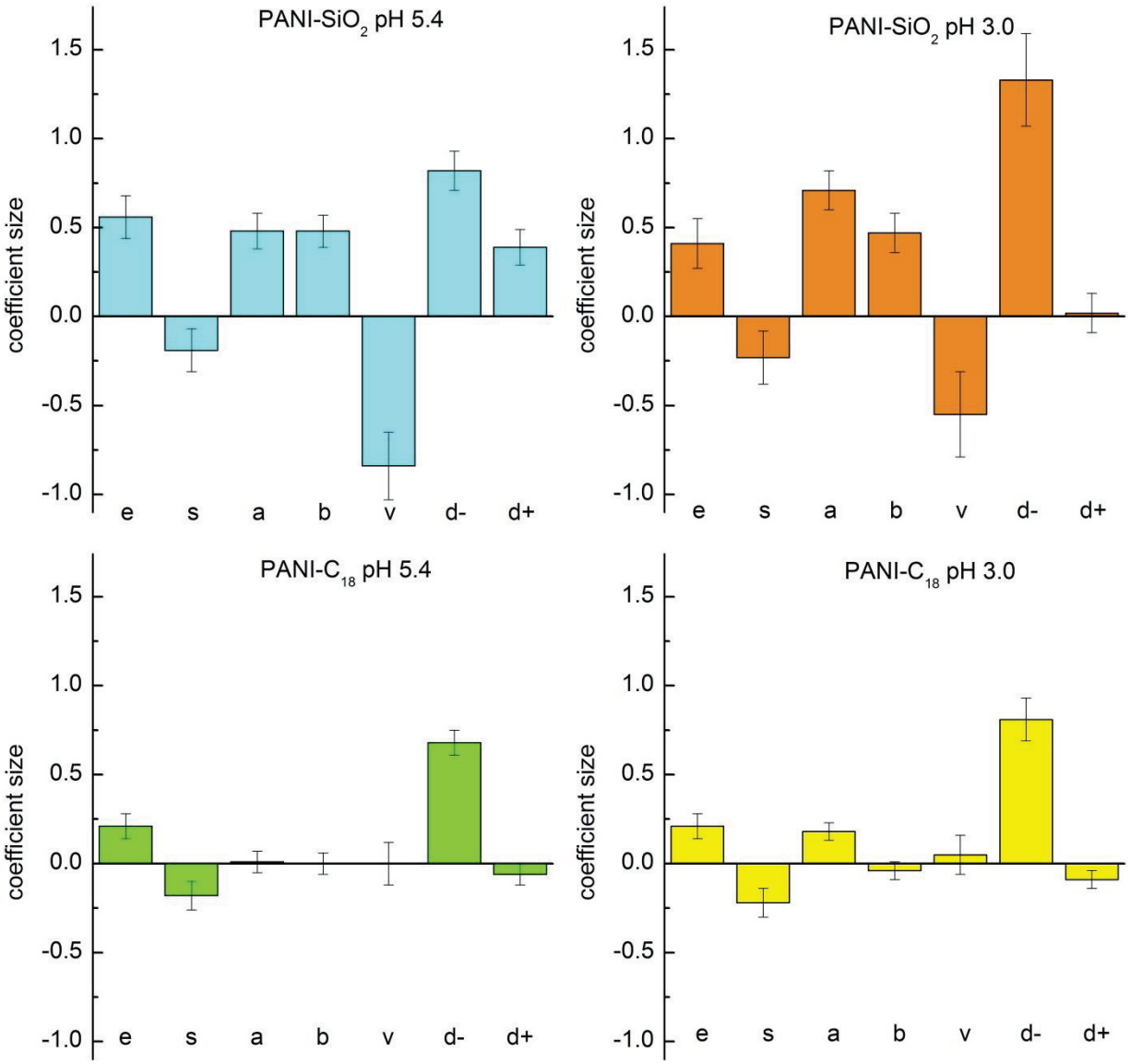

Figure S3 System coefficients of both the stationary phases for either ${}^{s}_{w}pH$ 5.4 or ${}^{w}_{w}pH$ 3.0.

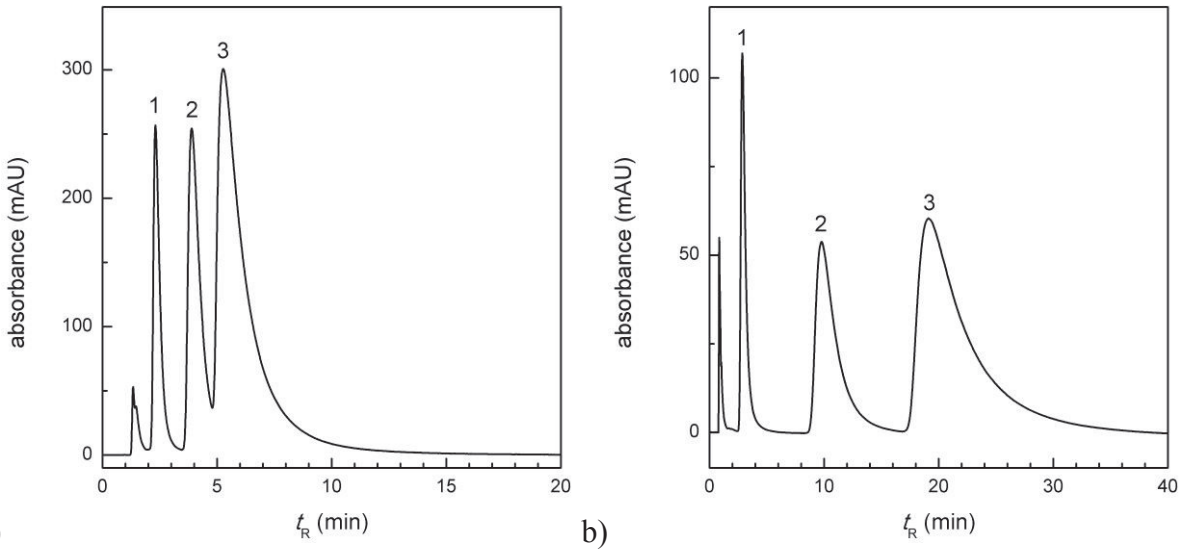

Figure S4 Separation of stucturally similar organic acids under LSER measurement conditions (a) and optimized conditions (b); (a) ACN/100 mM ammonium formate buffer 90/10 (v/v), flow rate 5 µl/min, 25 °C; (b) ACN/100 mM ammonium formate buffer 96.5/3.5 (v/v), flow rate 10 µl/min, 25 °C; UV detection at 298 nm. Elution order: 1 – cinnamic acid, 2 – 1,2-coumaric acid, 3 – 1,4-coumaric acid.

References

[S1] Schuster G., Lindner W., J. Chromatogr. A 2013, 1273, 73–94.

[S2] Chirita R. I., West C., Zubrzycki S., Finaru A.L., Elfakir C., J. Chromatogr. A 2011, 1218, 5939–5963.

[S3] Schuster G., Lindner W., J. Chromatogr. A 2013, 1301, 98–110.

4.1 Publication I – Non-published relevant data

Following section contains commented experimental data related to the polymerization mechanism of PANI under conditions described in the publication I and additional physicochemical characterization of PANI-SiO_2 sorbent that is not shown in the publication. The experiments performed during optimization of slurry packing procedure for PANI-SiO_2 and PANI-C_{18} and Walters' chromatographic test are also shown below.

4.1.1 UV-VIS-NIR characterization of PANI polymerization procedure

The experimental conditions of PANI-SiO_2 polymerization procedure described in publication I were adopted also to coat common glass microscopy slides in order to study the polymerization mechanism of PANI using UV-VIS-NIR spectroscopy under the given conditions. The parallelly arranged slides (thickness of 1 mm) were immersed into the polymerization mixture for different period of time.

Figure 4 A shows the slides that were pulled out from polymerization bath by 60 min from iniciation of the reaction, rinsed with water to stop the polymerization and dried at ambient temperature. Increasing intesity of coloration depending on the immersion time of originally colorless slides is clear. The slides pulled out by 15 min from the beginning of the reaction stayed completely colorless or very slightly, unevenly colored (Figure 4 A, slide 15) indicating thus too short time for the formation of PANI chains withstanding the subsequent wash. During next two hours, the slides, that were immersed for 20 min or longer, deepened/changed their color (Figure 4B). UV-VIS-NIR spectra of slides pulled out at different time were recorded using UV-visible Spectroscopy System 8453 (Agilent Technologies, Waldbronn, Germany). The spectra show a shift of local absorbance maxima from the original value of 550 nm, typical for pernigraniline base [63], over 720 nm (attributed to pernigraniline salt) to approximately 790 nm corresponding to emeraldine salt (Figure 5A). The local absorbance maxima approximately at 340 nm are common for both pernigraniline and emeraldine and are attributed to π-π^* transition [73]. The highest absorbance at local maximum near 790 nm for slide 60 compared to other slides may relate to the slide material, although presumed the same as for others.

PANI-coated slides were then immersed into a bath with 1 M hydrochloric acid for 10 min and dried at ambient temperature. UV-VIS-NIR spectra were recorded again (Figure 5B). The local maxima shifted from 790 nm to approximately 820 nm except for slide 30 which has local maximum at 710 nm. The possible explanation is that coating of the slide 30 comprises mostly of pernigraniline salt instead of emeraldine salt. Surprisingly, slide 20 and slide 25 show more significant bathochromic shift than the latter. In addition, the presence of a band shoulder at approximately 430 nm indicates that the slide coating is formed by emeraldine salt [63, 73, 296]. However, round-shaped curve of slide 60 at the same region is also considered as emeraldine salt [49, 65]. Both bands at 430 nm and 820 nm are related with π-polaron and polaron-π* transtions [32].

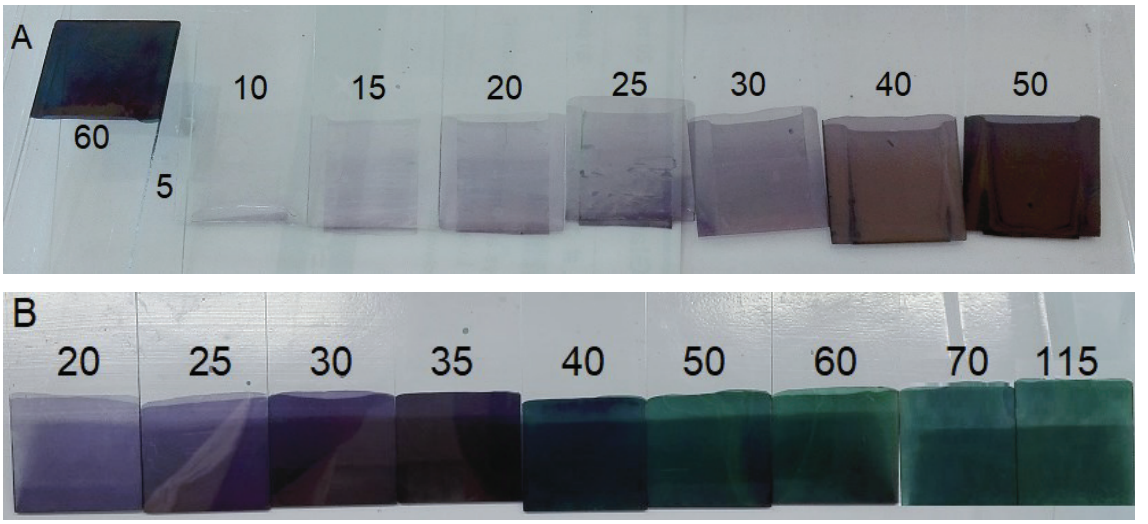

Figure 4 Water-rinsed microscopy slides coated with PANI by 60 min from the polymerization initiation (A); the same slides after three hours from the polymerization beginning (B); a number of individual slide reflects its immersion period (in min) in the polymerization bath; slides 5 and 10 remained colourless

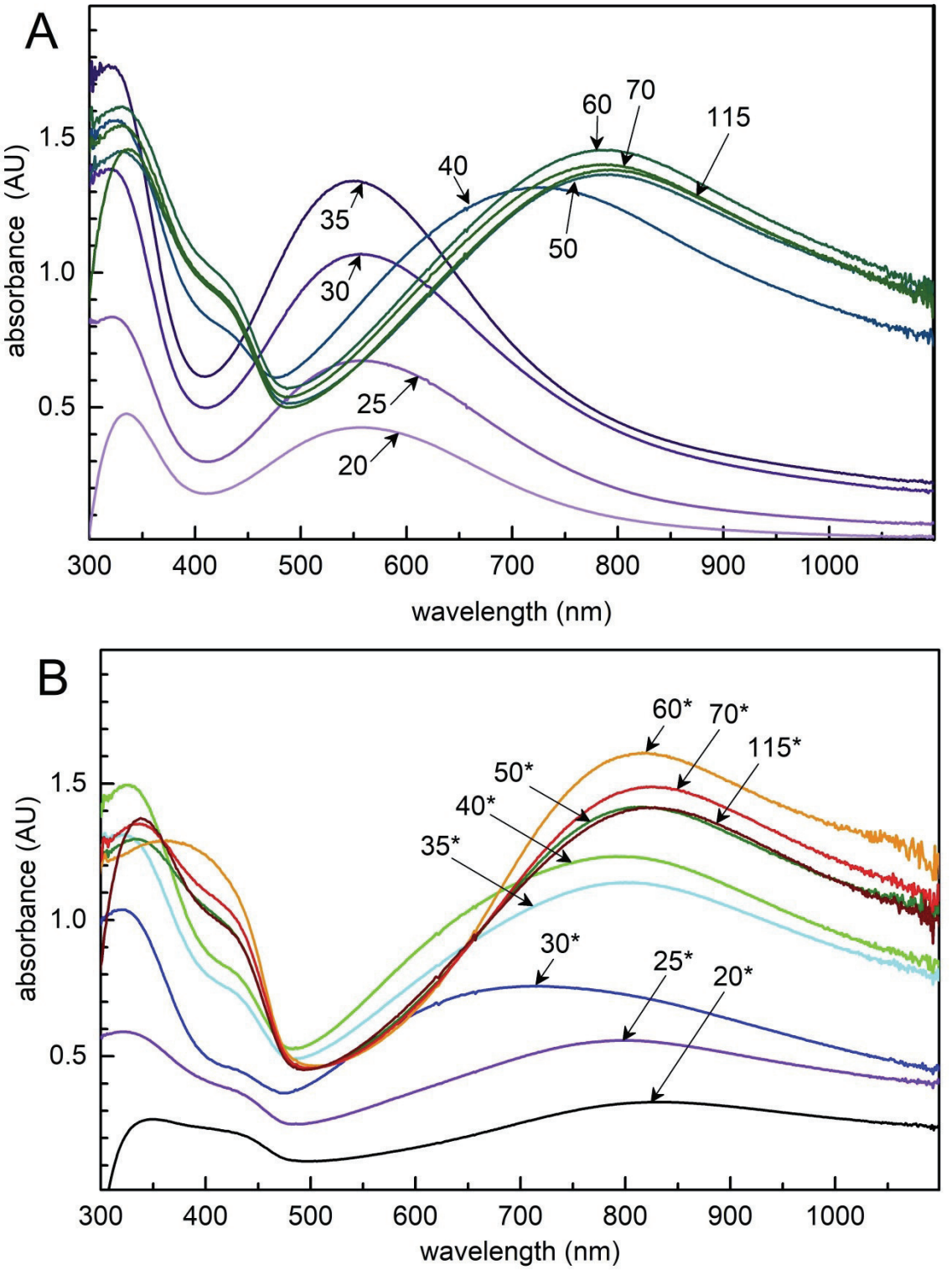

Figure 5 UV-VIS-NIR spectra of microscopy slides coated with PANI; the number of individual curve reflects the immersion period (in min) of the microscopy slide in the polymerization bath; curve color in upper graph correponds to observed color of PANI coating; asterisk denotes treatment of slides with 1 M hydrochloric acid

4.1.2 Characterization of PANI-SiO_2 using Raman and FTIR spectroscopy

Powder samples of PANI-SiO_2 particles were measured as prepared, without any pretreatment unless stated otherwise. Raman spectrum was recorded on MonoVista CRS+ dispersive confocal Raman microscope (Spectroscopy & Imaging, Germany) using diode excitation laser (laser excitation wavelength of 785 nm; laser power 10 mW; spectral range 40–3200 cm^{-1}; 150 lines/mm grating) at room temperature. The powder sample was evaluated in spectral range of 40 – 1700 cm^{-1}.

The infrared spectrum was recorded on Nicolet 6700 FTIR spectrometer (Thermo Scientific, USA) using the DRIFT technique at ambient temperature. Powder sample was dispersed in matrix of potassium bromide before measurement. FTIR spectrum was measured in range from 400 to 4000 cm^{-1} (4 cm^{-1} resolution, Happ-Genzel apodization, Mertz phase correction, zero filling 2, 128 scans).

Obtained Raman (Figure 6) and FTIR (Figure 7) spectra were processed in OMNIC 9 software [297]. Table 2 lists observed vibrational bands with the assignment according to literature [58, 73, 104, 122, 127, 138, 298-301]. Some FTIR bands were not possible to assign due to their overlap with intensive vibrational bands (468, 803, 1101, 1177, 1221 cm^{-1}) of the bare silica support (data not shown). Raman spectrum baseline is affected by the higher background caused by silica support and/or by luminescence of the PANI-SiO_2 sample.

The very broad structured band with maxima above 2000 cm^{-1} in FTIR spectrum is typical for the conducting form of PANI [73]. The hardly distinguishable absorption bands in FTIR region above 2000 cm^{-1} (weak local maxima at 3220, 3140, 3050, 2950 and 2830 cm^{-1}) relate with N–H stretching modes of secondary amine and protonated imine which are involved in the hydrogen bond interactions. These very weak local maxima of the broad bands can correspond to the hydrogen interactions among regularly aligned PANI chains which are perpendicular to the support surface [302, 303]. However, these maxima are of low intensity; which is common for PANI powder samples [301].

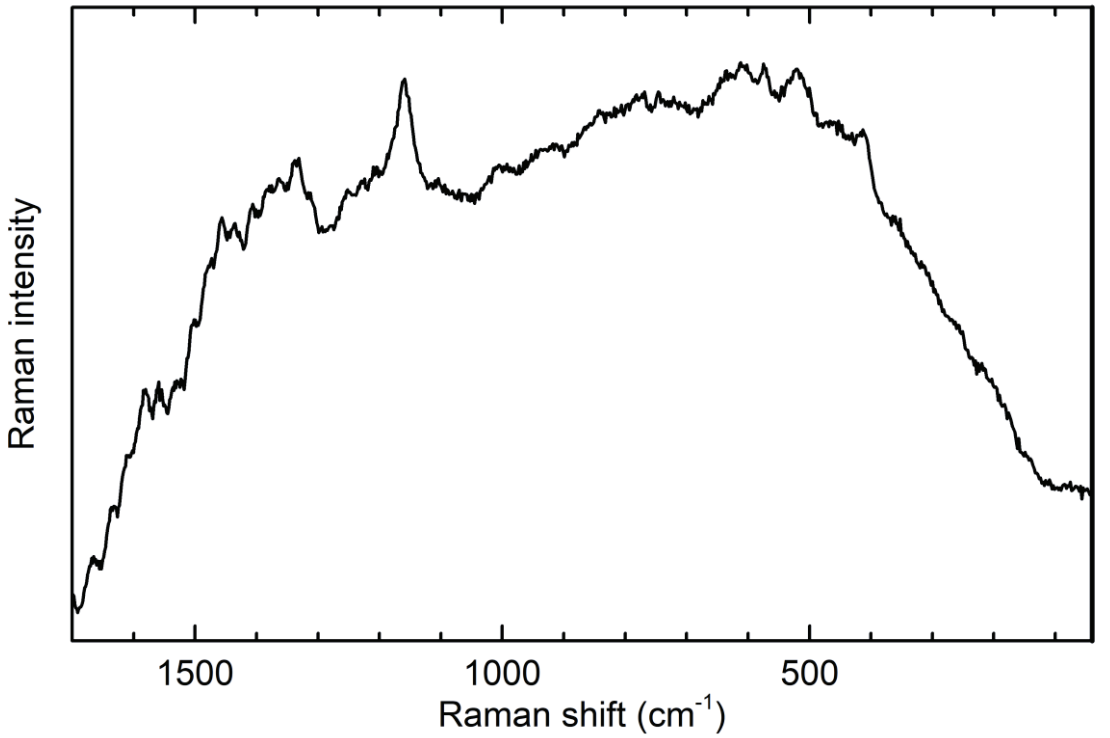

Figure 6 Raman spectrum of PANI-SiO_2 powder; the spectrum of pure SiO_2 was subtracted for easier peak identification

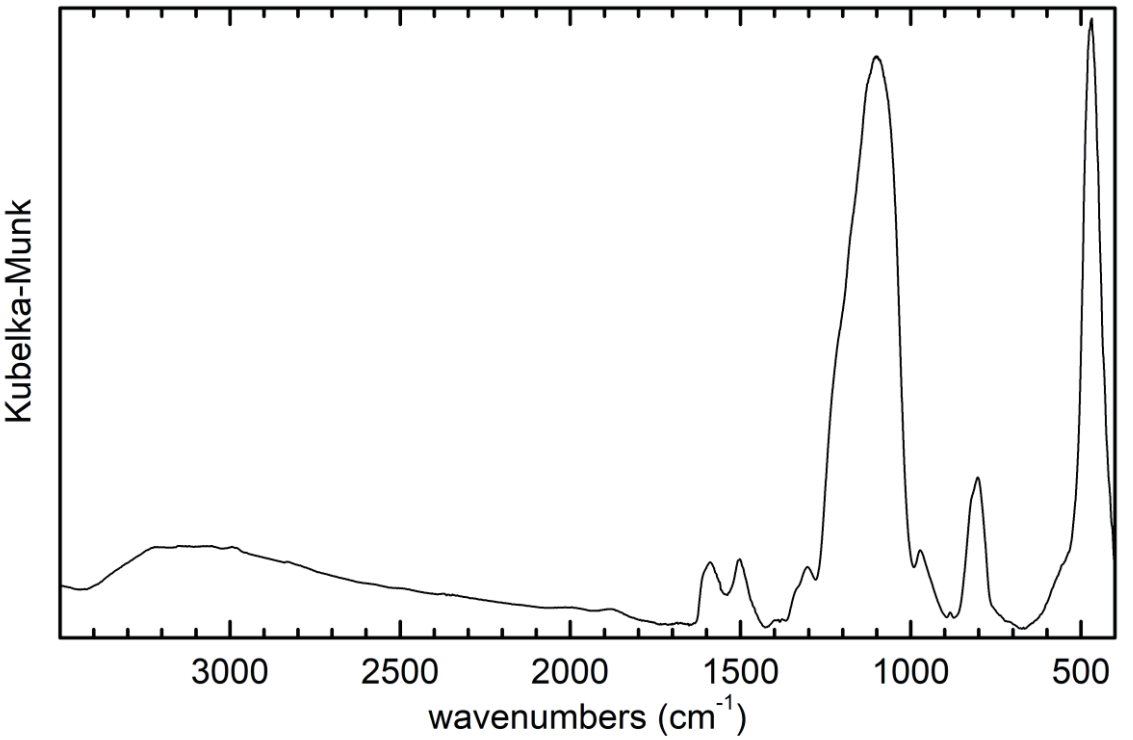

Figure 7 FTIR spectrum of PANI-SiO_2 powder

Table 2 Assignment of FTIR and Raman bands of PANI-SiO_2

FTIR [cm^{-1}]	Raman [cm^{-1}]	assignment
	411 **w**	**γ** C–C **rg**, **ω** C–H
468 **vsb**		
	519 **m**	**τ** C–N–C, **γ** C–C **rg**
540 **shb**		
	574 **w**	**δ** C–H, Pho
	745 **w**	**γ** C=C / **δ** C–C **Q**, Phz
	781 **w**	**δ** C=C **Q**
803 **sb**		?
820 **sh**		**γ** C–H of paradistributed aromatic rings indicating polymer
	838 **w**	**ω** C–H
884 **w**		?
972 **w**		**ω** N–H
1101 **vsb**		?
1177 **sh**		?
	1158 **vsb**	**δ** C–H **Q**
1221 **sh**		?
	1225 **w**	**ν** C=N **Q**, **ν** C–N **B**
	1252 **w**	**ν** C–$N^{+\bullet}$ **SQ**, **ν** C–C **Q**
1304 **w**		π-electron delocalization induced in polymer by protonation
	1337 **m**	**ν** C–$N^{+\bullet}$ **SQ**
	1407 **w**	**δ** N–H, **ν** C–C **rg**, Phz
	1456 **m**	**ν** C=N / **ν** C=C **Q**
	1472 **w**	**ν** C=N **Q**
1502 **w**	1505 **w**	**ν** C=N / **ν** C=C **Q** or **B**, δ N–H **SQ**
1589 **w**	1585 **m**	**ν** C=C **Q** corresponding to protonated polymer
1612 **sh**	1609 **sh**	**ν** C=C **B**
	1632 **w**	**ν** C–C **B**

Abbreviations: **B**, benzenoid segment; **Q**, quinoid segment; **SQ**, semiquinone segment; Phz, phenazine-like segment; Pho, phenoxazine-like segment; **b**, broad; **m**, medium; **rg**, aromatic ring; **s**, strong; **sh**, shoulder; **vs**, very strong; **w**, weak; **γ**, out-of-plane bending; **δ**, deformation or in-plane bending; **ν**, stretching; **τ**, torsion; **ω**, wagging.

4.1.3 Characterization of PANI-SiO_2 using XRD

Powder XRD spectrum of the PANI-SiO_2 sample was recorded on the X'Pert PRO MPD diffraction system (PANalytical, Netherlands) of Bragg-Brentan arrangement, equipped with the PIXcell position sensitive detector working with the Cu-K_α (λ = 1.54 Å) radiation. Measurements were performed at ambient temperature in the range of 5 – 70° 2θ. Total measurement time of one analysis was 15 min. Obtained spectrum was processed in X'Pert HighScore software [304]. According to a broad peak in the diffraction pattern the sample is amorphous, including supporting silica (Figure 8). The small peak at 22° can be assigned to loosely parallel arrangement of the PANI chains [58, 127, 300, 305-307].

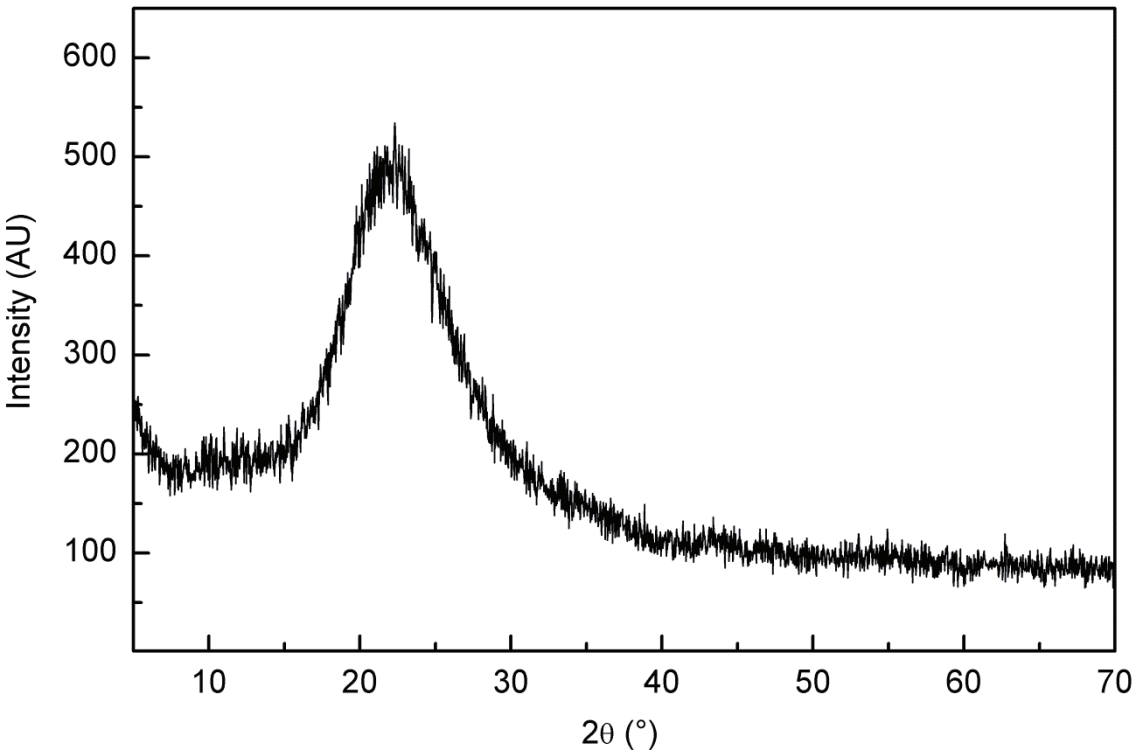

Figure 8 XRD record of PANI-SiO_2 powder

4.1.4 Characterization of PANI-SiO_2 using SEM and TEM

SEM images of sorbents used for coating with PANI (bare Hypersil silica and Nucleosil C_{18}) made before the polymerization (Figure 9A, B) show significantly different d_p values from the mean values (5 µm for both sorbents) stated by producers, especially for Hypersil sorbent.

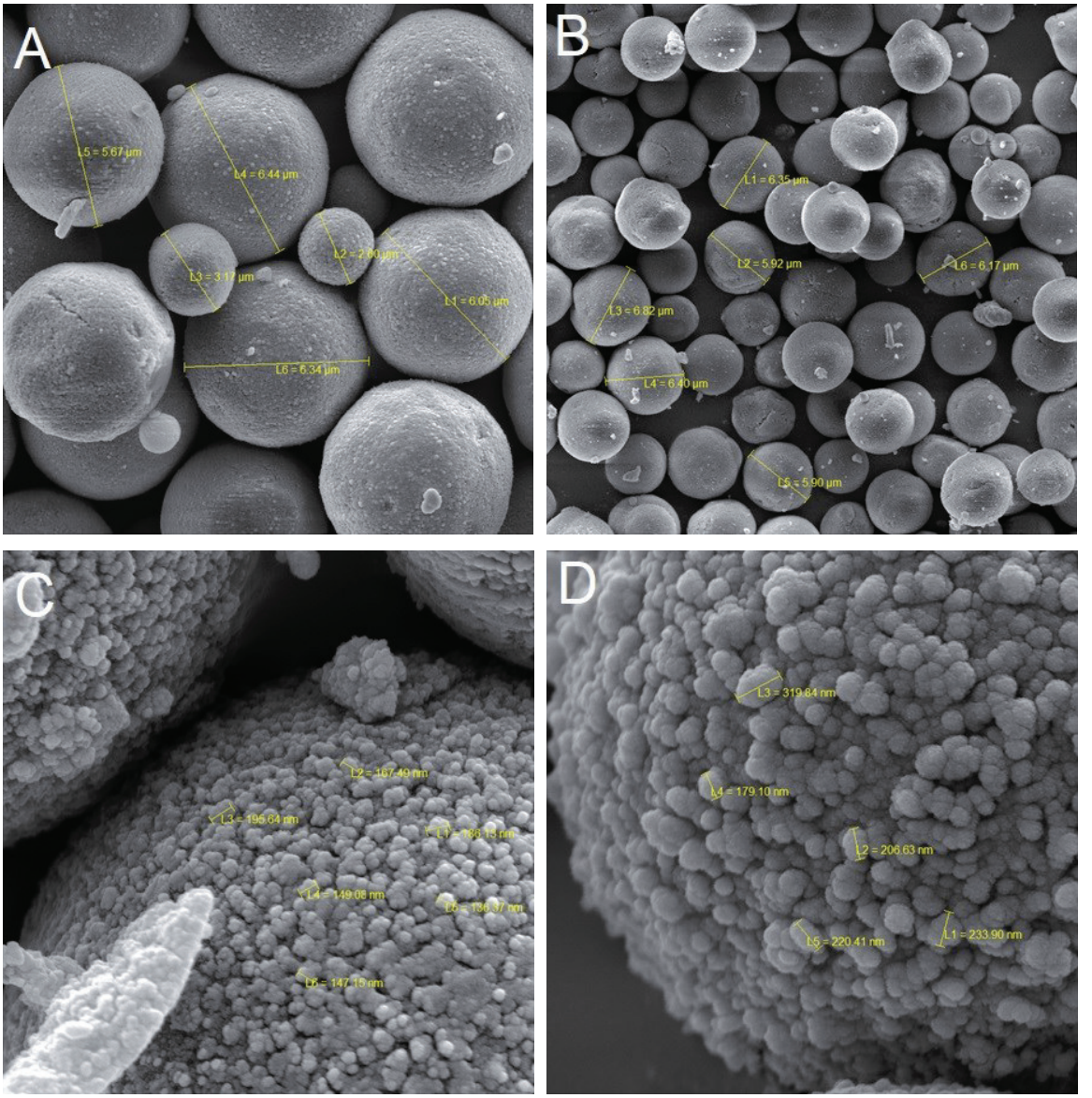

Figure 9 SEM images of bare Hypersil silica (A); bare Nucleosil C_{18} (B); PANI-SiO_2 (C); PANI-C_{18} (D); yellow lines denote diameter of the measured objects – sorbent particles (A, B) and grains forming the PANI coating (C, D)

Such a substantial non-uniformity in particle size may contribute to deteriorated column performance due to the increased eddy diffusion. All these SEM images were obtained

by MIRA SEM System (Tescan Orsay Holding, Brno, Czech Republic) thanks to the collaboration with the laboratory of visualization techniques of Zentiva pharmaceutical company (Prague, Czech Republic).

Figure 9C, D display PANI-coated sorbent surfaces. It seems that coating morphology is identical on both the sorbents. Originally smooth surfaces are covered with globular deposits of PANI that merge together to cover the surface (horizontal proliferation), albeit the vertical growth of grains on previously formed PANI layer was also observed. Approximate PANI layer thickness was estimated by the measurement of PANI grain diameter. Mean size of the PANI grain is 0.2 µm.

TEM images of bare silica and PANI-coated silica are shown in Figure 10. The PANI layer is indeed formed by merging, semi-globular lumps. However, surface coating is not always flawless. As can be observed in the bottom part of Figure 10B, some parts of the original sorbent area were not coated entirely. This can be explained by peeling the superficial layer off the damaged sorbent. The TEM images were recorded by JEOL 1011 transmission electron microscope (JEOL, Croissy Sur Seine, France) equipped with Veleta CCD camera and Olympus Soft Imaging Solution software for data acquisition.

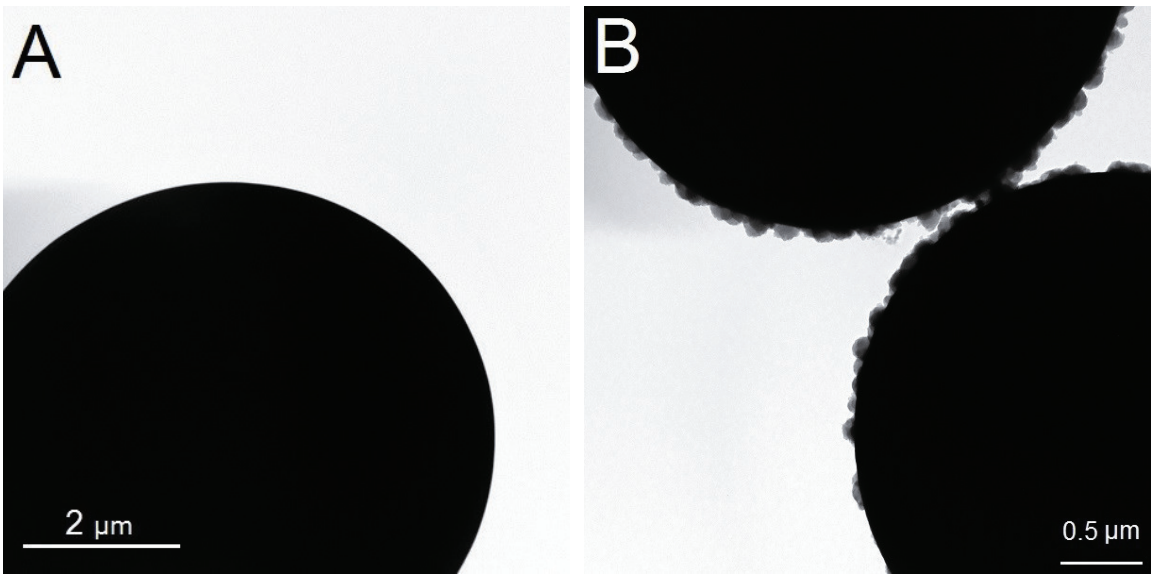

Figure 10 TEM images of bare silica sorbent without (A) and with the PANI coating (B)

4.1.5 Choice of slurry and packing solvents for PANI-coated sorbents

Several solvents and their mixtures were tested using the vial test [150] in order to find the optimal slurry and packing solvents for PANI-SiO_2 and PANI-C_{18}. The vial test is a simple test in which a small amount of sorbent particles is thoroughly dispersed in a solvent and then let to settle down at the bottom of vial; time necessary for complete particle sedimentation is a function of the solvent viscosity. Figure 11 shows progress of sedimentation for different solvents after 20 min and 40 min, respectively; settling development was observed in 5 min intervals. Sedimentation behavior of PANI-C_{18} was identical as for PANI-SiO_2 due to the same PANI coating (although the quality of coating may slightly differ). The results of sedimentation time for different solvents are shown in Table 3 together with other solvent properties.

A)

B)

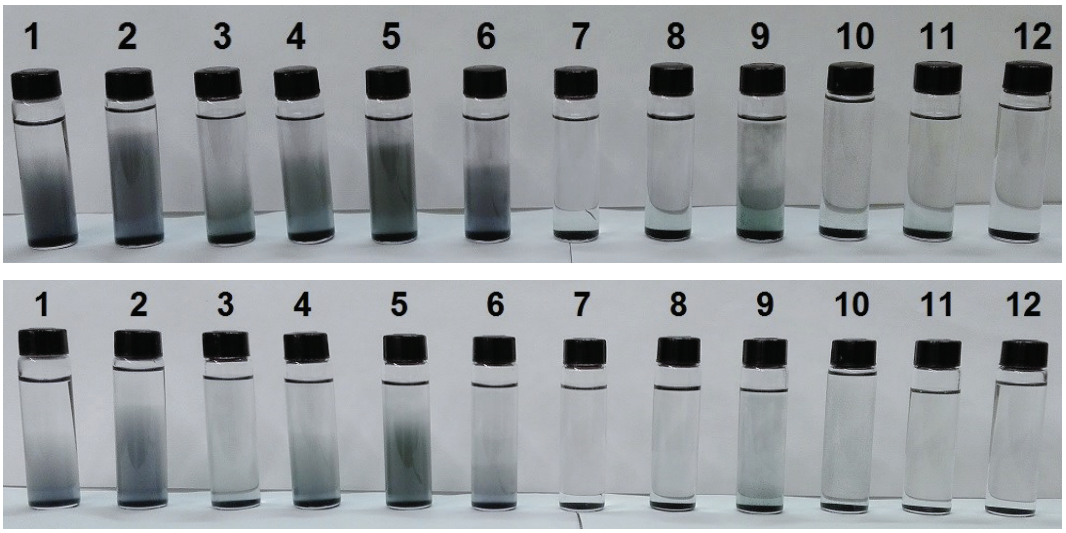

Figure 11 Illustration of sedimentation time measurement of PANI-SiO_2 particles in different solvents/mixtures of solvents after 20 min (A) and 40 min (B); slurry concentration of 5 mg/mL; (1) H_2O, (2) MeOH/H_2O (50/50 volume-to-volume ratio (v/v)), (3) MeOH, (4) ethanol, (5) *n*-propanol, (6) ACN/H_2O (50/50; v/v), (7) ACN, (8) mixture of xylene isomers, (9) chloroform, (10) *n*-pentane, (11) 2-butanone, (12) AC

For the solvents and solvent mixtures tested, a rapid settling of the particles was observed in ACN, AC, and 2-butanone, whereas the highest sedimentation time (t_{sed}) was achieved using 50/50 (v/v) MeOH/H_2O mixture. This result corresponds approximately to the values of calculated kinematic viscosity (Figure 12). Therefore, the latter was chosen as a suitable slurry solvent which presumably keeps the sorbent

particles dispersed for the longest time. Using *n*-pentane as a solvent, dispersion of PANI-SiO_2 particles was not possible at all.

Table 3 Properties of solvents tested in PANI-SiO_2 particles sedimentation time t_{sed} measurement

	solvent	ϱ_l [g/cm^3]	η [10^{-3} Pa·s]	η_{kin} [10^{-6} m^2/s]	UV cutoff [nm]	t_{sed} [min]
1	H_2O	0.998	1.002	1.004	190	70
2	50/50 (v/v) MeOH/H_2O	0.895[a)]	1.88[c)]	2.10	–	150
3	MeOH	0.791	0.591	0.747	205	30
4	ethanol	0.789	1.200	1.521	205	80
5	*n*-propanol	0.804	2.256	2.806	210	115
6	50/50 (v/v) ACN/H_2O	0.890[a)]	0.92[c)]	1.03	–	55
7	ACN	0.782	0.389	0.497	190	15
8	xylenes [b)]	~ 0.87	~ 0.69	~0.79	290	20
9	chloroform	1.488	0.580	0.390	245	40
10	*n*-pentane	0.626	0.235	0.375	200	– [d)]
11	2-butanone	0.805	0.403	0.501	329	15
12	AC	0.790	0.314	0.397	330	15
a	25/75 (v/v) ACN/H_2O	0.944[a)]	1.05[c)]	1.11	–	70
b	35/65 (v/v) ACN/H_2O	0.923[a)]	1.02[c)]	1.10	–	65
c	65/35 (v/v) ACN/H_2O	0.858[a)]	0.08[c)]	0.91	–	45
d	75/25 (v/v) ACN/H_2O	0.836[a)]	0.07[c)]	0.80	–	40

[a)] calculated by Amagat's law for liquid solutions

[b)] mixture of positional isomers, exact composition unspecified

[c)] dynamic viscosity values adapted from [292]

[d)] It was not possible to disperse PANI-SiO_2 particles by shaking or sonication

Then an appropriate packing solvent was sought. The recommendation says that the packing solvent for a polymer-containing stationary phase should include certain portion of water to prevent possible swelling/dissolution/peeling of the polymer when exposed to purely organic solvent for a long time [150, 152]; especially under high packing pressures. Moreover, tested use of pure ACN or AC led to the clogging of the slurry reservoir outlet by too fast agglomerating stationary phase particles. Therefore, further optimization was performed using ACN/H_2O mixtures of different volume ratios containing at least 25 % of water (v/v) (Figure 13); t_{sed} as a function of η_{kin} for these mixtures is plotted in Figure 12. This choice was preferred also because of intended use of ACN/H_2O mobile phase for the preliminary chromatographic experiments. The lowest t_{sed} of the particles was observed for 75/25 (v/v) ACN/H_2O mixture, however, the difference from 65/35 (v/v) ACN/H_2O mixture was almost insignificant. Therefore, the latter was preferred because of the higher content of water which should be more polymer coating-friendly.

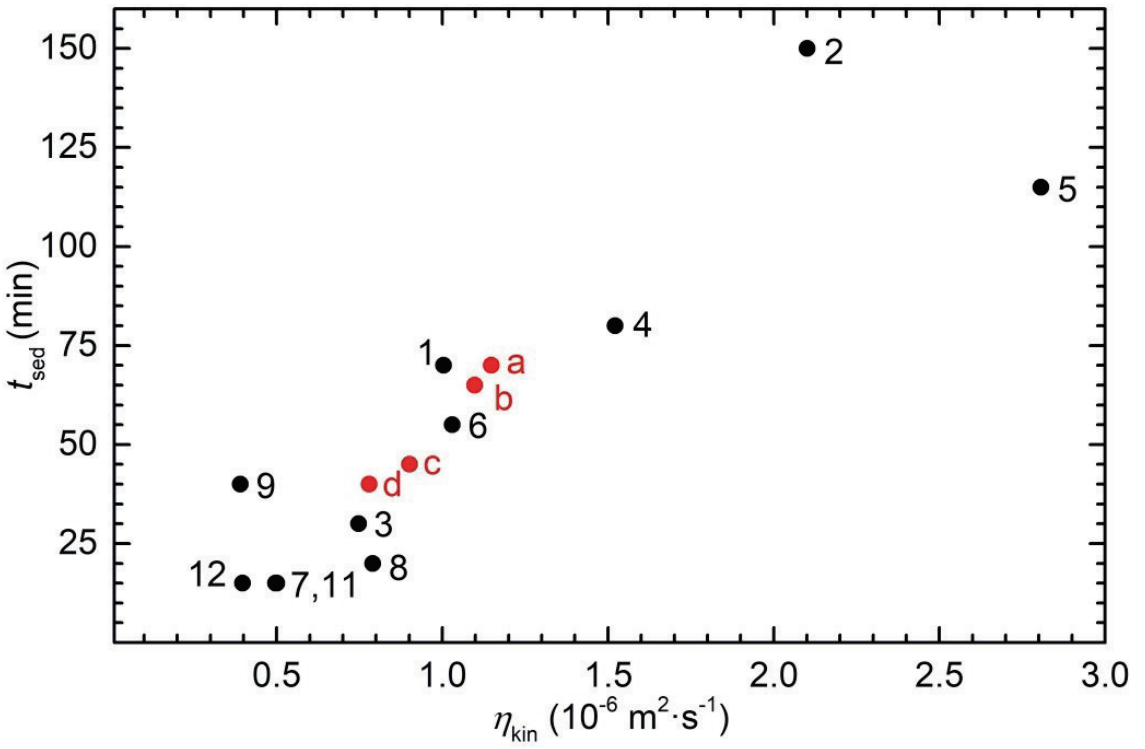

Figure 12 Sedimentation time of PANI-SiO_2 particles in different solvents as a function of kinematic viscosity of individual solvents; numerical and literal indication of solutes corresponds to Table 3

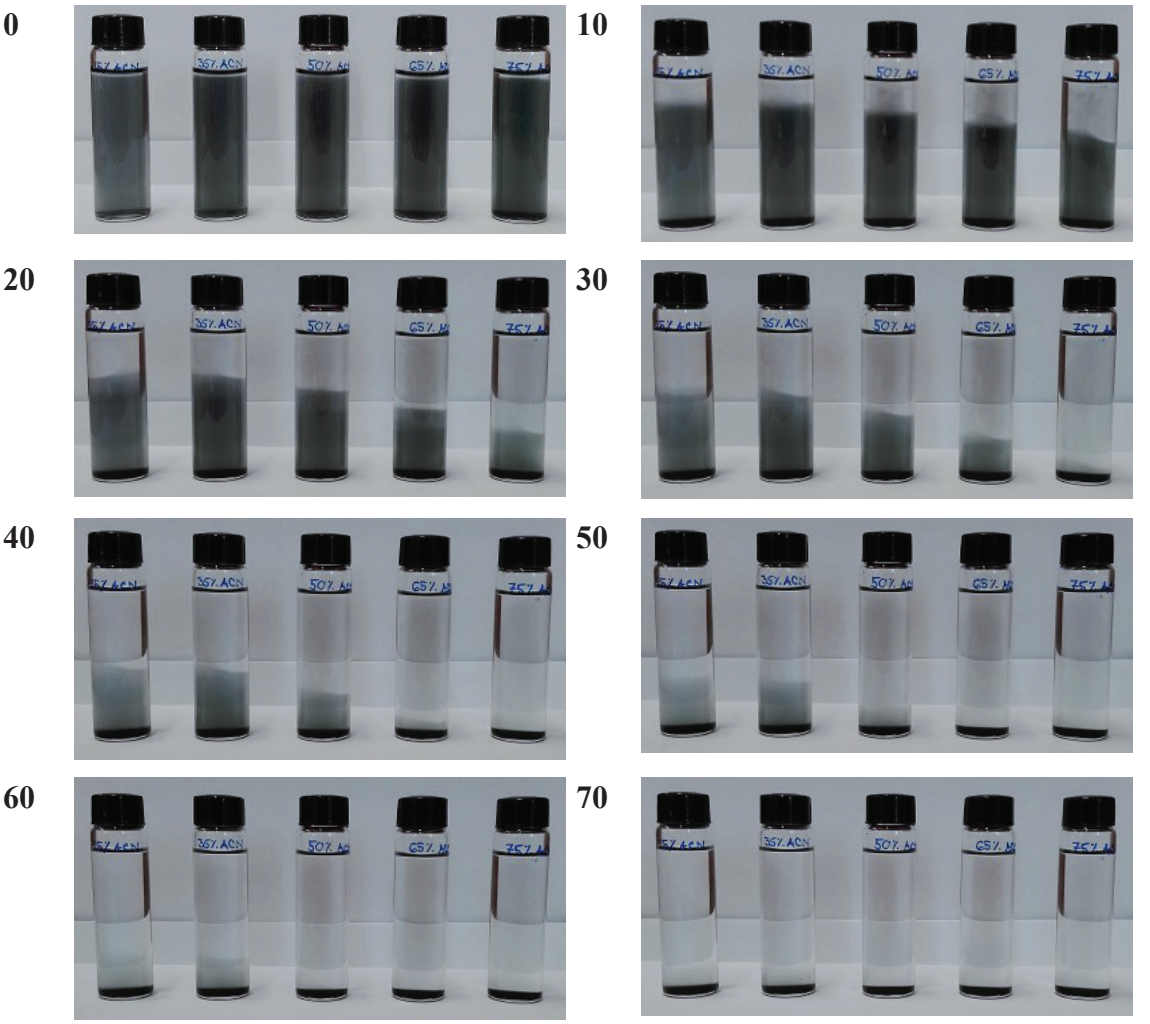

Figure 13 Sedimentation rate of PANI-SiO_2 particles in ACN/H_2O mixtures of different volume ratios; vials from the left to the right contain 25/75, 35/65, 50/50, 65/35, 75/25 of ACN/H_2O (v/v); numbers at left upper corners correspond to time (in min) that passed from the sedimentation start

Difference in behavior of PANI-SiO_2 particles in the slurry solvent and packing solvent was recorded using optical microscopy. The particles are mostly non-agglomerated in 50/50 (v/v) MeOH/H_2O solvent mixture (Figure 14A, B), whereas they tend to flocculate in 65/35 (v/v) ACN/H_2O solvent mixture (Figure 14C, D). On the basis of the above observed, it seems that both slurry and packing solvent were chosen appropriately [150, 176].

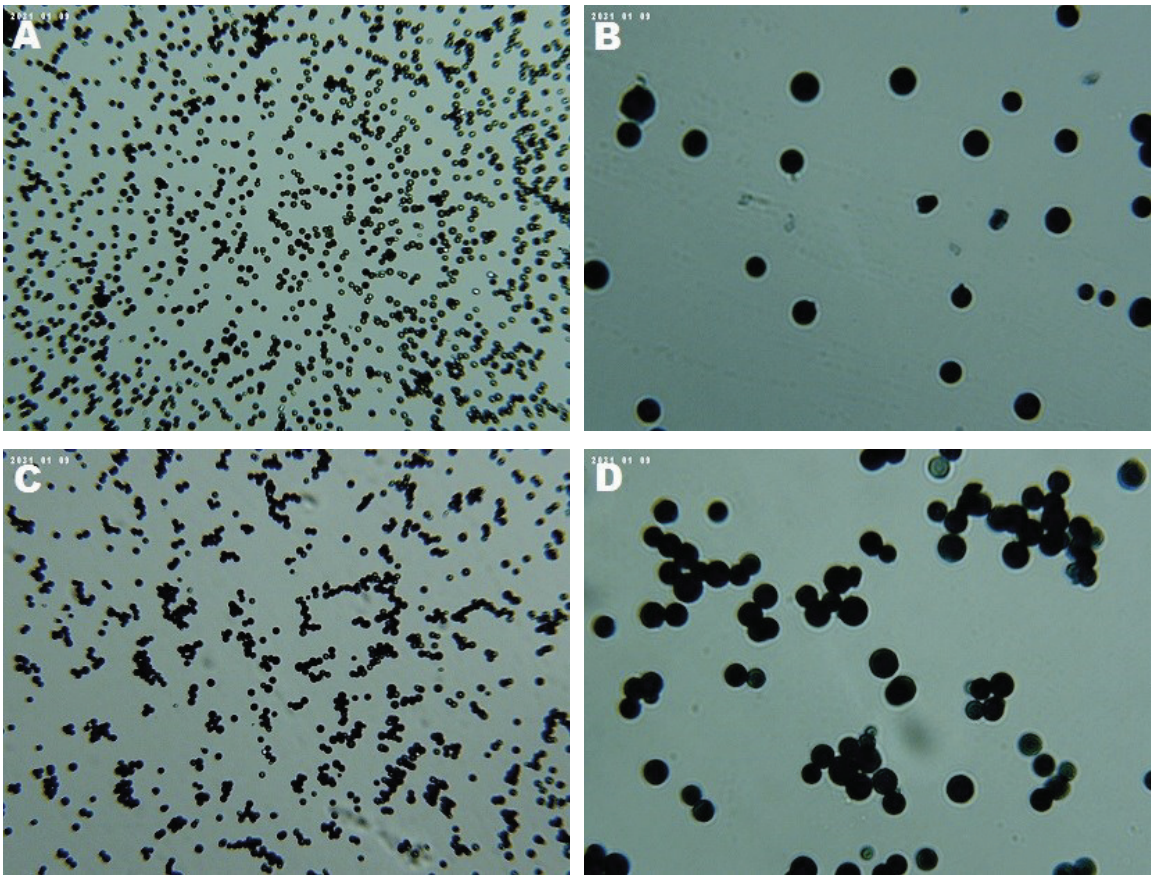

Figure 14 Optical microscopy images of PANI-SiO_2 particles dispersed in non-agglomerating slurry solvent (50/50 (v/v) MeOH/H_2O) magnified 400 × (A); 1200 × (B); and the same particles dispersed in agglomerating packing solvent (65/35 (v/v) ACN/H_2O) magnified 400 × (C); 1200 × (D)

4.1.6 Walters test

Besides the systematic characterization using LSER approach, PANI-SiO_2 and PANI-C_{18} stationary phases were subjected to the empirical Walters test. This chromatographic test was originally designed to evaluate hydrophobicity and activity of residual free silanols (related to polarity) of columns packed with RP stationary phases [208]. Hydrophobicity index (HI) is herein defined as the ratio of retention factor of anthracene to retention factor of benzene. Silanol index (SI) is defined as the ratio of retention factor of *N*,*N*-diethyl-*m*-toluamide to retention factor of anthracene. The mobile phase used to evaluate HI and SI consists of 65/35 (v/v) ACN/H_2O and pure ACN, respectively. The other experimental conditions were modified for capillary columns: flow rate was 5 µL/min (corresponding to 1 mL/min in 4.6 mm i.d.

conventional column), injection volume 0.1 µL, column temperature of 40 °C, and UV detection wavelength set to 254 nm. The stock solution concentrations were 1 mg/mL for anthracene, and 20 µL/mL for benzene and *N*,*N*-diethyl-*m*-toluamide, respectively.

The obtained parameters of Walters test are shown in Table 4. Hydrophobicity of both PANI-SiO_2 and PANI-C_{18} sorbents evaluated by Walters test is lower than of common RP stationary phases whose values range approximately from 2 to 6, depending on ligand used [308-310]. This observation can be explained by the nature of PANI which is less hydrophobic compared to $C_{18,}$ C_8 or phenyl alkyls due to presence of polar amino and imino moieties in the structure. Slightly higher HI value for PANI-C_{18} is attributed to C_{18} grafted to the supporting SiO_2. However, it is evident that PANI coating affects HI value dominantly.

Silanol activity is of medium value for both sorbents; moderate values of RP phases are set from 0.9 to 1.2. For PANI-SiO_2 sorbent, the original surface is coated with the protective layer of PANI hindering thus access of solutes to free silanols. For PANI-$C_{18,}$ the original surface is moreover sterically protected by long, grafted C_{18} ligands. The possible explanation of almost identical SI values for both sorbents is that the electrostatic attraction between deprotonated superficial silanols and partially protonated PANI layer is likely stronger than that when the non-polar C_{18} interface is embedded, therefore, lower amount of free silanols is available. Conversely, C_{18} ligand is grafted by silylation reaction directly to the silanol group, thus lowering the number of residual, un-modified silanols [6].

Table 4 Parameters of Walters test

	PANI-SiO_2	PANI-C_{18}
HI	1.73	1.86
SI	0.97	0.95

5. PUBLICATION II – Study of polyaniline-coated silica gel as a stationary phase in different modes of capillary liquid chromatography

Taraba L., Křížek T.

Monatshefte für Chemie 148 (2017) 1605–1611

Monatsh Chem (2017) 148:1605–1611
DOI 10.1007/s00706-017-1965-1

ORIGINAL PAPER

Study of polyaniline-coated silica gel as a stationary phase in different modes of capillary liquid chromatography

Lukáš Taraba[1] · Tomáš Křížek[1]

Received: 3 January 2017 / Accepted: 19 March 2017 / Published online: 3 July 2017

Abstract Separation potential of a stationary phase based on polyaniline-coated silica gel porous spherical particles was investigated in different chromatographic modes of capillary liquid chromatography. L-Tryptophan and three of its structural derivatives with modified amino or carboxylic functionality were used to investigate the retention factor curves under different mobile phase composition including pH variation. Some retention curves pass minimum which indicates that more than one chromatographic mode can be employed to retain the relevant solute. The positional isomers of aminoacetophenone and caffeine and its demethylated analogs—theobromine and theophylline—were used as separation probes in normal phase, hydrophilic interaction liquid chromatography, and reversed phase modes. The stationary phase exhibits the mixed-mode retention mechanism; therefore, it is not easy to predict the elution order of the solutes only according to their polarity. Even slightly hydrophilic compounds can be sufficiently retained in reversed phase mode using polyaniline-coated silica gel stationary phase. All positional isomers of aminoacetophenone were separated for the first time in normal phase and reversed phase modes.

Graphical abstract

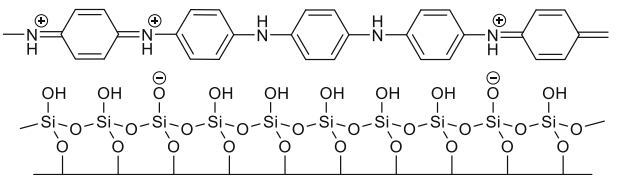

Keywords High pressure liquid chromatography · Material science · Stationary phase · Structure–activity relationships · Polyaniline

Introduction

Contemporary separation science must meet the requirements arising from steadily rising number of miscellaneous compounds with various chemical structures. The design, preparation and characterization of novel stationary phases are thus of unceasing interest.

Modification of the original sorbent, most often silica gel (either superficially or totally porous), by silylation and further attachment/interchange of a broad range of functionalities represent the most frequent technique at the present time [1]. However, it may include a rather complicated, multiple-step preparation process with low yields; especially for stationary phases with more than one functional moiety [2, 3]. Modification of the original sorbent with a polymer coating of a desirable structure offers a promising alternative [4–6]. This way comprises a rapid, sometimes only one-step procedure to obtain a required change of properties [7, 8]. The new sorbent maintains the mechanical stability of the original, usually inorganic,

✉ Tomáš Křížek
krizek@natur.cuni.cz

[1] Department of Analytical Chemistry, Faculty of Science, Charles University, Hlavova 8, 128 43 Prague, Czech Republic

substrate and acquires chemical resistance from the polymer [9, 10]. A combination of the two individual materials may lead to unexpected, even multimodal, retention ability and unique selectivity. It is generally supposed that polymer-coated stationary phases should provide better shielding of residual silanol groups and improve the protection of the silica support against alkaline mobile phase; moreover, they are significantly more resistant to acidic hydrolysis compared to the attached monomeric ligands [4].

The cohesion of the substrate and surface modifier is based either on chemisorption or physisorption. However, one has to take into account that only a small fraction of yet known polymers attach covalently to the silica substrate without initial silylation or gamma ray irradiation [11–13]. Besides covalent attachment, polymers can be immobilized on the surface of the substrate either by sorption of pre-synthesized polymer layers or in situ chemical/electrochemical polymerization of monomers sorbed onto the support [14–18]. Alas, the typical binding energy of physisorption is at least one order of magnitude lower than that of chemisorption; thus, it is not easy to find a suitable, satisfactorily cohesive polymer which has required properties.

Polyaniline (PANI) is a readily synthesized polymer occurring in three different states depending on the degree of protonation and the oxidation state as fully protonated leucoemeraldine, partly protonated emeraldine (Fig. 1) or fully deprotonated pernigraniline. PANI has an advantageous feature that during polymerization, besides a bulk precipitate, it forms thin layers on the surface of the material in direct contact with the polymerization mixture, regardless of the material [19–25].

Emeraldine, a highly stable, semiconductive form of polyaniline, has been investigated as a surface modifier for multiple applications, such as flexible electrodes, photovoltaic devices, anticorrosive coatings or catalysts [26, 27]. Some attempts have been made to employ polyaniline coatings as an inner-wall modifier in CZE and continuous flow analysis, monolith in microfluidic channel, or as a sorbent for SPME and TLC [28–34]. Stejskal et al. developed a simple coating method based on in situ polymerization of PANI on spherical silica gel dispersed in a reaction mixture containing aniline hydrochloride and ammonium persulfate [35]. Sowa et al. adopted the latter approach to synthesize the stationary phase and studied its potential application in non-suppressed ion chromatography [36, 37].

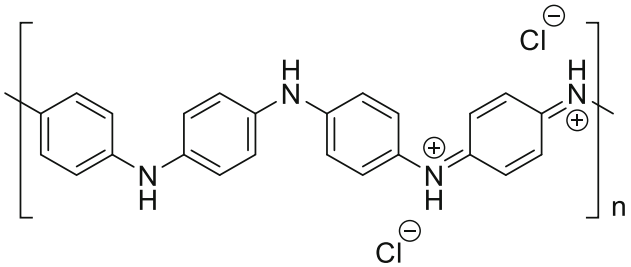

Fig. 1 Chemical structure of partly protonated polyaniline—emeraldine salt

In our previous work, we characterized polyaniline-coated silica gel (PANI–SiO_2) and octadecyl silica (PANI–C_{18}) spherical particles using the linear solvation energy relationship (LSER) approach extended with ionic interactions terms in hydrophilic interaction liquid chromatography (HILIC) mode [38]. A mixed-mode retention mechanism was observed. Individual interactions taking place here correspond to the structure of PANI–SiO_2; specifically, benzene rings enable π–π stacking, amino and imino moieties act as hydrogen bond (H-bond) acceptors or anion exchangers, and residual silanols behave as H-bond donors or cation exchangers. Especially anionic and zwitterionic solutes exhibit a considerable retention under HILIC conditions.

In this study, we have investigated the separation potential of this multimodal stationary phase using structurally similar compounds in HILIC mode as well as in normal phase (NP) and reversed phase (RP) modes.

Results and discussion

Investigation of retention factor curves

In the first part of the study, L-tryptophan (Trp) and its three derivatives L-tryptophan methyl ester hydrochloride (MeE-Trp), *N*-acetyl-L-tryptophan (NAc-Trp), and N_α-(*tert*-butoxycarbonyl)-L-tryptophan (Boc-Trp) were chosen to assess the retention ability of PANI–SiO_2 under different pH (50 mM HCOOH, pH 2.5 and 10 mM Tris–HCl buffer, pH 8.0) and content of acetonitrile (ACN; 10–90%; v/v) as an organic modifier in eluent. Chemical structures of relevant solutes are depicted in the top row in Fig. 2. These compounds have diverse values of pK_a and distribution coefficient (log $D_{o/w}$), see Table 1. Therefore, their combination in testing can provide a deeper insight into retention properties of the stationary phase.

As PANI–SiO_2 offers the mixed-mode retention mechanism, we assumed that the retention factor (k) curve would pass the minimum when the ratio of organic/aqueous constituent in the binary eluent is close to unity under both acidic and basic conditions. According to the obtained k values, our assumption was indeed confirmed and thus we can switch between different modes (Fig. 3).

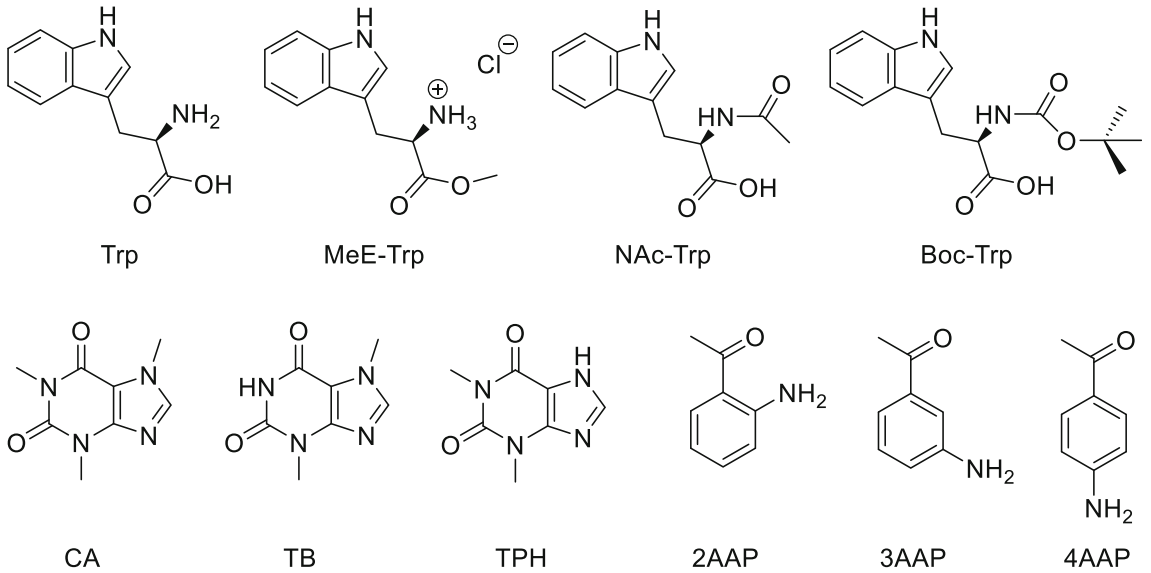

Fig. 2 Chemical structures of tested solutes; *Trp* L-tryptophan, *MeE-Trp* L-tryptophan methyl ester hydrochloride, *NAc-Trp* *N*-acetyl-L-tryptophan, *Boc-Trp* N_{α}-(*tert*-butoxycarbonyl)-L-tryptophan, *CA* caffeine, *TB* theobromine, *TPH* theophylline, *2AAP* 2′-aminoacetophenone, *3AAP* 3′-aminoacetophenone, *4AAP* 4′-aminoacetophenone

Table 1 Values of pK_a of functionalities and distribution coefficients of solutes used for retention factor measurement under different mobile phase composition

Solute	pK_a^a		log $D^a_{o/w}$	
	–COOH	–NH_2	pH 2.5	pH 8.0
Trp	2.54	9.40	−1.79	−1.58
MeE-Trp		6.92	−2.12	1.25
NAc-Trp	4.12		1.07	−2.39
Boc-Trp	4.13		2.53	−0.93

[a] The values were computed by Marvin software [39]

The retention of Boc-Trp and NAc-Trp is considerable as they are both hydrophobic in an acidic mobile phase with high content of water (RP mode). In addition, it appears that the presence of *tert*-butyl group in Boc-Trp contributes to the increased retention when compared to NAc-Trp. In contrast to this, Trp and MeE-Trp are retained very poorly since they are hydrophilic. Moreover, protonated nitrogen atoms of PANI repel their underivatized, positively charged amino moieties.

On the other hand, all solutes are retained to a certain extent in the eluent with the low content of acidic aqueous component (HILIC mode). Boc-Trp is the lowest retained solute as it has only partly dissociated carboxylic group and its carbonyl oxygen, able to act as an H-bond acceptor, is sterically shielded by a bulky branched-alkyl residue, as was confirmed by 3D structure modeling in the Marvin software [39]. Interaction of MeE-Trp with the stationary phase is limited by its methyl esterification and persisting protonation of the amino group. Compared to its derivatives, native Trp has relatively low value of the carboxylic group pK_a, which is close to the pH value of the mobile phase. Therefore, we can suppose its significant involvement in ionic or H-bonding interactions. Although NAc-Trp has almost identical calculated value of carboxylic pK_a as Boc-Trp (i.e., 4.12 and 4.13, respectively), its unshielded acetyl oxygen can act as a strong H-bond acceptor. The assumed ability of NAc-Trp to interact intensively with the stationary phase is in accordance with the observed highest retention time of NAc-Trp.

Also in the alkaline eluent, Boc-Trp and NAc-Trp are strongly retained despite their hydrophilic character given by dissociation of carboxylic groups. On the contrary, MeE-Trp turns hydrophobic. According to the retention factors of the solutes, it seems that ionic and/or H-bonding interactions can support or even outmatch the influence of hydrophobicity on overall solute retention on this multimodal stationary phase, despite the fact that hydrophobicity is generally considered as dominant criterion for solute retention in RP mode. The enhanced retention may also be affected by substantially lower electrostatic repulsion of solute's amino moiety and PANI–SiO_2 stationary phase.

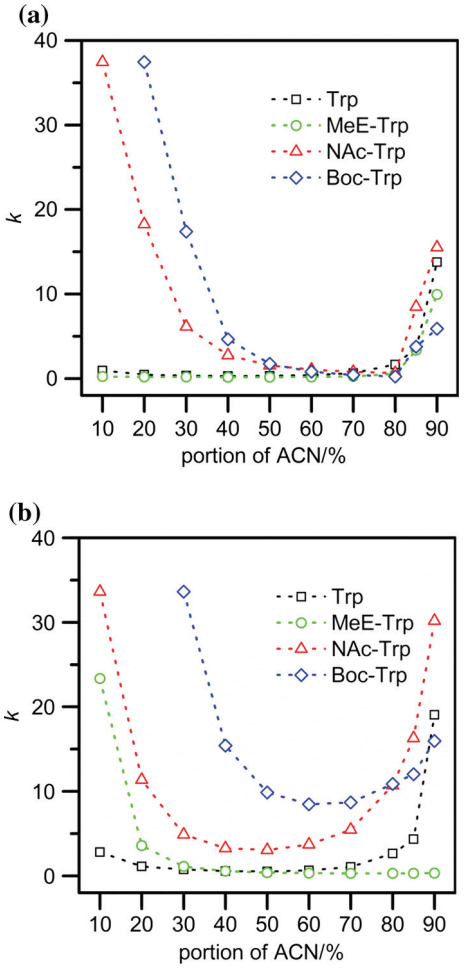

Fig. 3 Dependence of retention factor of Trp and its derivatives on content of ACN in the eluent with acidic—50 mM HCOOH, pH 2.5 (**a**) or alkaline—10 mM Tris–HCl, pH 8.0 (**b**) aqueous constituent, separation conditions: PANI–SiO_2 170 mm × 0.32 mm, temperature 50 °C, flow rate 15 mm^3/min, UV detection at 230 and 265 nm; *dotted lines* connect relevant points for better visualization of trends

Ionic interactions and H-bonding are obviously prevailing in HILIC mode, so only hydrophobic MeE-Trp has low retention factor in alkaline mobile phase. When comparing retention of the solutes in acidic or alkaline eluent, it is evident that the latter is always higher in both RP and HILIC mode. MeE-Trp in HILIC mode represents an exception from this behavior because of its sterically protected carboxylic group.

Separation of solutes in different chromatographic modes

In the second part of the study, two sets of structurally similar neutral compounds (Fig. 2, bottom row) having either slightly hydrophilic or hydrophobic character, were chosen for investigation of the separation potential of PANI–SiO_2 in NP, HILIC, and RP modes. The first set consisted of caffeine (CA, log $D_{o/w} = -0.79$) and its less methylated derivatives—theobromine (TB, log $D_{o/w} = -1.03$) and theophylline (TPH, log $D_{o/w} = -1.03$). The second one involved 2′-aminoacetophenone (2AAP, log $D_{o/w} = 1.22$) and its positional analogs 3′-aminoacetophenone (3AAP, log $D_{o/w} = 0.57$) and 4′-aminoacetophenone (4AAP, log $D_{o/w} = 0.57$).

In NP mode, the resolution higher than 1.5 was achieved for both sets of solutes using pure ACN (mild elution strength) as the eluent (Fig. 4a, d). Elution order of the compounds is given by their increasing polarity. Under the same conditions, CA and its derivatives are more retained and separated than positional analogs of AAP as they are more polar. For structurally similar solutes, having very similar log $D_{o/w}$ values and

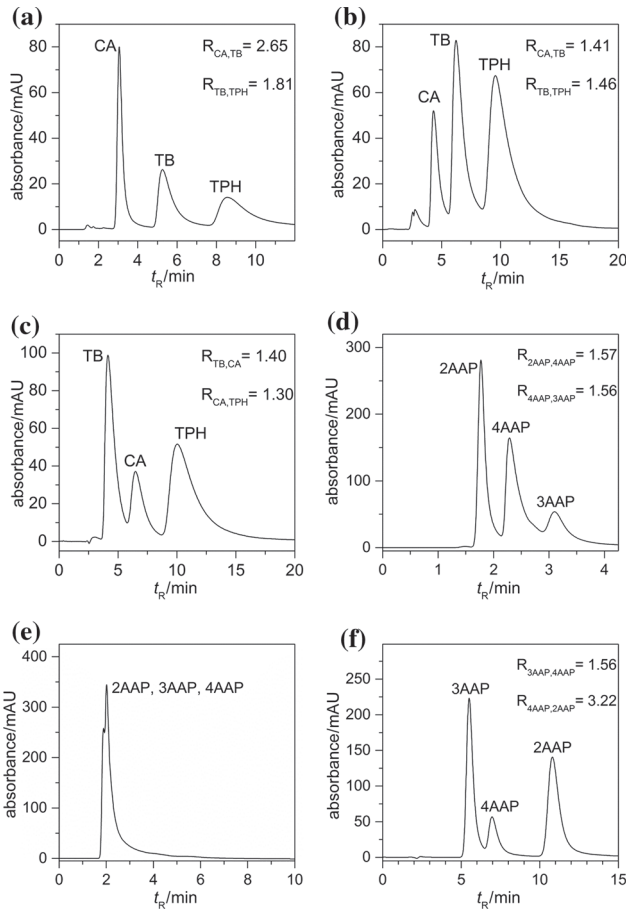

Fig. 4 Different chromatographic modes used for separation of CA and its demethylated derivatives in NP (**a**), HILIC (**b**) and RP (**c**) modes, and positional isomers of AAP in NP (**d**), HILIC (**e**) and RP (**f**) modes, separation conditions: PANI–SiO_2 170 mm × 0.32 mm, temperature 25 °C, flow rate 5 mm^3/min (AAPs in RP mode 10 mm^3/min), UV detection at 265 nm for mixture of CA, TB, TPH and 230 nm for mixture of AAPs, mobile phase composition: NP—100% ACN, HILIC—98/2 ACN/H_2O (v/v), RP—20/80 ACN/ H_2O (v/v); chromatograms are accompanied by peak resolution values

insignificant or irrelevant difference in functionalities pK_a, such as for TB–TPH or 3AAP–4AAP pairs, other effects on retention should be considered. In the first case, it is steric accessibility of less shielded secondary amine group (7-labeled nitrogen atom in TPH structure) for H-bonding compared to the same, however, shielded functionality in TB (1-labeled nitrogen atom). The other pair is an example of different dislocation of electron density provided by mesomeric effect of amino and acetyl functionalities of AAPs. Whereas amino group acts as an electron donor and *ortho* and *para* activator, acetyl acts as an electron withdrawing group and *meta*-directing deactivator. This results in an increased electron density in *meta* position of 4AAP as compared with 3AAP.

In HILIC mode (Fig. 4b), the resolution of CA, TB, and TPH is somewhat decreased but the overall retention of TB and TPH is higher in comparison with NP mode (Fig. 4a). On the other hand, very poor retention and separation of AAPs are attributed to their low polarity (Fig. 4e).

Despite the significant change of the eluent composition (i.e., portion of ACN), TPH remained the most retained solute of the set even in RP mode (Fig. 4c). We may find explanation in the very strong H-bonding interaction between TPH and the PANI–SiO_2 mixed-mode stationary phase. The expected shift of the elution order and a substantial increase of the retention were observed for AAPs in RP mode; it is worth noting that the resolution higher than 1.5 was maintained even with doubled flow rate (Fig. 4f).

Another chromatographic parameters such as the theoretical plate number (N) and peak asymmetry (A_s), giving the additional information about column performance, are stated in Tables 2 and 3 for both CA–TB–TPH and AAPs sets. Moreover, the tables include data about column performance of columns packed with commercially available sorbents such as bare silica gel (SiO_2) and octadecyl silica (C_{18}), packed under the same conditions as PANI–SiO_2 column.

In general, HILIC and RP modes offer quite comparable values of the resolution and analysis time for CA–TB–TPH solute set; nevertheless, the best results were achieved in NP mode. Also for AAP testing set the most suitable separation in terms of sufficient peak resolution and analysis time was observed in NP mode, although RP mode offers higher value of peak resolution. When comparing the solute sets in terms of column performance, the theoretical plate number is generally higher for less polar AAPs set, whereas peak asymmetry is comparable with the other set. Chromatographic performance of the PANI–SiO_2 sorbent was compared with commercial SiO_2 and C_{18} stationary phases using the same separation conditions. Significantly lower selectivity was achieved on the column packed with the commercial SiO_2 stationary phase where the analytes mostly co-eluted in a single peak. Column efficiency was also lower than for the other sorbents. Use of commercial C_{18} stationary phase provides column efficiency comparable to PANI–SiO_2 (with exception of N_{2AAP} that was roughly twice higher), although it needs twofold analysis time. It is worth noting that observed elution

Table 2 Comparison of chromatographic parameters for the separation of CA–TB–TPH set on different stationary phases in different chromatographic modes

Stationary phase	Chromatographic mode														
	NP					HILIC					RP				
	Solute	t_R/min	A_s	N	R[c]	Solute	t_R/min	A_s	N	R	Solute	t_R/min	A_s	N	R
PANI–SiO_2	CA	3.06	0.51	748			4.32	0.39	247			6.48	0.51	188	1.40
	TB	5.26	0.42	301	2.65		6.23	0.40	240	1.41		4.14	0.37	135	
	TPH	8.59	0.45	199	1.81		9.56	0.43	165	1.46		10.03	0.39	128	1.30
SiO_2[a]	Split[d]	3.09				Single[e]	4.05	0.50	116						
		3.87			0.63										
C_{18}[b]											Split	3.55			
												4.80			0.79

[a] Bare silica gel, other sorbent parameters are stated in the experimental section

[b] Octadecyl bonded silica gel, other sorbent parameters are stated in the experimental section

[c] The value of the peak resolution is always given next to the more retained solute

[d] Split means splitted peak of partially separated analytes

[e] Single means single peak of co-eluting analytes

Table 3 Comparison of chromatographic parameters for the separation of AAPs set on different stationary phases in different chromatographic modes

Stationary phase	Chromatographic mode														
	NP					HILIC					RP				
	Solute	t_R/min	A_s	N	R[c]	Solute	t_R/min	A_s	N	R	Solute	t_R/min	A_s	N	R
PANI–SiO_2	2AAP	1.77	0.52	955		Split[d]	1.88					10.80	0.61	1119	3.22
	3AAP	3.10	0.62	426	1.56		2.02			0.43		5.51	0.60	794	
	4AAP	2.29	0.32	489	1.57							6.96	0.63	714	1.56
SiO_2[a]	Single[e]	1.80	0.46	152		Single	1.78	0.39	194						
					0.63										
C_{18}[b]											2AAP	22.13	0.43	2478	2.54
											3AAP	8.72	0.40	561	1.13
											4AAP	7.73	0.80	634	

[a] Bare silica gel, other sorbent parameters are stated in the experimental section

[b] Octadecyl bonded silica gel, other sorbent parameters are stated in the experimental section

[c] The value of the peak resolution is always given next to the more retained solute

[d] Split means splitted peak of partially separated analytes

[e] Single means single peak of co-eluting analytes

order of 3AAP and 4AAP is inversed to PANI–SiO_2, thereby proving a unique selectivity of this stationary phase. In addition, use of the C_{18} stationary phase for more hydrophilic CA–TB–TPH set separation is unprofitable.

Conclusion

In this study, we confirmed our previous assumption that polyaniline-coated silica gel behaves as a multimodal stationary phase. On the basis of experimental data, it was testified that retention factor curve of different-polarity solutes passes the minimum when the portion of acetonitrile in the eluent is roughly the same as portion of the aqueous component. Therefore, it is possible to utilize more than only one separation mode. As the stationary phase exhibits the mixed-mode retention mechanism, it is not possible to simply predict the retention of solutes based only on their polarity. Other factors including hydrogen bonding and ionic interactions and even structural isomerism should be taken into account as well.

We investigated separation potential of this stationary phase on two sets of structurally similar, either slightly hydrophilic or hydrophobic solutes. We found out that even some hydrophilic solutes can be remarkably retained in reversed phase mode. Next, we successfully separated caffeine, theobromine and theophylline in normal, reversed and hydrophilic interaction liquid chromatography modes. Further, to the best of our knowledge, this is the first time when all three positional isomers of aminoacetophenone were sufficiently separated.

Experimental

Acetonitrile, methanol (both of HPLC gradient grade), aniline hydrochloride, ammonium persulfate, and all solutes used in this work (all of analytical grade purity) were purchased from Sigma-Aldrich (St. Louis, MO, USA). Formic acid, hydrochloric acid (35%) and tris(hydroxymethyl)aminomethane (Tris) were supplied by Lachner (Neratovice, Czech Republic). The deionized water was purified with a Milli-Q water purification system from Millipore (Bedford, MA, USA). The deionised water was used as a complementary solvent in all binary mixtures in this study. Tris–HCl buffer was prepared by dissolving the appropriate amount of Tris in deionized water; the required pH value was adjusted by titration with concentrated HCl. Solute solutions were prepared in a concentration range of 0.05–1.0 mg/cm^3 either in pure ACN or in ACN/water mixture (50/50; v/v), depending on their solubility.

Instrumentation

The preparation of PANI–SiO_2 sorbent and the capillary packing procedure are briefly described below (for the detailed description of the procedure, see Ref. [38]).

Original bare silica gel (Hypersil, Shandon Southern Instruments, Cheshire, UK; spherical, average particle size 5 μm, average pore size 12 nm) was modified with PANI coating by in situ chemical polymerization of aniline hydrochloride; ammonium persulfate was employed as the polymerization initiator. The sorbent was subsequently collected on a filter and repeatedly rinsed with small portions of diluted HCl, organic solvents and water to remove all possible impurities. Approximate thickness of PANI layer on silica gel substrate is 200 nm. Prepared PANI–SiO_2 sorbent was then slurry packed into a column made of a polyimide-coated fused silica capillary (Supelco, Bellefonte, PA, USA; 170 mm × 0.32 mm i.d., 0.43 mm o.d.) with an outlet stainless steel frit inserted into a PEEK union. As the slurry solvent 50% methanol (v/v) was used to obtain a slurry concentration of 20 mg/cm^3. The column was packed at a pressure of 25 MPa using 65% ACN (v/v) as a packing solvent. Other sorbents used in this study, i.e., the bare silica gel (Hypersil, for parameters description see above) and the octadecyl silica (Nucleosil C_{18}, Macherey-Nagel, Düren, Germany; spherical, average particle size 5 μm, average pore size 10 nm, carbon load 15%) were packed into columns under the same conditions as PANI–SiO_2.

Chromatographic measurements were performed using an Agilent 1200 Capillary LC System (Agilent Technologies, Waldbronn, Germany) consisting of a vacuum degasser, capillary binary pump, automated injector, column heating compartment and diode array detector. The ^{3D}HPLC ChemStation Software (Agilent Technologies) was used for acquisition and analysis of the experimental data. The injection volume was 0.1 mm^3 for all the solutes and the flow rate varied in the range of 5–15 mm^3/min. The capillary column was thermostated at 25 or 50 °C. UV detection was performed at 230 and 265 nm. The dead time was determined using a system peak.

Acknowledgements The study was financially supported by the Grant Agency of Charles University (Project No. 307015) and project SVV.

References

1. Kirkland JJ (2004) J Chromatogr A 1060:9
2. Zhang K, Liu X (2016) J Pharm Biomed Anal 128:73
3. Mansour FR, Danielson ND (2013) Anal Methods 5:4955
4. Faria AM, Collins CH, Jardim ICSF (2009) J Braz Chem Soc 20:1385
5. Zimmermann A, Horak J, Sievers-Engler A, Sanwald C, Lindner W, Kramer M, Lämmerhofer M (2016) J Chromatogr A 1436:73
6. Wang F, Dai X, Gong B (2010) J Appl Polym Sci 118:1513
7. Sapurina I, Riede A, Stejskal J (2001) Synth Met 123:503
8. Chriswanto H, Ge H, Wallace GG (1993) Chromatographia 37:423
9. Browne TE, Cohen Y (1993) Ind Eng Chem Res 32:716
10. Sowa I, Wojciak-Kosior M, Draczkowski P, Szwerc W, Tylus J, Pawlikowski A, Kocjan R (2015) Microchem J 118:88
11. Kurganov A, Davankov V, Isajeva T, Unger K, Eisenbeiss F (1994) J Chromatogr A 660:97
12. Hanson M, Kurganov A, Unger KK, Davankov VA (1993) J Chromatogr A 656:369
13. Tsuchida A, Suda M, Ohta M, Yamauchi T, Tsubokawa N (2006) J Polym Sci Part A Polym Chem 44:2972
14. Ohmacht R, Kele M, Matus Z (1989) Chromatographia 28:19
15. Schomburg G (1991) Trends Anal Chem 10:163
16. Janus L, Carbonnier B, Deratani A, Bacquet M, Crini G, Laureyns J, Morcellet M (2003) New J Chem 27:307
17. Carbonnier B, Janus L, Lekchiri Y, Morcellet M (2004) J Appl Polym Sci 91:1419
18. Chinn D, DuBow J, Liess M, Josowicz M, Janata J (1995) Chem Mater 7:1504
19. Riede A, Stejskal J, Helmstedt M (2001) Synth Met 121:1365
20. Ayad MM, Shenashin MA (2003) Eur Polym J 39:1319
21. Rozlivkova Z, Trchova M, Sedenkova I, Spirkova M, Stejskal J (2011) Thin Solid Films 519:5933
22. Salvatierry RV, Zitzer G, Savu SA, Alves AP, Zabrin AJG, Chasse T, Casu MB, Rocco MLM (2015) Synth Met 203:16
23. Job AE, Alves N, Zanin M, Ueki MM (2003) J Phys D Appl Phys 36:1414
24. Chen YJ, Kang ET, Neoh KG (2002) Appl Surf Sci 185:267
25. Ivanov S, Mokreva R, Tsakova V, Terlemezyan L (2003) Thin Solid Films 441:44
26. Boeva ZA, Sergeyev VG (2014) Polym Sci Ser C 56:144
27. Ibrahim M, Bassil M, Demirci UB, Khoury T, El Haj Moussa G, El Tahchi M, Miele P (2012) Mater Chem Phys 133:1040
28. Bossi A, Piletsky SA, Turner APF, Righetti PG (2002) Electrophoresis 23:203
29. Florea L, Diamond D, Benito-Lopez F (2013) Anal Chim Acta 759:1
30. Sowa I, Wojciak-Kosior M, Rokicka K, Kocjan R, Szymczak G (2014) Talanta 122:51
31. Mohammad A, Khatoon S, Khan AMT, Moheman A (2010) Arch Appl Sci Res 2:233
32. Siddiq A, Ansari MO, Mohammad A, Mohammad F, El-Desoky GE (2013) Int J Polym Mater Polym Biomater 63:277
33. Gorey B, Galineau J, White B, Smyth MR, Morrin A (2012) Electroanalysis 24:1318
34. Bagheri H, Banihashemi S (2014) Chromatographia 77:397
35. Stejskal J, Quadrat O, Sapurina I, Zemek J, Drelinkiewicz A, Hasik M, Krivka I, Prokes J (2002) Eur Polym J 38:631
36. Sowa I, Wojciak-Kosior M, Draczkowski P, Strzemski M, Kocjan R (2013) Anal Chim Acta 787:260
37. Sowa I, Kocjan R, Wojciak-Kosior M, Swieboda R, Zajdel D, Hajnos M (2013) Talanta 115:451
38. Taraba L, Krizek T, Hodek O, Kalikova K, Coufal P (2017) J Sep Sci 40:677
39. Marvin 16.4.11.0 (2015) ChemAxon, Budapest. http://www.chemaxon.com. Accessed 6 Oct 2015

5.1 Publication II - Non-published relevant data

This section contains non-published experimental data related to publication II with comments. The separation efficiency of PANI-SiO_2 stationary phase was evaluated with constructed van Deemter curves. Intraday repeatability and intermediate precision of retention time and peak area of selected probes as well as the comparison of chromatograms of solute separations on PANI-SiO_2 and commercial sorbents are shown below.

5.1.1 Separation efficiency – van Deemter curve

Chromatographic performance of the individual separation column is commonly described by parameters such as *k, α,* and *N* or HETP. In addition, van Deemter curve, expressing the separation efficiency as a function of the linear flow rate velocity *u* of the mobile phase allows description of diffusion-related processes taking place in the column. Unlike the plate model, van Deemter theory takes into account that solute equilibrium in the mobile and stationary phases is time-dependent [311, 312]. Van Deemter equation divides overall diffusion of the solute elution zone into three independent additive parts:

$$\mathrm{HETP} = A + \frac{B}{u} + (C_m + C_s)\,u = 2\lambda d_p + \frac{2\gamma_p D_m}{u} + \left[\frac{\psi' d_p}{D_m} + \frac{\psi d_f^2 k}{D_s(k+1)^2}\right] u \qquad (9)$$

where A term stands for eddy diffusion, B term is longitudinal diffusion, C_m and C_s terms express mass transfer resistance in the mobile phase and stationary phase, respectively, λ is flow path inequality coefficient, γ_p packing impedance factor, D_m stands for diffusion coefficient in the mobile phase, ψ' is dimensionless sorbent type related coefficient, ψ is coefficient comprising effects of sorbent shape and size distribution and pore shape and size distribution, d_f stands for thickness of particle porous layer, D_s is diffusion coefficient in the stationary phase.

Van Deemter curve was constructed for PANI-SiO_2 packed columns using caffeine (CA, log *D* = -0.79, concentration of 3 mg/mL) and toluene (TO, log *D* = 2.51, concentration of 10 μL/mL) as probes in mobile phases consisting of 95/5 (v/v) ACN/H_2O (HILIC mode, Figure 15A) and 50/50 (v/v) ACN/H_2O (RP mode, Figure 15B). The measurements were performed on single-piston 100DM syringe pump

(ISCO, Lincoln, NE, USA) equipped with automatic gearbox. UV detection at 254 nm was accomplished using UVIS-205 absorbance detector (Linear Instruments, San Jose, CA, USA). Connection of these instruments enables to perform chromatographic analysis with minimal extra-column contributions to the void volume, however, manual sample injection and hand-operated analysis launching are necessary. It is worth noting that all the measurements, related to van Deemter curve, were performed on a single column unless stated otherwise.

According to values of HETP as a function of u, it seems that van Deemter curve increases monotonously in both eluents tested without passing any minimum. CA was more retained on the stationary phase (data not shown) and showed higher values of HETP regardless of the mobile phase used. HETP values, calculated from experimental data (closed symbols in Figure 15), were fitted (dotted line) to the first part of Eq. (9) using Solver function in Microsoft Excel software in order to obtain values of A, B and ($C_m + C_s$) terms applying the least squares method; tightness of the fit was expressed by R^2. The terms C_m and C_s were evaluated as their sum. The relevant term values are attached in the form of a table to the corresponding van Deemter curves in Figure 15.

A term has the highest value in all cases (albeit it is lower for the less retained probe), therefore, eddy diffusion most contributes to the overall elution diffusion. This phenomenon can be explained by broad size distribution of packed particles size (as shown in Figure 9A) as well as by the loosely packed capillary column bed; within which wall effects manifest themselves significantly. Axial trans-column diffusion, covered by B term, is basically insignificant under the given conditions; B term has non-zero value only for the weakly retained probe, inhere TO in HILIC mode. Accordingly, no curve minimum was observed. The value of ($C_m + C_s$) sum is directly proportional to d_f^2 of fully porous SiO_2 particles coated with porous PANI layer whose D_s is not known. It is worth noting that PANI coating is substantially thicker (≈ 0.2 μm) than common organic-ligand-modified stationary phase (units of nm [313, 314]). Additionally, the higher value of ($C_m + C_s$) in 50/50 (v/v) ACN/H_2O mobile phase relates to its higher η_{kin} (i.e., $1.03 \cdot 10^{-6}$ m^2/s) compared to 95/5 (v/v) ACN/H_2O ($0.54 \cdot 10^{-6}$ m^2/s) because of D_m being inversely proportional to solvent viscosity. Taking into account that van Deemter equation is a non-trivial function, values of $R^2 \geq 0.9460$ prove well-fitted experimental data to the theory.

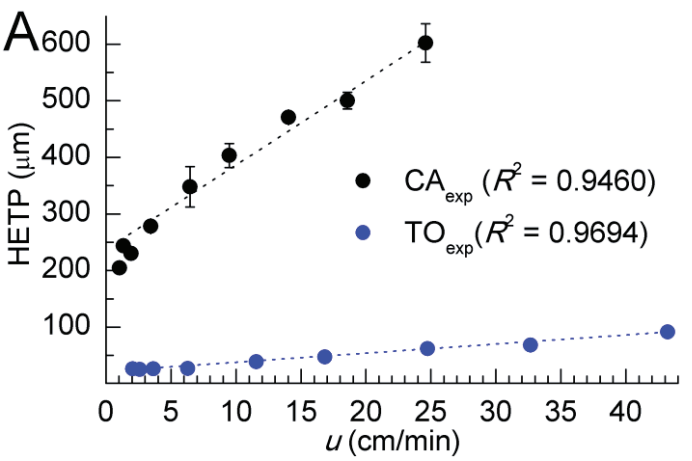

	CA	TO
A	237.4	18.4
B	0	6.1
$(C_m + C_s)$	14.9	1.7

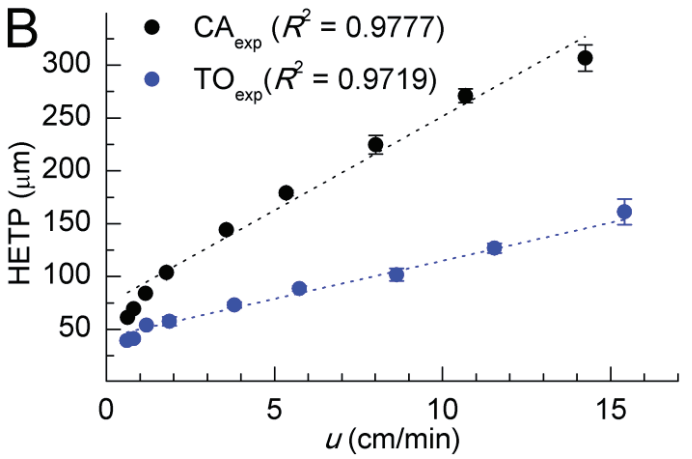

	CA	TO
A	73.3	42.7
B	0	0
$(C_m + C_s)$	17.8	7.2

Figure 15 Van Deemter curves for CA and TO probes in 95/5 (v/v) ACN/H_2O (A), 50/50 (v/v) ACN/H_2O (B) eluents accompanied with terms of van Deemter equation and R^2 expressing tightness of fit; dotted line denotes experimental data fit to Eq. (9)

To support the relevancy of found results, van Deemter curves for completely different probes in different eluents, tested in different PANI-SiO_2-packed capillary columns and measured in different settings (constant pressure vs. constant flow rate) were constructed (Figure 16). Thiourea (TU, $\log D$ = -0.57, concentration of 0.1 mg/mL, dissolved in 50/50 (v/v) ACN/H_2O and measured under constant pressure) and AC ($\log D$ = 0.38, concentration of 20 μL/mL, dissolved in H_2O and measured under constant flow rate) were used as probes. Mobile phases used are identical to the stock solution of the solutes.

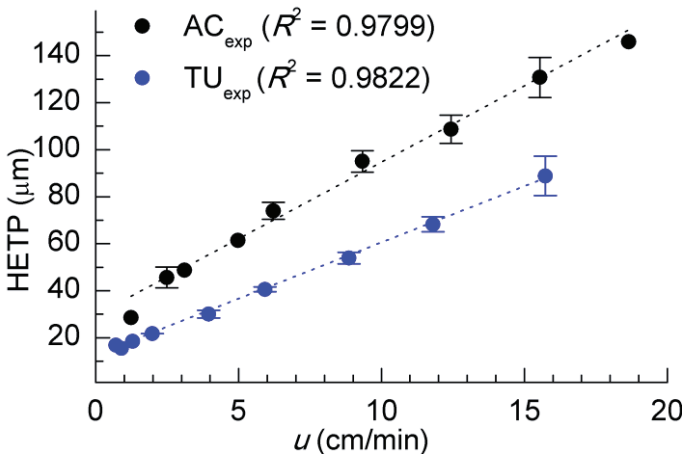

	AC	TU
A	29.4	10.2
B	0	1.9
$(C_m + C_s)$	6.5	4.9

Figure 16 Van Deemter curves for AC and TU probes in pure H_2O and 50/50 (v/v) ACN/H_2O eluents, respectively, accompanied with terms of van Deemter equation and R^2 expressing tightness of fit; dotted line denotes experimental data fit to Eq. (9)

Despite completely different setting of the measurement and the fact that AC was less retained than TU (data not shown), constructed van Deemter curves look similar to the previous ones, therefore the same conclusion applies. Interestingly, HETP value for TU at $u \approx 1$ cm/min reaches 3 d_p of average PANI-SiO_2 particle, which meets HETP requirements of contemporary commercial sorbents.

According to results for all constructed van Deemter curves, HETP value decreases with decreasing flow rate. However, to keep the stable flow rate lower than 3 μL/min without any pressure fluctuation or incidentally stopped flow is still demanding to contemporary instrumentation, especially when binary or quaternary pump is used. Therefore, flow rate of 5 μL/min was used mostly for the chromatographic measurements in this thesis. The used binary pump ensures stable pressure for such a value if a proper correction to compressibility of the used solvents and their mixtures is applied. Additionally, flow rate of 5 μL/min in the capillary column of 0.32 mm i.d. (Figure 17) corresponds to commonly used flow rate of 1.0 mL/min in analytical column of 4.6 mm i.d..

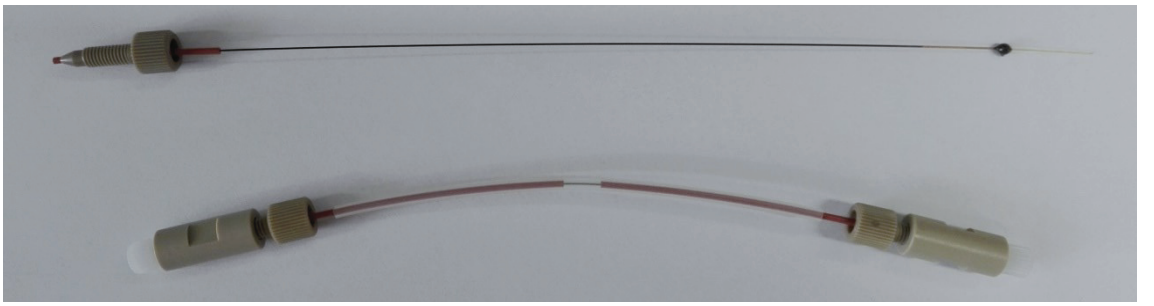

Figure 17 Capillary columns used in this thesis; both columns have equal dimensions of 170 mm × 0.32 mm; upper column type with inserted quartz wool frit and capillary of lower diameter cemented with epoxy adhesive was used for preliminary experiments and during measurements of van Deemter curves; bottom column type with stainless steel frit-like screens inserted into PEEK unions and mounted by tightened fitting, bare silica capillary was encased in PEEK and PTFE tubing to prevent its damage

5.1.2 Intraday repeatability and intermediate precision of retention time and peak area

Intraday repeatability of retention time and peak area of selected probes – TO and TU (concentration of 10 µL/mL and 0.1 mg/mL, respectively) – in capillary column packed with PANI-SiO_2 were assessed in HILIC and RP modes (Table 5); flow rate 5 µL/min, injection volume 0.1 µL, UV detection at 254 nm.

Table 5 Repeatability (RSD) and intermediate precision (ΔRSD) of retention time (t_R) and peak area (A_p) of selected probes (n = 5)

	HILIC[a)]				RP[b)]			
	TO		TU		TO		TU	
	t_R	A_p	t_R	A_p	t_R	A_p	t_R	A_p
RSD [%]	0.77	1.03	0.79	1.76	1.87	4.87	2.77	3.27
ΔRSD [%]	0.64	1.07	0.68	0.60	0.39	0.85	1.38	3.86

[a)] Mobile phase composition: 95/5 (v/v) ACN/H_2O

[b)] Mobile phase composition: 50/50 (v/v) ACN/H_2O

According to the results, intraday relative standard deviation (RSD) of retention time and peak area of both probes are higher in RP mode. However, the highest RSD value is < 3 % for the retention time and < 5 % for the peak area. Surprisingly,

intermediate precision (ΔRSD) expressing the difference of intraday RSD values is for both retention time and peak area higher for TU in RP mode, whilst for TO both these quantities are lower. However, all the values are still < 2 % for the retention time and < 4 % for the peak area. All the obtained values are acceptable for cLC.

5.1.3 Chromatographic comparison of stationary phases

The non-published comparison of chromatograms showing separations of three caffeine-related solutes and three aminoacetophenone positional isomers on PANI-SiO_2 and commercially available bare SiO_2 (Hypersil) or C_{18} (Nucleosil C_{18}) stationary phases is displayed in Figure 18. Bare SiO_2 was employed as comparative sorbent in NP and HILIC modes, whereas C_{18} was used in RP mode. From the chromatograms is clear that both selectivity and peak resolution are substantially higher on PANI-SiO_2 than on bare SiO_2 for both given sets of solutes in NP mode. The same applies for caffeine-related set of solutes in HILIC mode. The chromatograms of aminoacetophenone isomers in HILIC mode are very similar regardless the stationary phase used. Separation performance of both columns is poor presumably due to the lower polarity of aminoacetophenones.

In RP mode, certain separation of caffeine-related solutes was observed when C_{18} sorbent was used, however, theobromine (TB) and theophylline (TPH) were unresolved. Interestingly, all three solutes were almost baseline resolved on PANI-SiO_2 and selectivity different from C_{18} was observed. Further, the comparison of aminoacetophenones separation on PANI-SiO_2 and on C_{18} revealed again the different selectivity of these stationary phases. Surprisingly, peak resolution of solutes was higher on the former phase despite the time of the analysis being shorter by 50 %.

To summarize the observations, PANI-SiO_2 sorbent provides completely different selectivity than bare SiO_2 or C_{18} for the tested sets of solutes. In addition, the chromatographic performance of the column improves significantly after the modification of bare SiO_2 with PANI layer in NP and HILIC modes. Moreover, from the viewpoint of chromatographic performance, PANI-SiO_2 can compete successfully with the commercial C_{18} stationary phase in RP mode.

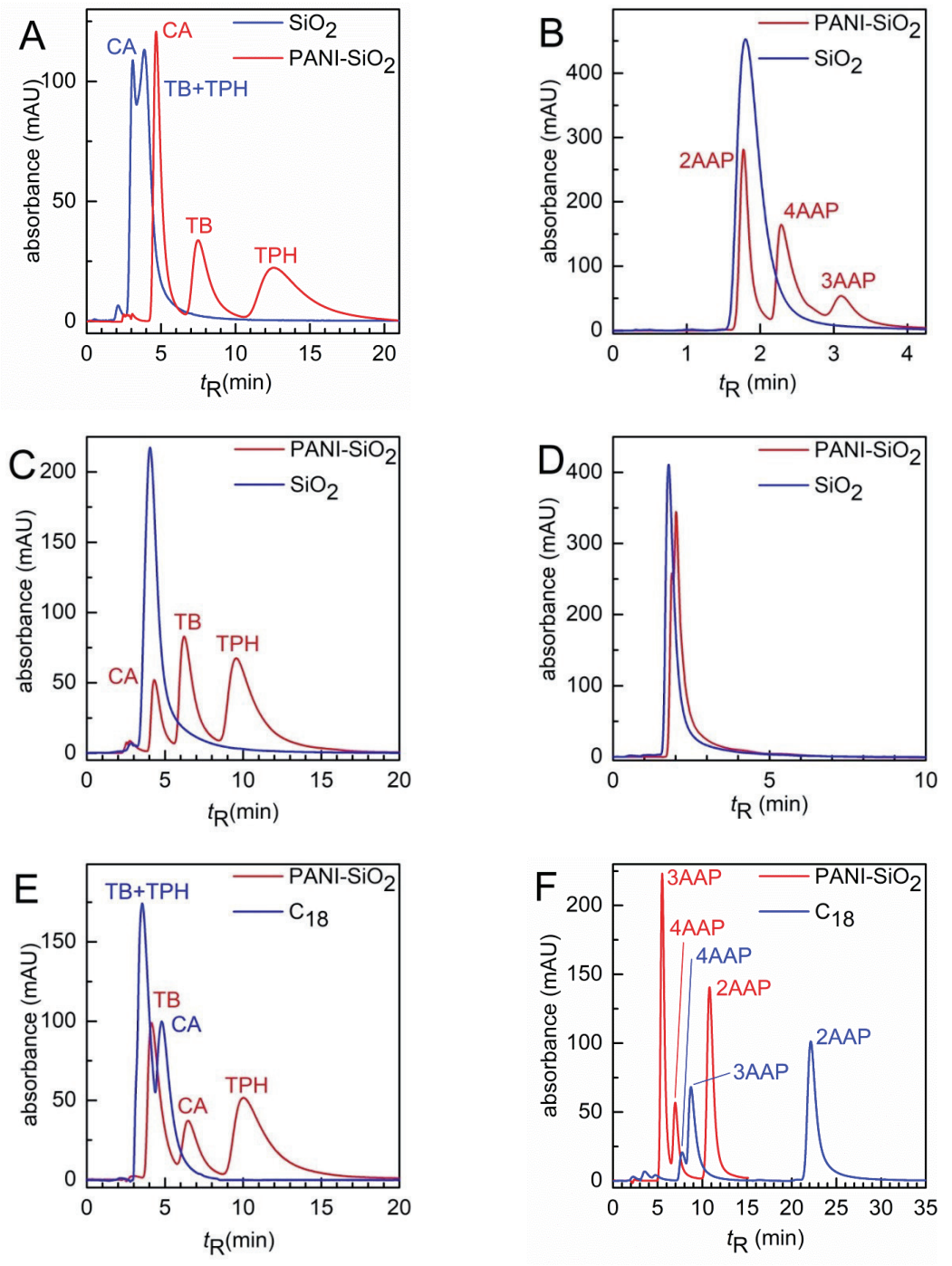

Figure 18 Separation of caffeine-related set of solutes and aminoacetophenone set of solutes comparing the separation performance of PANI-SiO_2 and bare SiO_2 or C_{18} packed columns in different chromatographic modes; preparation and experimental conditions for different columns were identical; NP mode (A, B), HILIC mode (C, D), RP mode (E, F); CA – caffeine, TB – theobromine, TPH – theophylline, 2AAP – 2´-aminoacetophenone, 3AAP– 3´-aminoacetophenone, 4AAP – 4´-aminoacetophenone; modified from Figure 4 in Publication II.

6. PUBLICATION III – Protonation of polyaniline-coated silica stationary phase affects the retention behavior of neutral hydrophobic solutes in reversed-phase capillary LC

Taraba L., Křížek T., Kozlík P., Hodek O., Coufal P.

Journal of Separation Science (2018) (available online), DOI: 10.1002/jssc.201800261

Received: 12 March 2018 | Revised: 4 May 2018 | Accepted: 4 May 2018

DOI: 10.1002/jssc.201800261

RESEARCH ARTICLE

JOURNAL OF SEPARATION SCIENCE

Protonation of polyaniline-coated silica stationary phase affects the retention behavior of neutral hydrophobic solutes in reversed-phase capillary liquid chromatography

Lukáš Taraba | Tomáš Křížek | Petr Kozlík | Ondřej Hodek | Pavel Coufal

Faculty of Science, Department of Analytical Chemistry, Charles University, Prague, Czech Republic

Correspondence
Dr. Tomáš Křížek, Faculty of Science, Department of Analytical Chemistry, Charles University, Hlavova 8, 128 43 Prague 2, Czech Republic.
Email: tomas.krizek@natur.cuni.cz

Because of its high conductivity when acid doped, polyaniline is known as a synthetic metal and is used in a wide range of applications, such as supercapacitors, biosensors, electrochromic devices, or solar and fuel cells. Emeraldine is the partly oxidized, stable form of polyaniline, consisting of alternating diaminobenzenoid and iminoquinoid segments. When acidified, the nitrogen atoms of emeraldine become protonated. Due to electrostatic repulsion between positive charges, the polarity and morphology of emeraldine chains presumably change; however, the protonation effects on emeraldine have not yet been clarified. Thus, we investigated these changes by reversed-phase capillary liquid chromatography using a linear solvation energy relationship approach to assess differences in dominant retention interactions under a significantly varied mobile phase pH. We observed that hydrophobicity dominates the intermolecular interactions under both acidic and alkaline eluent conditions, albeit to different extents. Therefore, by tuning the mobile phase pH, we can even modulate the retention of neutral hydrophobic solutes, such as aromatic hydrocarbons, because the pH-dependent charge and structure of polymer chains of the emeraldine-coated silica stationary phase show a mixed-mode separation mechanism.

KEYWORDS

capillary liquid chromatography, linear solvation energy relationships, polyaniline-coated silica, reversed-phase chromatography

1 | INTRODUCTION

Currently, polyaniline (PANI) is among the most intensively studied conducting polymers [1]. In addition to its high chemical and environmental stability and flexibility, PANI is easily prepared both in bulk and on substrates, either electrochemically on conductive substrates or chemically on insulants [2]. PANI generally occurs in three oxidation states: fully reduced leucoemeraldine, fully oxidized pernigraniline, or half-oxidized emeraldine [3]. Each PANI polymorph acts as an organic base in the undoped state and as a salt when acid doped and, therefore, protonated [4].

Unlike small molecules, polyelectrolyte polymers such as PANI lack a single, clearly defined value of dissociation constant of the functional group(s). Instead, they show a distribution of dissociation constants [5]. According to the available literature, the pK_a value of the transition from emeraldine salt (ES) to emeraldine base (EB) approximately ranges from 2 to 8 (Figure 1) [6]. It should be noted that such a wide pK_a range is most likely related to the different techniques used for pK_a determination and to the heterogeneous experimental conditions used for PANI preparation.

The electrostatic repulsion of positively charged nitrogen atoms of amino and imino groups necessarily lead to differences in the polarity of ES and deprotonated EB chains. Depending on the degree of protonation, the distance between the PANI chains and their spatial arrangement may also differ. However, to the best of our knowledge, this potential

Article Related Abbreviations: EB, emeraldine base; ES, emeraldine salt; LSER, linear solvation energy relationship; PAH, polycyclic aromatic hydrocarbon; PANI, polyaniline; PANI-SiO_2, polyaniline-coated silica

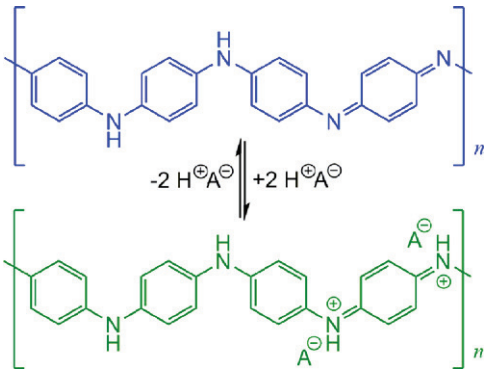

FIGURE 1 Emeraldine base (blue) reacts with an acid to form emeraldine salt (green)

structural difference has not been described yet. Theoretically, small-angle X-ray scattering could be used to estimate the distance between polymer chains to some extent [7]. However, only PANI material polymerized as a bulk can be studied using this technique, whereas PANI coating on a supporting material (our case) must be first detached from the substrate [8]. This pretreatment could affect the arrangement of the PANI polymer chains, resulting in a different material from the original PANI coating. Therefore, we sought an alternative approach to assess the effect of possible morphological changes of PANI by capillary LC assuming that the effect could be used in HPLC.

Fortunately, quantitative structure–retention relationship methods combining HPLC measurements with suitable mathematical and/or statistical approaches (e.g., multilinear regression) can also provide information about structure-related intermolecular interactions. These interactions occur between a solute of given physicochemical and structural parameters and the studied material, in this case, PANI-coated silica (PANI-SiO_2) stationary phase. Linear solvation energy relationship (LSER) is likely the best-known quantitative structure–retention relationship method and has been developed, modified, and widely applied to identify dominant intermolecular interactions in the last two decades [9–11]. The LSER model can divide the overall thermodynamics of the retention process, expressed as the retention factor k, into individual interactions between the solute and the chromatographic system [12]. The original Abraham equation comprising five solute descriptors was extended by including two additional interaction terms to account for interactions with ionic and ionizable solutes by Chirita et al. [13]:

$$\log k = eE + sS + aA + bB + vV + d^{-}D^{-} + d^{+}D^{+} + c \quad (1)$$

In Eq. (1), the uppercase letters stand for either the experimentally obtained or the calculated solute descriptors (information on individual solute descriptors is outlined in Supporting Information Table S1). The lowercase letters are the chromatographic system coefficients. The coefficient e expresses the interactions of lone electron pairs and π–π stacking, s shows the dipole–dipole interactions, a shows hydrogen bond basicity, b shows hydrogen bond acidity, v shows the dispersion interactions (in LC also regarded as hydrophobicity) and cavity-forming effect, d^{-} and d^{+} express the anion-exchange and cation-exchange interactions, respectively. The term c stands for the LSER model intercept and covers all unspecified interactions above (e.g., mobile and stationary phase ratio, throughput capacity or steric selectivity of the stationary phase) [14].

This modified Abraham equation has been used to describe dominant retention interactions in different chromatographic modes [13,15–17]. In contrast to simple chromatographic tests, experimental conditions can be changed and, therefore, the LSER model provides information related to changes in mobile phase composition [18–21].

Christwanto and Wallace performed a preliminary study of the chromatographic potential of PANI-SiO_2 beads with a few testing solute sets, including small organic molecules, inorganic ions, and polycyclic aromatic hydrocarbons (PAHs) in IEC, ANP, and RP chromatographic modes [22]. Sowa et al. adopted the PANI polymerization procedure proposed by Stejskal et al. [4] and investigated the pH and thermal stability of PANI-SiO_2 particles prepared in situ and their application potential in nonsuppressed ion chromatography and SPE [23–26].

In our recent studies, we extended the knowledge on the chromatographic behavior of PANI-SiO_2. We described PANI-SiO_2 as the stationary phase of the mixed-mode retention mechanism for various solutes in HILIC using the LSER approach [27]. Then, we studied the PANI-SiO_2 potential to separate structural analogues of either slightly hydrophilic or slightly hydrophobic solutes, in different chromatographic modes, and the changes in the elution order of structurally related solutes based on the variable portion of the organic modifier and on the eluent pH [28].

In this study, we assessed the effects of significantly varied values of eluent pH on the retention interactions of PANI-SiO_2 stationary phase by LSER in RP chromatographic mode. With respect to the charge difference between protonated ES and deprotonated EB, we expected to find the difference in extent of dominant interactions between solutes and this unique, chargeable, mixed-mode stationary phase.

2 | MATERIALS AND METHODS

2.1 | Chemicals and reagents

Methanol (HPLC gradient grade) was supplied by Sigma–Aldrich (St. Louis, MO, USA). Phosphoric acid, citric acid (purity > 99.5%), and sodium hydroxide (purity > 98%) were purchased from Lachner (Neratovice, Czech Republic).

Deionized water was prepared using a water purification system (Premier MFG'D, USA). All solutes used for the LSER measurements (all of analytical grade purity) were purchased from Sigma–Aldrich. The complete list of the 79 solutes used in this study, their molecular descriptor values, and other quantities are outlined in Supporting Information Table S2.

2.2 | Eluent and sample preparation

Sodium phosphate stock buffer (100 mmol/L) was prepared by diluting the appropriate quantity of phosphoric acid in deionized water; the required aqueous ${}^{w}_{w}$pH values of 2.5 and 7.0 were adjusted by titration with sodium hydroxide solution (10 mol/L). The mobile phase was prepared by mixing methanol and the buffer stock solution at a 50:50 v/v methanol/buffer ratio. The apparent hydroorganic ${}^{s}_{w}$pH values of 3.4 and 8.0 were measured with a glass electrode calibrated with aqueous calibration buffers. Standard solutions were prepared at a concentration of 0.05–1.0 mg/mL, either in methanol/water (50:50, v/v) or in the mobile phase.

2.3 | Instrumentation

Spherical bare silica gel with a mean diameter of 5 µm (mean pore size 12 nm; Hypersil, Shandon Southern, Cheshire, UK) was used as a substrate for PANI coating. PANI-SiO_2 stationary phase was prepared by in situ chemical polymerization of aniline hydrochloride using ammonium persulfate as a reaction initiator. A detailed description of the sorbent preparation can be found in our previous article [27]. The thickness of the PANI layer on silica substrate was estimated to be 0.2 µm (measured by TEM, see Supporting Information Figure S1). Slurry packing apparatus comprises an empty polyimide-coated fused-silica column (320 µm id/ 430 µm od; Supelco, Bellefonte, PA, USA) sealed with stainless steel screens inserted into the polyether ether ketone unions as column frits [29]. Slurry consisted of the PANI-SiO_2 suspension (2% w/v) in 50:50 v/v methanol/water sonicated before packing. The column was packed at 25 MPa using 65:35 v/v ACN/water as a packing solvent for 1 h. Then, the column was steadily depressurized and conditioned with the packing solvent overnight.

Chromatographic measurements were performed on an Agilent 1200 HPLC System (Agilent Technologies, Waldbronn, Germany) consisting of a degasser, binary pump, automated injector, thermostatted column compartment, and diode array detector. The ^{3D}HPLC ChemStation Software (Agilent Technologies) was used for data acquisition and analysis. The injection volume was 0.1 µL and the flow rate was 5 µL/min. The capillary column was thermostatted at 25°C. UV absorbance detection was performed at 230 and 254 nm. The dead time was determined using a system peak.

3 | RESULTS AND DISCUSSION

3.1 | Choice of RP eluent and solutes for the linear solvation energy relationship study

We selected phosphate buffer for the LSER investigation of the chromatographic behavior of PANI-SiO_2 as the stationary phase modulated by the pH of the mobile phase [30]. As one of only a few acids, phosphoric acid can dissociate more than one proton and still act as an acid. Additionally, the values of the phosphoric acid dissociation constants ($pK_{a,1} = 2.15$, $pK_{a,2} = 7.20$, and $pK_{a,3} = 12.32$) are near the marginal values of the EB dissociation constant range (see above) and, thus, suitable for our purpose. The exact pH values of aqueous sodium phosphate buffer (${}^{w}_{w}$pH) used in this study were 2.5 and 7.0. However, for the calculation of ionic descriptors (for exact formula, see Supporting Information or [13,15]) and for the subsequent LSER model building, we decided to use the apparent hydroorganic pH values (${}^{s}_{w}$pH) corresponding to the pH value of the final mobile phase.

In contrast to the generally accepted notion that the HILIC retention mechanism involves water-enriched layer adsorption onto the polar stationary phase surface, wherein the true pH value is supposedly closer to ${}^{w}_{w}$pH than to ${}^{s}_{w}$pH, the RP eluent components are presumably evenly spread in the mobile phase bulk [31]. A recent study evaluating the use of ${}^{w}_{w}$pH or ${}^{s}_{w}$pH performed by Schuster and Lindner supports our decision to use the apparent hydroorganic pH [16]. Regarding the pH values chosen, we suppose that a difference in eluent pH higher than four units should be satisfactory to assess the pH effect on the presumed polarity and protonation state of PANI-SiO_2. We did not perform the measurements for LSER evaluation using a ${}^{s}_{w}$pH lower than 3.4 or higher than 8.0 for two reasons. On the one hand, we assumed that PANI coating adhesion to the silica sorbent is mostly electrostatic. Therefore, the lower pH could cause the reprotonation of silanol groups and subsequently decrease the PANI-SiO_2 attraction, thereby damaging the modified sorbent [32]. On the other hand, we supposed that using a ${}^{s}_{w}$pH > 8 could result in the undesirable dissolution of silica substrate particles, despite their superficial protection with PANI coating [33].

The selected LSER test set consisted of 79 analytes of various types, such as small organic bases, carboxylic acids, zwitterions, polar and nonpolar neutral solutes, smaller PAHs, and even some positional isomers (Supporting Information Table S2). All Abraham solute descriptor values were adopted from the published literature [13,15,34–38]. Descriptors for ionic and ionizable solutes were calculated using the pK_a values computed by Marvin software [39]. Multiple linear regression analyses and evaluations of the proposed LSER models were performed using NCSS software [40].

3.2 | Evaluation of linear solvation energy relationship models

To ensure the reliability of the proposed LSER models, we used 79 solutes of various chemistries and with a wide range of polarities (i.e., log *D* from –2.64 to 4.37), thus meeting the statistical requirement of at least four solutes per independent variable [13,15]. The sufficient diversity in descriptors of the chosen analyte set was proven by the descriptive statistics (Supporting Information Table S3) and frequency plots (Supporting Information Figure S2). The correlation matrix (Supporting Information Table S4) supplemented with the mutual plotting of each solute descriptor showed no correlation; instead, only random data scattering was observed (not shown). In the text below, we discuss the proposed LSER models, focusing on major intermolecular interactions and on their differences for the PANI-SiO_2 stationary phase when using mobile phases consisting of (50:50 v/v) methanol/100 mM sodium phosphate buffer at ${}^{s}_{w}$pH 3.4 and 8.0.

Figure 2 shows the plots of the experimental versus predicted log *k* values for both pH-differing systems. All 75 solutes tested, considered in the final LSER models (four outliers were excluded from each individual model), were divided into the following five groups: neutral hydrophobic and hydrophilic compounds, cations, anions, and zwitterions. We considered solutes with a calculated log *D* value (using Marvin software) higher or equal to zero hydrophobic. Ionic state was attributed to solutes at least 10% dissociated at a given ${}^{s}_{w}$pH of the mobile phase.

Figure 2 clearly shows that cations (organic bases) were the least retained solutes, followed by the slightly more retained neutral hydrophilic compounds, in the acidic eluent. Zwitterions were approximately in the middle of the plot, as well as slightly hydrophobic neutral solutes. Anions (carboxylic acids) were somewhat more retained on the PANI-SiO_2 sorbent. However, the most retained solutes were neutral hydrophobic compounds (except for acetone), especially PAHs. The only positively charged solute with strong retention was 4-aminobenzoic acid (marked as solute 7 in Figure 2A); its amino group was protonated ($pK_{a,\text{-NH2}} = 2.69$), whereas its carboxylic group ($pK_{a,\text{-COOH}} = 7.77$) was insufficiently dissociated to be considered a zwitterion. The increase in solute retention with the number of aromatic rings in their structure (solutes marked as 2 – 6), which is proportionately related to the increase in hydrophobicity, should be highlighted because it corresponds to typical retention assumptions of RP mode.

The previous conclusions about the retention of individual solute groups at ${}^{s}_{w}$pH 3.4 also apply to the alkaline eluent at ${}^{s}_{w}$pH 8.0 (Figure 2B). The increase in the mobile phase pH caused the transformation of cations into neutral hydrophilic solutes and of neutral hydrophilic solutes into anions; zwitterions remained unchanged. The only cationic analyte with a high retention time was benzyltrimethylammonium (1+), most likely due to the presence of an aromatic ring and three hydrophobic methyl moieties in its structure. Interestingly, the results showed a twofold increase in both predicted and experimental log *k* values for some PAHs. Both plots clearly show that solutes are evenly scattered along the blue line denoting equal predicted and experimental log *k* values, with no solute clustering in any plot. The linear regression slopes are almost identical, albeit lower than one, indicating a slight underestimation of predicted log *k* values. Nevertheless, this feature is common for LSER models [15,16]. In principle,

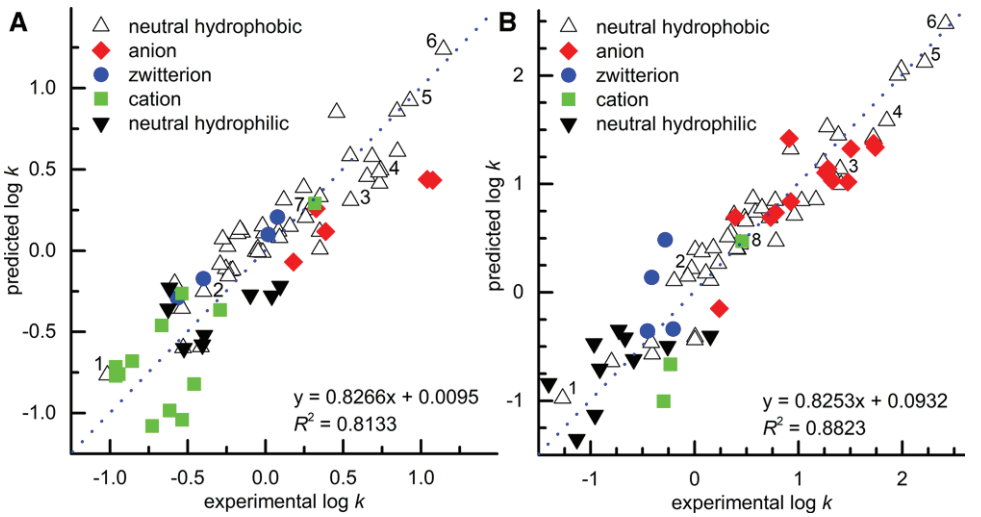

FIGURE 2 Plot of predicted log *k* versus experimental log *k* for acidic (A) and alkaline (B) eluents; the dotted line denotes equal log *k* values; the neutral hydrophobic solute has a value of log $D \geq 0$; ion is defined as a solute at least 10% ionized. Selected solutes discussed in the text: 1, acetone; 2, benzene; 3, naphthalene; 4, biphenyl; 5, anthracene; 6, pyrene; 7, 4-aminobenzoic acid; 8, benzyltrimethylammonium (1+) chloride; the equation expresses linear regression with R^2 of the linear fit

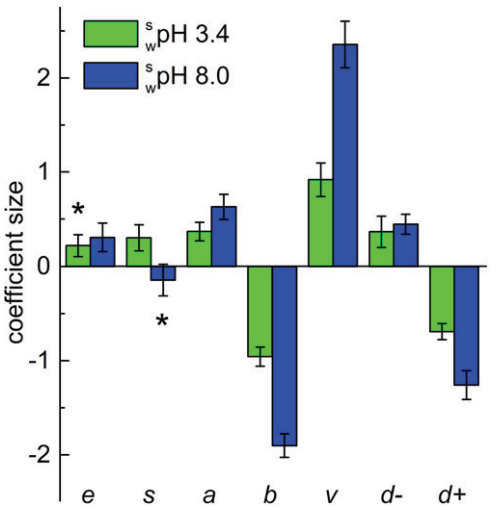

FIGURE 3 Column plot of LSER results—system coefficients of PANI-SiO_2 stationary phase and mobile phase consisting of 50:50 v/v methanol/100 mM sodium phosphate buffer of $^{s}_{w}$pH 3.4 (green) and 8.0 (blue), respectively; the error bars denote the standard error of the relevant coefficient; asterisk indicates statistically nonsignificant coefficient

mathematical multilinear regression disregards a system intercept significantly different from zero and any mutual effects of individual variables (chemical interactions), either synergic or antagonistic. However, those initial assumptions cannot be strictly implemented for chemical interactions [11]. Therefore, analysts should consider another LSER output to assess model reliability—the determination coefficient (R^2). The proposed models are highly reliable, with an R^2 of 0.8133 and 0.8823 for the chromatographic system with acidic and alkaline eluents, respectively.

The system coefficients calculated for both pH-differing chromatographic systems are shown in Figure 3 (the exact values along and the corresponding statistics are outlined in Supporting Information Table S5). Almost all system coefficients are statistically significant, with two exceptions. Coefficient *e* becomes significant under alkaline eluent conditions, whereas the *s* coefficient becomes nonsignificant under alkaline eluent conditions. However, this result may be affected by LSER modeling under different pH values of the mobile phase. In any case, the presence of lone electron pairs on nitrogen atoms of the protonated ES in the acidic mobile phase is less likely than in the alkaline eluent. Conversely, dipole–dipole interactions apparently decrease in the alkaline eluent.

The clear increase in the term *a* under conditions of higher pH is attributed to the expected (partial) deprotonation of nitrogen atoms of the PANI chains and consequent tendency to act as hydrogen bond acceptors. The negative value of the coefficient *b* describes the ability of the phosphate moiety included in the mobile phase to act as a proton donor, especially at a higher pH. In contrast, PANI-SiO_2 acts as a base. The doubled value of this coefficient in the alkaline eluent highlights the difference in behavior between mobile and stationary phases.

Dispersion forces (or hydrophobicity in RP) are the paramount retention-promoting interactions, regardless of the pH of the eluent in RP mode, as indicated by the regression coefficient *v* values. Under such conditions of both chromatographic systems, the stationary phase is more hydrophobic than the mobile phase containing 50% v/v of methanol. This result supports our previous conclusions, suggesting that PANI-SiO_2 acts as a unique, tunable, mixed-mode stationary phase (for more information, see Supporting Information Figure S3). In a similar study on the LSER characterization of PANI-SiO_2 in HILIC mode, the *v* coefficient was highly negative (albeit using a different mobile phase) [27].

The almost identical values of d^- indicate the persistent anion-exchange ability of PANI-SiO_2; therefore, the deprotonation of PANI chains is incomplete, even in the alkaline pH eluent. The negative d^+ value indicates that cationic solutes preferably interact with the mobile phase (more likely with phosphate anions than with methanol) than with the stationary phase. Similarly, the explanation is clear: negatively charged phosphate moieties attract more cations at higher pH due to the higher number of negatively charged sites per phosphate molecule, whereas incompletely deprotonated PANI chains still repulse solutes with the same charge. System intercepts ($c_{(3.4)} = -1.06$ and $c_{(8.0)} = -1.31$) are negative for both mobile phases; it should be noted that the negative value of *c* is a common feature for all LSER models. Unfortunately, various phenomena that contribute to the model intercept are overlooked by LSER, thereby precluding a simple discussion on its extent. LSER model generally provides more accurate, reliable, and clear description of the chemical interactions taking place in a given chromatographic system than simple chromatographic tests. However, many chromatographers prefer Tanaka test, which is often used for characterization of RP stationary phases, thus we performed this test as well (for details, see Supporting Information).

3.3 | Evaluation of partition and/or adsorption interaction mechanisms

We assessed the effect of the elution strength of the mobile phase on solute retention using empirical equations describing either partition or adsorption as the major interaction mechanism [13,34,41] to elucidate the interaction mechanism on the PANI-SiO_2 sorbent. For the measurements, we purposely selected several hydrophobic neutral solutes without functional groups to simplify the evaluation. As mentioned above, dispersion interactions play a key role in the retention interactions on PANI-SiO_2 in both acidic and alkaline eluents. The other interactions have substantially weaker effects on the retention of the analytes and, consequently, on the mechanism, based on chemical interactions. For the measurements,

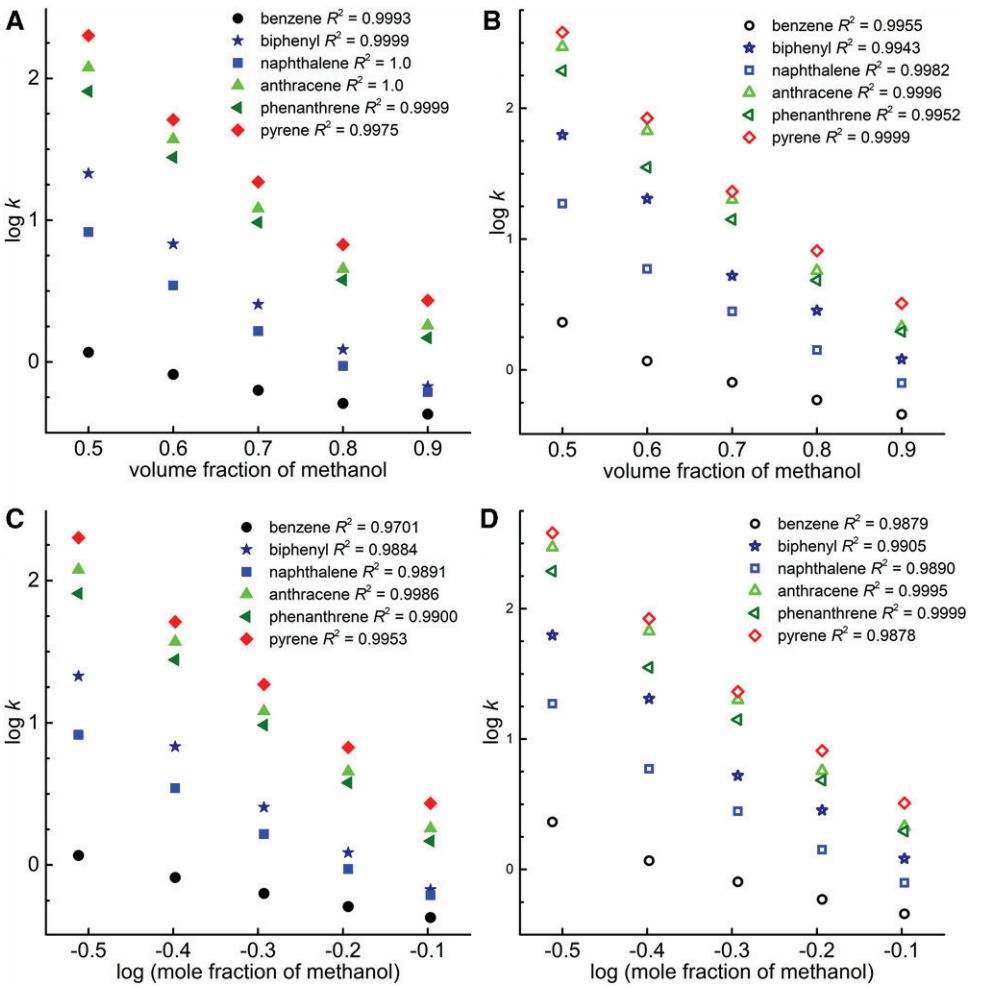

FIGURE 4 Plots of log k as a second-order polynomial function of the methanol volume fraction (A and B) or as a linear function of the logarithm of the methanol mole fraction (C and D) for selected neutral hydrophobic solutes in acidic–methanol/20 mM sodium citrate buffer (v/v; $^{w}_{w}$pH 2.5) (A and C) or alkaline–methanol/20 mM sodium citrate buffer (v/v; $^{w}_{w}$pH 7.0) eluents (B and D)

we replaced the phosphate buffer by a citrate buffer because the latter has similar chemical properties and does not precipitate readily in mixtures with more than 50% organic solvent [42,43].

To evaluate partitioning as the interaction mechanism on the RP stationary phase, we used the empirical equation proposed by Schoenmakers et al. [44,45]. According to this equation, the log k of a solute should be plotted as a function of the volume fraction of organic modifier (i.e., methanol) in the eluent. The relationship is expressed as a second-order polynomial function:

$$\log k = a\varphi^2 + b\varphi + c, \tag{2}$$

where φ is the volume fraction of organic solvent in the mobile phase and a, b, and c are the model coefficients of no physical significance [46]. Conversely, the adsorption process is described by a linear plot of log k versus the mole fraction of the stronger solvent B (i.e., methanol), according to the Snyder–Soczewinski equation [47]:

$$\log k = \log k_B - A_s/n_B \log N_B, \tag{3}$$

where k_B is the hypothetical retention factor of solute in the pure B eluent, A_s and n_B are the cross-sectional areas occupied by the solute molecule on the surface of the stationary phase and B molecules, respectively, and N_B is the mole fraction of the stronger B member in the eluent.

Figure 4 shows plots of log k as a function of the methanol volume fraction (second-order polynomial fit) or as a function of the logarithm of the methanol mole fraction (linear fit) for selected neutral hydrophobic analytes in acidic (i.e., methanol/20 mM sodium citrate v/v; $^{w}_{w}$pH 2.5) and alkaline (i.e., methanol/20 mM sodium citrate v/v; $^{w}_{w}$pH 7.0) eluents. The fitting of log k values using the function in Eq. (2) in the range of $\varphi = 0.5 - 0.9$ provided $R^2 \geq 0.9943$, in both acidic and alkaline eluents (Figure 4 A, B). The measurements of solute retention with methanol volume fractions lower than

0.5 were not performed because they would have irreversibly led to the retention of polyaromatic solutes.

The fitting of log k values in the same range of eluent composition using the function in Eq. (3) (Figure 4C and D) showed $R^2 \geq 0.9878$ (except for benzene, which is the least retained solute of the set, with $R^2 = 0.9701$ in the acidic eluent). The possible explanation for the lower determination coefficient values assessed when using the Snyder–Soczewinski equation is that this model was originally developed for adsorption mechanism on normal phases and not for RP phases [48] (frequently used for HILIC phases also [13, 34,41]).

Both retention (partitioning and adsorption) models illustrate the overall retention behavior and seem to corroborate the retention data of the neutral hydrophobic solutes used in this study. Therefore, based on the findings of this study and on the published literature [34,41,49], we presume a multimodal retention mechanism for PANI-SiO_2.

In addition, the results from the partitioning models showed a slightly better fit, which is in line with assumption that PANI-SiO_2 acts as the RP stationary phase under specific conditions (for more information, see Supporting Information).

An illustrative chromatogram of the separation of neutral hydrophobic solutes with different numbers of aromatic rings shows the effect of the mobile phase pH on retention time (Figure 5).

All peaks were baseline resolved. The tailing of more retained peaks was likely caused by the substantially thicker layer of PANI coating (approximately 0.2 μm), which is related to its higher mass transfer resistance than that of chemically attached, organic ligand-based stationary phases whose approximate layer thickness does not exceed units of nanometers [50,51]. The thinning of the PANI layer and the related improvement in separation performance will be the subject of future studies. Interestingly, the change in mobile phase pH accompanied by the change in eluent polarity affects the polarity of the stationary phase due to the rare protonation/deprotonation ability of EB. Therefore, the retention of solute with the constant value of log D also changes. The situation is more complicated for chargeable solutes when more interactions have to be considered, which can be shown on retention behavior of basic solutes (for details, see Supporting Information). Indeed, such an effect on the chromatographic system is rather unusual. Unfortunately, the chromatographic measurements did not provide clear evidence of the supposed change in distance between PANI chains. Therefore, further research will be required to precisely determine these values.

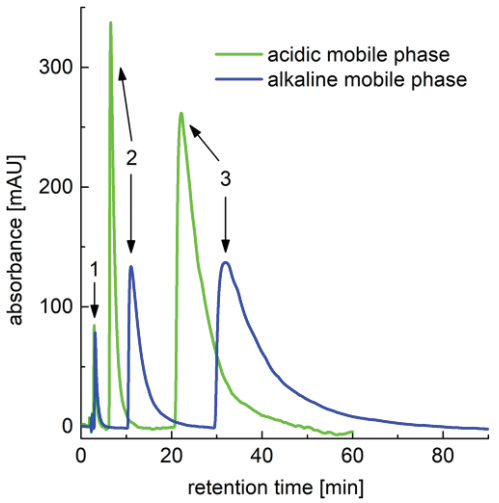

FIGURE 5 Chromatogram of separation of neutral hydrophobic solutes at different eluent pH values, using the following measurement conditions: 70:30 v/v methanol/20 mM sodium citrate (${}^{w}_{w}$pH 2.5; ${}^{s}_{w}$pH 3.7) acidic mobile phase; 70:30 v/v methanol/20 mM sodium citrate (${}^{w}_{w}$pH 7.0; ${}^{s}_{w}$pH 8.7) alkaline mobile phase; UV detection at 254 nm, 5 μL/min flow rate, 0.1 μL injection volume, 25°C column compartment temperature; and the following solutes: 1, benzene; 2, biphenyl; 3, anthracene

4 | CONCLUDING REMARKS

We assessed the effect of changes in eluent pH on the retention interactions occurring in the chromatographic system consisting of the PANI-SiO_2 stationary phase and the methanol/phosphate buffer mobile phase by RP capillary LC for the first time. For systematic chromatographic evaluation, we used the linear solvation energy relationship model extended with ionic solute descriptors with regard to the protonation ability of the stationary phase under acid doping. The results showed that dispersion interactions are the dominant retention-promoting interactions, along with hydrogen bond basicity and anion-exchange interactions, whereas hydrogen bond acidity and cation-exchange interactions promote solutes elution from the separation column. Individual interactions were stronger under alkaline mobile phase conditions. According to our observations, the retention of neutral hydrophobic solutes with no functional moieties can be significantly modulated by changing the pH of the eluent, especially of those with more aromatic rings. Furthermore, we also assessed whether the interaction mechanism of PANI-SiO_2 is dominated by partition or adsorption. Using empirical equations that describe the retention process, we found that both mechanisms were engaged; therefore, PANI-SiO_2 is associated with a multimodal retention mechanism.

In conclusion, PANI-SiO_2 can be considered a pH-tunable, chargeable, mixed-mode stationary phase with unique selectivity and key potential applications in RP LC.

ACKNOWLEDGMENTS

We gratefully acknowledge the financial support of the Grant Agency of Charles University, project no. 307015, project

SVV260440, and of the Charles University Research Centre program no. UNCE/CSI/014. The authors also thank Carlos V. Melo for proofreading the manuscript.

CONFLICT OF INTEREST

The authors declare no potential conflict of interest.

ORCID

Tomáš Křížek http://orcid.org/0000-0002-1623-8844

REFERENCES

1. Yishai-Aviram, L., Grushka, E., in: P. R. Brown, E. Grushka, S. Lunte (Eds.), Advances in chromatography: Volume 43. CRC Press Taylor & Francis, New York 2004, pp. 273–304.
2. Tran, H. D., D'Arcy, J. M., Wang, Y., Beltramo, P. J., Strong, V. A., Kaner, R. B., The oxidation of aniline to produce "polyaniline": a process yielding many different nanoscale structures. *J. Mater. Chem.* 2011, *11*, 3534–3550.
3. Boeva, Z. A., Sergeyev, V. G., Polyaniline: synthesis, properties, and application. *Polym. Sci. Ser. C* 2014, *56*, 144–153.
4. Stejskal, J., Quadrat, O., Sapurina, I., Zemek, J., Drelinkiewicz, A., Hasik, M., Krivka, I., Prokes, J., Polyaniline-coated silica gel. *Eur. Polym. J.* 2002, *38*, 631–637.
5. Tanford, C., Physical chemistry of macromolecules. Second Edition, Wiley-VCH, New York 1961.
6. Marmisolle, W. A., Florit, M. I., Posadas, D., Acid-base equilibrium in conducting polymers. The case of reduced polyaniline. *J. Electroanal. Chem.* 2014, *734*, 10–17.
7. Sanches, E. A., Soares, J. C., Mafud, A. C., Fernandes, E. G. R., Leite, F. L., Mascarenhas, Y. P., Structural characterization of chloride salt of conducting polyaniline obtained by XRD, SAXD, SAXS, and SEM. *J. Mol. Struct.* 2013, *1036*, 121–126.
8. Wessling, B., in: H. S. Nalwa (Ed.) Handbook of Nanostructured Materials and Nanotechnology, Vol. 5: Organics, Polymers, and Biological Materials, Academic Press, Cambridge, MA 1999, pp. 525–553.
9. Poole, C. F., Poole, S. K., Column selectivity from the perspective of the solvation parameter model. *J. Chromatogr. A* 2002, *965*, 263–299.
10. Abraham, M. H., Ibrahim, A., Zissimos, A. M., Determination of sets of solute descriptors from chromatographic measurements. *J. Chromatogr. A* 2004, *1037*, 29–47.
11. Vitha, M., Carr, P. W., The chemical interpretation and practice of linear solvation energy relationships in chromatography. *J. Chromatogr. A* 2006, *1126*, 143–194.
12. Sykora, D., Vozka, J., Tesarova, E., Chromatographic methods enabling the characterization of stationary phases and retention prediction in high-performance liquid chromatography and supercritical fluid chromatography. *J. Sep. Sci.* 2016, *39*, 115–131.
13. Chirita, R.-I., West, C., Zubrzycki, S., Finaru, A. L., Elfakir, C., Investigations on the chromatographic behaviour of zwitterionic stationary phases used in hydrophilic interaction chromatography. *J. Chromatogr. A* 2011, *1218*, 5939–5963.
14. Kirkland, J. J., Development of some stationary phases for reversed-phase high-performance liquid chromatography. *J. Chromatogr. A* 2004, *1060*, 9–21.
15. Schuster, G., Lindner, W., Comparative characterization of hydrophilic interaction liquid chromatography columns by linear solvation energy relationships. *J. Chromatogr. A* 2013, *1273*, 73–94.
16. Schuster, G., Lindner, W., Additional investigations into the retention mechanism of hydrophilic interaction liquid chromatography by linear solvation energy relationships. *J. Chromatogr. A* 2013, *1301*, 98–110.
17. VanMiddlesworth, B. J., Stalcup, A. M., Characterization of surface confined ionic liquid stationary phases: impact of cation revisited. *J. Chromatogr. A* 2014, *1364*, 171–182.
18. Blackwell, J. A., Stringham, R. W., Characterization of temperature dependent modifier effects in SFC using linear solvation energy relationships. *Chromatographia* 1997, *46*, 301–308.
19. West, C., Lesellier, E., Effects of mobile phase composition on retention and selectivity in achiral supercritical fluid chromatography. *J. Chromatogr. A* 2013, *1302*, 152–162.
20. West, C., Auroux, E., Deconvoluting the effects of buffer salt concentration in hydrophilic interaction chromatography on a zwitterionic stationary phase. *J. Chromatogr. A* 2016, *1461*, 92–97.
21. Kiridena, W., Poole, C. F., Koziol, W. W., Effect of solvent strength and temperature on retention for a polar-endcapped, octadecylsiloxane-bonded silica stationary phase with methanol-water mobile phases. *J. Chromatogr. A* 2004, *1060*, 177–185.
22. Chriswanto, H., Wallace, G. G., Characterization of polyaniline using chromatographic studies. *Chromatographia* 1996, *42*, 191–198.
23. Sowa, I., Wojciak-Kosior, M., Draczkowski, P., Strzemski, M., Kocjan, R., Synthesis and properties of a newly obtained sorbent based on silica gel coated with a polyaniline film as the stationary phase for non-suppressed ion chromatography. *Anal. Chim. Acta* 2013, *787*, 260–266.
24. Sowa, I., Wojciak-Kosior, M., Draczkowski, P., Szwerc, W., Tylus, J., Pawlikowski, A., Kocjan, R., Evaluation of pH and thermal stability of sorbent based on silica modified with polyaniline using high-resolution continuum source graphite furnace atomic absorption spectrometry and Raman spectroscopy. *Microchem. J.* 2015, *118*, 88–94.
25. Sowa, I., Wojciak-Kosior, M., Rokicka, K., Kocjan, R., Szymczak, G., Application of solid phase extraction with the use of silica modified with polyaniline film for pretreatment of samples from plant material before HPLC determination of triterpenic acids. *Talanta* 2014, *122*, 51–57.
26. Sowa, I., Wojciak-Kosior, M., Strzemski, M., Sawicki, J., Staniak, M., Szwerc, W., Moldoch, J., Dresler, S., Latalski, M., Silica modified with polyaniline as a potential sorbent for matrix solid phase dispersion (MSPD) and dispersive solid phase extraction (d-SPE) of plant samples. *Materials* 2018, *11*. https://doi.org/10.3390/ma11040467.
27. Taraba, L., Krizek, T., Hodek, O., Kalikova, K., Coufal, P., Characterization of polyaniline-coated stationary phase by using the linear solvation energy relationship in the hydrophilic interaction liquid chromatography mode using capillary liquid chromatography. *J. Sep. Sci.* 2017, *40*, 677–687.

28. Taraba, L., Krizek, T., Study of polyaniline-coated silica gel as a stationary phase in different modes of capillary liquid chromatography. *Monatsh. Chem.* 2017, *148*, 1605–1611.

29. Franc, M., Vojta, J., Sobotnikova, J., Coufal, P., Bosakova, Z., Performance and lifetime of slurry packed capillary columns for high performance liquid chromatography. *Chem. Pap.* 2014, *68*, 22–28.

30. Han, D. D., Row, K. H., Study of chromatographic retention in phosphate solution on the basis of linear solvation energy relationships. *Asian J. Chem.* 2010, *22*, 2717–2726.

31. Buszewski, B., Noga, S., Hydrophilic interaction liquid chromatography (HILIC) – a powerful separation technique. *Anal. Bioanal. Chem.* 2012, *402*, 231–247.

32. Mendez, A., Bosch, E., Roses, M., Neue, U. D., Comparison of the acidity of residual silanol groups in several liquid chromatography columns. *J. Chromatogr. A* 2003, *986*, 33–44.

33. Claessens, H. A., van Straten, M. A., Review on the chemical and thermal stability of stationary phases for reversed-phase liquid chromatography. *J. Chromatogr. A* 2004, *1060*, 23–41.

34. Kozlik, P., Simova, V., Kalikova, K., Bosakova, Z., Armstrong, D. W., Tesarova, E., Effect of silica gel modification with cyclofructans on properties of hydrophilic interaction liquid chromatography stationary phases. *J. Chromatogr. A* 2012, *1257*, 58–65.

35. Fields, P. R., Sun, Y., Stalcup, A. M., Application of a modified linear solvation energy relationship (LSER) model to retention on a butylimidazolium-based column for high performance liquid chromatography. *J. Chromatogr. A* 2011, *1218*, 467–475.

36. Stephens, T. W., Loera, M., Quay, A. N., Chou, V., Shen, C., Wilson, A., Acree, W. E., Jr., Abraham, M. H., Correlation of solute transfer into toluene and ethylbenzene from water and from the gas phase based on the Abraham model. *Open Thermodynamics J.* 2011, *5*, 104–121.

37. Yeatts, J. L., Jr., Baynes, R. E., Xia, X.-R., Riviere, J. E., Application of linear solvation energy relationships to a custom-made polyaniline solid-phase microextraction fiber and three commercial fibers. *J. Chromatogr. A* 2008, *1188*, 108–117.

38. Dunkle, M., West, C., Pereira, A., Van der Plas, S., Madder, A., Farrell, W., Lesellier, E., Lynen, F., Sandra, P., Increasing the dielectric breakdown strength of poly(ethylene terephthalate) films using a coated polyaniline layer. *Scientia Chromatographica* 2014, *6*, 85–103.

39. Marvin 16.4.11.0, (2015), ChemAxon, Budapest, Hungary 2015. Available at: http://www.chemaxon.com.

40. Hintze, J. L., NCSS User's Guide I. NCSS, Kaysville 2007.

41. Kalikova, K., Kozlik, P., Gilar, M., Tesarova, E., Properties of two amide-based hydrophilic interaction liquid chromatography columns. *J. Sep. Sci.* 2013, *36*, 2421–2429.

42. Schellinger, A. P., Carr, P. W., Solubility of buffers in aqueous-organic eluents for reversed-phase liquid chromatography. *LCGC North America* 2004, *22*, 544–548.

43. Oliviera, M. L. N., Malagoni, R. A., Franco, M. R. Jr., Solubility of citric acid in water, ethanol, n-propanol and in mixtures of ethanol + water. *Fluid Phase Equilibria* 2013, *352*, 110–113.

44. Schoenmakers, P. J., Billiet, H. A. H., De Galan, L., Influence of organic modifiers on the retention behaviour in reversed-phase liquid chromatography and its consequences for gradient elution. *J. Chromatogr.* 1979, *185*, 179–195.

45. Kaczmarski, K., Prus, W., Kowalska, T., Adsorption/partition model of liquid chromatography for chemically bonded stationary phases of the aliphatic cyano, reversed-phase C8, and reversed-phase C18 types. *J. Chromatogr. A* 2000, *869*, 57–64.

46. Poole, C. F., Kiridena, W., DeKay, C., Koziol, W. W., Rosencrans, R. D., Insights into the retention mechanism on an octadecylsiloxane-bonded silica stationary phase (HyPURITY C18) in reversed-phase liquid chromatography. *J. Chromatogr. A* 2006, *1115*, 133–141.

47. Snyder, L. R., Poppe, H., Mechanism of solute retention in liquid-solid chromatography and the role of the mobile phase in affecting separation. Competition versus "sorption". *J. Chromatogr. A* 1980, *184*, 363–413.

48. Kurbatova, S. V., Saifutdinov, B. R., The influence of the eluent composition on the retention of derivatives of some aromatic heterocyclic compounds in reversed-phase high-performance liquid chromatography. *Russ. J. Phys. Chem. A* 2009, *83*, 1223–1229.

49. Kozlik, P., Krajicek, J., Kalikova, K., Tesarova, E., Cabala, R., Exnerova, A., Stys, P., Bosakova, Z., Hydrophilic interaction liquid chromatography with tandem mass spectrometric detection applied for analysis of pteridines in two Graphosoma species (Insecta: Heteroptera). *J. Chromatogr. B* 2013, *930*, 82–89.

50. Meyer, R., Schneider, C., Jira, T., Considerations of the behaviour of C18-chains and calixarenes and their application for determination of stationary phase volume in RP-chromatography. *Pharmazie* 2008, *63*, 619–627.

51. Gritti, F., Guiochon, G., Adsorption mechanism in RPLC. Effect of the nature of the organic modifier. *Anal. Chem.* 2005, *77*, 4257–4272.

SUPPORTING INFORMATION

Additional supporting information may be found online in the Supporting Information section at the end of the article.

How to cite this article: Taraba L, Křížek T, Kozlík P, Hodek O, Coufal P. Protonation of polyaniline-coated silica stationary phase affects the retention behavior of neutral hydrophobic solutes in reversed-phase capillary liquid chromatography. *J Sep Sci* 2018;1–9. https://doi.org/10.1002/jssc.201800261

Supporting Information

Protonation of polyaniline-coated silica stationary phase affects the retention behavior of neutral hydrophobic solutes in reversed-phase capillary LC

Lukáš Taraba, Tomáš Křížek*, Petr Kozlík, Ondřej Hodek, Pavel Coufal
Charles University, Faculty of Science, Department of Analytical Chemistry, Hlavova 8, 128 43 Prague 2, Czech Republic

* Corresponding author: RNDr. Tomáš Křížek, Ph.D., Charles University, Faculty of Science, Department of Analytical Chemistry, Hlavova 8, 128 43 Prague 2, Czech Republic.
Tel.: +420 221 951 229. E-mail address: tomas.krizek@natur.cuni.cz (T. Křížek)

Table S1 List of solute descriptors and system coefficients of the LSER model

solute descriptor	described solute characteristics
E	excess molar refraction
S	dipolarity/polarizability
A	effective H-bond acidity
B	effective H-bond basicity
V	McGowan's characteristic molecular volume
D^-	effective dissociation ability
D^+	effective protonation ability
system coefficient	**reflected type of interaction (behavior of mobile and stationary phase)**
e	π-π stacking, lone electron pairs interactions
s	dipole-dipole type
a	H-bond basicity
b	H-bond acidity
v	dispersion interactions (hydrophobicity)
d^-	anion exchange ability
d^+	cation exchange ability
c	model intercept – interactions unspecified by LSER

The following formulas were used to calculate the ionic descriptors of the solutes [1]:

$$D^{-} = \frac{10^{(pH^{*}-pK^{*})}}{1+10^{(pH^{*}-pK^{*})}} \quad (1)$$

$$D^{+} = \frac{10^{(pK^{*}-pH^{*})}}{1+10^{(pK^{*}-pH^{*})}} \quad (2)$$

where D^{-} corresponds to the negative charge of the anion or zwitterion, and D^{+} represents the positive charge of the cation or zwitterion, expressing the degree of dissociation and protonation of the solute, respectively. Dissociation constants of either the acid or the base in the hydro-organic mobile phase are expressed as pK*, pH* describes the effective ${}^{s}_{s}pH$ obtained after mixing the aqueous buffer with the organic solvent and is, hence, different from the aqueous ${}^{w}_{w}pH$ of the buffer before mixing with the organic solvent. Although organic buffers are in principle necessary to calibrate the electrode before correctly measuring the ${}^{s}_{s}pH$, in practice, the ${}^{s}_{w}pH$ of the hydro-organic mobile phase is commonly estimated after calibrating the electrode in purely aqueous buffers, and the aqueous dissociation constant pK_a is often used [1-4]. pK_a values of the solutes used in this study were computed by Marvin software [5].

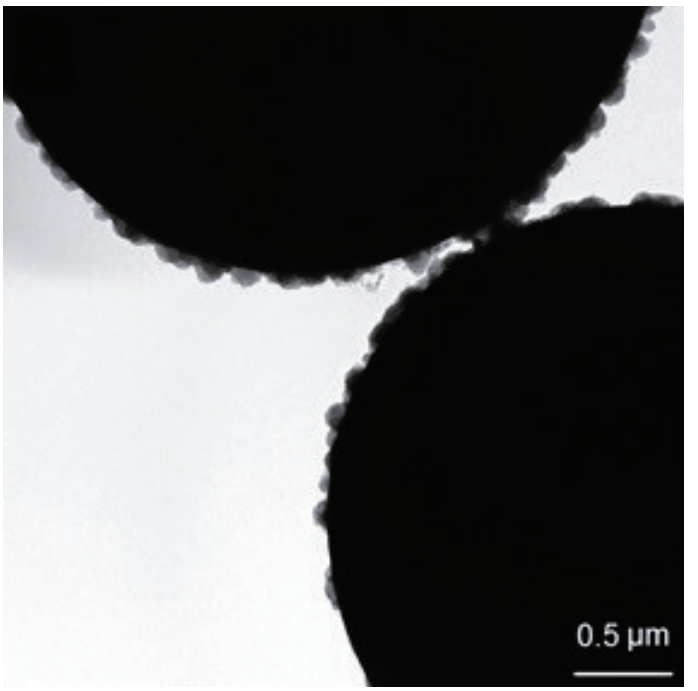

Figure S1 Transmission electron microscopy image of PANI-SiO_2 particles.

Table S2 LSER test solutes with their molecular descriptors, log *D* values, acidic and basic pK_a values, and log *k* values (values in parentheses denote the corresponding hydro-organic pH values)

No.	solute	*E*	*S*	*A*	*B*	*V*	D^- (3.4)	D^+ (3.4)	D^- (8.0)	D^+ (8.0)	log *D* (3.4)	log *D* (8.0)	acid pK_a	base pK_a	ch.[c)] (3.4)	ch.[c)] (8.0)	log *k* (3.4)	log *k* (8.0)
1	2-hydroxypyridine[a)]	0.83	1.03	0.50	0.67	0.734	0.00		0.00		1.11	1.15	11.40		0	0	-0.56	-1.22
2	3-hydroxypyridine	0.83	1.03	0.50	0.67	0.734	0.00	0.99	0.06	0.00	-0.55	0.42	9.16	5.26	(+)	0	-0.53	0.01
3	4-hydroxypyridine	0.83	1.03	0.50	0.67	0.734	0.00	0.00	0.00	0.00	0.26	0.45			0	0	-0.54	0.01
4	nicotinamide	1.01	1.09	0.63	1.00	0.932	0.00	0.63	0.00	0.00	-0.99	-0.61	13.39	3.63	(+)	0	-0.46	-0.97
5	dopamine	1.35	1.46	1.20	1.04	1.215	0.00	1.00	0.01	0.95	-2.60	-0.95	10.01	9.27	(+)	(+)	-0.67	-0.23
6	uracil	0.81	1.00	0.44	1.00	0.752	0.00		0.04		-0.41	-0.48	9.36		0	0	-0.53	-0.58
7	5-methyltryptophan	1.64	1.74	1.09	1.23	1.684	0.86	1.00	1.00	0.96	-1.15	-1.12	2.61	9.41	zw	zw	0.08	-0.28
8	tryptophan	1.62	1.80	1.09	1.23	1.543	0.88	1.00	1.00	0.96	-1.61	-1.58	2.54	9.40	zw	zw	0.02	-0.41
9	tyrosine	1.18	1.60	1.28	1.29	1.372	0.96	1.00	1.00	0.94	-1.97	-1.98	2.00	9.19	zw	zw	-0.40	-0.21
10	phenylalanine	0.95	1.39	0.78	1.02	1.313	0.89	1.00	1.00	0.97	-1.71	-1.68	2.47	9.45	zw	zw	-0.57	-0.45
11	benzoic a.	0.73	0.90	0.59	0.40	0.932	0.17		1.00		1.48	-1.92	4.08		(-)	(-)	0.39	1.33
12	4-aminobenzoic a.	1.08	1.65	0.94	0.60	1.032	0.04	0.16	1.00	0.00	0.66	-2.34	4.77	2.69	(+)	(-)	0.32	1.26
13	salicylic a.[b)]	0.89	0.84	0.71	0.38	0.990	0.80		1.00		1.22	-1.74	2.79		(-)	(-)	1.45	1.74
14	acetylsalicylic a.	0.78	0.80	0.49	1.00	1.288	0.49		1.00		0.77	-2.57	3.41		(-)	(-)	0.18	0.39
15	cinnamic a.[b)]	1.14	1.00	0.58	0.57	1.171	0.07		1.00		2.37	-0.87	4.51		0	(-)	0.73	1.72
16	mandelic a.[b)]	0.90	1.05	0.74	0.89	1.131	0.31		1.00		0.79	-2.63	3.75		(-)	(-)	0.50	0.73
17	1,2-coumaric a.[a)]	1.13	1.39	1.07	0.79	1.229	0.19		1.00		2.03	-1.40	4.04		(-)	(-)	1.08	2.23
18	1,4-coumaric a.[a)]	1.13	1.39	1.07	0.79	1.229	0.20		1.00		2.02	-1.41	4.00		(-)	(-)	1.04	2.25
19	4-hydroxyphenylacetic a.	0.94	1.32	0.97	0.78	1.131	0.20		1.00		1.3	-2.13	4.00		(-)	(-)	0.33	1.48
20	theophylline	1.50	1.60	0.54	1.34	1.222	0.00		0.15		-1.03	-1.38	8.77		0	(-)	0.09	0.24
21	theobromine	1.50	1.60	0.50	1.38	1.222	0.00		0.05		-1.03	-1.06	9.28		0	0	-0.10	-0.26

No.	solute	E	S	A	B	V	D^- (3.4)	D^+ (3.4)	D^- (8.0)	D^+ (8.0)	log D (3.4)	log D (8.0)	acid pK_a	base pK_a	ch.[c)] (3.4)	ch.[c)] (8.0)	log k (3.4)	log k (8.0)
22	caffeine	1.50	1.60	0.00	1.33	1.364					-0.79	-0.79			0	0	0.04	0.15
23	benzene	0.61	0.52	0.00	0.14	0.716					2.05	2.05			0	0	-0.40	-0.03
24	toluene	0.60	0.52	0.00	0.14	0.857					2.51	2.51			0	0	-0.23	0.35
25	ethylbenzene	0.61	0.51	0.00	0.15	0.998					2.91	2.91			0	0	-0.06	0.56
26	propylbenzene	0.60	0.50	0.00	0.15	1.139					3.31	3.31			0	0	0.08	1.24
27	butylbenzene	0.60	0.51	0.00	0.15	1.280					3.70	3.70			0	0	0.28	1.28
28	1,2-xylene	0.66	0.56	0.00	0.16	0.998					2.98	2.98			0	0	-0.05	1.17
29	1,3-xylene	0.62	0.52	0.00	0.16	0.998					2.98	2.98			0	0	-0.03	0.78
30	1,4-xylene	0.61	0.52	0.00	0.16	0.998					2.98	2.98			0	0	-0.02	1.03
31	biphenyl	1.36	0.99	0.00	0.26	1.324					3.73	3.73			0	0	0.74	1.85
32	naphthalene	1.34	0.92	0.00	0.20	1.085					3.05	3.05			0	0	0.55	1.40
33	anthracene	2.29	1.34	0.00	0.26	1.454					4.05	4.05			0	0	0.93	2.22
34	phenanthrene	2.06	1.29	0.00	0.26	1.454					4.05	4.05			0	0	0.85	1.99
35	phenol	0.81	0.89	0.60	0.30	0.775	0.00		0.01		1.76	1.76	10.02		0	0	-0.24	0.44
36	2-nitrophenol	1.02	1.05	0.05	0.37	0.949	0.00		0.96		1.72	0.35	6.63		0	(-)	0.35	0.93
37	3-nitrophenol	1.05	1.57	0.79	0.23	0.949	0.00		0.56		1.72	1.36	7.89		0	(-)	0.69	1.50
38	4-nitrophenol	1.07	1.72	0.82	0.26	0.949	0.00		0.89		1.72	0.75	7.07		0	(-)	0.85	0.91
39	pyrocatechol	0.97	1.07	0.88	0.47	0.834	0.00		0.04		1.48	1.46	9.34		0	0	-0.01	0.78
40	resorcinol	0.98	1.11	1.09	0.52	0.834	0.00		0.05		1.48	1.45	9.26		0	0	-0.02	0.32
41	phloroglucinol	1.36	1.12	1.40	0.82	0.893	0.00		0.07		1.19	1.16	9.13		0	0	0.35	0.42
42	1,2-cresol	0.84	0.86	0.52	0.31	0.916	0.00		0.00		2.23	2.23	10.37		0	0	-0.15	0.38
43	1,3-cresol	0.82	0.88	0.57	0.34	0.916	0.00		0.01		2.23	2.23	10.13		0	0	-0.18	0.48
44	1,4-cresol	0.82	0.87	0.57	0.31	0.916	0.00		0.00		2.23	2.23	10.36		0	0	-0.16	0.58
45	acetone	0.18	0.70	0.04	0.49	0.547					0.38	0.38			0	0	-1.02	-1.27

No.	solute	E	S	A	B	V	D^- (3.4)	D^+ (3.4)	D^- (8.0)	D^+ (8.0)	log D (3.4)	log D (8.0)	acid pK_a	base pK_a	ch.[c)] (3.4)	ch.[c)] (8.0)	log k (3.4)	log k (8.0)
46	anisole	0.71	0.75	0.00	0.29	0.916					1.79	1.79			0	0	-0.21	0.41
47	acetophenone	0.82	1.01	0.00	0.48	1.014					1.36	1.36			0	0	-0.26	0.23
48	aniline	0.96	0.96	0.26	0.41	0.816		0.95		0.00	0.00	1.26		4.64	(+)	0	-0.96	-0.07
49	4-nitroaniline	1.22	1.83	0.45	0.38	0.990		0.01		0.00	1.21	1.22		1.43	0	0	0.65	0.72
50	1,2-toluidine	0.97	0.92	0.23	0.45	0.957		0.92		0.00	0.62	1.73		4.48	(+)	0	-0.86	0.01
51	1,4-toluidine	0.92	0.95	0.23	0.45	0.957		0.97		0.00	0.14	1.73		4.99	(+)	0	-0.96	0.07
52	bromobenzene	0.88	0.73	0.00	0.09	0.891					2.84	2.84			0	0	0.09	0.65
53	chlorobenzene	0.72	0.65	0.00	0.07	0.839					2.56	2.56			0	0	-0.05	0.49
54	1,2-dichlorobenzene	0.87	0.78	0.00	0.04	0.961					3.08	3.08			0	0	0.26	1.36
55	1,2,3-trichlorobenzene	1.03	0.86	0.00	0.00	1.084					3.60	3.60			0	0	0.73	1.72
56	3-chlorophenol	0.91	1.06	0.69	0.15	0.898	0.00		0.14		2.28	2.22	8.79		0	(-)	0.25	1.28
57	4-chlorophenol	0.92	1.08	0.67	0.21	0.898	0.00		0.10		2.28	2.24	8.96		0	0	0.35	1.41
58	2-nitrotoluene	0.87	1.11	0.00	0.27	1.032					2.47	2.47			0	0	0.16	0.96
59	benzaldehyde	0.82	1.00	0.00	0.39	0.873					1.72	1.72			0	0	-0.24	0.16
60	3-hydroxybenzaldehyde	0.99	1.38	0.74	0.40	0.932	0.00		0.10		1.44	1.39	8.94		0	(-)	0.12	0.78
61	benzamide	0.99	0.50	0.49	0.67	0.973					0.70	0.70			0	0	-0.42	-0.41
62	benzonitrile	0.74	1.11	0.00	0.33	0.871					1.86	1.86			0	0	-0.29	0.11
63	benzophenone	1.45	1.50	0.00	0.50	1.481					3.27	3.27			0	0	0.55	1.38
64	benzylalcohol	0.80	0.87	0.33	0.56	0.916					1.21	1.21			0	0	-0.58	-0.20
65	dibenzothiophene	1.96	1.31	0.00	0.18	1.379					3.87	3.87			0	0	0.46	1.96
66	2-naphthol	1.52	1.08	0.61	0.40	1.144	0.00		0.02		2.76	2.76	9.78		0	0	0.73	0.93
67	pyridine[b)]	0.63	0.84	0.00	0.52	0.675		0.98		0.00	-0.25	0.73		5.12	(+)	0	-0.55	-0.80
68	ethyl acetate	0.11	0.62	0.00	0.45	0.747					0.21	0.21			0	0	-0.53	-0.42
69	hydroquinone	1.00	1.00	1.16	0.60	0.834	0.00		0.02		1.48	1.47	9.68		0	0	-0.28	0.18

No.	solute	E	S	A	B	V	D^- (3.4)	D^+ (3.4)	D^- (8.0)	D^+ (8.0)	log D (3.4)	log D (8.0)	acid pK_a	base pK_a	ch.[c)] (3.4)	ch.[c)] (8.0)	log k (3.4)	log k (8.0)
70	pyrene	2.81	1.71	0.00	0.29	1.585					4.37	4.37			0	0	1.15	2.42
71	urea	0.50	1.49	0.83	0.84	0.465					-1.30	-1.30			0	0	-0.41	-1.13
72	thymine	0.80	1.00	0.44	1.03	0.893	0.00		0.08		-0.14	-0.17	9.06		0	0	-0.39	-0.73
73	tyramine	1.01	1.17	0.71	0.94	1.157	0.00	1.00	0.01	0.97	-2.31	-0.64	10.27	9.58	(+)	(+)	-0.94	-0.30
74	cytosine	1.43	1.90	0.60	1.02	0.793	0.00	0.92	0.00	0.00	-0.31	-0.27	12.20	4.45	(+)	0	-0.54	-1.41
75	uridine	1.88	2.35	0.90	2.29	1.582	0.00		0.02		-2.19	-2.20	9.70		0	0	-0.63	-0.96
76	2-aminopyridine	0.98	1.10	0.32	0.63	0.775		1.00		0.06	-1.11	-0.79		6.84	(+)	0	-0.62	-0.67
77	2-deoxyuridine	1.65	2.14	0.74	1.92	1.524	0.00		0.02		-1.28	-1.28	9.71		0	0	-0.62	-0.91
78	4-aminopyridine[a)]	0.90	1.21	0.23	0.71	0.775		1.00		0.90	-1.11	-0.79		8.95	(+)	(+)	-0.73	-0.06
79	benzyltrimethyl-ammonium chlorid	0.36	0.56	0.00	0.15	1.401		1.00		1.00	-2.64	-2.64			(+)	(+)	-0.29	0.46

a) Excluded from the LSER model as outliers under alkaline eluent conditions.

b) Excluded from the LSER model as outliers under acidic eluent conditions.

c) ch. denotes the charge state at a given hydro-organic pH; 0 – neutral, (+) – cation, (-) – anion, zw – zwitterion.

Table S3 Descriptive statistics of the solute set outlined in Table S1:

acidic eluent (75 solutes, 4 outliers excluded)

	E	*S*	*A*	*B*	*V*	*D-*	D^+
minimum	0.110	0.500	0.000	0.000	0.465	0.000	0.000
maximum	2.810	2.350	1.400	2.290	1.684	1.000	1.000
mean	1.036	1.115	0.429	0.566	1.037	0.084	0.196
standard deviation	0.451	0.417	0.412	0.442	0.259	0.238	0.389

alkaline eluent (75 solutes, 4 outliers excluded)

	E	*S*	*A*	*B*	*V*	*D-*	D^+
minimum	0.110	0.500	0.000	0.000	0.465	0.000	0.000
maximum	2.810	2.350	1.400	2.290	1.684	1.000	1.000
mean	1.031	1.098	0.417	0.558	1.037	0.237	0.104
standard deviation	0.453	0.417	0.404	0.443	0.257	0.407	0.301

Table S4 Correlation matrix of the solute descriptors of the solute set outlined in Table S1:

acidic eluent (75 solutes, 4 outliers excluded)

	E	*S*	*A*	*B*	*V*	D^-	D^+
E	1.000	0.686	0.171	0.340	0.691	0.099	0.015
S		1.000	0.527	0.679	0.468	0.158	0.079
A			1.000	0.552	0.072	0.384	0.224
B				1.000	0.357	0.370	0.259
V					1.000	0.352	0.146
D^-						1.000	0.490
D^+							1.000

alkaline eluent (75 solutes, 4 outliers excluded)

	E	*S*	*A*	*B*	*V*	D^-	D^+
E	1.000	0.689	0.171	0.339	0.696	0.028	0.078
S		1.000	0.510	0.672	0.470	0.190	0.142
A			1.000	0.548	0.063	0.440	0.348
B				1.000	0.365	0.311	0.301
V					1.000	0.196	0.304
D^-						1.000	0.331
D^+							1.000

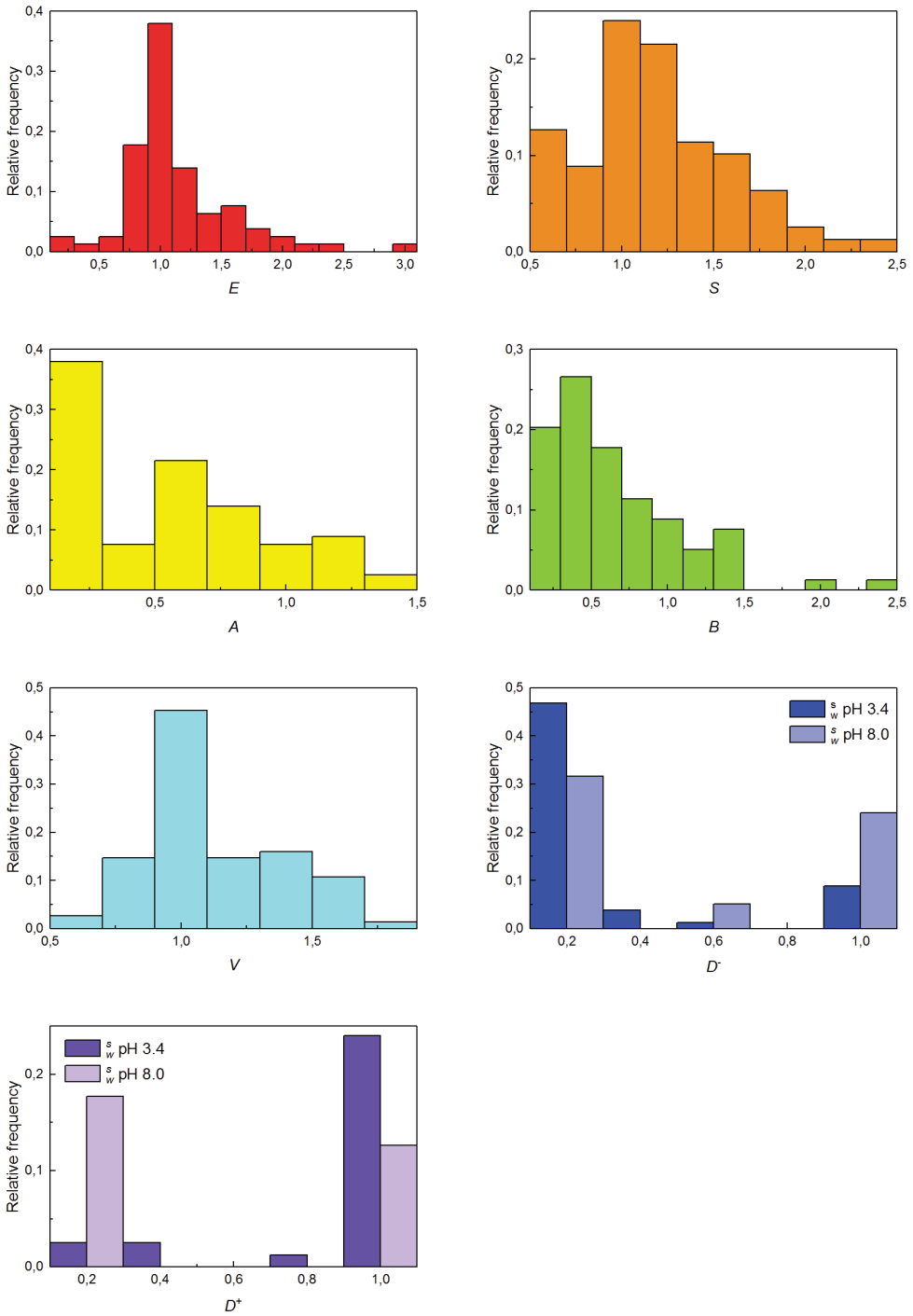

Figure S2 Frequency plots of the solute descriptors of the solute set outlined in Table S1.

Table S5 System coefficients (significant values are shown in bold) and statistics of the acidified and neutralized stationary phases

stationary phase	model	*e*	*s*	*a*	*b*	*v*	d^-	d^+	*c*	R^2	*n*	*F*
acid. PANI-SiO_2		0.22	**0.30**	**0.37**	**-0.96**	**0.92**	**0.36**	**-0.69**	-1.06	0.81	75	38
	p-value	0.06	0.03	0.00	0.00	0.00	0.03	0.00	0.00			
	SE	0.12	0.14	0.10	0.10	0.18	0.17	0.09	0.14			
	±CI	0.24	0.28	0.20	0.20	0.36	0.33	0.17	0.29			
alkal. PANI-SiO_2		**0.30**	-0.14	**0.63**	**-1.90**	**2.36**	**0.44**	**-1.26**	-1.31	0.88	75	75
	p-value	0.05	0.40	0.00	0.00	0.00	0.00	0.00	0.00			
	SE	0.15	0.17	0.13	0.12	0.25	0.10	0.15	0.19			
	±CI	0.30	0.34	0.27	0.25	0.49	0.21	0.31	0.38			

CI represents the ±95% confidence interval; SE is the standard error of the coefficients; the statistical *p*-value expresses the probability of the error that the individual coefficient does not contribute to the model; *F* corresponds to Fisher's statistics; *n* is the number of solutes considered in the regression. Chromatographic conditions: the acidic mobile phase consisted of a methanol/100 mM sodium phosphate aqueous solution at ${}^{s}_{w}pH$ 3.4, (50/50; v/v); alkaline mobile phase consisted of a methanol/100 mM sodium phosphate aqueous solution at ${}^{s}_{w}pH$ 8.0, (50/50; v/v), 25 °C temperature and 5 µL/min flow rate.

Additional information proving the mixed-mode retention mechanism of the PANI-SiO_2 stationary phase

Fig. S3 plotting the experimental log *k* value as a function of log *D* clearly shows that neutral hydrophobic compounds are the most retained solutes in the acidic eluent and are accompanied by a few partly dissociated carboxylic acids. The blue line represents the linear regression fit and is approximately in the middle of oblong-like scattered solutes, although anions are somewhat above this curve. However, in the alkaline mobile phase, the solutes are scattered far more randomly.

Surprisingly, dissociated and thus hydrophilic carboxylic acids are also strongly retained under these conditions, which indicates the involvement of more than one major retention-promoting interaction (Fig S3 B). Not only hydrophobicity but also hydrogen bonding and anion-exchange interactions strongly affect solute retention. Thus, anion-exchange interactions should be considered in the overall retention

mechanism of PANI-SiO_2, especially when using alkaline eluents. Therefore, we conclude that PANI-SiO_2 behaves as mixed-mode stationary phase also in RP mode.

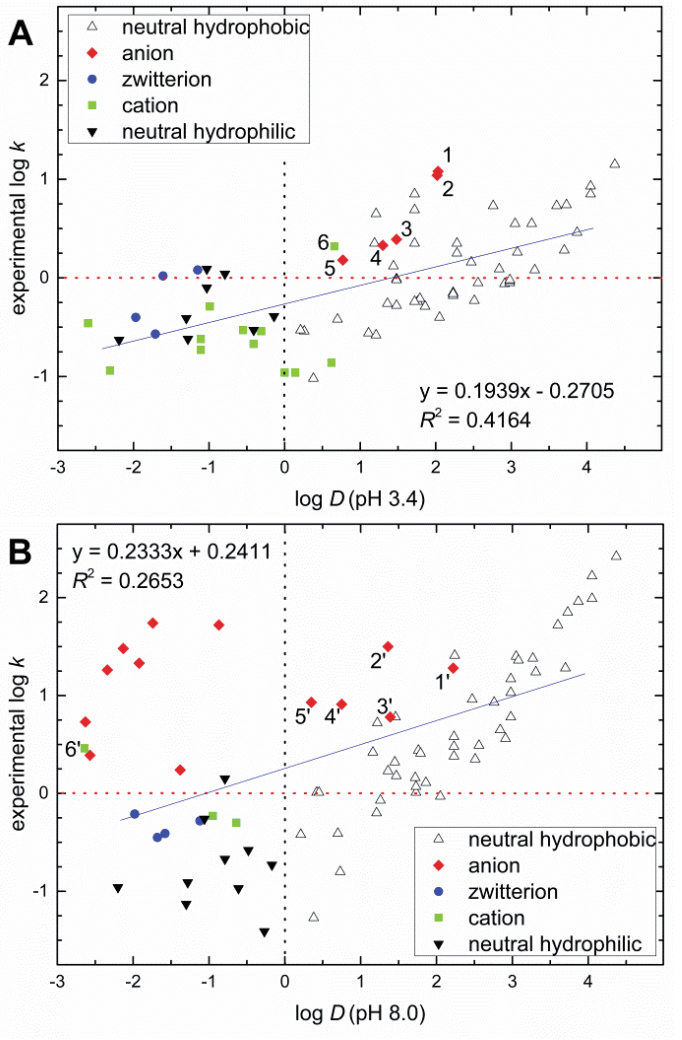

Figure S3 Experimental log k value as a function of log D under varied ${}^{s}_{w}pH$ of the mobile phase; horizontal red dotted line denotes the zero value of the experimental log k; the vertical black dotted line denotes the zero value of the log D; analytes – anions: 1, 1,2-coumaric acid; 2, 1,4-coumaric acid; 3, benzoic acid; 4, 4-hydroxyphenylacetic acid; 5, acetylsalicylic acid; 1', 3-chlorophenol; 2', 3-nitrophenol; 3', 3-hydroxybenzaldehyde; 4', 4-nitrophenol; 5', 2-nitrophenol; cations: 6, 4-aminobenzoic acid; 6', benzyltrimethylammonium chloride; blue line expresses the linear regression curve. Chromatographic conditions: acidic mobile phase consisted of a methanol/100 mM sodium phosphate aqueous solution at ${}^{s}_{w}pH$ 3.4, (50/50; v/v); alkaline mobile phase consisted of a methanol/100 mM sodium phosphate aqueous solution at ${}^{s}_{w}pH$ 8.0, (50/50; v/v), 25 °C temperature, 5 µL/min flow rate, 0.1 µL injection volume.

Evaluation of partition and/or adsorption interaction mechanism – additional equation comparison describing the partitioning mechanism

Reversed-phase chromatography has its roots in liquid–liquid chromatography, and thus the retention is considered (ideally) controlled only by partition [6]. Before applying the equation proposed by Schoenmakers [7], the partition interaction mechanism of RP stationary phases was considered using another empirical equation:

$$\log k = \log k_w + a\varphi + b\varphi^2 \quad (3)$$

where k stands for the solute retention factor, k_w is the solute retention factor with pure water as the mobile phase, φ is the volume fraction of the organic solvent (inhere methanol), and a and b are constants for a given solute and eluent combination, respectively. This equation is presumably applicable in 0.1 – 0.9 range of the organic solvent volume fraction [8]. Indeed, from the practical aspect of the partitioning mechanism evaluation, Eq. (3) does not differ from the more general equation proposed by Schoenmakers. However, for mobile phases of intermediate composition, the following equation can be applied as a reasonable approximation for variations in retention with the volume fraction of the organic solvent in the eluent:

$$\log k = \log k_w - S \quad (4)$$

where k_w corresponds to the analyte retention factor in the pure weaker component of eluent (inhere water), φ is the volume fraction of the stronger member of a binary eluent mixture (inhere methanol), and S is a solute-dependent factor related to the elution strength of the organic solvent (or simply the slope of log k versus φ when fitted with a linear regression model; for methanol typical S value is 2.6) [8]. Eq. (4) is more restricted in the applicable range of eluent composition than Eq. (3), but the former provides more insight into the selection of mobile phases of constant elution strength for method development in RP mode. Our methanol volume fraction only ranged from 0.5 to 0.9; thus, we used Eq. (3) and discussed the results. When comparing the values of R^2 for the linear fitting (Fig. S4 A, B), based on Eq. (4), with the second-order polynomial fitting (Fig. S4 C, D), based on Eq. (3), the latter is best fitted in all cases. The explanation is that our elution strength range is still too broad for linear dependence. Therefore, Eq. (4) is applicable, even for smaller differences in organic solvent volume fraction [9]. Moreover, a methanol volume fraction ≥ 0.8 corresponds to hydrophilic interaction liquid chromatography (HILIC) mobile phase composition [10].

Additionally, the R^2 of the parabolic equation fitting shows a generally better fit than that of linear fitting because the constructed parabola can be almost infinitely opened and thus mimic a linear function, whereas the reverse does not apply.

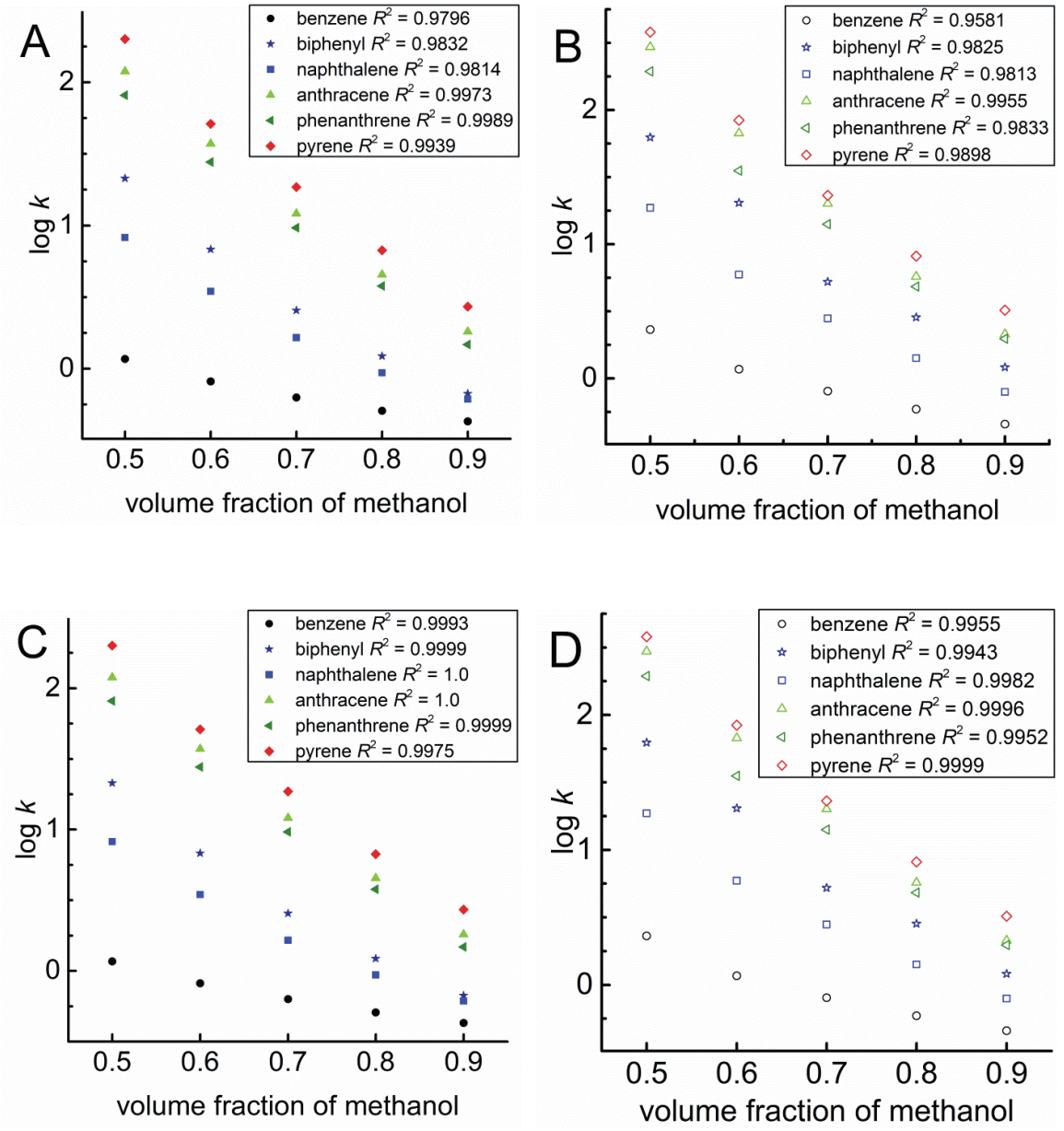

Figure S4 Plots of log k as a function of volume fraction of methanol using linear (A, B) or parabolic (C, D) fitting for selected neutral hydrophobic solutes in both acidic (A, C) – methanol/20 mM sodium citrate (v/v; ${}^{w}_{w}pH$ 2.5; ${}^{s}_{w}pH$ 3.7) and alkaline (B, D) – methanol/20 mM sodium citrate (v/v; ${}^{w}_{w}pH$ 7.0; ${}^{s}_{w}pH$ 8.7) eluents.

Difference in PANI-SiO_2 selectivity towards basic solutes under varied pH of the eluent buffer

Selectivity of PANI-SiO_2 stationary phase changes also for small organic bases under varied pH of the eluent. To prove this statement we selected adenine ($pK_{a,1} = 4.25$, $pK_{a,2} = 9.90$), aniline ($pK_a = 4.64$), and pyridine ($pK_a = 5.12$) as probes (concentration of 0.1 – 0.3 mg/mL) and studied their separation in varied eluent pH. As the mobile phase buffer we chose Britton-Robinson buffer (40 mM acetic acid, 40 mM phosphoric acid, 40 mM boric acid, pH adjusted by titration with sodium hydroxide) due to its buffering capacity covering pH range from 2 to 12. The chosen pH values are 3, 5, 7, 8, and 10 to show the separations in moderate acidic, weak acidic, neutral, weak alkaline and moderate alkaline aqueous pH. Selectivity of the PANI-SiO_2 changes with increasing pH because of successive deprotonation of the probes and PANI chains and the related change of their polarity. The elution order of aniline and pyridine changes after the transition from acidic to neutral pH of the eluent buffer. Additionaly, the retention time of adenine shortens with the increasing pH, and thus the shift of aniline and adenine elution order was also observed in alkaline pH.

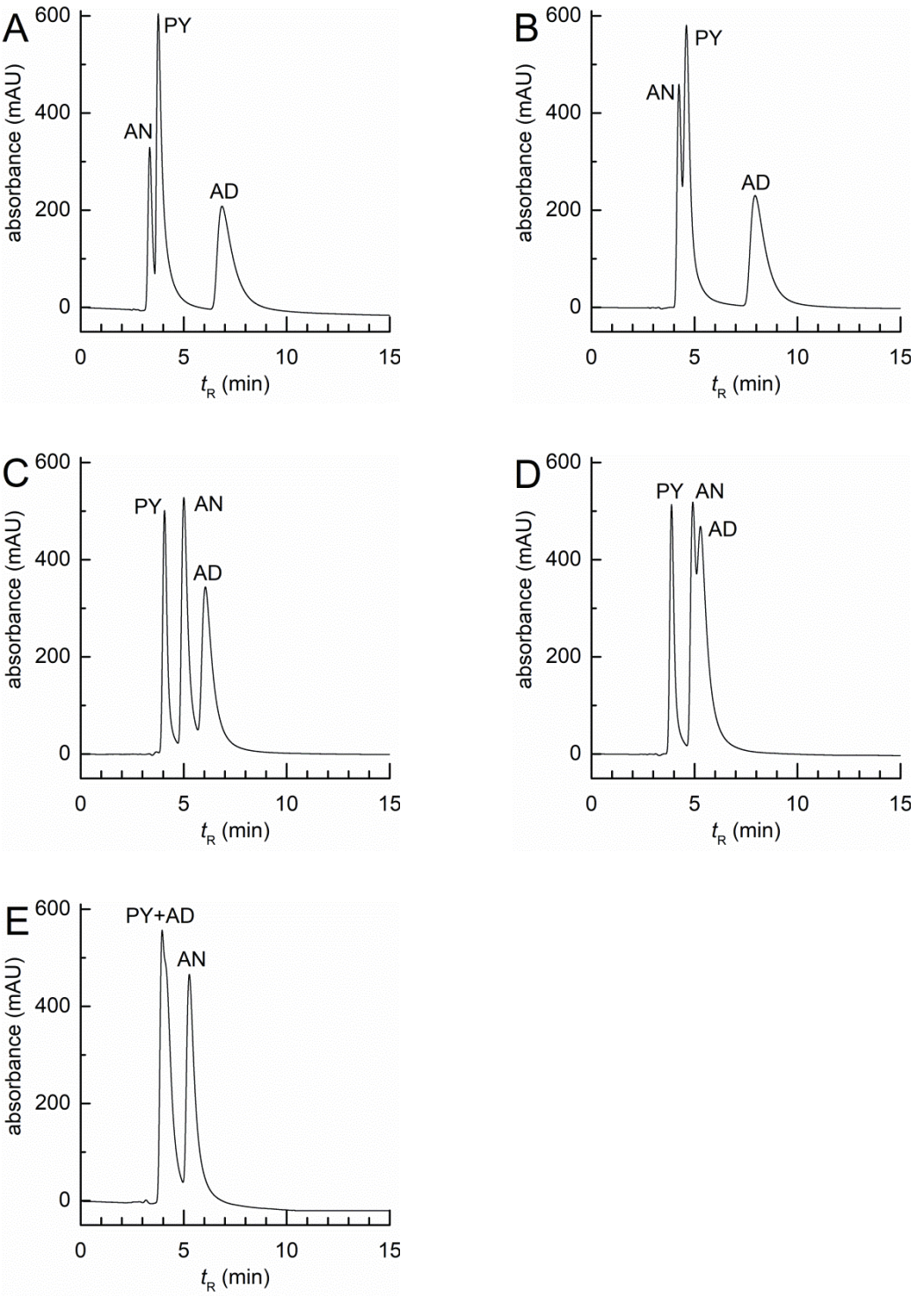

Figure S5 Chromatograms of separations of basic solutes under different pH of the eluent buffer – ${}^{w}_{w}pH$ 3.0/ ${}^{s}_{w}pH$ 4.0 (A), ${}^{w}_{w}pH$ 5.0/ ${}^{s}_{w}pH$ 5.9 (B), ${}^{w}_{w}pH$ 7.0/ ${}^{s}_{w}pH$ 8.0 (C), ${}^{w}_{w}pH$ 8.0/ ${}^{s}_{w}pH$ 8.7 (D), ${}^{w}_{w}pH$ 10.0/ ${}^{s}_{w}pH$ 10.4 (E); AD, adenine; AN, aniline; PY, pyridine; separation conditions: mobile phase consisting of 50/50 (v/v) methanol/Britton-Robinson buffer, flow rate 5 µl/min, column compartment temperature 25 °C, UV detection at 254 nm.

Tanaka chromatographic test

Tanaka test is one of the most used chromatographic tests for characterization of RP stationary phases, especially C_{18}-based ones. This test provides information about stationary phase retention capacity, hydrophobic selectivity, shape selectivity, hydrogen-bonding capacity, and ion-exchange capacity according to the retention and selectivity factors of seven selected solutes whose retention times are measured under the specific conditions (Table S6) [11].

Table S6 Parameters and obtained values of Tanaka test for PANI-SiO_2

parameter		value	mobile phase
retention capacity	$k_{n\text{-pentylbenzene}}$	0.64	80/20 (v/v) methanol/water
hydrophobic selectivity	$\alpha_{n\text{-pentylbenzene / } n\text{-butylbenzene}}$	1.18	80/20 (v/v) methanol/water
shape selectivity	$\alpha_{\text{triphenylene / } o\text{-terphenyl}}$	7.38	80/20 (v/v) methanol/water
hydrogen-bonding (silanol) capacity	$\alpha_{\text{caffeine / phenol}}$	1.65	30/70 (v/v) methanol/water
acidic cation exchange capacity	$\alpha_{\text{benzylamine / phenol}}$	0.24	30/70 (v/v) methanol/ 20 mM phosphate buffer ($^{w}_{w}pH$ 2.7)
total cation exchange capacity	$\alpha_{\text{benzylamine / phenol}}$	0.30	30/70 (v/v) methanol/ 20 mM phosphate buffer ($^{w}_{w}pH$ 7.6)

Other experimental conditions: flow rate 5 μL/min (in the 320 μm i.d. capillary column corresponding to 1 mL/min of 4.6 mm i.d. conventional HPLC column), column compartment temperature 40 °C, sample injection 0.1 μL, UV detection at 254 nm.

Obtained values of individual parameters show that PANI-SiO_2 mixed-mode stationary phase differs from most RP stationary phases, which however also differ from each other [12, 13]. PANI-SiO_2 retention capacity towards *n*-pentylbenzene is low, hydrophobic (methylene) selectivity is also low because this stationary phase does not contain any methylene moieties. Shape selectivity is higher than for most of C_{18} stationary phases which is likely given by the arrangement of PANI chains. Hydrogen-bonding capacity is relatively high not only because the supporting silica is not chemically modified but also due to the presence of amino and imino moieties in PANI.

Cation exchange capacity is lower under acidic conditions due to presumably higher electrostatic repulsion between cationic analytes and positively charged nitrogen atoms in PANI structure.

References:

[1] Chirita R.-I., West C., Zubrzycki S., Finaru A. L., Elfakir C., Investigations on the chromatographic behaviour of zwitterionic stationary phases used in hydrophilic interaction chromatography. *J. Chromatogr. A* 2011, *1218*, 5939–5963.

[2] Schuster G., Lindner W., Comparative characterization of hydrophilic interaction liquid chromatography columns by linear solvation energy relationships. *J. Chromatogr. A* 2013, *1273*, 73–94.

[3] Schuster G., Lindner W., Additional investigations into the retention mechanism of hydrophilic interaction liquid chromatography by linear solvation energy relationships. *J. Chromatogr. A* 2013, *1301*, 98–110.

[4] West C., Auroux E., Deconvoluting the effects of buffer salt concentration in hydrophilic interaction chromatography on a zwitterionic stationary phase. *J. Chromatogr. A* 2016, *1461*, 92–97.

[5] Marvin 16.4.11.0, (2015), ChemAxon, Budapest, Hungary 215. Available from: http://www.chemaxon.com.

[6] Poole C. F., Kiridena W., DeKay C., Koziol W. W., Rosencrans R. D., Insights into the retention mechanism on an octadecylsiloxane-bonded silica stationary phase (HyPURITY C18) in reversed-phase liquid chromatography. *J. Chromatogr. A* 2006, *1115*, 133–141.

[7] Schoenmakers P. J., Billiet H. A. H., De Galan L., Influence of organic modifiers on the retention behaviour in reversed-phase liquid chromatography and its consequences for gradient elution. *J. Chromatogr.* 1979, *185*, 179–195.

[6] Poole C. F., Kiridena W., DeKay C., Koziol W. W., Rosencrans R. D., Insights into the retention mechanism on an octadecylsiloxane-bonded silica stationary phase (HyPURITY C18) in reversed-phase liquid chromatography. *J. Chromatogr. A* 2006, *1115*, 133–141.

[8] Poole C. F., Poole S. K., Chromatography today. First Edition, Elsevier, Amsterdam 1991.

[9] Fasoula S., Zisi Ch., Gika H., Pappa-Louisi A., Nikitas P., Retention prediction and separation optimization under multilinear gradient elution in liquid chromatography with Microsoft Excel macros. *J. Chromatogr. A* 2015, *1395*, 109–115.

[10] Hemstrom P., Irgum K., Hydrophilic interaction chromatography. *J. Sep. Sci.* 2006, *29*, 1784–1821.

[11] Kimata K., Iwaguchi K., Onishi S., Jinno K., Eksteen R., Hosoya K., Araki M.,Tanaka N., Chromatographic characterization of silica C18 packing materials. Correlation between a preparation method and retention behavior of stationary phase. *J. Chromatogr. Sci*. 1989, *27*, 721–728.

[12] Petersson P., Euerby M. R., Characterization of RPLC columns packed with porous sub-2 μm particles. *J. Sep. Sci.* 2007, *30*, 2012–2024.

[13] Euerby M. R., James M., Axelsson B.-O., Rosen O., Petersson P., Validation of the extended Tanaka column characterization protocol by multivariate analysis of chromatographic retention of low-molecular-weight analytes on reversed phase columns using methanol and acetonitrile as organic modifiers. *J. Chromatogr. Sci*. 2012, *35*, 2592–2598.

7. CONCLUDING SUMMARY

This dissertation thesis deals with physicochemical and chromatographic characterization of polyaniline-coated stationary phases and it is based on three related studies that have been published in international journals.

The first part of the thesis is focused on surface modification of bare silica and octadecyl silica sorbents by in-situ chemical polymerization of aniline hydrochloride and their subsequent systematic characterization using the linear solvation energy relationship approach in HILIC mode. In addition to that, several common physicochemical techniques were used to characterize properties of the altered materials. The modified sorbents were packed into capillary columns using the developed slurry packing procedure. The retention interactions taking place between solute and the separation system were evaluated on the basis of retention data of a number of various solutes. It was shown that polyaniline coating has a substantial effect on the retention-promoting interactions of both polyaniline-coated stationary phases. However, the extent of these interactions differs according to the supporting material used. The assumed mixed-mode retention mechanism was proven for both the stationary phases, although the polyaniline-coated bare silica sorbent was concluded as more promising for separation of polar solutes in HILIC mode.

In the second study, the separation potential of polyaniline-coated silica stationary phase was investigated in different chromatographic modes. The retention factor curves of structurally similar solutes, albeit of different polarity, were constructed as a function of organic modifier content in the mobile phase, pH variation of the eluent was also included. The results showed that this stationary phase is applicable in more than one chromatographic mode. Further, the separation performance of polyaniline-coated sorbent was assessed for two sets of either hydrophobic or hydrophilic structural analogues in NP, RP and HILIC modes. The changes of elution order and selectivity were observed for related solutes. As the stationary phase exhibits mixed-mode retention mechanism, the elution order of solutes is not governed only by their polarity. Interestingly, even slightly hydrophilic solutes can be sufficiently retained on this sorbent in the RP mode. Surprisingly, polyaniline-coated silica sorbent is selective for distinction of the functional group position in the solute aromatic ring in NP and RP modes. In addition, selectivity of this stationary phase was compared to the selectivity of unmodified bare silica and octadecyl silica commercial sorbents. It was shown that

polyaniline-modified stationary phase provides different selectivity from the latter sorbents for the tested sets of solutes. Furthermore, the chromatographic performance of the column improves significantly after the modification of bare silica with polyaniline layer in NP and HILIC modes.

The last study deals with protonation ability of polyaniline-coated silica sorbent and its effect on retention behavior of various solutes in the mobile phase of different pH investigated by the linear solvation energy relationship in RP mode of capillary LC. The obtained results show that pH of the eluent has a significant effect on the extent of dominant retention interactions. When the alkaline mobile phase is used, the stationary phase exhibits remarkably more hydrophobic behavior which is provided by deprotonation of nitrogen atoms in the structure of the polyaniline. Moreover, by tuning the mobile phase pH, we can even modulate the retention of neutral hydrophobic solutes, such as aromatic hydrocarbons, because the pH-dependent charge and structure of polymer chains of the polyaniline-coated silica stationary phase shows a mixed-mode separation mechanism also in RP mode. Additionally, investigation of partitioning or adsorption retention processes on the stationary phase was performed. According to the results, both processes participate in the retention of solutes.

To conclude, this thesis broadened our knowledge of retention behavior of tunable, mixed-mode polyaniline-coated stationary phases under various conditions, their unique selectivity and potential applications in LC.

REFERENCES

[1] Pino V., Afonso A. M.: *Surface-bonded ionic liquid stationary phases in high performance liquid chromatography – a review*. Anal. Chim. Acta 714 (2012) 20–37.

[2] Bakry R., Rainer M., Huck C. W., Bonn G. K.: *New stationary phases for enrichment and separation in the 'omics' era*. Bioanalysis 1 (2009) 151–169.

[3] Barhate C. L., Lopez D., Makarov A. A., Bu X., Morris W. J., Lekhal A., Hartman R., Armstrong D. A., Regalado E. L.: Macrocyclic glycopeptide chiral selectors bonded to core-shell particles enables enantiopurity analysis of the entire verubecestat synthetic route. J. Chromatogr. A 1539 (2018) 87–92.

[4] Borges E. M.: *Silica, hybrid silica, hydride silica and non-silica stationary phases for liquid chromatography*. J. Chromatogr. Sci. 53 (2015) 580–597.

[5] Tanaka N., McCalley D. V.: *Core-shell, ultrasmall particles, monoliths, and other support materials in high-peformance liquid chromatography*. Anal. Chem. 88 (2016) 279–298.

[6] Kirkland J. J.: *Development of some stationary phases for reversed-phase high-performance liquid chromatography*. J. Chromatogr. A 1060 (2004) 9–21.

[7] Hui Y., Cunyu J., Haibo W., Guangjun S., Yu J., Yanxiong K., Xinmiao L.: *Highly stable high performance liquid chromatography stationary phase based on direct chemical modification of organic bridges in hybrid silica*. J. Chromatogr. A 1247 (2012) 63–70.

[8] Iverson C. D., Lucy C. A.: *Aniline-modified porous graphitic carbon for hydrophilic interaction and attenuated reverse phase liquid chromatography*. J. Chromatogr. A 1373 (2014) 17–24.

[9] Kurganov A., Truedinger U., Isaeva T., Unger K.: *Native and modified alumina, titania and zirconia in normal and reversed-phase high-performance liquid chromatography*. Chromatographia 42 (1996) 217–222.

[10] Arrua R. D., Strumia M. C., Alvarez Igarzabal C. I.: *Macroporous monolithic polymers: preparation and applications.* Materials 2 (2009) 2429–2466.

[11] Lee W.-C., Cheng C.-H., Pan H.-H., Chung T.-H., Hwang C.-C.: *Chromatographic characterization of molecularly imprinted polymers*. Anal. Bioanal. Chem. 390 (2008) 1101–1109.

[12] Claessens H. A., van Straten M. A.: *Review on the chemical and thermal stability of stationary phases for reversed-phase liquid chromatography*. J. Chromatogr. A 1060 (2004) 23–41.

[13] Silva C. R., Collins C. H., Jardim I. C. S. F., Airoldi C.: *Chromatographic and column stability at pH 7 of a C18 dimethylurea polar stationary phase*. J. Chromatogr. A 1030 (2004) 157–166.

[14] Wirth M. J., Fatunmbi H. O.: *Horizontal polymerization of mixed trifunctional silanes on silica: a potential chromatographic stationary phase*. Anal. Chem. 64 (1992) 2783–2786.

[15] Paek C., Huang Y., Filgueira M. R., McCormick A. V., Carr P. W.: *Development of a carbon clad core-shell silica for high speed two-dimensional liquid chromatography.* J. Chromatogr. A 1229 (2012) 1239–139.

[16] Doyle C. A., Dorsey J. G.: Handbook of HPLC 78, *Chapter 8: Reversed-phase HPLC: Preparation and characterization of reversed-phase stationary phases* (1998) 293–323 New York, NY, USA: Marcel Dekker ISBN 0-8247-9444-3.

[17] Nawrocki J., Dunlap C., Li J., Zhao J., McNeff C. V., McCormick A., Carr P. W.: *Part II. Chromatography using ultra-stable metal oxide-based stationary phases for HPLC*. J. Chromatogr. A 1028 (2004) 31–62.

[18] Wang Y., Wahab M. F., Breitbach Z. S., Armstrong D. W.: *Carboxylated cyclofructan 6 as a hydrolytically stable high efficiency stationary phase for hydrophilic interaction liquid chromatography and mixed mode separations*. Anal. Meth. 8 (2016) 6038–6045.

[19] Zhang K., Liu X.: *Mixed-mode chromatography in pharmaceutical and biopharmaceutical applications*. J. Pharm. Biomed. Anal. 128 (2016) 73–88.

[20] Petro M., Berek D.: *Polymers immobilized on silica gels as stationary phases for liquid chromatography*. Chromatographia 37 (1993) 549–561.

[21] Wu J. Y., Bicker W., Lindner W.: *Separation properties of novel and commercial polar stationary phases in hydrophilic interaction and reversed-phase liquid chromatography mode*. J. Sep. Sci. 31 (2008) 1492–1503.

[22] Novotny M. V.: *Development of capillary liquid chromatography: A personal perspective*. J. Chromatogr. A 1523 (2017) 3–16.

[23] Lesellier E., West C.: *Description and comparison of chromatographic tests and chemometric methods for packed column classification*. J. Chromatogr. A 1158 (2007) 329–360.

[24] Sykora D., Vozka J., Tesarova E.: *Chromatographic methods enabling the characterization of stationary phases and retention prediction in high-performance liquid chromatography and supercritical fluid chromatography*. J. Sep. Sci. 39 (2016) 115–131.

[25] Faria A. M., Collins C. H., Jardim I. C. S. F.: *State-of-the-art in immobilized polymer stationary phases for high-performance liquid chromatography*. J. Braz. Chem. Soc. 20 (2009) 1385–1398.

[26] Bottoli C. B. G., Collins K. E., Carol H.: *Chromatographic evaluation of self-immobilized stationary phases for reversed-phase liquid chromatography*. J. Chromatogr. A 987 (2003) 87–92.

[27] Yishai-Aviram L., Grushka E.: Advances in chromatograph: Volume 43*, Chapter 5: Polyelectrolytes as stationary phases in liquid chromatography* (2004) 273–304, New York, NY, USA: CRC Press Taylor & Francis ISBN 978-0-203-99695-9.

[28] Hirayama C., Ihara H., Nagaoka S., Makise H.: *Porous polymer packings from vinyl ether derivatives for reversed-phase liquid chromatography*. Chromatographia 33 (1992) 19–24.

[29] Svec F.: *Organic polymer monoliths as stationary phases for capillary HPLC*. J. Sep. Sci. 27 (2004) 1419–1430.

[30] Pirogov A.V., Buchberger W.: *Ionene-coated sulfonated silica as a packing material in the packed-capillary mode of electrochromatography*. J. Chromatogr. A 916 (2001) 51–59.

[31] Carbonnier B., Janus L., Lekchiri Y., Morcellet M.: *Coating of porous silica beads by in situ polymerization/crosslinking of 2-hydroxypropyl β-cyclodextrin for reversed-phase high performance liquid chromatography applications*. J. Appl. Polym. 91 (2004) 1419–1426.

[32] Wallace G. G., Spinks G. M., Kane-Maguire L. A. P., Teasdale P. R.: *Conductive electroactive polymers. Intelligent polymer systems* (2009) Boca Raton, FL, USA: CRC Press Taylor & Francis, 3rd ed. ISBN 978-1-4200-6709-5.

[33] MacDiarmid A. G.: *"Synthetic metals": A novel role for organic polymers (Nobel lecture)*. Angew. Chem. Int. Ed. 40 (2001) 2581–2590.

[34] Tran H. D., D'Arcy J. M., Wang Y., Beltramo P. J., Strong V. A., Kaner R. B: *The oxidation of aniline to produce "polyaniline": a process yielding many different nanoscale structures*. J. Mater. Chem. 21 (2011) 3534–3550.

[35] Green A. G., Woodhead A. E.: *Aniline black and allied compounds*. J. Chem. Soc. 101 (1910) 2388–2403.

[36] Chiang J.-C., MacDiarmid A. G.: *"Polyaniline": Protonic acid doping of the emeraldine form to the metallic regime*. Synth. Met. 13 (1986) 193–205.

[37] Stejskal J., Kratochvil P., Jenkins A. D.: *The formation of polyaniline and the nature of its structures*. Polymer 37 (1996) 367–369.

[38] Lux F.: *Properties of electronically conductive polyaniline: a comparison between well-known literature data and some recent experimental findings*. Polymer 35 (1994) 2915–2936.

[39] Pron A., Rannou P.: *Processible conjugated polymers: from organic semiconductors to organic metals and superconductors*. Prog. Polym. Sci. 27 (2002) 135–190.

[40] Kulkarni V. G., Campbell L. D., Mathew W. R.: *Thermal stability of polyaniline*. Synth. Met. 30 (1989) 321–325.

[41] Gvozdenovic M. M., Jugovic B. Z., Stevanovic J. S., Trisovic T. L., Grgur B. N.: Electropolymerization. *Chapter 4: Electrochemical Polymerization of Aniline* (2011) 77–96 Rijeka, Croatia: InTech ISBN 978-953-307-693-5.

[42] Chinn D., DuBow J., Liess M., Josowicz M., Janata J.: *Comparison of chemically and electrochemically prepared polyaniline films: 1. Electrical properties*. Chem. Mater. 7 (1995) 1504–1509.

[43] Stejskal J., Gilbert R. G.: *Polyaniline. Preparation of a conducting polymer (IUPAC Technical Report)*. Pure Appl. Chem. 74 (2002) 857–867.

[44] Wang Y., Levon K.: *Influence of dopant on electroactivity of polyaniline*. Macromol. Symp. 317 (2012) 240–247.

[45] Pron A., Genoud F., Menardo C., Nechtschein M.: *The effect of the oxidation conditions on the chemical polymerization of polyaniline*. Synth. Met. 24 (1988) 193–201.

[46] Armes S. P., Miller J. F.: *Optimum reaction conditions for the polymerization of aniline in aqueous solution by ammonium persulphate*. Synth. Met. 22 (1988) 385–393.

[47] Cao Y., Andreatta A., Heeger A. J., Smith P.: *Influence of chemical polymerization conditions on the properties of polyaniline*. Polymer 30 (1989) 2305–2311.

[48] Travain S. A., de Souza N. C., Balogh D. T., Giacometti J. A.: *Study of the growth process of in situ polyaniline deposited films*. J. Colloid Interface Sci. 316 (2007) 292–297.

[49] Sapurina I., Riede A., Stejskal J.: *In-situ polymerized polyaniline films 3. Film formation*. Synth. Met. 123 (2001) 503–507.

[50] Osaka T., Nakajima T., Naoi K., Owens B. B.: *Electroactive polyaniline film deposited from nonaqueous organic media II. Effect of acid concentration in solution*. J. Electrochem. Soc. 137 (1990) 2139–2142.

[51] Melad O., Alhendawi H., Fayyad M.: *The influence of organic solvents on the polymerization of polyaniline*. Res. Rev. J. Chem. 3 (2014) 40–47.

[52] Werake L. K., Story J. G., Bertino M. F., Pillalamarri S. K., Blum F. D.: *Photolithographic synthesis of polyaniline nanofibers*. Nanotechnology 16 (2005) 2833–2837.

[53] Pillalamarri S. K., Blum F. D., Tokuhiro A. T., Story J. G., Bertino M. F.: *Radiolytic synthesis of polyaniline nanofibers: A new templateless pathway*. Chem. Mater. 17 (2005) 227–229.

[54] Heinze J., Frontana-Uribe B., Ludwigs S.: *Electrochemistry of conducting polymers – persistent models and new concepts*. Chem. Rev. 110 (2010) 4724–4771.

[55] Sheridan E. M., Breslin C. B.: *Enantioselective detection of D- and L-phenylalanine using optically active polyaniline*. Electroanalysis 17 (2005) 532–537.

[56] Riede A., Stejskal J., Helmstedt M.: *In-situ prepared composite polyaniline films*. Synth. Met. 121 (2001) 1365–1366.

[57] Gorey B., Galineau J., White B., Smyth M. R., Morrin A.: *Inverse-opal conducting polymer monoliths in microfluidic channels*. Electroanalysis 24 (2012) 1318–1323.

[58] Zhang L., Ma H., Cao F., Gong J., Su Z.: *Nonaqueous synthesis of uniform polyaniline nanospheres via cellulose acetate template*. J. Polym. Sci. A Polym. Chem. 50 (2012) 912–917.

[59] Mazur M., Blanchard G. J.: *Electroless Deposition of Poly(2-alkoxyaniline)s*. Langmuir 20 (2004) 3471–3476.

[60] Sapurina I., Shishov M. A.: New Polymers for Special Applications. *Chapter 9: Oxidative Polymerization of Aniline: Molecular Synthesis of Polyaniline and the Formation of Supramolecular Structures* (2012) 251–312 Rijeka, Croatia: InTech ISBN 978-953-51-0744-6.

[61] Steskal J., Trchova M.: *Surface polymerization of aniline on silica gel*. Langmuir 19 (2003) 3013–3018.

[62] Stejskal J., Spirkova M., Kratochvil P.: *Polyaniline dispersions 4. Polymerization seeded by polyaniline particles*. Acta Polym. 45 (1994) 385–388.

[63] Stejskal J., Kratochvil P., Jenkins, A. D.: *Polyaniline: forms and formation*. Collect. Czech. Chem. Commun. 60 (1995) 1747–1755.

[64] Boeva Zh. A., Sergeyev V. G.: *Polyaniline: synthesis, properties, and application*. Polymer Sci., Ser. C 56 (2014) 144–153.

[65] Stejskal J., Sapurina I.: Polyaniline: *Thin films and colloidal dispersions (IUPAC Technical Report)*. Pure Appl. Chem. 77 (2005) 815–826.

[66] Ayad M. M., Shenashin M. A.: *Polyaniline film deposition from the oxidative polymerization of aniline using K2Cr2O7*. Eur. Polym. J. 40 (2003) 197–202.

[67] Sapurina I., Osadchev A. Y., Volchek B. Z., Trchova M., Riede A., Stejskal J.: *In-situ polymerized polyaniline films 5. Brush-like chain ordering*. Synth. Met. 129 (2002) 29–37.

[68] Kemp N. T., Cochrane J. W., Newbury R.: *Characteristics of the nucleation and growth of template-free polyaniline nanowires and fibrils*. Synth. Met. 159 (2009) 435–444.

[69] Forveille J. L., Olmedo L.: *Controlling the quality of deposits of polyaniline synthesized on glass fiber fabric*. Synth. Met. 65 (1994) 5–11.

[70] Ayad M. M., Shenashin M. A.: *Film thickness studies for the chemically synthesized conducting polyaniline*. Eur. Polym. J. 39 (2003) 1319–1324.

[71] Riede A., Helmstedt M., Saurina I., Stejskal J.: *In situ polymerized polyaniline films 4. Film formation in dispersion polymerization of aniline*. J. Colloid Sci. 248 (2002) 413–418.

[72] Riede A., Helmstedt M. Riede V., Stejskal, J.: *Polyaniline dispersions 7. Dynamic light scattering study of particle formation*. Colloid. Polym. Sci. 275 (1997) 814–820.

[73] Rozlivkova Z., Trchova M., Sedenkova I., Spirkova M., Stejskal J.: *Structure and stability of thin polyaniline films deposited in situ on silicon and gold during precipitation and dispersion polymerization of aniline hydrochloride*. Thin Solid Films 519 (2011) 5933–5941.

[74] Chen Y. J., Kang E. T., Neoh K. G.*: Electroless polymerization of aniline on platinum and palladium surfaces*. Appl. Surf. Sci. 185 (2002) 267–276.

[75] Liu Z., Miao Y.-E., Liu M., Ding Q., Tjiu W. W., Cui X., Liu T.: *Flexible polyaniline-coated TiO2/SiO2 nanofiber membranes with enhanced visible-light photocatalytic degradation performance*. J. Colloid Interface Sci. 424 (2014) 49–55.

[76] Job A. E., Alves N., Zanin M., Ueki M. M.*: Increasing the dielectric breakdown strength of poly(ethylene terepthalate) films using a coated polyaniline layer*. J. Phys. D Appl. Phys. 36 (2003) 1414–1417.

[77] Ince A., Bayramoglu G., Karagoz B., Altintas B., Bicak N., Arica M. Y.: *A method for fabrication of polyaniline coated polymer microspheres and its application for cellulase immobilization*. Chem. Eng. J. 189 (2012) 404–412.

[78] Chen J., Zeng X., Aoki K. J., Nishiumi T.: *Voltammetry of suspensions of polyaniline-coated graphene composites*. Int. J. Chem. 7 (2015) 1–11.

[79] Salvatierra R. V., Zitger G., Savu S. A., Alves A. P., Zarbin A. J. G., Chasse T, Casu M. B., Rocco M. L. M.: *Carbon nanotubes/polyaniline nanocomposites: Electronic structure, doping level and morphology investigations*. Synth. Met. 203 (2015) 16–21.

[80] Huang J.: *Syntheses and applications of conducting polymer polyaniline nanofibers*. Pure Appl. Chem. 78 (2006) 15–27.

[81] Mansour M. S., Ossman M. E., Farag H. A.: *Removal of Cd (II) ion from waste water by adsorption onto polyaniline coated on sawdust*. Desalination 272 (2011) 301–305.

[82] Ivanov S., Mokreva P., Tsakova V., Terlemezyan L.: *Electrochemical and surface structural characterization of chemically and electrochemically synthesized polyaniline coatings*. Thin Solid Films 441 (2003) 44–49.

[83] Bagheri H., Banihashemi S.: *Silver nanoparticles-polyaniline nanocomposite for microextraction in packed syringe*. Chromatographia 77 (2014) 397–403.

[84] Fedorczyk A., Ratajczak J, Czerwinski A., Skompska M.: *Selective deposition of gold nanoparticles on the top or inside a thin conducting polymer film, by combination of electroless deposition and electrochemical reduction*. Electrochim. Acta 122 (2014) 267–274.

[85] Drelinkiewicz A., Stejskal J., Waksmundzka A., Sobczak J. W.: *Physicochemical and catalytic properties of palladium deposited on polyaniline-coated silica gel*. Synth. Met. 140 (2004) 233–246.

[86] Khosrozadeh A., Darabi M. A., Xing M., Wang Q.: *Flexible electrode design: Fabrication of freestanding polyaniline-based composite films for high-performance supercapacitors*. ACS Appl. Mater. Interfaces 8 (2016) 11379–11389.

[87] Ibrahim M., Bassil M., Demirci U. B., Khoury T., Moussa G. E. H., Tahchi M. E., Miele P.: *Polyaniline-titania solid electrolyte for new generation photovoltaic single-layer devices*. Mater. Chem. Phys. 133 (2012) 1040–1049.

[88] Ghanbari Kh., Mousavi M. F., Shamsipur M.: *Preparation of polyaniline nanofibers and their use as a cathode of aqueous rechargeable batteries*. Electrochim. Acta 52 (2006) 1514–1522.

[89] Luo X., Killard A. J., Morrin A., Smyth M. R.: *In situ electropolymerised silica-polyaniline core-shell structures: Electrode modification and enzyme biosensor enhancement*. Electrochim. Acta 52 (2007) 1865–1870.

[90] Tanwar S., Ho J. A.: *Green synthesis of novel polyaniline nanofibers: Application in pH sensing*. Molecules 20 (2015) 18585–18596.

[91] Seidel K. F., Rossi L., Mello R. M. Q., Huemmelgen I. A.: *Vertical organic field effect transistor using sulfonated polyaniline/aluminium bilayer as intermediate electrode*. J. Mater. Sci-Mater. El. 24 (2013) 1052–1056.

[92] Eftekhari A., Li L., Yang Y.: *Polyaniline supercapacitators*. J. Power Sources 347 (2017) 86–107.

[93] Watanabe A., Mori K., Iwasaki Y., Nakamura Y., Niizuma S.: *Electrochromism of polyaniline film prepared by electrochemical polymerization*. Macromolecules 20 (1987) 1793–1796.

[94] Zambri M. S. M., Mohamed N. M., Kait C. F.: *Preparation of electrochromic material using carbon nanotubes*. J. Appl. Sci. 11 (2011) 1321–1325.

[95] Yeh J.-M., Liou S.-J., Lai C.-Y., Wu P.-C., Tsai T.-Y.: *Enhancement of corrosion protection effect in polyaniline via the formation of polyaniline-clay nanocomposite materials*. Chem. Mater. 13 (2001) 1131–1136.

[96] Orlov A. V., Kiseleva S. G., Karpacheva G. P., Teplyakov V. V., Syrtsova D. A., Starannikova L. E., Lebedeva T. L.: *Structure and gas separation properties of composite films based on polyaniline*. J. Appl. Polym. Sci. 89 (2003) 1379–1384.

[97] Shaban M., Rabia M., Fathallah W., El-Mawgoud N. A., Mahmoud A., Hissien H., Said O.: *Preparation and characterization of polyaniline and Ag/polyaniline composite*

nanoporous particles and their antimicrobial activities. J. Polym. Environ. 26 (2017) 434–442.

[98] Drelinkiewicz A., Waksmundzka-Gora A., Makowski W., Stejskal J.: *Pd/polyaniline(SiO2) a novel catalyst for the hydrogenation of 2-ethylanthraquinone*. Catal. Commun. 6 (2005) 347–356.

[99] Schwartz I. T., Jonke A. P., Josowicz M., Janata J.*: Polyaniline electrodes with atomic Au_nPd_1 alloys: oxidation of methanol and ethanol*. Catal. Lett. 143 (2013) 636–641.

[100] Gawron E. L., Krizek T., Kowalik M. A., Josowicz M., Janata J.: *Preparation of a carbon-platinum-polyaniline support for atomic metal deposition*. J. Electrochem. Soc. 162 (2015) H423–H427.

[101] Bossi A., Piletsky S. A., Turner A. P. F., Righetti P. G.: *Repartition effect of aromatic polyaniline coatings on the separation of bioactive peptides in capillary electrophoresis*. Electrophoresis 23 (2002) 203–208.

[102] de Sa P. F. G., Robb C., Resende E., McCarthy P., Yang S. C., Phyllis R., Dain J. A.: *Capillary electrophoretic separation by doublestrand polyaniline-coated capillaries of the advanced glycation endproducts formed from N-α-acetyl-L-lysine with reducing sugars*. J. Capill. Electrophor. Microchip Technol. 7 (2002) 61–65.

[103] Bossi A., Castelletti L., Piletsky S. A., Turner A. P. F., Righetti P. G.: *Towards the development of an integrated capillary electrophoresis optical biosensor*. Electrophoresis 24 (2003) 3356–3363.

[104] Florea L., Diamond D., Benito-Lopez F.: *Polyaniline coated micro-capillaries for continuous flow analysis of aqueous solutions*. Anal. Chim. Acta 759 (2013) 1–7.

[105] Floris P., Connolly D., White B., Morrin A.: *Development and characterization of switchable polyaniline-functionalised flow-through capillary monoliths*. RSC Adv. 4 (2014) 43934–43941.

[106] Zhang J., Zhang W., Bao T., Chen Z.: *Enhancement of capillary electrochromatographic separation performance by conductive polymer in a layer-by-layer fabricated graphene stationary phase*. J. Chromatogr. A 1339 (2014) 192–199.

[107] Nagaoka T., Fujimoto M., Nakao H., Kakuno K., Yano J., Ogura K.: *Electrochemical separation of ionic compounds using a conductive stationary phase coated with polyaniline or polypyrrole film, and ion exchange properties of conductive polymers*. J. Electroanal. Chem. 364 (1994) 179–188.

[108] Nagaoka T., Kakuno K., Fujimoto M., Nakao H., Yano J., Ogura K.: *Electrochemical chromatography using a polyaniline stationary phase II: Effects of pH of the mobile phase and column length*. J. Electroanal. Chem. 368 (1994) 315–317.

[109] Teasdale P. R., Wallace G. G.: *Characterizing the chemical interactions that occur on polyaniline with inverse thin layer chromatography*. Polym. Int. 35 (1994) 197–205.

[110] Mohammad, A., Khatoon, S., Khan, A. M. T., Moheman, A.: *Synthetic and chromatographic studies on silica polyaniline: A new approach*. Arch. Appl. Sci. Res. 2 (2010) 233–240.

[111] Siddiq, A., Ansari, M. O., Mohammad, A., Mohammad, F., El-Desoky, G. E.: *Synergistic effect pf polyaniline modified silica gel for highly efficient separation of non-resolvable amino acids*. Int. J. Polym. Mater. Polym. Biomater. 63 (2014) 277–281.

[112] Mohammad A., Khan M., Mobin R., Mohammad F.: *A new thin-layer chromatographic system for the identification and selective separation of brilliant blue food dye: Application of a green solvent*. J. Planar Chromat. 29 (2016) 446–452.

[113] Ghassempour A., Najafi N., Mehdinia A., Davarani S. S. H., Fallahi M., Nakhshab M.: *Analysis of anatoxin-A using polyaniline as a sorbent in solid-phase microextraction coupled to gas chromatography-mass spectrometry*. J. Chromatogr. A 1078 (2005) 120–127.

[114] Huang M., Jiang G., Cai Y.: *Electrochemical preparation of composite polyaniline coating and its application in the determination of bisphenol A, 4-n-nonylphenol, 4-tert-octylphenol using direct solid phase microextraction coupled with high performance liquid chromatography*. J. Sep. Sci. 28 (2005) 2218–2224.

[115] Sowa I., Wojciak-Kosior M., Rokicka K., Kocjan R., Szymczak G.: *Application of solid phase extraction with the use of silica modified with polyaniline film for pretreatment of samples from plant material before HPLC determination of triterpenic acids*. Talanta 122 (2014) 51–57.

[116] Sowa I., Pizon M., Swieboda R., Kocjan R., Zajdel D.: *Properties of chelating sorbent prepared by modification of silica gel with polyaniline and acid alizarin violet N*. Sep. Sci. Technol. 47 (2012) 1194–1198.

[117] Tanford C.: *Physical chemistry of macromolecules* (1961) New York, NY, USA: Wiley-VCH, Inc. ISBN 978-0-471-84447-1.

[118] Marmisolle W. A., Florit M. I., Posadas D.: *Acid-base equilibrium in conducting polymers. The case of reduced polyaniline.* J. Electroanal. Chem. 734 (2014) 10–17.

[119] Chriswanto H., Wallace G. G.: *Characterization of polyaniline using chromatographic studies*. Chromatographia 42 (1996) 191–198.

[120] Stejskal J., Quadrat O., Sapurina I., Zemek J., Drelinkiewicz A., Hasik M., Krivka I., Prokes J.: *Polyaniline-coated silica gel*. Eur. Polym. J. 38 (2002) 631–637.

[121] Sowa I., Zajdel D., Kocjan R., Pizon M., Wojciak-Kosior M.: *Silica gel modified with polyaniline as a stationary phase in the ion chromatography of nitrate(III) and nitrate(V) ions*. Acta Chromatogr. 25 (2013) 423–429.

[122] Sowa I., Wojciak-Kosior M., Draczkowski P., Strzemski M., Kocjan R.: *Synthesis and properties of a newly obtained sorbent based on silica gel coated with a polyaniline film as the stationary phase for non-suppressed ion chromatography*. Anal. Chim. Acta 787 (2013) 260–266.

[123] Sowa I., Kocjan R., Wojciak-Kosior M., Swieboda R., Zajdel D., Hajnos M.: *Physicochemical properties of silica gel coated with a thin layer of polyaniline (PANI) and its application in non-suppressed ion chromatography*. Talanta 115 (2013) 451–456.

[124] Sowa I., Wojciak-Kosior M., Draczkowski P., Szwerc W., Tylus J., Pawlikowski A., Kocjan R.: *Evaluation of pH and thermal stability of sorbent based on silica modified with polyaniline using high-resolution continuum source graphite furnace atomic absorption spectrometry and Raman spectroscopy*. Microchem. J. 118 (2015) 88–94.

[125] Buszewski B., Gadzala-Kopciuch R. M., Markuszewski M., Kaliszan R.: *Chemically bonded silica stationary phases, physicochemical characterization, and molecular mechanism of reversed-phase HPLC retention*. Anal. Chem. 69 (1997) 3277–3284.

[126] El-Naggar A. Y.: *Thermal analysis of the modified and unmodified silica gels to estimate their applicability as stationary phase in gas chromatography*. J. Emerg. Trends Eng. Appl. Sci. 4 (2013) 144–148.

[127] Divya V., Sangaranarayanan M. V.: *A facile synthesis strategy for mesoporous crystalline copper-polyaniline composite*. Eur. Pol. J. 48 (2012) 560–568.

[128] Lu C., Ben T., Xu S., Qiu S.: *Electrochemical synthesis of a microporous conductive polymer based on a metal-organic framework thin film*. Angew. Chem. Int. Ed. 53 (2014) 6454–6458.

[129] Abell A. B., Willis K. L., Lange D. A.: *Mercury intrusion porosimetry and image analysis of cement-based materials*. J. Colloid Interface Sci. 211 (1999) 39–44.

[130] Hegel C., Jones C., Cabrera F., Yanez M. J., Bucala V.: *Particle size characterization: comparison of laser diffraction (LD) and scanning electron microscopy (SEM)*. Acta Microsc. 23 (2014) 11–17.

[131] Gritti F., Bell D. S., Guiochon G. J.: *Particle size distribution and column efficiency. An ongoing debate revived with 1.9 µm Titan-C18 particles*. J. Chromatogr. A 1355 (2014) 179–192.

[132] Aslzadeh M. M., Abdouss M., Shoushtari A. M., Ghanbari F.: *A comparative study on anti-UV non-spherical methacrylate polymer particles and anti-UV PVA nanofibers*. Iran. Polym. J. 25 (2016) 145–156.

[133] Catani M., Ismail O. H., Cavazzini A., Ciogli A., Villani C., Pasti L., Bergantin C., Cabooter D., Desmet G., Gasparrini F., Bell D. S.: *Rationale behind the optimum efficiency of columns packed with new 1.9 µm fully porous particles of narrow particle size distribution*. J. Chromatogr. A 1454 (2016) 78–85.

[134] Iffelsberger C., Vatsyayan P., Matysik F.-M.: *Scanning electrochemical microscopy with forced convection introduced by high-precision stirring*. Anal. Chem. 89 (2017) 1658–1664.

[135] Erni R., Rossell M. D., Kisielowski C., Dahmen U.: *Atomic-resolution imaging with a sub-50-pm electron probe*. Phys. Rev. Lett 102 (2009) 96101–96104.

[136] Sfez R., De-Zhong L., Turyan I., Mandler D., Yitzchai, S.: *Polyaniline monolayer self-assembled on hydroxyl-terminated surfaces*. Langmuir 17 (2001) 2556–2559.

[137] Jansen W., Slaughter M.: *Elemental mapping of minerals by electron microprobe*. Amer. Miner. 67 (1982) 521–533.

[138] Jagminas A., Balciunaite A., Niaura G., Tamasauskaite-Tamasiunaite L.: *Electrochemical synthesis and characterization of polyaniline in TiO_2 nanotubes*. Int. J. Surf. Eng. Coat. 90 (2012) 311–315.

[139] Tanami G., Gutkin V., Mandler D.: *Thin nanocomposite films of polyaniline/Au nanoparticles by the Langmuir-Blodgett technique*. Langmuir 26 (2010) 4239–4245.

[140] Kabumoto A., Shinozaki K., Watanabe K., Nishikawa N.: *Electrochemical degradation of polyaniline*. Synth. Met. 26 (1988) 349–355.

[141] Neoh K. G., Kang E. T., Khor S. H., Tan K. L.: *Stability studies of polyaniline*. Polym. Degrad. Stab. 27 (1990) 107–117.

[142] Lancas F. M., Rodrigues J. C., de Freitas S. S.: *Preparation and use of packed capillary columns in chromatographic and related techniques*. J. Sep. Sci. 27 (2004) 1475–1482.

[143] Fermier A. M., Colon L. A.: *Capillary electrochromatography in columns packed by centripetal forces*. J. Microcolumn Sep. 10 (1998) 439–447.

[144] Koh J.-H., Broyles B. S., Guan-Sajonz H., Hu M. Z.-C., Guiochon G.: *Consolidation and column performance of several packing materials for liquid chromatography in a dynamic axial compression column*. J. Chromatogr. A 813 (1998) 223–238.

[145] Yin H., Brennen R. A., Lyster E., Slocum R.: *Liquid chromatography columns with structured walls*. U.S. patent application 20160231293 (11. 8. 2016).

[146] Fee C., Nawada S., Dimartino S.: *3D printed porous media columns with fine control of column packing morphology*. J. Chromatogr. A 1333 (2014) 18–24.

[147] Franc M., Sobotnikova J., Coufal P., Bosakova Z.: *Comparison of different types of outlet frits in slurry-packed capillary columns*. J. Sep. Sci. 37 (2014) 2278–2283.

[148] Cheong W. J.: *Fritting techniques in chromatography*. J. Sep. Sci. 37 (2014) 603–617.

[149] Tan F., Chen S. O., Zhang Y. J., Cai Y., Qian X. H.: *A simple and efficient frit preparation method for one-end tapered-fused silica-packed capillary columns in nano-LC-ESI MS*. Proteomics 10 (2010) 1724–1727.

[150] Wahab M. F., Patel C. D., Wimalasinghe R. M., Armstrong D. W.: *Fundamental and practical insights on the packing of modern high-efficiency analytical and capillary columns*. Anal. Chem. 89 (2017) 8177–8191.

[151] Franc M., Vojta J., Sobotnikova J., Coufal P., Bosakova Z.: *Performance and lifetime of slurry packed capillary columns for high performance liquid chromatography*. Chem. Papers 68 (2014) 22–28.

[152] Wahab M. F., Pohl C. A., Lucy C.A.: *Colloidal aspects and packing behaviour of charged micro-particulates in high efficiency ion chromatography*. J. Chromatogr. A 1270 (2012)139–146.

[153] Leonardis I. Capriotti F., Cappiello A., Famiglini G., Palma P.: *Temperature effects on nano-LC column packing technology*. J. Sep. Sci. 35(2012) 1589–1595.

[154] Andreolini F., Borra C., Novotny M.: *Preparation and evaluation of slurry-packed capillary columns for normal-phase liquid chromatography*. Anal. Chem. 59 (1987) 2428–2432.

[155] Boughtflower R. J., Underwood T., Maddin J.: *The production of packed capillaries using a novel pressurized ultrasound device*. Chromatographia 41 (1995) 398–402.

[156] Ehlert S., Roesler T., Tallarek U.: *Packing density of slurry-packed capillaries at low aspect ratios*. J. Sep. Sci. 31 (2008) 1719–1728.

[157] Meyer R. F., Hartwick R. A.: *Efficient packing of small particle microbore columns*. Anal. Chem. 56 (1984) 2211–2214.

[158] Wong V., Shalliker R. A., Guiochon G.: *Evaluation of the uniformity of analytical-size chromatography columns prepared by the downward packing of particulate slurries*. Anal. Chem. 76 (2004) 2601–2608.

[159] Lynen F., Buica A., de Villiers A., Crouch A., Sandra P.: *An efficient slurry packing procedure for the preparation of column applicable in capillary electrochromatography and capillary electrochromatography-electrospray-mass spectrometry*. J. Sep. Sci. 28 (2005) 1539–1549.

[160] Karlsson K. E., Novotny M.: *Separation efficiency of slurry-packed liquid chromatography microcolumns with very small inner diameters*. Anal. Chem. 60 (1988) 1662–1665.

[161] Roulin S., Dmoch R., Carney R., Bartle K. D., Myers P., Euerby M. R., Johnson C.: *Comparison of different packing methods for capillary electrochromatography columns.* J. Chromatogr. A 887 (2000) 307–312.

[162] Kirkland J. J., DeStefano J. J.: *The art and science of forming packed analytical high-performance liquid chromatography columns*. J. Chromatogr. A 1126 (2006) 50–57.

[163] MacNair J. E., Lewis K. C., Jorgensson J. W.: *Ultrahigh-pressure reversed-phase liquid chromatography in packed capillary columns*. Anal. Chem. 69 (1997) 983–989.

[164] Shen Y., Yang Y. J., Lee M. L.: *Fundamental considerations of packed-capillary GC, SFC, and LC using non-porous silica particles*. Anal. Chem. 69 (1997) 628–635.

[165] Lottes F., Arlt W., Minceva M., Stenby E. H.: *Hydrodynamic impact of particle shape in slurry packed liquid chromatography columns.* J. Chromatogr. A 1216 (2009) 5687–5695.

[166] Yang P., McCabe T., Pursch M.: *Practical comparison of LC columns packed with different superficially porous particles for the separation of small molecules and medium size natural products*. J. Sep. Sci. 34 (2011) 2975–2982.

[167] Gritti F., Farkas T., Heng J., Guiochon G.: *On the relationship between band broadening and the particle-size distribution of the packing material in liquid chromatography: Theory and practice*. J. Chromatogr. A 1218 (2011) 8209–8221.

[168] Cabooter D., Billen J., Terryn H., Lynen F., Sandra P., Desmet G.: *Kinetic plot and particle size distribution analysis to discuss the performance limits of sub-2µm and supra-2µm particle columns*. J. Chromatogr. A 1204 (2008) 1–10.

[169] Billen J., Guillarme D., Rudaz S., Veuthey J.-L., Ritchie H., Grady B., Desmet G.: *Relation between the particle size distribution and the kinetic performance of packed columns.* J. Chromatogr. A 1161 (2007) 224–233.

[170] Hiestand E. N.: *Theory of coarse suspension formulation*. J. Pharma. Sci. 53 (1964) 1–18.

[171] Harkins W. D., Feldman A.: *Films. The spreading of liquids and the spreading coefficient*. J. Am. Chem. Soc. 44 (1922) 2665–2685.

[172] Binks B. P., Clint J. H.: *Solid wettability from surface energy components: Relevance to Pickering emulsions*. Langmuir 18 (2002) 1270–1273.

[173] Tyrrell E., Hilder F., Shalliker R. A., Dicinoski G. W., Shellie R. A., Breadmore M. C., Pohl C. A., Haddad P. R.: *Packing procedures for high efficiency, short ion-*

exchange columns for rapid separation of inorganic anions. J. Chromatogr. A 1208 (2008) 95–100.

[174] Zimina T. M., Smith R. M., Myers P., King B.W.: *Effects of kinematic viscosity of the slurry on the packing efficiency of PEEK microbore columns for liquid chromatography*. Chromatographia 40 (1995) 662–668.

[175] Neue U. D.: *HPLC Columns: Theory, Technology, and Practice* (1997) New York, NY, USA: Wiley-VCH, Inc. ISBN 978-0-471-19037-0.

[176] Vissers J. P. C., Claessens H. A., Laven J., Cramers C. A.: *Colloid chemical aspects of slurry packing techniques in microcolumn liquid chromatography*. Anal. Chem. 67 (1995) 2103–2109.

[177] Patel D. C., Breitbach Z. S., Wahab M. F., Barhate C. L., Armstrong D. W.: *Gone in seconds: Praxis, performance, and peculiarities of ultrafast chiral liquid chromatography with superficially porous particles*. Anal. Chem. 87 (2015) 9137–9148.

[178] Wahab M. F., Patel D. C., Armstrong D. W.: *A new peak shape analysis approach: detection and quantitation of concurrent fronting, tailing, and their effect on asymmetry measurements*. J. Chromatogr. A 1509 (2017) 163–170.

[179] Blue L. E., Jorgenson J. W.: *1.1 μm superficially porous particles for liquid chromatography Part II: Column packing and chromatographic performance*. J. Chromatogr. A 1308 (2015) 71–80.

[180] Godinho J. M., Reising A. E., Tallarek U., Jorgenson J.W.: *Implementation of high slurry concentration and sonication to pack high-efficiency, meter-long capillary ultrahigh pressure liquid chromatography columns*. J. Chromatogr. A 1462 (2016) 165–169.

[181] Shalliker R. A., Broyles B. S., Guiochon G.: *Physical evidence of two wall effects in liquid chromatography*. J. Chromatogr. A 888 (2000) 1–12.

[182] Reising A. E., Godinho J. M., Hormann K., Jorgenson J. W.: *Larger voids in mechanically stable, loose packing of 1.3 μm frictional, cohesive particles: Their reconstruction, statistical analysis, and impact on separation efficiency*. J. Chromatogr. A 1436 (2016) 118–132.

[183] Gritti F., Guiochon G.: *Perspectives on the evolution of the column efficiency in liquid chromatography*. Anal. Chem. 85 (2013) 3017–3035.

[184] Guiochon G., Farkas T., Guan-Sajonz H., Koh J., Sarker M., Stanley B. J., Yun T.: *Consolidation of particle beds and packing of chromatographic columns*. J. Chromatogr. A 762 (1997) 83–88.

[185] Dong L., Johnson D.: *Surface tension of charge-stabilized colloidal suspensions at the water-air interface*. Langmuir 19 (2003) 10205–10209.

[186] Bruns S., Franklin E. G., Grinias J. P., Godinho J. M., Jorgenson J. W., Tallarek U.: *Slurry concentration effects on the bed morphology and separation efficiency of capillaries packed with sub-2 μm particles*. J. Chromatogr. A 1318 (2013) 189–197.

[187] Reising A. E., Godinho J. M., Jorgenson J. W., Tallarek U.: *Bed morphological features associated with an optimal slurry concentration for reproducible preparation of efficient capillary ultrahigh pressure liquid chromatographic columns*. J. Chromatogr. A 1504 (2017) 71–82.

[188] Liu Y., Shamsi S. A.: *Chiral capillary electrophoresis-mass spectrometry: developments and applications in the period 2010-2015: a review*. J. Chromatogr. Sci. 54 (2016) 1771–1786.

[189] Fung Y. S.: Current achievements and future perspectives. *Chapter 17: Microfluidic Chip-Capillary Electrophoresis Devices* (2016) 347–368 Boca Raton, FL, USA: CRC Press Taylor & Francis ISBN 978-1-4822-5164-7.

[190] Povarov V. G., Lopatnikov A. I.: *A simple multisensory detector based on tin dioxide in capillary gas chromatography*. J. Anal. Chem. 71 (2016) 901–906.

[191] Darko E., Thurbide K. B.: *Capillary gas chromatographic separation of carboxylic acids using an acidic water stationary phase*. Chromatographia 80 (2017) 1225–1232.

[192] Pyo D.: *Temperature controlled restrictor for packed capillary column supercritical fluid chromatography*. J. Liq. Chromatogr. Relat. Technol. 30 (2007) 3085–3092.

[193] Murakami J. N., Thurbide K. B.: *Coating properties of a novel water stationary phase in capillary supercritical fluid chromatography*. J. Sep. Sci. 38 (2015) 1618–1624.

[194] Blue L. E., Franklin E. G., Godinho J. M., Grinias J. P., Grinias K. M., Lunn D. B., Moore S. M.: *Recent advances in capillary ultrahigh pressure liquid chromatography*. J. Chromatogr. A 1523 (2017) 17–39.

[195] Shimizu H., Smirnova A., Mawatari K., Kitamori T.: *Extended-nano chromatography*. J. Chromatogr. A 1490 (2017) 11–20.

[196] Nazario C. E. D., Silva M. R., Franco M. S., Lancas F. M.: *Evolution in miniaturization column liquid chromatography instrumentation and applications: An overview*. J. Chromatogr. A 1421 (2015) 18–37.

[197] Stulik K., Pacakova V., Suchankova J., Coufal P.: *Monolithic organic polymeric columns for capillary liquid chromatography and electrochromatography*. J. Chromatogr. B 841 (2006) 79–87.

[198] Sestak J., Moravcova D., Kahle V.: *Instrument platforms for nano liquid chromatography*. J. Chromatogr. A 1421 (2015) 2–17.

[199] Horvath C. G., Preiss B. A., Lipsky S. R.: *Fast liquid chromatography. Investigation of operating parameters and the separation of nucleotides on pellicular ion exchangers*. Anal. Chem. 39 (1967) 1422–1428.

[200] Ishii D., Asai K., Hibi K., Jonokuchi T., Nagaya M.: *A study of micro-high-performance liquid chromatography. I. Development of technique for miniaturization of high-performance liquid chromatography*. J. Chromatogr. 144 (1977) 157–168.

[201] Scott R. P. W., Kucera P.: *Mode of operation and performance characteristics of microbore columns for use in liquid chromatography*. J. Chromatogr. 169 (1979) 51–72.

[202] Takeuchi T.: *Development of capillary liquid chromatography*. Chromatography 26 (2005) 7–10.

[203] Kawachi Y., Ikegami T., Takubo H., Ikegami Y., Miyamoto M., Tanaka N.: *Chromatographic characterisation of hydrophilic interaction liquid chromatography*

stationary phases: Hydrophilicity, charge effects, structural selectivity, and separation efficiency. J. Chromatogr. A 1218 (2011) 5903–5919.

[204] Andres A., Broeckhoven K., Desmet G.: *Methods for experimental characterization and analysis of the efficiency and speed of chromatographic columns: A step-by-step tutorial*. Anal. Chim. Acta 894 (2015) 20–34.

[205] Cruz E., Euerby M. R., Johnson C. M., Hackett C. A.: *Chromatographic classification of commercially available reversed-phase HPLC columns*. Chromatographia 44 (1997) 151–161.

[206] Visky D., Heyden Y. V., Ivanyi T., Baten P., De Beer J., Kovacs Z., Noszal B., Dehouck P., Roets E., Massart D. L., Hoogmartens J.: *Characterisation of reversed phase liquid chromatographic columns by chromatographic tests. Evaluation of 36 test parameters: repeatability, reproducibility and correlation*. J. Chromatogr. A 977 (2002) 39–58.

[207] Neue U. D., Serowik E., Iraneta P., Alden B. A., Walter T. H.: *Universal procedure for the assessment of the reproducibility and the classification of silica-based reversed-phase packings I. Assessment of the reproducibility of reversed-phase packings*. J. Chromatogr. A 849 (1999) 87–100.

[208] Walters M. J.: *Classification of octadecyl-bonded liquid chromatography columns*. J. Assoc. Off. Anal. Chem. 70 (1987) 465–469.

[209] Kimata K., Iwaguchi K., Onishi S., Jinno K., Eksteen R., Hosoya K., Araki M.,Tanaka N.: *Chromatographic characterization of silica C18 packing materials. Correlation between a preparation method and retention behavior of stationary phase*. J. Chromatogr. Sci. 27 (1989) 721–728.

[210] Sander L. C., Wise S. A.: *Recent advances in bonded phases for liquid chromatography*. Crit. Rev. Anal. Chem. 18 (1987) 299–415.

[211] Galushko S. V.: *The calculation of retention and selectivity in reversed-phase liquid-chromatography. 2. Methanol-water eluents*. Chromatographia 36 (1993) 39–42.

[212] Engelhardt H., Jungheim M.: *Comparison and characterization of reversed phases*. Chromatographia 29 (1990) 59–68.

[213] Neue U. D., Alden B. A., Walter T. H.: *Universal procedure for the assessment of the reproducibility and the classification of silica-based reversed-phase packings II. in hydrophilic interaction liquid chromatography*. J. Chromatogr. A 1260 (2012) 126–131.

[214] Ibrahim M. E. A., Liu Y., Lucy C. A.: *A simple graphical representation of selectivity in hydrophilic interaction liquid chromatography*. J. Chromatogr. A 1260 (2012) 126–131.

[215] Galea C., Mangelings D., Vander Heyden Y.: *Characterization and classification of stationary phases in HPLC and SFC – a review*. Anal. Chim. Acta 886 (2015) 1–15.

[216] McCalley D. V., Brereton R. G.: *High-performance liquid chromatography of basic compounds: problems, possible solutions and tests of reversed-phase columns*. J. Chromatogr. A 828 (1998) 407–420.

[217] Claessens H.: *Trends and progress in the characterization of stationary phases for reversed-phase liquid chromatography*. TrAC Trends Anal. Chem. 20 (2001) 563–583.

[218] Wilson N. S., Gilroy J., Dolan J. W., Snyder L. R.: *Column selectivity in reversed-phase liquid chromatography. VI. Columns with embedded or end-capping polar groups*. J. Chromatogr. A 1026 (2004) 91–100.

[219] Dolan J. W., Snyder L. R., Jupille T. H., Wilson N. S.: *Variability of column selectivity for reversed-phase high-performance liquid chromatography compensation by adjustment of separation conditions*. J. Chromatogr. A 960 (2002) 51–67.

[220] Cole L. A., Dorsey J. G.: *Temperature-dependence of retention in reversed-phaseliquid-chromatography. 1. Stationary-phase considerations*. Anal. Chem. 64 (1992) 1317–1323.

[221] Cole L. A., Dorsey J. G., Dill K. A.: *Temperature-dependence of retention in reversed-phase liquid-chromatography. 2. Mobile-phase considerations*. Anal. Chem. 64 (1992) 1324–1327.

[222] Liu M., Chen E. X., Ji R., Semin D.: *Stability-indicating hydrophilic interaction liquid chromatography method for highly polar and basic compounds*. J. Chromatogr. A 1188 (2008) 255–263.

[223] Tyteca E., Guillarme D., Desmet G.: *Use of individual retention modeling for gradient optimization in hydrophilic interaction chromatography: Separation of nucleobases and nucleosides*. J. Chromatogr. A 1368 (2014) 125–131.

[224] Baeza-Baeza J. J., Ortiz-Bolsico C., Torres-Lapasio J. R., Garcia-Alvarez-Coque M. C.: *Approaches to model the retention and peak profile in linear gradient reversed-phase liquid chromatography*. J. Chromatogr. A 1284 (2013) 28–35.

[225] Cheng C. Y., Chen T. L., Wang B. C.: *Molecular dynamics simulation of separation mechanisms in bonded phase liquid chromatography*. J. Mol. Struct. 577 (2002) 81–90.

[226] Lindsey R. K., Rafferty J. L., Eggimann B. L., Siepmann J. I., Schure M. R.: *Molecular simulation studies of reversed-phase liquid chromatography*. J. Chromatogr. A 1287 (2013) 60–82.

[227] Al-Haj M. A., Kaliszan R., Buszewski B.: *Quantitative structure-retention relationships with model analytes as a means of an objective evaluation of chromatographic columns*. J. Chromatogr. Sci. 39 (2001) 29–38.

[228] Jandera P.: *Correlation of retention and selectivity of separation in reversed-phase high-performance liquid-chromatography with interaction indexes and with lipophilic and polar structural indexes*. J. Chromatogr. A 656 (1993) 437–467.

[229] Snyder L. R., Dolan J. W., Carr P. W.: *The hydrophobic-subtraction model of reversed-phase column selectivity*. J. Chromatogr. A 1060 (2004) 77–116.

[230] Croes K., Steffens A., Marchand D. H., Snyder L. R.: *Relevance of π- π and dipole-dipole interactions for retention on cyano and phenyl columns in reversed-phase liquid chromatography*. J. Chromatogr. A 1098 (2005) 123–130.

[231] Wilson N. S., Nelson M. D., Dolan J. W., Snyder L. R., Wolcott R. G., Carr P. W.: *Column selectivity in reversed-phase liquid chromatography: I. A general quantitative relationship*. J. Chromatogr. A 961 (2002) 171–193.

[232] Johnson A. R., Johnson C. M., Stoll D. R., Vitha M. F.: *Indentifying orthogonal and similar reversed phase liquid chromatography stationary phases using the system*

selectivity cube and the hydrophobic subtraction model. J. Chromatogr. A 1249 (2012) 62–82.

[233] Wang J., Guo Z., Shen A., Yu L., Xiao Y., Xue X., Zhang X., Liang X.: *Hydrophilic-subtraction model for the characterization and comparison of hydrophilic interaction liquid chromatography columns*. J. Chromatogr. A 1398 (2015) 29–46.

[234] Sykora D., Ridka K., Tesarova E., Kalikova K., Kaplanek R., Kral V.: *Characterization of novel metallacarborane-based sorbents by linear solvation energy relationships*. J. Chromatogr. A 1371 (2014) 220–226.

[235] Sandi A., Nagy M., Szepesy L.: *Characterization of reversed-phase columns using the linear free energy relationship. III. Effect of the organic modifier and the mobile phase composition*. J. Chromatogr. A 893 (2000) 215–234.

[236] Giaginis C., Tsantili-Kakoulidou A.: *Quantitative structure-retention relationships as useful tool to characterize chromatographic systems and their potential to simulate biological processes*. Chromatographia 76 (2013) 211–226.

[237] Vitha M., Carr P. W.: *The chemical interpretation and practice of linear solvation energy relationships in chromatography*. J. Chromatogr. A 1126 (2006) 143–194.

[238] Blackwell J. A., Stringham R. W.: *Characterization of temperature dependent modifier effects in SFC using linear solvation energy relationships*. Chromatographia 46 (1997) 301–308.

[239] West C., Auroux E.: *Deconvoluting the effects of buffer salt concentration in hydrophilic interaction chromatography on a zwitterionic stationary phase*. J. Chromatogr. A 1461 (2016) 92–97.

[240] West C., Lesellier E.: *Effects of mobile phase composition on retention and selectivity in achiral supercritical fluid chromatography*. J. Chromatogr. A 1302 (2013) 152–162.

[241] Jandera P., Hajek T., Skerikova V., Soukup J.: *Dual hydrophilic interaction-RP retention mechanism on polar columns: Structural correlations and implementation for 2-D separations on a single column*. J. Sep. Sci. 33 (2010) 841–852.

[242] Abraham M. H., Whiting G. S., Doherty R. M., Shuely W. J.: *Hydrogen bonding. XVI. A new solute solvation parameter, n2H, from gas chromatographic data*. J. Chromatogr. 587 (1991) 213–228.

[243] Abraham M. H., Andonianhaftvan J., Whiting G. S., Leo A., Taft R. S.: *Hydrogen-bonding 34. The factors that influence the solubility of gases and vapors in water at 298 K, and a new method for its determination*. J. Chem. Soc. Perkin Trans. 2 (1994) 1777–1791.

[244] Abraham M. H., McGowan J. C.: *The use of characteristic volumes to measure cavity terms in reversed phase liquid chromatography*. Chromatographia 23 (1987) 243–246.

[245] Poole C. F., Poole S. K.: *Column selectivity from the perspective of the solvation parameter model*. J. Chromatogr. A 965 (2002) 263–299.

[246] Abraham M. H.: *Scales of solute hydrogen-bonding: their construction and application to physicochemical and biochemical processes*. Chem. Soc. Rev. 22 (1993) 73–83.

[247] http://www.acdlabs.com/products/percepta/predictors/absolv/ (webpage visited on 24.1.2018)

[248] Kirkland J. J., van Straten M. A., Claessens H. A.: *High pH Mobile-Phase Effects on Silica-Based Reversed-Phase High-Performance Liquid-Chromatographic Columns*. J. Chromatogr. A 691 (1995) 3–19.

[249] Kalikova K., Lokajova J., Tesarova E.: *Linear free energy relationship as a tool for characterization of three teicoplanin-based chiral stationary phases under various mobile phase compositions*. J. Sep. Sci. 29 (2006) 1476-1485.

[250] Michel M., Baczek T., Studzinska S., Bodzioch K., Jonsson T., Kaliszan R., Buszewski B.: *Comparative evaluation of high-performance liquid chromatography stationary phases used for the separation of peptides in terms of quantitative structure-retention relationships*. J. Chromatogr. A 1175 (2007) 49–54.

[251] D'Archivio A. A., Giannitto A., Maggi M. A., Ruggieri F.: *Cross-column retention prediction in reversed-phase high-performance liquid chromatography by artificial network modelling*. Anal. Chim. Acta 717 (2012) 52–60.

[252] Van Middlesworth B. J., Stalcup A. M.: *Characterization of surface confined ionic liquid stationary phases: Impact of cation revisited*. J. Chromatogr. A 1364 (2014) 171–182.

[253] Quiming N. S., Denola N. L., Saito Y., Catabay A. P., Jinno K.: *Chromatographic behavior of uric acid and methyl uric acids on a diol column in HILIC*. Chromatographia 67 (2008) 507–515.

[254] Quiming N. S., Denola N. L., Bin Samsuri S. R., Saito Y., Jinno K.: *Development of retention predictionmodels for adrenoreceptor agonists and antagonists on a polyvinyl alcohol-bonded stationary phase in hydrophilic interaction chromatography*. J. Sep. Sci. 31 (2008) 1537–1549.

[255] Kalikova K., Kozlik P., Gilar M., Tesarova E.: *Properties of two amide-based hydrophilic interaction liquid chromatography columns*. J. Sep. Sci. 36 (2013) 2421–2429.

[256] Kozlik P., Simova V., Kalikova K., Bosakova Z., Armstrong D. W., Tesarova E.: *Effect of silica gel modification with cyclofructans on properties of hydrophilic interaction liquid chromatography stationary phases*. J. Chromatogr. A 1257 (2012) 58–65.

[257] Buszewski B., Noga S.: *Hydrophilic interaction liquid chromatography (HILIC) – a powerful separation technique*. Anal. Bioanal. Chem. 402 (2012) 231–247.

[258] Noga S., Bocian S. Buszewski B.: *Hydrophilic interaction liquid chromatography columns classification by effect of solvation and chemometric methods*. J. Chromatogr. A 1278 (2013) 89–97.

[259] Jandera P.: *Stationary phases for hydrophilic interaction chromatography, their characterization and implementation into multidimensional chromatography concepts.* J. Sep. Sci. 31 (2008) 1421–1437.

[260] Chirita R. I., West C., Zubrzycki S., Finaru A. L., Elfakir C.: *Investigations on the chromatographic behaviour of zwitterionic stationary phases used in hydrophilic interaction chromatography*. J. Chromatogr. A 1218 (2011) 5939–5963.

[261] Schuster G., Lindner W.: *Comparative characterization of hydrophilic interaction liquid chromatography columns by linear solvation energyrelationships*. J. Chromatogr. A 1273(2013) 73–94.

[262] Schuster G., Lindner W.: *Additional investigations into the retentionmechanism of hydrophilic interaction liquid chromatography by linearsolvation energy relationships*. J. Chromatogr. A 1301 (2013) 98–110.

[263] Zichová J.: *Plánování experimentů a predikční vícerozměrová analýza* (2008) Praha, Czech Republic: Karolinum ISBN 978-80-246-1407-6.

[264] Kiridena W., Poole C. F.: *Structure-driven retention model for optimization of ternary solvent systems in reversed-phase liquid chromatography*. Chromatographia 48 (1998) 607–614.

[265] Bolliet D., Poole C. F.: *Mixture-design approach to retention prediction using the solvation parameter model and ternary solvent systems in reversed-phase liquid chromatography*. Anal. Commun. 35 (1998) 253–256.

[266] Vozka J., Kalikova K., Roussel C., Armstrong D. W., Tesarova E.: *An insight into the use of dimethylphenyl carbamate cyclofructan 7 chiral stationary phase in supercritical fluid chromatography: The basic comparosin with HPLC*. J. Sep. Sci. 36 (2013) 1711–1719.

[267] Janeckova L., Kalikova K., Vozka J., Armstrong D. W., Bosakova Z., Tesarova E.: *Characterization of cyclofructan-based chiral stationary phases by linear free energy relationship*. J. Sep. Sci. 34 (2011) 2639–2644.

[268] Du C. M., Valko K., Bevan C., Reynolds D., Abraham M. H.: *Characterizing the selectivity of stationary phases and organic modifiers in reversed-phase high-performance liquid chromatographic systems by a general solvation equation using gradient elution*. J. Chromatogr. Sci. 38 (2000) 503–511.

[269] Li J., Cai B.: *Evaluation of the retention dependence on the physicochemical properties of solutes in reversed-phase liquid chromatographic linear gradient elution based on linear solvation energy relationships*. J. Chromatogr. A 905 (2001) 35–46.

[270] Li J., Carr P. W.: *Gas chromatographic study of solvation enthalpy by solvatochromically based linear solvation energy relationships*. J. Chromatogr. A 659 (1994) 367–380.

[271] Li J., Dallas A. J., Carr P. W.: *Empirical scheme for the classification of gas chromatographic stationary phases based on solvatochromic linear solvation energy relationships*. J. Chromatogr. 517 (1990) 103–121.

[272] Poole C. F., Poole S. K.: *Separation characteristics of wall-coated open-tubular columns for gas chromatography*. J. Chromatogr. A 1184 (2008) 254–280.

[273] West C., Lesellier E.: *Characterization of stationary phases in supercritical fluid chromatography with the solvation parameter model*. V. Elaboration of a reduced set of test solutes for rapid evaluation. J. Chromatogr. A 1169 (2007) 205–219.

[274] Poole C. F., Poole S. K., Abraham M. H.: *Recommendations for the determination of selectivity in micellar electrokinetic chromatography*. J. Chromatogr. A 798 (1998) 207–222.

[275] Snyder L. R.: *Linear elution adsorption chromatography. IX. Strong eluents and alumina. The basis of eluent strength*. J. Chromatogr. 16 (1964) 55–88.

[276] Mongay C., Pastor A., Olmos C.: *Determination of carboxylic acids and inorganic anions in wines by ion-exchange chromatography*. J. Chromatogr. A 736 (1996) 351–357.

[277] Adrian A., Ruettimann T. B.: *Simultaneous determination of small organic and inorganic anions in environmental water samples by ion-exchange chromatography*. J. Chromatogr. A 706 (1995) 259–269.

[278] Tijssen R., Schoenmakers P. J., Boehmer M. R., Koopal L. K., Billiet H. A. H.: *Lattice models for the description of partitioning/adsorption and retention in reversed-phase liquid chromatography, including surface and shape effects*. J. Chromatogr. A 656 (1993) 135–196.

[279] Sander L. C., Pursch M., Wise S. A.: *Shape selectivity for constrained solutes in reversed-phase liquid chromatography*. Anal. Chem. 71 (1999) 4821–4830.

[280] Jandera P., Engelhardt H.: *Liquid chromatography separation of organic acidic compounds*. Chromatographia 13 (1980) 18–23.

[281] Gritti F., Guiochon G.: *Critical contribution on nonlinear chromatography to the understanding of retention mechanism in reversed-phase liquid chromatography*. J. Chromatogr. A 1099 (2005) 1–42.

[282] Alpert A. J.: *Hydrophilic-interaction chromatography for the separation of peptides, nucleic acids and other polar compounds*. J. Chromatogr. 499 (1990) 177–196.

[283] Hemstrom P., Irgum K.: *Hydrophilic interaction chromatography*. J. Sep. Sci. 29 (2006) 1784–1821.

[284] Greco G., Letzel T.: *Main interactions and influences of the chromatographic parameters in HILIC separations*. J. Chromatogr. Sci. 51 (2013) 684–693.

[285] Gritti F., Hoeltzel A., Tallarek U., Guiochon G.: *The relative importance of the adsorption and partitioning mechanism in hydrophilic interaction liquid chromatography*. J. Chromatogr. A 1376 (2015) 112–125.

[286] Liu X. D., Pohl C. A.: *HILIC behavior of a reversed-phase/cation-exchange/anion-exchange trimode column*. J. Sep. Sci. 33 (2010) 779–786.

[287] Davies N. H., Euerby M. R., McCalley D. V.: *A study of retention and overloading of basic compounds with mixed-mode reversed-phase/cation-exchange columns in high performance liquid chromatography*. J Chromatogr. A 1138 (2007) 65–72.

[288] Apfelthaler E., Bicker W., Laemmerhofer M., Sulyok M., Krska R., Lidner W., Schuhmacher R.: *Retention pattern profiling of fungal metabolites on mixed-mode reversed-phase/weak anion exchange stationary phases in comparison to reversed-phase and weak anion exchange separation materials by liquid chromatography–electrospray ionisation-tandem mass spectrometry*. J. Chromatogr. A 1191 (2008) 171–181.

[289] Liu X., Pohl C.: *New hydrophilic interaction/reversed-phase mixed-mode stationary phase and its application for analysis of nonionic ethoxylated surfactants*. J. Chromatogr. A 1191(2008) 83–89.

[290] Szabo Z.-I., Foroughbakhshfasaie M., Noszal B., Toth G.: *Enantioseparation of racecadotril using polysaccharide-type chiral stationary phases in polar organic mode.* Chirality 30 (2018) 95–105.

[291] Nováková L, Douša M.: *Moderní HPLC separace v teorii a praxi I.* (2013) Praha, Czech Republic: Europrint a.s. 1st ed. ISBN 978-80-260-4243-3.

[292] Nováková L, Douša M.: *Moderní HPLC separace v teorii a praxi II.* (2013) Praha, Czech Republic: Europrint a.s. 1st ed. ISBN 978-80-260-4244-0.

[293] Van Kreveld M. E., Van Den Hoed N.: *Mechanism of gel permeation chromatography distribution coefficient*. J. Chromatogr. A 83 (1973) 111–124.

[294] Sun J., Guo H. X., Semin D., Cheetham J.: *Direct separation and detection of biogenic amines by ion-pair liquid chromatography with chemiluminescent nitrogen detector*. J. Chromatogr. A 1218 (2011) 4689–4697.

[295] Queiroz J. A., Tomaz C. T., Carbral J. M. S.: *Hydrophobic interaction chromatography of proteins*. J. Biotechnol. 87 (2001) 143–159.

[296] Stejskal J., Sapurina I., Prokes J., Zemek J.: *In-situ polymerized polyaniline films*. Synth. Met. 105 (1999) 195–202.

[297] OMNIC 9, Thermo Nicolet, Madison, Wisconsin, USA.

[298] Trchova M., Moravkova Z., Blaha M., Stejskal J.: *Raman spectroscopy of polyaniline and oligoaniline thin films*. Electrochim. Acta 122 (2014) 28–38.

[299] Blaha M., Trchova M., Bober P., Moravkova Z., Zujovic Z. D., Filippov S. K., Prokes J., Pilar J., Stejskal J.: *Structure and properties of polyaniline interacting with H-phosphonates*. Synth. Met. 232 (2017) 79–86.

[300] Ashokan S., Ponnuswamy V., Jayamurugan P., Chandrasekaran J., Subba Rao Y. V.: *Influence of the counter ion on the properties of organic and inorganic acid doped polyaniline and their Schottky diodes*. Superlattices Microstruct. 85 (2015) 282–293.

[301] Trchova M., Sapurina I., Prokes J., Stejskal J.: *FTIR spectroscopy of ordered polyaniline films*. Synth Met. 135–136 (2003) 305–306.

[302] Wu C.-G., Yeh Y.-R., Chen J.-Y., Chiou Y.-H.: *Electroless surface polymerization of ordered conducting polyaniline films on aniline-primed substrates*. Polymer 42 (2001) 2877–2885.

[303] Sedenkova I., Trchova M., Blinova N. V., Stejskal J.: *In-situ polymerized polyaniline films. Preparation in solutions of hydrochloric, sulfuric, or phosphoric acid*. Thin Solid Films 515 (2006) 1640–1646.

[304] X'Pert HighScore 2.2e, PANalytical B. V., Netherlands (2009).

[305] Luzny W., Sniechowski M., Laska J.: *Structural properties of emeraldine base and the role of water contents: X-ray diffraction and computer modelling study*. Synth. Met. 126 (2002) 27–35.

[306] Sanches E. A., Soares J. C., Mafud A. C., Fernandes E. G. R., Leite F. L., Mascarenhas Y. P.: *Structural characterization of chloride salt of conducting polyaniline obtained by XRD, SAXD, SAXS and SEM*. J. Mol. Struct. 1063 (2013) 121–126.

[307] Tang Q., Wu J., Sun X., Li Q., Lin J.: *Shape and size control of oriented polyaniline microstructure by a self-assembly method*. Langmuir 25 (2009) 5253–5257.

[308] Claessens H. A., van Straten M. A., Cramers C. A., Jezierska M., Buszewski B.: *Comparative study of test methods for reversed-phase columns for high-performance liquid chromatography*. J. Chromatogr. A 826 (1998) 135–156.

[309] Janeckova L., Kalikova K., Bosakova Z., Tesarova E.: *Study of interaction mechanisms on zirconia-based polystyrene HPLC column*. J. Sep. Sci. 33 (2010) 3043–3051.

[310] Jandera P., Novotna K., Beldean-Galea M. S., Jisa K.: *Retention and selectivity tests of silica-based and metal-oxide bonded stationary phases for RP-HPLC*. J. Sep. Sci. 29 (2006) 856–871.

[311] van Deemter J. J., Zuiderweg F. J., Klinkenberg A.: *Longitudinal diffusion and resistance to mass transfer as causes of noideality in chromatography*. Chem. Eng. Sci. 5 (1956) 271–89.

[312] Usher K. M., Simmons C. R., Dorsey J. G.: *Modeling chromatographic dispersion: A comparison of popular equations*. J. Chromatogr. A 1200 (2008) 122–128.

[313] Gritti F., Guiochon G.: *Adsorption mechanism in RPLC. Effect of the nature of the organic modifier*. Anal. Chem. 77 (2005) 4257–4272.

[314] Meyer R., Schneider C., Jira T.: *Considerations of the behaviour of C18-chains and calixarenes and their application for determination of stationary phase volume in RP-chromatography*. Pharmazie 63 (2008) 619–627.

LIST OF PUBLICATIONS

1. Bierhanzl V. M., Riesová M., **Taraba L.**, Čabala R., Seydlová G.: *Analysis of phosphate and phosphate containing headgroups enzymatically cleaved from phospholipids of Bacillus subtilis by capillary electrophoresis*. Anal. Bioanal. Chem. 407 (2015) 7215-7220, DOI 10.1007/s00216-015-8885-x, IF 3.125.

2. **Taraba L.**, Křížek T., Kubíčková A., Coufal P.: *Sample pretreatment for the capillary electrophoretic determination of organic acids in chromium(III) plating baths*. J. Sep. Sci. 38 (2015) 4255-4261, DOI 10.1002/jssc.201500946, IF 2.741.

3. Garcia Gonzalez A., **Taraba L.**, Hraníček J., Kozlík P., Coufal P.: *Determination of dasatinib in the tablet dosage form by ultra-high performance liquid chromatography, capillary zone electrophoresis, and sequential injection analysis*. J. Sep. Sci. 40 (2016) 400-406, DOI 10.1002/jssc.201600950, IF 2.557.

4. **Taraba L.**, Křížek T., Hodek O., Kalíková K., Coufal P.: *Characterization of polyaniline-coated stationary phases by using the linear solvation energy relationship in the hydrophilic interaction liquid chromatography mode using capillary liquid chromatography*. J. Sep. Sci. 40 (2017) 677-687, DOI 10.1002/jssc.201600785, IF 2.557

5. **Taraba L.**, Křížek T.: *Study of polyaniline-coated silica gel as a stationary phase in different modes of capillary liquid chromatography*. Monatsh. Chem. 148 (2017) 1605-1611, DOI 10.1007/s00706-017-1965-1, IF 1.282

6. **Taraba L.**, Křížek T., Kozlík P., Hodek O., Coufal P.: *Protonation of polyaniline-coated silica stationary phase affects the retention behavior of neutral hydrophobic solutes in reversed-phase capillary LC*. J. Sep. Sci. (2018) (online available), DOI: 10.1002/jssc.201800261.

DECLARATION OF CO-AUTHORS

On behalf of the co-authors I declare that Mgr. Lukáš Taraba contributed substantially to paper 4 entitled *Characterization of polyaniline-coated stationary phases by using the linear solvation energy relationship in the hydrophilic interaction liquid chromatography mode using capillary liquid chromatography*. His share was 90 %.

On behalf of the co-authors I declare that Mgr. Lukáš Taraba contributed substantially to paper 5 entitled *Study of polyaniline-coated silica gel as a stationary phase in different modes of capillary liquid chromatography*. His share was 90 %.

On behalf of the co-authors I declare that Mgr. Lukáš Taraba contributed substantially to paper 6 entitled *Protonation of polyaniline-coated silica stationary phase affects the retention behavior of neutral hydrophobic solutes in reversed-phase capillary LC*. His share was 90 %.

Prague, June 2018 RNDr. Tomáš Křížek, Ph.D.

LIST OF CONFERENCE CONTRIBUTIONS

List of oral presentations

- **Taraba, L.**, Křížek, T.: *Electrophoretic determination of organic acids in matrices containing chromium* (*Elektroforetické stanovení organických kyselin v matricích obsahujících chrom).* 17th National Competition for the Best Student Scientific Work in the Field of Analytical Chemistry, Pardubice, Czech Republic (5. 2. - 6. 2. 2014)

- **Taraba, L.**, Křížek, T.: *Determination of oxalic and citric acid in chromium(III)-containing industrial solutions by capillary zone electrophoresis*. 10th International Students Conference "Modern Analytical Chemistry", Prague, Czech Republic (22. 9. - 23. 9. 2014).

- **Taraba, L.**, Křížek, T.: *Sample pre-treatment and electrophoretic determination of organic acids in chromium(III)-based plating baths* (*Úprava vzorku a elektroforetické stanovení organických kyselin v pokovovacích lázních na bázi trojmocného chromu)*. Cycle of Lectures for Collaborating Czech Universities "Perspektivy v analytické chemii 2015", University of Chemistry and Technology Prague, Prague, Czech Republic (19. 3. 2015)

- **Taraba, L.**: *Characterization of stationary phases for HPLC.* Cycle of lectures "Advances in Separation Science", Charles University, Prague, Czech Republic (4. 4. 2016)

- **Taraba, L.**, Křížek, T.: *Investigation of polyaniline-coated silica gel as a stationary phase for separations in different modes of capillary liquid chromatography*. 12th International Students Conference "Modern Analytical Chemistry", Prague, Czech Republic (22. 9. - 23. 9. 2016)

- **Taraba, L.** Křížek, T.: *pH-effect on retention behavior of polyaniline-coated silica gel stationary phase investigated using linear solvation energy*

relationships. Seminar of the Institute of Analytical Chemistry, Chemo- and Biosensors, Regensburg, Germany (19. 7. 2017)

- **Taraba, L.**, Křížek, T.: *Influence of pH on retention behavior of polyaniline-coated silica gel stationary phase investigated by using linear solvation energy relationships in capillary liquid chromatography*. 13th International Students Conference "Modern Analytical Chemistry", Prague, Czech Republic (21. 9. - 22. 9. 2017)

List of posters

- **Taraba, L.**, Křížek, T., Kubíčková, A., Coufal, P.: *Determination of oxalic and citric acid in chromium(III)-containing industrial solutions by capillary zone electrophoresis.* 20th International Symposium on Separation Sciences ISSS 2014, Prague, Czech Republic (30. 8. - 2. 9. 2014)

- **Taraba, L.**, Křížek, T., Coufal, P.: *Application of polyaniline-coated silica gel particles as the stationary phase for separation of structural isomers.* 43rd International Symposium on High Performance Liquid Phase Separations and Related Techniques HPLC 2015, Beijing, China (21. 9. - 25. 9. 2015)

- **Taraba, L.**, Křížek, T., Coufal, P.: *Characterization of polyaniline-coated stationary phases using linear solvation energy relationship in HILIC mode by capillary LC*. 31st International Symposium on Chromatography ISC 2016, Cork, Ireland (28. 8. - 1. 9. 2016)

- **Taraba, L.**, Křížek, T.: *Modulated retention of neutral hydrophobic solutes on charged polyaniline-coated silica stationary phase by change of mobile phase pH*. 2nd International Caparica Christmas Congress on Translational Chemistry IC_3TC, Caparica, Portugal (4. 12. - 7. 12. 2017) – **Excellent Poster Presentation Award**

ACKNOWLEDGEMENT

First of all, I am very grateful to my supervisor RNDr. Tomáš Křížek, Ph.D. whose encouragement, leading, expertise in separation science, and friendship helped me to make this dissertation thesis. I also thank to prof. RNDr. Pavel Coufal, Ph.D. for his willingness to help anytime and valuable advice on slurry packing instrumentation. Next, I would like to express my thank to RNDr. Petr Kozlík, Ph.D. for his help with continual repairs of capillary LC system and related troubleshooting. I am also grateful to Mgr. Ondřej Hodek who, besides his collaboration on common projects, made a hilarious working atmosphere.

I thank to RNDr. Květa Kalíková, Ph.D. and RNDr. Jitka Zichová, Dr. for consulting the issues related to LSER evaluation. Next, I would like to express my gratitude to RNDr. Irena Matulková, Ph.D. for recording of Raman and FTIR spectra of PANI-SiO_2 powder samples and help with their evaluation. Similarly, I thank to doc. RNDr. David Havlíček, CSc. for XRD measurement of the PANI-SiO_2.

Further, I would like to thank to Ing. Lukáš Krejčík, Ph.D. and Bc. Radka Mikešová for measurement of SSA of the sorbents and for recording SEM images thereof. I also thank to Mgr. Martina Havelcová, Ph.D. for performed elemental analysis of the sorbents and RNDr. Miroslav Hyliš, Ph.D. who allowed me to record SEM and TEM images of my sorbents in his laboratory.

Na závěr chci velmi poděkovat svým rodičům a přítelkyni za jejich podporu a porozumění během mého doktorského studia.